

FINAL REPORT – PART I

Innovative In-Situ Remediation of Contaminated Sediments for Simultaneous Control of Contamination and Erosion

SERDP Project ER-1501

AUGUST 2011

Kenneth Dixon
Savannah River National Laboratory

Danny Reible
University of Texas

Jesse Roberts
Sandia National Laboratory

Iona Petrisor
Haley & Aldrich

This document has been cleared for public release



Report Documentation Page				Form Approved OMB No. 0704-0188		
Public reporting burden for the collection of information is estimated to average 1 hour per response, including the time for reviewing instructions, searching existing data sources, gathering and maintaining the data needed, and completing and reviewing the collection of information. Send comments regarding this burden estimate or any other aspect of this collection of information, including suggestions for reducing this burden, to Washington Headquarters Services, Directorate for Information Operations and Reports, 1215 Jefferson Davis Highway, Suite 1204, Arlington VA 22202-4302. Respondents should be aware that notwithstanding any other provision of law, no person shall be subject to a penalty for failing to comply with a collection of information if it does not display a currently valid OMB control number.						
1. REPORT DATE AUG 2011		2. REPORT TYPE Final		3. DATES COVERED -		
4. TITLE AND SUBTITLE Innovative In-Situ Remediation of Contaminated Sediments for Simultaneous Control of Contamination and Erosion - Part I				5a. CONTRACT NUMBER		
				5b. GRANT NUMBER		
				5c. PROGRAM ELEMENT NUMBER		
6. AUTHOR(S)				5d. PROJECT NUMBER		
				5e. TASK NUMBER		
				5f. WORK UNIT NUMBER		
7. PERFORMING ORGANIZATION NAME(S) AND ADDRESS(ES) Savannah River National Laboratory				8. PERFORMING ORGANIZATION REPORT NUMBER		
9. SPONSORING/MONITORING AGENCY NAME(S) AND ADDRESS(ES)				10. SPONSOR/MONITOR'S ACRONYM(S)		
				11. SPONSOR/MONITOR'S REPORT NUMBER(S)		
12. DISTRIBUTION/AVAILABILITY STATEMENT Approved for public release, distribution unlimited						
13. SUPPLEMENTARY NOTES The original document contains color images.						
14. ABSTRACT Active or reactive capping, is the application of a relatively thin layer of reactive material to the sediment to physically and chemically reduce contaminant mobility and/or bioavailability. This project addressed high priority research needs related to developing/selecting active capping materials and cap designs for contaminant sequestration under a range of aquatic sediment conditions and assessing the ability of innovative amendments to immobilize a variety of organic and inorganic contamination and resist erosion in situ.						
15. SUBJECT TERMS						
16. SECURITY CLASSIFICATION OF:				17. LIMITATION OF ABSTRACT SAR	18. NUMBER OF PAGES 303	19a. NAME OF RESPONSIBLE PERSON
a. REPORT unclassified	b. ABSTRACT unclassified	c. THIS PAGE unclassified				

This report was prepared under contract to the Department of Defense Strategic Environmental Research and Development Program (SERDP). The publication of this report does not indicate endorsement by the Department of Defense, nor should the contents be construed as reflecting the official policy or position of the Department of Defense. Reference herein to any specific commercial product, process, or service by trade name, trademark, manufacturer, or otherwise, does not necessarily constitute or imply its endorsement, recommendation, or favoring by the Department of Defense.

ACKNOWLEDGEMENTS

This research was supported wholly by the U.S. Department of Defense, through the Strategic Environmental Research and Development Program (SERDP) under project ER 1501. Performers of this project would like to thank to all commercial companies for supplying sequestering agents. We would also like to extend appreciation to X. Ma, J. Galjour, C. Forest, L. Moretti, and X. Lu, University of Texas, and Y. G. Kritzas and M. Brim, University of South Carolina at Aiken, X. Ma, J. Galjour, C. Forest, L. Moretti, and X. Lu, University of Texas, W. J. Macky, P.A. Allen, R. Roseberry, C. Turick, D. Coughlin, M. T. Whiteside, M. Serrato, E. Caldwell, and L. Bagwell, Savannah River National Laboratory for assistance in the laboratory, in the field, data analysis, and project support.

TABLE OF CONTENTS

LIST OF ACRONYMS	vii
LIST OF FIGURES	ix
LIST OF TABLES	xvi
LIST OF PICTURES.....	xix
ABSTRACT.....	1
OBJECTIVES	8
BACKGROUND	10
TECHNICAL APPROACH.....	12
MATERIALS AND METHODS	15
TASK 1. LABORATORY STUDY – EFFECT OF AMENDMENTS ON CONTAMINANT MOBILITY AND BIOAVAILABILITY	15
SUBTASK 1.1. SORPTION AND DESORPTION OF CONTAMINANTS BY SEQUESTERING AGENTS.....	15
Sorption and Desorption of As, Cd, Cr, Co, Cu, Pb, Ni, Se, and Zn in Fresh and Salt Water.....	15
Sorption of Organic Contaminants by Sequestering Agents.....	16
Development of Cross-linked Biopolymers and Biopolymer Coated Sand	18
Sorption of Organic Contaminants on Cross-linked Biopolymers Coated Sand.....	22
Sorption of Metals on Cross-linked Biopolymer Coated Sand.....	22
SUBTASK 1.2. EFFECT OF SEQUESTERING AGENTS ON MOBILITY, BIOAVAILABILITY, AND RETENTION OF CONTAMINANTS IN SEDIMENTS	22
Kinetic Studies on Retention of Organic Contaminants	22
Effect of Sequestering Agents on Availability and Retention of Metals.....	24
TASK 2. STUDIES FOR DETERMINATION OF THE BEST COMBINATION OF AMENDMENTS FOR PLACEMENT AND CONSTRUCTION OF ACTIVE SEDIMENT CAPS	26
SUBTASK 2.1. EVALUATION OF MECHANICAL PROPERTIES.....	26
Physical Properties of Biopolymer Products and Other Amendments	26
SUBTASK 2.2. EVALUATION OF DIFFUSIVE TRANSPORT	27
Diffusion of Metals through Active Caps – Laboratory Experiment	27
Diffusion of Metals through Active Caps – Modeling	28
SUBTASK 2.3. EVALUATION OF ADVECTIVE TRANSPORT.....	29
Advective Transport of Metals through Cap Materials – Laboratory Experiments .	29
Diffusive and Advective Transport of Organic Contaminants - Column Studies	31
Tracer Study for Column Experiments	33
SUBTASK 2.4. EVALUATION OF POTENTIAL AMENDMENT TOXICITY.....	34
Analysis of Extracts	34
Sediment Toxicity Tests for Fresh and Salt Water.....	34
Bioaccumulation Study.....	36
Recovering California Blackworms from Sediments and Amendments	36
Laboratory Survival Studies.....	36
SUBTASK 2.5. BIODEGRADABILITY OF BIOPOLYMER PRODUCTS	37
Biodegradability of Biopolymer Products	37
Microbial Effects on the Properties of Biopolymers.....	37

TASK 3. EVALUATION OF THE RESISTANCE OF CAPS TO PHYSICAL DISTURBANCE	39
Evaluation of Suspension by Shaker Tests	39
Evaluation of Cap Resistance to Physical Disturbance by Adjustable Shear Stress	
Erosion and Transport (ASSET) Flume	43
Description of the ASSET Flume	43
Hydrodynamics	44
Sample Collection and Preparation for the ASSET Flume Test	45
Measurements of Sediment Erosion Rates and Critical Shear Stress	45
Erosion Rate Ratio Analysis	45
TASK 4. GENERATION OF CONCEPTUAL AND MATHEMATICAL MODELS FOR CONTAMINANTS ATTENUATION	47
1-D Metal Transport Modeling	47
Model Grid Construction	47
Material Properties and Other Input Parameters	48
TASK 5. FIELD DEPLOYMENT	50
SUBTASK 5.1. SELECTION AND CHARACTERIZATION OF A STUDY SITE FOR A PLOT STUDY.....	50
Selection of a Study Site	50
Characterization of a Study Site.....	50
SUBTASK 5.2. CAP CONSTRUCTION	56
Cap Construction.....	56
SUBTASK 5.3. POST - CAP MONITORING.....	62
Sample Collection and Analysis after Cap Construction.....	63
Sediment Characterization after Treatment.....	64
Evaluation of Zone of Influence (ZOI)	64
DGT Probes for Assessment of Active Cap Effectiveness.....	65
Statistical Analysis	66
Cap Monitoring for Erosion	66
Active Biomonitoring.....	67
RESULTS AND DISCUSSION	71
TASK 1. EFFECT OF AMENDMENTS ON CONTAMINANT MOBILITY AND BIOAVAILABILITY – LABORATORY STUDY.....	71
SUBTASK 1.1. SORPTION AND DESORPTION OF CONTAMINANTS BY SEQUESTERING AGENTS.....	71
Effect of Sequestering Agents on pH.....	71
Sorption and Desorption of Metals in Fresh and Salt Water	73
Sorption of Organic Contaminants by Sequestering Agents	89
Development of Biopolymer Products	90
Sorption of Metals and Organic Contaminants by Biopolymers	94
SUBTASK 1.2. EFFECT OF SEQUESTERING AGENTS ON THE MOBILITY, BIOAVAILABILITY, AND RETENTION OF CONTAMINANTS IN SEDIMENT ..	96
Removal and Retention of Organic Contaminants.....	96
Kinetic Study and Sorption/ Desorption of Organic Contaminants by Selected Amendments.....	99
Cap Effectiveness for Organics	106

Effect of Selected Sequestering Agents on Mobility and Retention of Metals	109
TASK 2. STUDIES FOR DETERMINATION OF THE BEST COMBINATION OF AMENDMENTS FOR PLACEMENT AND CONSTRUCTION OF ACTIVE SEDIMENT CAPS	131
Subtask 2.1. Evaluation of Mechanical Properties.....	131
Physical Properties of Biopolymer Materials and Other Amendments	131
SUBTASK 2.2. EVALUATION OF DIFFUSIVE TRANSPORT	135
Diffusion of Metals through Active Caps – Laboratory Experiment	135
Diffusive Transport of Metals through Active Caps – Modeling	142
SUBTASK 2.3. EVALUATION OF ADVECTIVE TRANSPORT	151
Advective Transport of Metals through Active Caps – Laboratory Evaluation	151
Evaluation of Advective Transport of Organic Contaminants	152
Diffusive and Advective Transport of Organic Contaminants -Measured Breakthrough and Model Comparison.....	157
SUBTASK 2.4. EVALUATION OF POTENTIAL AMENDMENT TOXICITY.....	162
Analysis of extracts	162
Sediment Toxicity Tests for Fresh and Salt Water.....	166
Development of Biomonitoring Method for the Field Study	172
Recovery Methods and Efficiency	172
Survival.....	172
SUBTASK 2.5. BIODEGRADABILITY OF BIOPOLYMER PRODUCTS	173
TASK 3. EVALUATION OF THE RESISTANCE OF CAPS TO PHYSICAL DISTURBANCE	178
Evaluation of Biopolymer Resistance to Physical Disturbance	178
Shaker Tests	178
Adjustable Shear Stress Erosion and Transport (ASSET) Flume	181
TASK 4. GENERATION OF CONCEPTUAL AND MATHEMATICAL MODELS FOR CONTAMINANT ATTENUATION	187
Transport of Metals through Active Caps – 1-D Metal Transport Modeling	188
TASK 5. FIELD DEPLOYMENT	199
SUBTASK 5.1. SELECTION AND CHARACTERIZATION OF A STUDY SITE FOR A PLOT STUDY.....	199
Site Selection.....	199
Characteristics and Chemistry of Surface Water and Pore Water before Cap Placement.....	200
Sediment Properties before Cap Placement.....	201
SUBTASK 5.2. FIELD DEPLOYMENT - CAP CONSTRUCTION	207
Characteristics and Chemistry of Surface Water and Pore Water after Cap Placement.....	210
Sediment Characterization Twelve Months after Cap Placement.....	225
Simultaneously Extracted Metals/Acid Volatile Sulfide (SEM/AVS) Evaluation of Sediment	227
Evaluation of Zone of Influence (ZOI) – Laboratory Study.....	233
Evaluation of Zone of Influence (ZOI) –Field Study.....	235
Effect of Active Caps on Metal Bioavailability – Comparison of DGT Probes and Pore Water Results	239

Cap Erosion	243
Cap Erosion – Field Evaluation by Adjustable Shear Stress Erosion Transport (ASSET) Flume	247
Active Biomonitoring.....	250
SUMMARY AND CONCLUSIONS	257
REFERENCES.....	260
APPENDIX 1- ADDITIONAL DATA	270
APPENDIX 2- PUBLICATIONS	276
APPENDIX 3 - TRANSITION PLAN	283

LIST OF ACRONYMS

A – apatite

ANOVA – one-way analysis of variance

As – arsenic

ASSET – adjustable shear stress erosion transport

AVS – acid volatile sulfide

B – biopolymer

C – chitosan, biopolymer

Cd – cadmium

Co – cobalt

Cr – chromium

Cu – copper

DGT – diffusive gradients in thin films

DI – deionized water

DO – dissolved oxygen

DOC – dissolved organic carbon

DoD – Department of Defense

EC – electrical conductivity

G – guar gum, biopolymer

HPLC- high performance liquid chromatography

ICP-MS – inductively coupled plasma – mass spectrometry

K_d – partition coefficient

Meq – milliequivalents

MNR – monitored natural recovery

NCA – North Carolina apatite

Ni – nickel

O – organoclay

ORP – oxidation reduction potential

PAHs – polycyclic aromatic hydrocarbons

Pb – lead

PCBs – polychlorinated biphenyls

PM – organoclay PM-199

S – sand

Se – selenium

SEM – simultaneously extracted metals

SNL – Sandia National Laboratories

SPME- solid phase microextraction

SRNL – Savannah River National Laboratory

SRS – Savannah River Site

TC – total carbon

TCLP- toxicity characteristic leaching procedure

TIC – total inorganic carbon

TOC – total organic carbon

X – xanthan, biopolymer

Zn – zinc

ZOI – zone of influence

LIST OF FIGURES

Figure 1. Shaker Test Experimental Design (after Tsai and Lick, 1986)	41
Figure 2. Shear Stress as a Function of Oscillation Period (Tsai and Lick, 1986)	42
Figure 3. Fitting of Tsai and Lick's (1986) data	42
Figure 4. Schematic Illustration of the ASSET Flume.	43
Figure 5. Map of the Savannah River Site showing Potential Field Study Locations on Steel Creek and Tims Branch (red diamonds).	51
Figure 6. Scheme of Field Deployment.	52
Figure 7. Top and Cross-section Views of Cap and Locations of the Sippers.	55
Figure 8. Three Types of Caps were Tested in the Field Deployment.	62
Figure 9. Effect of Sequestering Agents on Spike Solution pH. Ctrl – control (spike solution), RPT – rock phosphate from Tennessee, NCA- North Carolina apatite, BA- biological apatite, CaP – calcium phytate, OC or OCB – organoclays from Biomin Inc., AB8 – aquablok with clay coating, AB-ZVI aquablok with zero valent iron, ZC – clinoptilolite zeolite, ZP – phillipsite zeolite, BPC – chitosan biopolymer.	72
Figure 10. Partition Coefficients (K_d) (mL g^{-1}) for As, Cd, Cr, Co, Cu, Ni, Pb, Se, and Zn in Fresh Water; RPT – rock phosphate from Tennessee, NCA- North Carolina apatite, BA- biological apatite, CaP – calcium phytate, OCB – organoclays from Biomin Inc., AB8 – aquablok with clay coating, AB-ZVI aquablok with zero valent iron, ZC – clinoptilolite zeolite, ZP – phillipsite zeolite, BPC – chitosan biopolymer.	75
Figure 11. Sorption of As, Cd, Cr, Co, Cu, Ni, Pb, Se, and Zn in Fresh Water (concentration of each metal in the spike solution was $\sim 1 \text{ mg L}^{-1}$).	78
Figure 12. Sorption of As, Cd, Cr, Co, Cu, Ni, Pb, Se, and Zn in Salt Water (concentration of each metal in the spike solution was $\sim 1 \text{ mg L}^{-1}$).	80
Figure 13. Comparison of Sorption of As, Cd, Cr, Co, Cu, Ni, Pb, Se, and Zn in Fresh and Salt Water (concentration of each metal in the spike solution was $\sim 1 \text{ mg L}^{-1}$).	81
Figure 14. Retention of Metals by Amendments in Fresh Water.	84
Figure 15. Retention of Metals by Amendments in Salt Water.	88
Figure 16. Viscosity of Alginate before and after Cross-linking with CaCl_2	93
Figure 17. Viscosity of Xanthan before and after Cross-linking.	93
Figure 18. Removal of Metals by Biopolymers from a Spike Solution with an Initial Concentration of 5000 mg L^{-1} of Cd, Co, Cr, Cu, Ni, Pb, Se, and Zn; NCA - North Carolina apatite, XG - xanthan cross-linked with guar gum, XC - xanthan cross-linked with chitosan.	95
Figure 19. Carbon Fraction of Biopolymer Coated Sand; C – chitosan, G – guar gum, B - borax, X – xanthan, c – calcium chloride.	95
Figure 20. Dissolved Naphthalene and Phenanthrene Release from Columns in which Creosote Mixtures were Continuously Injected. Vertical lines indicate NAPL breakthrough	98
Figure 21. Phenanthrene Released by Gas Migration from a Weathered Creosote Mixture Showing the Effectiveness of an Organoclay Layer.	99
Figure 22. Sorption of Three PAHs to Zeolite (Clinoptilolite).	101
Figure 23. Sorption of Two PAHs to PIMS (Biological Apatite).	102
Figure 24. Sorption of Phenanthrene and Pyrene to CETCO-199.	103
Figure 25. North Carolina Apatite Desorption Kinetics. Reported data were the average of three replicates. The error bars are standard deviations.	105

Figure 26. Organoclay (OCB750) Desorption Kinetics. Reported data were the average of three replicates. The error bars are standard deviations.....	105
Figure 27. Organoclay (CETCO PM 200) Desorption Kinetics. Reported data were the average of three replicates. The error bars are standard deviations.....	106
Figure 28. Effect of Amendments on Anacostia River Sediment Properties under Oxidized and Reduced Conditions; NCA – North Carolina apatite, OCB – organoclay 750 from Biomin, Inc., BPC – biopolymer chitosan, Z- zeolite.....	110
Figure 29. Effect of Amendments on Metal Concentrations in the Water Extracted from the Anacostia Sediment after Eight Weeks of Contact with Amendments under Reduced Conditions (~-200mV); the amount of added amendments - 2 % by dry weight.	114
Figure 30. Effect of Amendments on Metal Concentrations in the Water Extracted from the Anacostia Sediment after Eight Weeks of Contact with Amendments under Oxidized Conditions (~-200mV); the amount of added amendments - 2 % by dry weight.	115
Figure 31. Effect of North Carolina Apatite (NCA) and Organoclay (OCB) on Partitioning of As in Elizabeth River Sediment (ES); F1 - exchangeable fraction, F2 - carbonate fraction, F3 - amorphous fraction, F4 – crystalline oxide, F5 – organic, F6 – sulfide, and F7 – residual; doses of amendments in % by dry weight: 2.5, 5, and 10.....	121
Figure 32. Effect of NCA and OCB on Partitioning of Cd in Elizabeth River Sediment (ES); F1 - exchangeable fraction, F2 - carbonate fraction, F3 - amorphous fraction, F4 – crystalline oxide, F5 – organic, F6 – sulfide, and F7 – residual; doses of amendments in % by dry weight: 2.5, 5, and 10.	122
Figure 33. Effect of NCA and OCB on Partitioning of Co in Elizabeth River Sediment (ES); F1 - exchangeable fraction, F2 - carbonate fraction, F3 - amorphous fraction, F4 – crystalline oxide, F5 – organic, F6 – sulfide, and F7 – residual; doses of amendments in % by dry weight: 2.5, 5, and 10.	123
Figure 34. Effect of NCA and OCB on Partitioning of Cr in Elizabeth River Sediment (ES); F1 - exchangeable fraction, F2 - carbonate fraction, F3 - amorphous fraction, F4 – crystalline oxide, F5 – organic, F6 – sulfide, and F7 – residual; doses of amendments in % by dry weight: 2.5, 5, and 10.	124
Figure 35. Effect of NCA and OCB on Partitioning of Ni in Elizabeth River Sediment (ES); F1 - exchangeable fraction, F2 - carbonate fraction, F3 - amorphous fraction, F4 – crystalline oxide, F5 – organic, F6 – sulfide, and F7 – residual; doses of amendments in % by dry weight: 2.5, 5, and 10.	125
Figure 36. Effect of NCA and OCB on Partitioning of Pb in Elizabeth River Sediment (ES); F1 - exchangeable fraction, F2 - carbonate fraction, F3 - amorphous fraction, F4 – crystalline oxide, F5 – organic, F6 – sulfide, and F7 – residual; doses of amendments in % by dry weight: 2.5, 5, and 10.	126
Figure 37. Effect of NCA and OCB on Partitioning of Zn in Elizabeth River Sediment (ES); F1 - exchangeable fraction, F2 - carbonate fraction, F3 - amorphous fraction, F4 – crystalline oxide, F5 – organic, F6 – sulfide, and F7 – residual; doses of amendments in % by dry weight: 2.5, 5, and 10.	127
Figure 38. Average Potentially Mobile Fraction (PMF) and Recalcitrant Factor (RF) for As, Cd, Co, Cr, Ni, Pb, and Zn in Untreated and Treated Elizabeth River Sediment (ES). The red line represents the partitioning of untreated sediment; doses of amendments in % by dry weight: 2.5, 5, and 10.	130

Figure 39. Metal Release in Diffusion Experiment after Six Months; average of five samplings.	136
Figure 40. pH Changes with Time in Diffusion Experiment.	137
Figure 41. Electrical Conductivity in Diffusion Experiment.	138
Figure 42. Total Inorganic (TIC) and Total Organic (TOC) Carbon in Water and Sediment....	139
Figure 43. Carbon Content in Water and Sediment Layers under Two Biopolymer Caps and in Biopolymer Caps at Start and End of Diffusion Experiment.	140
Figure 44. Predicted Breakthrough Curves for Cd, Co, Cr, and Cu for the no cap case.	143
Figure 45. Predicted Breakthrough Curves for Pb, Ni, Se, and Zn for the no cap case.	144
Figure 46. Predicted Breakthrough Curves for Cd, Co, Cr, and Cu for the sand cap case.	145
Figure 47. Predicted Breakthrough Curves for Pb, Ni, Se, and Zn for the sand cap case.	146
Figure 48. Predicted Breakthrough Curves for Cd, Co, Cr, and Cu for Apatite (NCA) Cap Case. The sediment concentration curves are plotted against the left y-axis and all others against the right y-axis.	147
Figure 49. Predicted Breakthrough Curves for Pb, Ni, Se, and Zn for Apatite (NCA) Cap Case. The sediment concentration curves are plotted against the left y-axis and all others against the right y-axis.	148
Figure 50. Predicted Breakthrough Curves for Cd, Co, Cr, and Cu for the organoclay (OCB750) cap case. The sediment concentration curves are plotted against the left y-axis and all others against the right y-axis.	149
Figure 51. Predicted Breakthrough Curves for Pb, Ni, Se, and Zn for Organoclay (OCB750) Cap Case. The sediment concentration curves are plotted against the left y-axis and all others against the right y-axis.	150
Figure 52. Breakthrough Curves as a Function of Pore Volume for Sand Column.	151
Figure 53. Breakthrough Curves for Apatite Column as a Function of Pore Volume.	152
Figure 54. Predicted Breakthrough Curves for Biopolymer Coated Sand (CGB3) for Phenanthrene, Naphthalene, and Pyrene.	155
Figure 55. Predicted Breakthrough Curves for Organoclay PM-199 for Phenanthrene and Naphthalene.	156
Figure 56. Measured Effluent Concentrations and Comparison to Model.	159
Figure 57. Total Breakthrough Curve Predictions.	160
Figure 58. Comparison of Experimental and Model Data of Phenanthrene Breakthrough of 15 cm XCc Cap.	160
Figure 59. Comparison of Experimental and Model Data of Naphthalene Breakthrough of 15 cm XCc Cap.	161
Figure 60. Comparison of Experimental and Model Data of Phenanthrene Breakthrough of 15 cm CGB3 Cap.	161
Figure 61. Comparison of Experimental and Model Data of Naphthalene Breakthrough of 15 cm CGB3 Cap.	161
Figure 62. Comparison of the Concentrations of As, Ba, Cd, Cr, Pb, Sb, and Se in the TCLP Extract Solution to TCLP Limits (in ppb); NCA = North Carolina Apatite, TRP = rock phosphate from TN, OCB750 = organoclay 750 from Biomin Inc., PM-199 organoclay from CETCO, CS = coated sand with xanthan, chitosan and cross-linked with calcium chloride, PS = sand.	165
Figure 63. Effects of Organoclay on Survival of <i>Hyalella</i> and <i>Leptocheirus</i> ; S – sediment, OC – Organoclay	169

Figure 64. Effects of Organoclay on Survival and Growth of of <i>Ilyodrilus</i>	170
Figure 65. Effect of Organoclay on Lipid Normalized Bioaccumulation of PAHs in <i>Ilyodrilus</i> ; OC - Organoclay.	171
Figure 66. Recovery of California Blackworms (based on aggregate worm weight) from Silt and Sand over 17 Days. Recovery was a combined function of survival and growth.....	173
Figure 67. Release of CO ₂ (measured by GC-MS) from Several Cross-linked Biopolymers: B - borax, C - chitosan, G - guar gum, X - xanthan, c - calcium chloride, 1 & 3 - without glutaral-dehyde, 2 - with glutaraldehyde, 3 – with NaOH.....	174
Figure 68. Evaluation of Biopolymer Degradation under Wet/Dry Conditions and Different Temperatures; X - xanthan, G - guar gum, C- chitosan, c - calcium chloride.	174
Figure 69. Microscopic Analyses of Biopolymer Surfaces using 4',6-Diamidino-2-Phenylindole (DAPI) and Epifluorescence Microscopy. Biopolymer XCc (left) contained fewer bacteria than CGB after 6 months of contact with sediment suggesting limited biodegradation.....	176
Figure 70. Evaluation of Biopolymer Degradation for 45 Days; X - xanthan, G - guar gum, and C- chitosan. Metal sorption of biopolymers inhibited bacterial activity.....	176
Figure 71. Morphological Differences in Bacterial Populations after Exposure to Xanthan Biopolymers without (left) and with (right) Sorbed Metals.....	177
Figure 72. Metals Remaining in Biopolymers after 3 Months of Biodegradation (initial concentration of the spike solution was 5000 µg L ⁻¹).	177
Figure 73. Effects of Equivalent Shear Stresses on Resuspension of Sand and Three Types of Dry and Rewetted Biopolymer Coated Sand.	179
Figure 74. Effects of Equivalent Shear Stresses on Sand and Slurries of Biopolymer Coated Sand: 2 – sand with chitosan/guar gum/borax, 7 – sand with xanthan/guar gum and apatite, 8 - sand with xanthan/guar gum and organoclay (PM-199), 9 - sand with xanthan/guar gum and apatite, and organoclay.....	179
Figure 75. Plain Sand Resuspension at 3.7 m/s (A) and Erosion at (11 m/s) (B).....	180
Figure 76. Coated Sand with Xanthan and Guar Gum did not Erode at 3.7 m/s (A) or 11m/s (B).	180
Figure 77. Sand and Organoclay (PM-199) Mixed with Biopolymers Xanthan and Guar Gum did not Erode at 3.7m/s (A) or 11m/s (B).	180
Figure 78. Resuspension of Organoclay (PM-199) leading to Cloudiness (A) and Surface Suspension (B).	181
Figure 79. (A) #9 XG/AO 10 Day Consolidation Erosion Rate as a Function of Depth at Shear Stresses of 0.5, 0.75, 1.0, 1.5, 2.0, and 4.0 Pa. (B) #9 XG/AO 10 Day Consolidation Erosion Rate Ratio for the 3 Erosion Intervals. (C) #8 OXG 10 Day Consolidation Erosion Rate as a Function of Depth at Shear Stresses of 0.75, 1.0, 1.5, 2.0, 3.0, and 4.0 Pa. (D) #8 OXG 10 Day Consolidation Erosion Rate Ratio for the 3 Erosion Intervals.....	183
Figure 80. Erosion Rate Ratio for Six Primary Cap Materials comparing All Erosion Intervals and Core Average Erosion at Consolidation Times of 2, 10, and 175 Days.....	185
Figure 81. Comparison of Core Average Erosion Rates at 2, 10, and 175 Day Consolidation Including the Time Average of All Three.....	186
Figure 82. Critical Shear Stress Comparison among Biopolymer Materials at 2, 10, and 175 Days. Each value is an average of measurements taken at two to five different depths in a core sample. Error bars represent standard deviations.....	186

Figure 83. Breakthrough Curves for Cd, Co, Cr, and Cu for the No cap Case. The sediment concentration curves are plotted against the left y-axis and all others against the right y-axis.	190
Figure 84. Breakthrough Curves for Pb, Ni, Se, and Zn for No Cap Case. The sediment concentration curves are plotted against the left y-axis and all others against the right y-axis.	191
Figure 85. Breakthrough Curves for Cd, Co, Cr, and Cu for Sand Cap Case. The sediment concentration curves are plotted against the left y-axis and all others against the right y-axis.	192
Figure 86. Breakthrough Curves for Pb, Ni, Se, and Zn for Sand Cap Case. The sediment concentration curves are plotted against the left y-axis and all others against the right y-axis.	193
Figure 87. Breakthrough Curves for Cd, Co, Cr, and Cu for Apatite Cap Case. The sediment concentration curves are plotted against the left y-axis and all others against the right y-axis.	194
Figure 88. Breakthrough Curves for Pb, Ni, Se, and Zn for Apatite Cap Case. The sediment concentration curves are plotted against the left y-axis and all others against the right y-axis.	195
Figure 89. Breakthrough Curves for Cd, Co, Cr, and Cu for Organoclay Cap Case. The sediment concentrations curves are plotted against the left y-axis and all others against the right y-axis.	196
Figure 90. Breakthrough Curves for Pb, Ni, Se, and Zn for Organoclay Cap Case. The sediment concentration curves are plotted against the left y-axis and all others against the right y-axis.	197
Figure 91. Apatite Thickness as a Function of Breakthrough Time for Cr Concentration of $2 \mu\text{g L}^{-1}$	198
Figure 92. Total Carbon (TC), Total Inorganic Carbon (TIC), and Total Organic Carbon (TOC) in Surface Water Collected at each Plot before Cap Deployment.	204
Figure 93. Total Carbon (TC), Total Inorganic Carbon (TIC), and Total Organic Carbon (TOC) in Pore Water Collected at each Plot before Cap Deployment.	204
Figure 94. Average Metal Concentrations in Surface Water (n=9) from Steel Creek Experimental Area.	205
Figure 95. Average Metal Concentrations in Pore Water (n=20) from Steel Creek Experimental Area.	205
Figure 96. Total Carbon Content (TC), Total Inorganic Carbon (TIC), and Total Organic Carbon (TOC) in Sediment Core Samples (n = 8) Collected at each Plot before Cap Deployment; the core samples were divided in three parts: A 0-5 cm, B 5-10 cm, and C 10-20 cm.	206
Figure 97. Acid-Volatile Sulfide Concentrations ($\mu\text{mole sulfide} \times \text{gram dry sediment}^{-1}$) in Samples from each Plot.	206
Figure 98. Effect of Cap Amendments on pH of Pore Water – 12 Month Evaluation; Cap – pore water collected within the cap, UC – pore water collected beneath the cap, OC – pore water collected outside the cap.	213
Figure 99. Effect of Cap Amendments on Electrical Conductivity (EC) of Pore Water – 12 Month Evaluation; Cap – pore water collected within the cap, UC – pore water collected beneath the cap, OC – pore water collected outside the plot.	214

Figure 100. Effect of Cap Amendments on ORP Values of Pore Water –12-Month Evaluation; A/S – apatite/sand, B/A/S – biopolymer/apatite/sand; B/A/O/S - biopolymer/apatite/organoclay/sand.	215
Figure 101. Total Carbon in Surface Water Collected before Cap Placement and One, Two, and Five, and 12 Months after Cap Placement.	217
Figure 102. Total Carbon Concentrations in Pore Water Samples Collected from each Type of Cap before Cap Placement (BCP), and One, Two, Five, and 12 Months after Cap Placement. Pore water was collected within each cap (cap), beneath each cap (beneath cap), and outside of each cap (outside).	218
Figure 103. Element Concentrations in Surface Water; BCP- before cap placement, A1M – One Month after Cap Placement, A2M - two months, A5M – five months, A9M – nine months, A12M – twelve months.	219
Figure 104. Effect of Cap Materials on Metal Concentrations in Pore Water Two and Five Months after Cap Placement; BCP- before cap placement (n = 8), 2M – pore water collected two months after cap placement(n = 8 for each type of cap), 5M- pore water collected five months after cap placement (n = 8 for each type of cap); A/S – apatite/sand, B/A/S – biopolymer/apatite/sand; B/A/O/S – biopolymer/apatite/organoclay/sand.	220
Figure 105. Effect of Cap Materials on Metal Concentrations in Pore Water 12 Months after Cap Placement.	221
Figure 106. Average P Concentrations (ppm) in Pore Water Collected within and beneath each Cap. The P concentrations are presented for three sampling events: one, two and five months after cap placement; A/S – apatite/sand, B/A/S – biopolymer/apatite/sand; B/A/O/S – biopolymer/apatite/organoclay/sand.	223
Figure 107. Average P Concentrations (ppm) in Pore Water Collected within and outside each Cap. The P concentrations are presented only for one sampling event - five months after cap placement; A/S – apatite/sand, B/A/S – biopolymer/apatite/sand; B/A/O/S – biopolymer/apatite/organoclay/sand.	223
Figure 108. Effect of Cap Amendments on Sediment pH Values; Sediment Samples Collected Six and 12 Months after Cap Placement: Control, untreated sediment, A – apatite cap, B/A – biopolymer/apatite cap, B/A/O – biopolymer/apatite/organoclay cap.....	226
Figure 109. Effect of Cap Amendments on Total Carbon (TC) Content in Sediment beneath Caps; Sediment Samples Collected before, six, and 12 Months after Cap Placement; A – apatite cap, B/A – biopolymer/apatite cap, B/A/O – biopolymer/apatite/organoclay cap...	227
Figure 110. AVS, SEM, and SEM/AVS in Steel Creek Sediment before and after Cap Placement; treatments: control (untreated sediment), biopolymer/apatite/organoclay (B/A/O) cap, and apatite cap.	229
Figure 111. Effect of Cap Amendments on the SEM/AVS Ratio in the Sediment beneath the Caps in Steel Creek – 12 Month Evaluation.	230
Figure 112. Regression Lines and 95% Confidence Intervals (CIs) Describing Temporal Changes in the SEM/AVS Ratio in Sediment Located in the Control Plot and beneath the Apatite Cap during the One Year Test Period.....	231
Figure 113. Lead Concentration in Water Extracts from Sediment Collected from below Each Cap; four types of caps were evaluated: sand, NCA – apatite, organoclay, and B/NCA/O – biopolymer, apatite and organoclay; A – layer 0-1.5 cm, B – layer 1.5-2.5 cm, C – layer 2.5- 5 cm, and D – layer 5-10cm.	233

Figure 114. Metal Concentrations in Water Extracts from Sediment Collected from below each Cap; four types of caps were evaluated: sand, NCA – apatite, organoclay, and B/NCA/O – biopolymer, apatite and organoclay cap.....	234
Figure 115. Double Acid Extractions of Metals from Sediment Layers beneath the Caps – Six Month Evaluation; A- apatite cap, B/A – biopolymer/apatite cap, and B/A/O – biopolymer/apatite/organoclay cap.	236
Figure 116. Double Acid Extractions of Metals from Sediment Layers beneath the Caps – Six Month Evaluation; A- apatite cap, B/A – biopolymer/apatite cap, and B/A/O – biopolymer/apatite/organoclay cap.	237
Figure 117. Double Acid Extractions of Metals from Sediment Layers beneath Caps – 12 Month Evaluation; A- apatite cap, B/A – biopolymer/apatite cap, and B/A/O – biopolymer/apatite/organoclay cap.	238
Figure 118. Metal Concentrations Measured by Field and Laboratory DGT and in Pore Water Collected with Sippers in Field; US – untreated sediment, PW – pore water.....	241
Figure 119. Effect of Apatite Active Cap on Metals in Sediments – DGT in Comparison with Pore Water Results; US – untreated sediment, PW – pore water.	242
Figure 120. Erosion Rate Ratio - Comparison of All Samples: control plot – samples 1 and 2; biopolymer/apatite/organoclay plot – samples 3, 4, and 5; apatite/sand plot – 6, 7, and 8..	248
Figure 121. Erosion Rate Ratio - Comparison of the Depth Average for all Samples: control plot – samples 1 and 2; biopolymer/apatite/organoclay plot – samples 3, 4, and 5; apatite/sand plot – 6, 7, and 8; A – average.	249
Figure 122. Erosion Rate Ratio - Comparison of Material Types: native material (control plot – samples 1 and 2), biopolymer/apatite/organoclay material (samples 3, 4, and 5) and apatite/sand material (samples – 6, 7, and 8).	250
Figure 123. Percent Recovery (average and standard deviation, n=4) Based on Aggregate Weight of California Blackworms Held for 28 Days in Screened Cages Buried within Experimental Active Caps composed of Different Materials (A/S/3 = apatite and sand, Plot 3; OC/S/8 = organoclay and sand, Plot 8; B/A/S/8 = biopolymer, apatite, and sand, Plot 8; B/A/S/4 = biopolymer, apatite, and sand, Plot 4; C/5 = natural substrate, Control Plot 5).....	252
Figure 124. Survival of <i>Corbicula fluminea</i> Held in Cages within Experimental Active Caps in Steel Creek (A = apatite, OC = organoclay, S = sand, B = biopolymer, C = control [native sediment], numbers refer to plot designations).	255
Figure 125. Survival of <i>Hyalella azteca</i> Held in Cages within Experimental Active Caps in Steel Creek (A = apatite, OC = organoclay, S = sand, B = biopolymer, C = control [native sediment], numbers refer to plot designations).	256

LIST OF TABLES

Table 1. Biopolymer Products Used for Sand Coating and Contaminant Sorption; C- chitosan; G-guar gum, B-borax, X-xanthan; c- calcium chloride; 1 – without glutaraldehyde, 2 – with glutaraldehyde, 3 - without glutaraldehyde but with NaOH.	20
Table 2. Preparation Method for Biopolymer Coated Sand Materials. Materials selected for erosion tests in an Adjustable Shear Stress Erosion and Transport (ASSET) flume are marked by an asterisk; C-chitosan; G-guar gum, B-borax, X-xanthan; c- calcium chloride; 1 – without glutaraldehyde, 2 – with glutaraldehyde, 3 - without glutaraldehyde but with NaOH.	20
Table 3. Sequential Extraction Procedure for Geochemical Fractionation of Untreated and Amended Sediments.....	25
Table 4. Predicted Breakthrough ($C/C_o = 0.5$) of Selected Metals for the Apatite Column.....	31
Table 5. Estimated Shear Stresses for the Shaker Test.....	40
Table 6. Material Properties Used in Transport Modeling.	49
Table 7. Diffusion Coefficients Used in Transport Modeling.	49
Table 8. Partitioning Coefficients Used in Transport Modeling.....	49
Table 9. Material Composition of Experimental Caps in Steel Creek; plot numbers correspond with numbers on the field deployment scheme (Figure 6).....	57
Table 10. Average K_d Values (standard deviation) for Nine Elements for each Tested Amendment (in mL g^{-1}).	74
Table 11. Metal Sorption (%) by the Tested Amendments in Fresh Water ^a	77
Table 12. Evaluation of Amendment Effectiveness for the Removal of Metals from Fresh Water Based on Sorption Data ^a	79
Table 13. Average Metal Retention by Amendments (%) in Fresh Water ^a	83
Table 14. Evaluation of Amendment Effectiveness in Fresh Water Based on Retention Data....	85
Table 15. Average Metal Retention by Amendments (in %) in Salt Water.	86
Table 16. Evaluation of Amendment Effectiveness in Salt Water Based on Retention Data ^a	87
Table 17. Partitioning Coefficients (ml g^{-1}) for Sorption of Organic Compounds on Various Amendments	90
Table 18. Development of Cross-linked Biopolymer Products – Procedures and Characteristics	91
Table 19. Average Sorption Coefficients of Sand and Sand Coated by Biopolymers (standard deviation in parentheses); B - borax, C - chitosan, G - guar gum, X - xanthan, c - calcium chloride; 1 – without glutaraldehyde, 2 – with glutaraldehyde, 3 - without glutaraldehyde but with NaOH.	96
Table 20. Sorption Capacities of Two Commercial Organoclays for LNAPLs and DNAPLs from Different Weathered Creosote Mixtures.	97
Table 21. Sorption and Desorption Coefficients for Selected Amendments (L kg^{-1}).....	104
Table 22. Estimation of Cap Penetration Time (in years) for 15 and 2.5 cm Active Layers Subject to a 100 cm yr^{-1} Groundwater Upwelling Velocity.....	104
Table 23. Breakthrough Times under Upwelling (1 cm yr^{-1}) and Diffusion ($0.124 \text{ cm}^2 \text{ day}^{-1}$) Conditions for a Thin Cap Layer.	108
Table 24. Comparison of Element Concentrations in Water Extracts from Anacostia River Sediment under Reduced and Oxidized Conditions.....	112
Table 25. Effect of Amendments on Ca, Fe, Mn, and P Concentrations in Water Extracts from Reduced and Oxidized Treatments of Anacostia River Sediment.	113

Table 26. Carbon Fractions of Biopolymer Materials.	132
Table 27. Bulk Density of Sequestering Agents (g mL^{-1}).	133
Table 28. Bulk Density of Coated Sand (g mL^{-1}).	133
Table 29. Porosity of Sorbents.	134
Table 30. Porosity of Biopolymer Materials.	134
Table 31. Model Inputs and Parameters for Diffusion Advection Transient Models for Biopolymer Coated Sand.	153
Table 32. Diffusion Advection Transient Model and Parameters for Modeling Breakthrough Time Curve for Organoclay as an Active Cap Component.	154
Table 33. Model Results.	159
Table 34. Metal Concentrations ($\mu\text{g L}^{-1}$) in Water Extracts from Amendments. These metal concentrations are compared with ecological screening values (ESVs ¹).	163
Table 35. Evaluation of Amendments for Toxicity Characteristic Leaching Procedure (TCLP) (data in ppb).	164
Table 36. Sediment Toxicity Test Results for Amendments and Mixtures of Amendments and Sediment.	168
Table 37. Summary of Erosion Properties for 2, 10 and 175 Days of Consolidation.	184
Table 38. Effects of Transport Processes on Sediment Capping Effectiveness.	188
Table 39. Metal Concentrations in Sediments from the Proposed Steel Creek Study Area and in Tinker Creek, a Nearby Uncontaminated Stream.	200
Table 40. Properties of Surface and Pore Water Collected from each Plot in Steel Creek before Cap Deployment.	202
Table 41. Average Element Concentrations in Surface Water (n=9) from the Steel Creek Experimental Area.	203
Table 42. Properties of Surface Water Collected Before and One, Two, Five, Nine, and Twelve Months after Cap Placement; EC - electrical conductivity, DO – dissolved oxygen, pH, and ORP - oxidation/reduction potential.	212
Table 43. Effect of Cap Amendments on the pH Values of Pore Water -12 Month Evaluation; A/S – apatite/sand, B/A/S – biopolymer/apatite/sand; B/A/O/S – biopolymer/apatite/organoclay/sand; C- cap, B – beneath cap, O – outside cap, PW – pore water, A1M – after one month, A2M – after 2 months, A5M – after 5 months, A9M – after 9 months, and A12M – after 12 months.	216
Table 44. Effect of Cap Amendments on the EC Values of Pore Water – 12 Month Evaluation; A/S – apatite/sand, B/A/S – biopolymer/apatite/sand; B/A/O/S – biopolymer/apatite/organoclay/sand; C- cap, B – beneath cap, O – outside cap, PW – pore water, A1M – after one month, A2M – after 2 months, A5M – after 5 months, A9M – after 9 months, and A12M – after 12 months.	216
Table 45. Effect of Cap Amendments on the ORP Values of Pore Water – 12 Month Evaluation; A/S – apatite/sand, B/A/S – biopolymer/apatite/sand; B/A/O/S – biopolymer/apatite/organoclay/sand; C- cap, B – beneath cap, O – outside cap, PW – pore water, A1M – after one month, A2M – after 2 months, A5M – after 5 months, A9M – after 9 months, and A12M – after 12 months.	217
Table 46. Effect of Cap Amendments on Element Concentration (mg kg^{-1}) in Pore Water – 12 Month Evaluation; A – apatite/sand, BA – biopolymer/apatite/sand; BAO – biopolymer/apatite/organoclay/sand; C- cap, B – beneath cap, O – outside cap; Before –	

element concentration in pore water before cap placement; AVG – averages; STDEV – standard deviations.	222
Table 47. Average P Concentration (ppm) in Pore Water Collected within, beneath, and outside of each Cap. The P concentrations are presented for four sampling events: one, two, five, and 12 months after cap placement; A – apatite/sand, BA – biopolymer/apatite/sand; BAO – biopolymer/apatite/organoclay/sand; C- cap, B – beneath cap, O – outside cap; Before – element concentration in pore water before cap placement; Avg – averages; Stdev – standard deviations.	224
Table 48. Statistical Comparison of Regression Slopes Describing Temporal Changes in the SEM/AVS Ratio in Sediment Located in the Control Plot and beneath the Apatite Cap during the One Year Test Period.	232
Table 49. Analysis of Variance of Metal Concentrations Measured by DGT in Sediment from Apatite Caps and Control Plots. Data were collected from the field (i.e., with DGT probes deployed in-situ) and from sediment samples maintained in the laboratory.	240
Table 50. Analysis of Variance of Metal Concentrations Measured by DGT and by Collection of Pore Water Samples Using Sippers. Data were collected from sediments located beneath apatite caps and from control plots with untreated sediment.	240
Table 51. Twelve month Evaluation of Cap Thickness; A/S- apatite/sand cap, B/A – biopolymer/apatite sand cap, and B/A/O – biopolymer/apatite/organoclay sand cap.	244

LIST OF PICTURES

Picture 1. Setting of the Experiment on Advective Transport of Metals through Cap Materials.	30
Picture 2. Shaker for Simulating Erosion.	41
Picture 3. In-situ Measurement of Pore Water Properties.	53
Picture 4. Measurement of Water Flow with Portable Water Flow Meter (Marsh-McBirney, Inc., Model 201).	53
Picture 5. Amendments were Mixed in a Multi-Use Portable Mixer (Kobalt™).....	59
Picture 6. Mixed Amendments were Transported in All-Terrain Vehicle.....	59
Picture 7. All Terrain Vehicle in Use.....	60
Picture 8. Cap Frame during Deployment.	60
Picture 9. Cap Frame was Removed in Sections after Cap Construction was Completed.	61
Picture 10. Coring Tubes and Sediment Cores used for Evaluation of Erosion Resistance by an ASSET Flume.	67
Picture 11. Installation of Cages with California Blackworms on November 13, 2008 and Collection of Cages after 28 days in the Field (December 9, 2008).	68
Picture 12. Installation of Cages with Clams on March 5, 2009.	69
Picture 13. Collection of Clam Cages after 4 weeks in the Field (April 3, 2009).	70
Picture 14. Installation of Cages with <i>Hyalella azteca</i>	70
Picture 15. Adhesive Product of Sand Coated with Guar Gum Cross-linked by Borax.....	94
Picture 16. Diffusion Experiment at Start (9/28/07) and after Six Months (2/14/2008).	141
Picture 17. Plot 3 -- One-layer Cap Composed of Apatite (50%) and Sand (50%) with a Sand Transition Zone. Two sets of pore water sampler tubes were located near the top of the cap (white tubes for samplers beneath the cap and black tubes for samplers in the middle of the cap).	208
Picture 18. Plot 4 Cap Composed of Two Layers including a Two Inch Layer of Biopolymer/Sand Slurry over a Four Inch Layer of 50% Apatite and 50% Sand.	208
Picture 19. Plot 8 -- Three-layer Cap Composed of Biopolymer/Sand Slurry, a Two Inch Middle Layer of 50% Apatite and 50% Sand, and a Two Inch Bottom Layer of 25% Organoclay and 75% Sand.	209
Picture 20. The Average Cap Thickness was about 6 Inches.	209
Picture 21. Sediment DGT Probe.....	240
Picture 22. One Layer Cap Composed of Apatite (50%) and Sand (50%) in Creek Channel with High Flow One Month after Deployment. Erosion of the plot was visible within the first week (Picture A). After one month the cap material was transported up to 20 feet (Picture B) and about one or two inches of native sediment was deposited on the top of cap.	245
Picture 23. Sediment Cores from Caps in Depositional Areas (Flow Rate Lower than 0.4fps) after Two Months: A) plot #3 -- Apatite/Sand cap; B) plot #4 -- Biopolymer/Apatite/Sand cap; C) plot #8 -- Biopolymer/Apatite/Organoclay/Sand. Two months after cap placement, the cap thickness in all plots in depositional areas was about 6 inches.	246
Picture 24. Sediment Cores Collected from Depositional Areas after Six Months - biopolymer/apatite/organoclay/sand cap (A), apatite/sand cap (B), and biopolymer/apatite/sand cap (C).	246
Picture 25. California Blackworms after One Month of Exposure to Amendments in Field; B/A/S -- biopolymer/apatite/sand; A/S -- apatite/sand; O/S -- organoclay/sand.	253

ABSTRACT

Objectives

Active or reactive capping, is the application of a relatively thin layer of reactive material to the sediment to physically and chemically reduce contaminant mobility and/or bioavailability. This project addressed high priority research needs related to developing/selecting active capping materials and cap designs for contaminant sequestration under a range of aquatic sediment conditions and assessing the ability of innovative amendments to immobilize a variety of organic and inorganic contamination and resist erosion in situ.

Technical Approach

The active capping technology under study consisted of the in situ application of phosphate materials, organoclays, and biopolymer products. The amendments were selected based on the proven ability of phosphate-based materials to stabilize metals, of organoclays to bind nonpolar pollutants such as PCBs and PAHs, and of biopolymers and their cross-link networks to act as plugging agents that bind contaminants. We theorized that phosphate amendments, organoclays, and the cross-link biopolymer products would complement each other to stabilize a wider range of organic and inorganic compounds than they could individually. This project included laboratory studies that researched fundamental aspects of active cap design followed by a pilot-scale field study that evaluated newly developed active caps under realistic conditions. Numerical simulations were used to determine how active caps composed of promising amendments and amendment mixtures affected the diffusive and advective transport of contaminants from the sediment surface into the water column. Procedures were developed for making biopolymer materials that contributed to erosion resistance.

Results

This project identified beneficial active cap materials, active cap compositions, and the effects of active cap components on metal bioavailability, retention, toxicity, and erosion under laboratory and field conditions. Apatite, organoclay, and cross-linked biopolymers showed high potential for the design of an environmentally benign, multiple-amendment active cap that is effective for the remediation of organic and inorganic contaminants in fresh and salt water. In situ bioassays employing multiple organisms showed the advantages of providing realistic conditions of exposure and provided one of the first quantitative measures of the toxicity of active cap amendments. The results showed that apatite and organoclay at concentrations useful for remediation are acceptable to benthic organisms. Numerical modeling was used to evaluate the long term performance of active cap amendments. The results showed that reactive amendments were effective in delaying the release of contaminants compared to passive cap materials. The field deployment provided a realistic evaluation of the ability of the innovative capping technologies to control the movement, bioavailability, and environmental toxicity of contaminants commonly found at Department of Defense installations and other sites. Lastly, this project tested a new method, diffusion gradients in thin-films (DGT), for evaluating active caps in the field. Because of its ability to mimic the uptake of contaminants by biota (i.e., bioavailability), DGT may be able to more accurately assess the performance of active caps than other analytical techniques.

Benefits

Active capping has the potential for in situ remediation of a variety of contaminants in a range of sediments (fresh and salt water), especially in the areas where dredging or passive capping may not be effective or practical. This project improved the understanding of active cap design and deployment, sequestration mechanisms occurring within active caps and underlying sediments, and the environmental impact of active caps. It also resulted in the development of a flexible multi-amendment active cap design that can be used to remediate a variety of contaminants and contaminant mixtures under a range of environmental conditions.

EXECUTIVE SUMMARY

One of the conventional remedies for contaminated sediments is passive capping, which is the installation of a subaqueous covering or cap of clean, inert material over contaminated sediment. Passive caps physically isolate the sediment from the surrounding environment and reduce contaminant migration into the overlying water. Conventional remedies have been proven effective for contaminants in marine and freshwater environments; however, these technologies cannot be successfully applied at all sites. Particularly problematic situations are those where dredging or passive capping are impractical due to physical constraints such as depth or presence of overlying structures (e.g., docks, proximity to breakwaters). Active or reactive capping, which is targeted by the current study, is the application of a relatively thin layer of reactive material to the sediment to physically and chemically reduce contaminant mobility and/or bioavailability. This comprehensive project investigated the use of sequestering agents to develop active sediment caps that stabilize mixtures of contaminants and act as a barrier to mechanical disturbance under a broad range of environmental conditions. Efforts focused on the selection of effective sequestering agents for use in active caps, the composition of active caps, and the effects of active cap components on contaminant bioavailability, retention, toxicity, and erosion resistance.

Results from this project showed that phosphate amendments, some organoclays, and the biopolymer, chitosan, were very effective at removing metals from both fresh and salt water. The amendments also exhibited high retention (80% or more) of most metals indicating low potential for remobilization of contaminants to the water column. Experiments on metal speciation and retention in contaminated sediment showed that apatite and organoclay can immobilize a broad range of metals under both reduced and oxidized conditions. These studies were followed by sequential extractions to evaluate the bioavailability and retention of metals in treated sediments. Metal fractions recovered in early extraction steps, which are more likely to be bioavailable, were termed the Potentially Mobile Fraction (PMF). Less bioavailable fractions collected in later extraction steps were termed the Recalcitrant Factor (RF). Apatite and organoclay reduced the PMF and increased the RF for several elements, especially Pb, Zn, Ni, Cr, and Cd.

One goal of this project was to develop modeling approaches for the design and evaluation of sediment caps that incorporated all the complexities of sediment cap systems. Sorption onto cap materials, desorption resistance from sediments, sorption onto dissolved organic matter, pore water advection, sediment deposition/erosion, molecular diffusion, pore water dispersion, and contaminant decay are the processes that control the fate and transport of contaminants in sediment caps. Modeling showed that amendments can significantly delay the breakthrough of contaminants compared with sand. This illustrates the promise of amendments such as apatite or organoclay for use in active cap systems. Numerical models were also used to estimate the cap thickness needed to delay contaminant breakthrough for a specified time period for various flow rates, thereby showing that models are cost effective tools for designing active cap systems.

Biopolymer products were considered for inclusion in active caps because of their potential to produce a barrier that resists mechanical disturbance and sorbs contaminants. They were evaluated on the basis of mechanical properties (e.g., plugging), resistance to biodegradation,

sorption capacity for organic and inorganic contaminants, and resistance to erosion. More than 20 biopolymer products were evaluated resulting in the selection of a few products such as chitosan/guar gum cross-linked with borax, xanthan/chitosan cross-linked with calcium chloride, and guar gum cross-linked with xanthan for future evaluation. A process was developed for coating sand with cross-linked biopolymers to provide a means for biopolymer delivery to the sediment surface. Biopolymer materials showed potential for immobilization of metals and some organic contaminants. Most of the tested products demonstrated good erosion resistance capabilities in the laboratory. Slurry mixtures consisting of xanthan and guar gum with entrained amendments and sand showed the greatest resistance to erosion.

Although the ability of active cap materials to remediate contaminants was emphasized in this study, it was also important to ensure that these materials were environmentally benign. Therefore, promising amendments were evaluated for toxicity using 10 day sediment toxicity tests, the standardized Toxicity Characteristic Leaching Procedure (TCLP), and measurement of metal concentrations in aqueous extracts from the amendments. Metal concentrations in the TCLP extracts were below TCLP limits, and metal concentrations in the aqueous extracts were below EPA ambient water quality criteria, and other ecological screening values. These results showed that apatite, organoclay, and biopolymer coated sand do not leach toxic metals. The sediment toxicity tests indicated that apatite and organoclay are nontoxic at concentrations (up to 50% and 25% by weight, respectively) needed for the construction of active caps that are useful for the remediation of metals and organic contaminants in sediments.

Steel Creek at the Savannah River Site (SRS), Aiken, SC was chosen for a field deployment of the capping technologies developed in the laboratory. Steel Creek is a third order stream averaging about 6-8 m wide and 30-40 cm deep during typical low flow conditions. The bottom substrate is composed primarily of sand in high energy areas and silt in depositional environments. Contaminant concentrations for several metals substantially exceeded those in Tinker Creek, a nearby uncontaminated stream. The field deployment in Steel Creek included eight plots with four treatments: two control treatments consisting of uncapped sediments (i.e., no amendments added); two caps composed of a single six inch layer of 50% apatite and 50% sand; two caps composed of two layers including a two inch layer of biopolymer/sand slurry over a four inch layer of 50% apatite and 50% sand; and two caps composed of three layers including a two inch top layer of biopolymer/sand slurry, a two inch middle layer of 50% apatite and 50% sand, and a two inch bottom layer of 25% organoclay and 75% sand.

An aluminum frame was used to deflect downstream flow, stabilize the working area, reduce turbulence, and avoid loss of amendment materials during the construction of each cap. The leading edge of each cap was preceded by a sloped transition zone rising from the sediment to the top of the cap to prevent the undercutting likely to occur with a vertical leading edge. The transition zone was composed of sand (in apatite/sand plots) or biopolymer/sand slurry in plots with a top layer composed of biopolymer/sand slurry (xanthan crossed linked with guar gum). Upper cap layers that contained low density materials like biopolymers were applied as slurry to prevent material separation and differential settling. After cap placement, sediment cores were collected to confirm and characterize cap thickness. The average cap thickness was about 6 inches. The thickness of individual layers in the caps composed of three layers was about 2 inches.

The test plots were evaluated for contaminant immobilization, environmental impact, and erosion for twelve months. Sediment samples from the test area were collected three times: before cap placement and six and twelve months after cap placement. Surface water and pore water samples from the test area were collected six times: before cap placement and one, two, five, nine, and twelve months after cap placement. The surface and pore water samples were characterized for metals and other parameters including pH, total organic carbon, total inorganic carbon, and redox potential.

Sediment samples collected beneath the caps were characterized and assessed for the effects of cap amendments on sediment chemistry. Acid volatile sulfide (AVS), simultaneously extracted metals (SEM), and SEM/AVS were measured to assess the applicability of the SEM/AVS method for evaluating sediment remediation by active caps. The SEM concentrations in sediment from plots with apatite or biopolymer and apatite caps were lower after cap placement. The active caps lowered SEM/AVS in the sediment beneath the caps resulting in substantially lower metal bioavailability during the one year test period.

The zone of influence (ZOI) of the amendments in the active caps was evaluated by collecting sediment cores from the test plots six and twelve months after cap placement. Sediment samples from beneath the caps were extracted with a double acid method to assess the available pool of metals in the sediment below the cap and to evaluate the ZOI of sequestering materials that were used in the caps. The concentrations of metals [e.g., cadmium (Cd), cobalt (Co), copper (Cu), and zinc (Zn)] in extracts from the sediments beneath the apatite and apatite/biopolymer caps declined in both the upper (0 – 2.5 cm) and lower (2.5 – 5.0 cm) sediment layers. In the sediment beneath the biopolymer/apatite/organoclay cap, where organoclay was placed at the bottom, the extracted metal concentrations were reduced only in the upper sediment layer (0 – 2.5 cm). Extracted metal concentrations in the lower layer (2.5 – 5.0 cm) were similar to those in the control plot. These data showed that the active cap amendments can immobilize contaminants located deeper in the sediment profile (i.e., in the ZOI).

The effect of the active apatite cap on metal bioavailability was also evaluated by diffusion gradients in thin-films (DGT). DGT techniques can be used to accumulate dissolved contaminants in a controlled fashion while quantifying the mean contaminant concentration in pore water at the surface of the device. This measurement reflects the concentration in the pore water and the release of contaminants from the solid phase. Because of their ability to mimic the uptake of contaminants by biota (i.e., bioavailability), DGT may be able to more accurately assess the performance of active caps than other analytical techniques. DGT sediment probes were used to evaluate metal bioavailability in the apatite active caps and control sediments (untreated). The DGT results were compared with metal concentrations in pore water samples and assessed for their ability to accurately evaluate the remedial effectiveness of active caps. Active caps composed of apatite significantly ($P < 0.05$) lowered the concentration of some metals as indicated by DGT and pore water samples. Results from DGT sediment probes used in the field and laboratory were in good agreement. However, metal concentrations in pore water from the field were slightly higher than concentrations measured by DGT, except for Pb and Zn. More research is needed to assess the usefulness of DGT sediment probes for evaluating the bioavailable pool of metals in remediated sediments.

Erosion was evaluated based on visual observations, sediment core characterization for integrity of the cap layers, and measurement of erosion rates and critical shear stresses by an Adjustable Shear Stress Erosion Transport (ASSET) flume. Seven months after cap deployment, sediment cores were collected from the apatite cap plot, the biopolymer/apatite/organoclay cap plot, and the untreated plot. All cores were analyzed by the ASSET flume. The results indicated that the cap most resistant to erosion was the cap with apatite, which became increasingly harder to erode with depth. However, differences among the average erosion rates of the cores and material types were relatively small. For example, the differences for all eight cores and material types were less than twice the overall mean. These results, using samples collected from the field, were consistent with the laboratory evaluation of biopolymers. Both laboratory and field studies showed that guar gum cross-linked with xanthan (Kelzan) became less resistant to erosion after two months. The application of xanthan/guar gum in the field as the top layer of active caps is beneficial for a short time for erosion resistance. This mixture also reduced sediment suspension during cap construction and caused the rapid settling of other amendments that were placed below the biopolymer layer. Biopolymers can also increase the pool of carbon in the sediment beneath caps and lower the release of metals and other elements, especially phosphorous (P), in comparison with apatite only. However, more research is needed on the type of biopolymers applied to caps and methods for delivering biopolymers to the cap. Further research is especially needed on the biodegradability of biopolymers under extreme aquatic conditions (e.g., high summer temperature, changing ratios of iron (Fe)-sulfur (S)-P in sediment pore water and surface water, and other factors). Finally, the applicability of biopolymer products in active capping technology is also dependent on the effects of these products on benthic organisms. Although biopolymers are nontoxic, the viscous matrix produced by biopolymers may have the potential to physically entrap or suffocate burrowing organisms.

Active biomonitoring (i.e., in situ bioassay) was conducted in the experimental plots using three types of benthic organisms including *Hyalella azteca*, *Lumbriculus variegates*, and *Corbicula fluminea*. The organisms were placed in small screened cages that contained cap materials, and the cages were placed in the caps. The cages were retrieved after one month or ten days, and the organisms were removed from the cages to assess their survival. Active biomonitoring showed that all test organisms survived well in all experimental caps except those containing biopolymer (guar gum cross-linked with xanthan).

This project identified and evaluated beneficial active cap materials, active cap compositions, and the effects of active cap components on metal bioavailability, retention, toxicity, and erosion under laboratory and field conditions. Apatite, organoclay, and cross-linked biopolymers have high potential for the design of an environmentally benign, multiple-amendment active cap that is effective for the remediation of organic and inorganic contaminants in fresh and salt water. This project also tested a new method for evaluating active caps in the field. DGT techniques, because of their ability to mimic the uptake of contaminants by biota (i.e., bioavailability), may be able to more accurately assess the performance of active caps than other analytical techniques. Active biomonitoring applied in this study showed the advantage of providing realistic conditions of exposure while maintaining control over important variables such as species and life stage, sample size, and exposure period. Numerical modeling was used as a tool to evaluate the long term performance of the active cap amendments. Results from the modeling effort

showed that reactive amendments were effective in delaying the release of contaminants compared to sand. Lastly, the field deployment of selected cap materials provided a realistic evaluation of the ability of the innovative capping technologies to control the movement, bioavailability, and environmental toxicity of contaminants commonly found at Department of Defense installations and other sites. Taken together, the results of this project provide a firm basis for transitioning the proposed technology from the laboratory to full field deployment. The results of this project indicate that multiple amendment active caps (MAACs) composed of mixtures of apatite, organoclay, and inert materials have the potential to create durable active caps that can economically treat a variety of sediment contaminants under a variety of conditions. MAACs are described more fully in final report Part II of this project.

OBJECTIVES

Project ER-1501 addressed two identified high priority research needs related to:

- Developing/selecting active capping materials and different cap designs for contaminant sequestration
- Development, application and in situ assessment of innovative amendments for stabilization of a large variety of organic and inorganic contamination under a range of aquatic sediment conditions

The primary objective of this project was to identify and evaluate promising sequestering materials for active caps that stabilize sediment contaminants and resist physical disturbance. Active or reactive capping, which is targeted by this study, involves the use of capping materials that react with sediment contaminants to reduce their toxicity or bioavailability.

Specific objectives of this research were to:

- Evaluate the ability of innovative chemical and biological sequestering materials (in different combinations) to stabilize a broad range of contaminants in different types of sediments (e.g. marine versus fresh water, oxic versus anoxic) under controlled laboratory conditions
- Determine the best amendments for construction of active sediment caps
- Evaluate the resistance of different active caps to physical disturbance
- Develop conceptual and mathematical models for contaminant attenuation in active caps
- Evaluate the effects of the proposed active caps on contaminant mobility, retention, toxicity, and bioavailability under field conditions

To obtain the data necessary to meet the specific objectives listed above, a combination of laboratory and field studies were designed and implemented to examine the proposed capping materials in the following five tasks:

Task 1: Laboratory study – effect of amendments on contaminant mobility and bioavailability

Task 2: Studies for determination of the best combination of amendments for placement and construction of active sediment caps

Task 3: Evaluation of the resistance of caps to physical disturbance

Task 4: Generation of conceptual and mathematical models for contaminants attenuation

Task 5: Field deployment.

The first task consisted of two subtasks. In the first subtask, sorption and desorption laboratory experiments were conducted to evaluate the ability of several amendments to sequester organic and inorganic contaminants. Additionally, cross-linked biopolymer and biopolymer coated sand and sand/amendments were developed and evaluated for sorption of contaminants. The second subtask concerned the effects of the amendments on contaminant mobility and bioavailability. The bioavailability and retention of contaminants in treated sediments under oxic and reduced conditions were evaluated by sequential extraction techniques in the laboratory. The second task consisted of column studies that identified the best amendments for various contaminants and application methods that produce the best cap. The following experiments were conducted in this task: diffusive transport, advective transport, mechanical tests, contaminant mobility and retention, evaluation of attenuation, and evaluation of potential toxicity of active cap materials.

The third task consisted of studies that evaluated the resistance of the caps to physical disturbance.

The fourth task consisted of analysis and integration of laboratory results with the objective of developing conceptual and mathematical models for effective deployment of the capping amendments under field conditions.

The fifth task consisted of a small-scale field deployment and evaluation of the capping technology at a contaminated site at the Savannah River Site, Aiken, SC. The field deployment of selected cap materials provided a realistic evaluation of the ability of capping technologies to control the movement, bioavailability, and environmental toxicity of contaminants commonly found at Department of Defense (DoD) sites and other sites.

BACKGROUND

Current remediation/risk management options for contaminated sediments include no action, monitored natural recovery, institutional controls (land use restrictions, etc.), in situ treatment and management, and ex situ treatment and management. In-situ management of contaminated sediments is potentially less expensive than ex-situ management, but there are relatively few alternatives for in-situ treatment, and some are still under development. Capping is the most commonly used alternative for in situ remediation of sediments.

Passive (inactive) capping is defined as the installation of a subaqueous covering or cap of clean, neutral material over contaminated sediment, thus isolating it from the surrounding environment and reducing contaminant migration in the water phase. Passive capping commonly employs clean dredged material that contains silt, clay, and organic carbon. This alternative can be an effective approach for the remediation of contaminated sediment and is relatively economical. However, passive caps can release toxic contaminants and are not suitable, due to their thickness, in shallow areas, under existing marine structures (e.g., docks, piers), and in sensitive habitats such as marshes.

In contrast to passive capping, active or reactive capping, which is targeted by the current study, involves the use of capping materials that react with sediment contaminants to reduce their toxicity or bioavailability. Active capping is a less mature technology that holds great potential for a more permanent solution that avoids residual risks resulting from contaminant migration through the cap or breaching of the cap and can be applied in areas where a more traditional thick passive cap cannot be employed. Active caps, although directly reducing the bioavailability and toxicity of sediment contaminants (rather than simply making them less accessible), often require additional protection, such as a layer of armoring material to protect them from physical disturbance in dynamic aquatic environments.

Apart from types of amendments potentially useful in active capping, little is known regarding amendment application techniques, application rates, and amendment combinations that will maximize immobilization of contaminants. The current research was designed to extend the range of potential active cap technologies to address a variety of contaminants more effectively. This project studied the use of a combination of sequestering and binding agents to develop a sediment capping system that combines many of the advantages of active and passive methods by simultaneously creating a resistant barrier that protects sediments from physical disturbance while reducing the toxicity of contaminants migrating through the cap and within the underlying sediments. The tested amendments immobilized a broad range of contaminants through the in-situ application of phosphate materials in solid (rock phosphate), organoclays, and biopolymer cross-link (gel forming) products, individually and in different combinations. These treatments were based on the abilities of phosphate-based materials to stabilize metals, the ability of organoclays to stabilize nonpolar pollutants (e.g., polychlorinated biphenyls (PCBs)), and the ability of biopolymers and of their cross-linked networks to act as plugging agents that bind and stabilize metals, radionuclides, and organic contaminants (e.g., polycyclic aromatic hydrocarbons (PAHs)) in porous media, while being stable to biodegradation. The selection of the best treatment as well as the study of its mechanism of action and effect on the sediment environment were investigated by chemical and biological tests that addressed: 1) contaminant mobility and

availability/bioavailability before and after remediation, 2) contaminant retention on capping materials and treated sediments, 3) resistance of the cap to physical disturbance, and 4) overall reduction of ecological risks resulting from the proposed active capping materials.

TECHNICAL APPROACH

This research integrated development and design of an active capping system for sediment remediation, its placement for optimal environmental protection, and evaluation of the ecological effects of the capping system. Success was measured using various short-term and long-term geochemical and biological approaches.

This study evaluated low-cost, commercially available sequestering agents such as phosphate, organoclays, AquablokTM, zeolites, and biopolymers. Phosphate sources included rock phosphate from Tennessee and North Carolina, biological apatite (ground fish bones), and calcium phytate (Appendix 1, Table 1). Apatite is a common surface and subsurface amendment (Knox et al., 2004) that effectively immobilizes Pb and other constituents (e.g., Cd, Ni, Zn, and U) in contaminated soils/sediments (Ma et al., 1995, 1997; Chlopecka and Adriano, 1996; Knox, et al., 2000 a, b; Singh et al., 2001; Knox et al., 2003 and 2004), thus offering an economical, simple, and environmentally friendly alternative to treat contaminated environments. Properly selected phosphate-containing amendments mixed in contaminated sediment or soils can effectively reduce metal mobility, bioavailability, and toxicity. Rock phosphates and biological apatite have been used at several contaminated remediation sites (Knox, et al., 2004; Knox et al., 2006 b).

Calcium phytate removes contaminants in the same manner as apatite minerals. Recent studies have suggested that phytate (IP6) can be applied in a soluble form for delivery to remote contaminated sediments, where it undergoes various reactions that eventually result in the precipitation of the contaminant metals (Jensen et al., 1996; Nash et al., 1997, 1998 a, b). Metal interactions with the numerous phosphate ligands present on IP6 can lead to both intra- and intermolecular bonding resulting in the simultaneous formation of numerous monomeric and polymeric species, which can lead to the coprecipitation of nonstoichiometric solid-phase mixtures as the metal to ligand ratio increases (Wise, 1986). Naturally occurring metal ions like Ca^{2+} have been demonstrated to have a positive influence on the effectiveness of the process in both the ion exchange and mineralization stages (Nash et al., 1997). Contaminant metals may be coprecipitated or exchanged with Ca in Ca-IP6 at concentrations that are insufficient to promote precipitation by themselves (Wise, 1986). Additionally, metals such as Pb may be strongly sorbed to precipitated Ca-IP6 without resulting in the stoichiometric release of Ca^{2+} (Wise, 1986). Although coprecipitation or metal exchange with Ca-IP6 may initially reduce contaminant metal solubility, Nash and coworkers (Jensen et al., 1996; Nash et al., 1997, 1998a, b) suggest Ca-IP6 hydrolysis and mineralization release inorganic PO_4 , which can result in further contaminant immobilization through the formation of insoluble secondary contaminant-phosphate precipitates in a manner similar to the addition of apatite or hydroxyapatite (HA) to metal contaminated sediment/soil.

Three organoclays from Biomin, Inc. (Clayfloc TM 200, 202, and 750) were tested in this study. Appendix 1, Table 1 lists some properties of these materials. Organoclays consist of bentonite that is modified with quaternary amines. Bentonite is a volcanic rock whose main constituent is the clay mineral montmorillonite, which imparts an ion exchange capacity of 70-90 milliequivalents (meq)/gram. The bentonite becomes organically modified by exchanging the nitrogen end of a quaternary amine onto the surface of the clay platelets through cation exchange (Lagaly 1984). Organoclays are particularly effective at sequestering non-polar pollutants such

as oil, polychlorinated biphenols, chlorinated solvents, and polycyclic aromatic hydrocarbons (Xu et al., 1997; Alther 2002). The organoclay appears to be a stable complex; i.e., the surfactants are not easily desorbed (Zhang et al. 1993). Organoclays can be used in a number of settings; for example, as liners in landfills to diminish the transport of pollutants into water supplies (Xu et al., 1997) and in wastewater treatment (Soundarajan et al., 1990).

Zeolites are crystalline aluminosilicate minerals consisting of three-dimensional networks of linked SiO_4 and AlO_4 tetrahedra. Zeolites are porous, with channels as large as 0.8-1.0 nm in diameter that lead into large framework cavities or cages, allowing for selective entry of cations and molecules. The system of chemicals and cages is unique to each zeolite mineral, giving rise to a variety of materials with sorption properties that are selective for specific molecules or cations (Knox et al., 2000 a, b). The unique physical and chemical properties combined with their natural abundance in sedimentary deposits and volcanic parent materials have resulted in their widespread use in numerous agricultural and industrial processes. The use of zeolites for pollution control depends primary on their ion-exchange properties. Clinoptilolite and phillipsite, natural zeolites, were evaluated in this study.

Commercially available biopolymers such as xanthan, guar gum, alginate and chitosan were used in this study based on their performance in previous studies (Appendix1, Table 1). Biopolymers are high-molecular weight compounds with repeated sequences that may become multiple reactive sites with high opportunity for chemical interaction with other compounds. Depending on their functional groups, biopolymers can bind metals or soil particles, and can form interpenetrating cross-linking networks with other polymers. In general, the ability of biopolymers (cross-linked or not) to bind a large variety of metals (including Cu, Pb, Cd, As, Cr, Hg, Zn, Ni, Au) is supported by many studies (Eiden et al., 1980; McKay et al., 1989; Udaybhaskar et al., 1990; Deans and Dixon, 1992; Wan Ngah and Liang, 1999; Schmuhl et al., 2001; Vankar and Tiwari, 2001; Yen, 2001; Khor, 2001).

Apart from their contaminant binding ability, the use of biopolymers as plugging agents is well known. They are easily introduced in subsurface environments by injection under pressure using drilling equipment similar to that in the oil industry. Several studies (Li et al., 1993; Martin et al., 1996; Yen et al., 1996; Stewart and Fogler, 2001) reported the application of biopolymers and associated microorganisms as plugging agents to construct a range of impervious barriers. The application of biopolymers to soils or sediments may result in the formation of barriers that isolate the contaminants, with possible permanent encapsulation of some contaminants and fixation of soils or sediments thereafter. Such barriers are permeable to some extent and permit the flow of water, thus permitting the continuance of chemical and physical processes in the benthic environment.

Cross-linking agents are used to enhance the strength of polymers and to decrease their biodegradability. Cross-linking agents are chosen based on the functional groups of polymers. The interpenetrating polymer networks (IPNs) developed by cross-linking may stop or slow the migration of contaminants as a result of increased viscosity and reduced permeability of porous media.

The study consisted of five tasks. The first task consisted of two subtasks. In the first subtask, sorption and desorption laboratory experiments were conducted to evaluate the ability of the amendments to sequester organic and inorganic contaminants. The second subtask concerned the effects of the amendments on contaminant mobility and bioavailability. The bioavailability and retention of contaminants in treated sediments under oxic and reduced conditions were evaluated by sequential extraction techniques in the laboratory. The second task consisted of column studies that identified the best amendments for various contaminants and application methods that produce the best cap. The following experiments were conducted in this task: diffusive transport, advective transport, mechanical tests, contaminant mobility and retention, evaluation of attenuation, and evaluation of potential toxicity of active cap materials. The third task consisted of studies that evaluated the resistance of the caps to physical disturbance. The fourth task consisted of analysis and integration of laboratory results with the objective of developing conceptual and mathematical models for effective deployment of the capping amendments under field conditions. The fifth task consisted of small-scale field deployment and evaluation of the capping technology at contaminated site at the Savannah River Site, Aiken, SC. The field deployment of selected cap materials provided a realistic evaluation of the ability of the innovative capping technologies to control the movement, bioavailability, and environmental toxicity of contaminants commonly found at DoD sites and other sites.

MATERIALS AND METHODS

TASK 1. LABORATORY STUDY – EFFECT OF AMENDMENTS ON CONTAMINANT MOBILITY AND BIOAVAILABILITY

The first task consisted of two subtasks. In the first subtask sorption and desorption laboratory experiments were conducted to evaluate the ability of the amendments to sequester organic and inorganic contaminants. The second subtask investigated the effects of the amendments on contaminant mobility/bioavailability and retention. The experiments were conducted under oxidized and reduced conditions to prove that the amendments are effective in both types of environments. The bioavailability and retention of inorganic contaminants in treated sediments were evaluated by sequential extraction techniques. Additionally under this task we investigated development of cross-linked biopolymers and biopolymer coated sand and sorption and desorption of contaminants on these novel products.

SUBTASK 1.1. SORPTION AND DESORPTION OF CONTAMINANTS BY SEQUESTERING AGENTS

Sorption and Desorption of As, Cd, Cr, Co, Cu, Pb, Ni, Se, and Zn in Fresh and Salt Water

Sorption of As, Cd, Cr, Co, Cu, Pb, Ni, Se, and Zn in fresh water was evaluated for 12 amendments. The 12 amendments included two rock phosphates (from Tennessee and North Carolina), biological apatite (ground fish bones), calcium phytate, three organoclays from Biomin, Inc. (Clayfloc™ 200, 202, and 750), two types of Aquablok™ from AquaBlok, Ltd. (one with clay coating and one with zero valent iron coating), two types of zeolite (phyllosite and clinoptilolite), chitosan (a biopolymer), and sand (as a control). The experiment was conducted in 50 mL centrifuge tubes for one week. Each treatment had three replicates: two for metal analysis by inductively coupled plasma-mass spectrometry (ICP-MS) and a third for pH measurements. The spike solution used in the experiment was obtained from Inorganic Ventures, Lakewood, NJ. The metal concentration in the spike solution was 1 mg L⁻¹ of As, Cd, Cr, Co, Cu, Pb, Ni, Se, and Zn. Suspensions composed of 0.2 g of solid (the sequestering agent) and 15 mL of spike solution were shaken for one week, phase separated by centrifugation, and then analyzed for metal content by ICP-MS and pH. There were 12 treatments with individual amendments and six with mixtures of amendments. The mixtures were tested to determine if their sorption capacity and removal effectiveness was greater than that of individual amendments.

The metal concentration data obtained in this experiment were used to calculate percent sorption and partition coefficient (K_d) values, defined as the ratio of the concentration of solute sorbed to the solid divided by its concentration in solution. The K_d (mL g⁻¹) was calculated using equation 1 (American Society for Testing and Materials, 1993):

$$K_d = V_{\text{spike}} (C_{\text{spike}} - C_{\text{final}}) / C_{\text{final}} \times M_{\text{Mineral}} \quad (1)$$

where:

C_{spike} = metal concentration in spike solution before addition of amendment (mg L^{-1})

C_{final} = metal concentration in solution after contact with the amendment (mg L^{-1})

M_{mineral} = amendment mass (g)

V_{spike} = volume of spike solution (mL)

The desorption study was run on the residue from the sorption study. The residue was washed twice with deionized water and extracted with 1 M MgCl_2 to determine the readily available pool of sorbed metals. After 1 hour, the samples were centrifuged and the supernatant decanted. The extract was analyzed for metals by ICP-MS. The desorption and sorption data were used to calculate percentage retention on each tested amendment using equation 2:

$$\% \text{ retention} = [(C_{\text{adsorbed}} - C_{\text{desorbed}})/C_{\text{spike}}] \times 100 \quad (2)$$

where:

C_{adsorbed} = concentration of metal adsorbed at the end of the adsorption experiment

C_{desorbed} = concentration of metal desorbed at the end of the desorption experiment

C_{spike} = concentration of metal in the spike solution

The sorption and desorption experiments in salt water were conducted as described for fresh water, except the spike solution was made from artificial ocean water (Instant OceanTM, salinity 3.5%, pH 7.2). The following amendments were evaluated: sand (as a control), rock phosphate from Tennessee, North Carolina apatite, calcium phytate, organoclay (OCB-750), two AquablokTM materials, zeolite (clinoptilolite), chitosan, and a mixture of North Carolina apatite and chitosan.

Sorption of Organic Contaminants by Sequestering Agents

Twelve amendments were evaluated to determine their sorption capacity for the three PAHs: phenanthrene, pyrene, and benzo[a]pyrene. The amendments included organoclays (PM-199 from CETCO, IL and ClayflocTM 200, 202 and 750 from Biomin Inc, MI), zeolites (clinoptilolite - powder; clinoptilolite TSM 140, -4 mesh; clinoptilolite TSM, 8x14 mesh; and phillipsite TSM 180), apatite/rock phosphate (apatite from North Carolina and washed phosphate ore from Tennessee), PIMS biological apatite (ground fish bones), and calcium phytate. The sorption capacity of these amendments was compared with the sorption capacity of untreated sediments from the Anacostia River, Washington.

Partitioning coefficient measurements were carried out in 50 mL centrifuge tubes (VWR, PA). A piece of aluminum foil was attached to the inside of each tube cap to minimize sorption loss. Twenty mg of each sorbent was weighed and transferred to individual tubes. Three to five replicates were prepared for each sorbent. Fifty mL of pre-made contaminated solution was then added to each tube, and the tubes were tumbled for 48 hours. After tumbling the tubes were centrifuged for 30 minutes at 3000 rpm, and 1 mL of supernatant from each tube was transferred to 2 mL vials. The concentrations of PAHs remaining in the supernatant were determined immediately by high performance liquid chromatography (HPLC). In addition, 15 mL of supernatant from each tube was transferred to a 15 mL vial containing a one cm

polydimethylsiloxane (PDMS)-coated fiber. The vials were then shaken on a shaker table for two hours. The fibers were quickly removed after the shaking and put into small inserts of the 2mL HPLC vials. One hundred μ L of acetonitrile was added to the inserts to desorb contaminants on the fiber. The acetonitrile solution was analyzed with HPLC, and the concentrations were compared with external standards. External standards were prepared by serial dilutions of pre-made stock solution with known concentrations. The standards were treated exactly the same as the samples. The detection limit was approximately 0.03 μ g/L by direct injection and 0.02 ng/L by SPME.

For highly sorptive materials such as Clayfloc 750 and CETCO-199, benzo(a)pyrene in the supernatant was lower than the detection limits for both direct injection and solid phase microextraction (SPME). In this case, the experiment was repeated as described above except that solvent extraction was utilized in the final stage to analyze contaminants in the supernatant. After centrifugation, 40 mL of liquid was transferred to 100 mL tubes and 10 mL of hexane was used to extract the contaminants. The mixture was allowed to shake on a shaker table for approximately 12 hours. The extraction rate of hexane was determined to be over 95%. Following the extraction, as much hexane as possible was taken out with a pipette and blown down with a N-evaporator (Labcono, MO) to about 0.2 mL. The exact volume of hexane was recorded. Acetonitrile was then added to bring the volume back to 2 mL and re-blown down to approximately 0.1 mL. The concentrations were then determined by HPLC. Due to the effect of dissolved organic carbon (DOC), the concentrations of PAHs were higher than measured from direct injection or SPME. To remove the effect of DOCs, the dissolved water concentrations were determined with equation 3:

$$C_w = \frac{C_{WM}}{1 + C_{DOC} K_{DOC}} \quad (3)$$

where

C_{WM} = water concentration measured via extraction (mg/L)

C_w = free or truly dissolved water concentration (mg/L)

C_{DOC} = DOC content in water

K_{DOC} = DOC water partition coefficient determined from the following correlation:

$$\log K_{DOC} = \log K_{OW} - 0.58 \quad (4)$$

This DOC was then used to correct the partitioning coefficient of benzo(a)pyrene of these materials obtained from solvent extraction. The concentrations of phenanthrene and pyrene obtained by solvent extraction were compared with those obtained by direct injection and SPME, which were similar.

Studies on organic contaminants also included column experiments designed to characterize the potential of organoclays to contain organic contaminants, with containment of dissolved organics the primary focus. There were two experiments:

- 1) measurement of the flux of dissolved contaminants released while pumping nonaqueous phase liquids (NAPL) into columns of organoclay to evaluate the capacity for simultaneous control of dissolved and separate phase contamination,

- 2) measurement of the flux of dissolved contaminants released by pumping gas through columns of organoclay to simulate the effects of gas generation and migration by microbial degradative processes.

In addition to the column studies, procedures were developed for quantitatively measuring sorption/desorption partitioning coefficients between water and solid phases in ongoing studies. The protocol for organic contaminants is shown below.

1. Prepare stock solutions in methanol for each compound (e.g., phenanthrene, pyrene and benzo(a) pyrene).
2. Prepare solutions of different concentrations in deionized water with the stock solution. The solutions are allowed to shake in a shaker table for a day before they are used.
3. Sieve contaminated sediment samples with an ASTM 10 sieve (2 mm).
4. Weigh one g of the sieved sediment in amber bottles of different volumes. The volumes of bottles will range from 125 mL to 1000 mL for different chemicals.
5. Add pre-made solutions to the bottles. Two replicates are prepared for each concentration.
6. Prepare one control without sediment to evaluate loss from sorption to the walls, evaporation and other escaping mechanisms.
7. Add sodium azide (0.01 mM) to each bottle.
8. Place the bottles on a shaker table for 4-5 days to equilibrate (2 days for organoclay).
9. After five days, take the bottles from the shaker and allow them to stand for 4 hours for the sediment to settle.
10. Take supernatant (20 mL) from each bottle and extract with 5 ml hexane to concentrate the compound.
11. Take the hexane (2 mL) and blow down the solution to 0.2 mL.
12. Add acetone to bring back the volume to 2 mL, and analyze the samples with HPLC with photoiodide array detection.
13. For samples with initial concentrations over 100 ppb, directly analyze with HPLC after centrifugation.
14. Use SPME to analyze samples with extremely low concentrations (mainly in the water-organoclay partition coefficient measurement experiment). The liquid after equilibrium will be centrifuged and transferred to a clean glass bottle. One-five cm of fiber will be added to the samples for up to 10 days to achieve equilibration with the aqueous solution. The fibers will be picked out and chemicals will be desorbed into 100 μ l hexane.
15. Conduct desorption experiments on selected samples by placing the same amount of distilled water with the contaminated sediment/organoclay to measure the desorption coefficient. Desorption experiments should last at least 5 days, and liquid samples are analyzed by SPME.
16. Measure the moisture content of all samples by weight difference after drying in an oven at 103-110°C for one day.

Development of Cross-linked Biopolymers and Biopolymer Coated Sand

Biopolymer experiments included: 1) the production and characterization of cross-linked biopolymer products, and 2) the development of sediment deliverable forms of cross-linked biopolymers by coating sand particles. The objective of the first experiment was to obtain and

characterize different biopolymer cross-link products. Cross-linking agents were selected for study based on the functional groups of the polymers. The tested biopolymers included chitosan, guar gum (high density), xanthan (kelzan), and alginate. Two and 3 g/L solutions were prepared for each biopolymer using deionized water. Chitosan (which is insoluble in water) was first dissolved in acetic acid (10% in the final solution). Guar gum was cross-linked with borax. Xanthan was cross-linked with guar gum and Ca phytate. Alginate was cross-linked with Ca chloride and Ca phytate. Chitosan was cross-linked with a mixture of guar gum and borax and with a mixture of guar gum, borax, and glutaraldehyde. The pH and viscosity (at different shear rates) were measured for each biopolymer solution and cross-link product using a VMR Symphony SP90M5 pH meter and a Brookfield Digital Viscometer.

The objective of the second experiment was to prepare cross-linked biopolymers that are deliverable to sediments by coating sand particles. Ideal deliverable products should be easy to deploy on sediments, exhibit mechanical characteristics that bind sediments, and efficiently adsorb metals and organic contaminants. Several cross-linked products were tested using two coating procedures.

1. Liquid – treatment of sand with liquid or gel cross-linked biopolymers (obtained in the previous experiments) followed by acidification, mixing and neutralization, and filtration.
2. Solid – treatment of sand with a mixture of biopolymer and cross-linker in solid phases (for cross-linking directly on the sand) followed by addition of water only or water and other reagents (e.g., acids).

Description and detailed development methods of cross-linked biopolymer and biopolymer coated sand or sand/amendments are presented in Tables 1 and 2. The six most promising products which had high carbon fractions (indicating greater coverage of biopolymer) and high viscosity were evaluated further for metal and organic sorption, biodegradability, and physical disturbance/erosion.

Table 1. Biopolymer Products Used for Sand Coating and Contaminant Sorption; C- chitosan; G-guar gum, B-borax, X-xanthan; c- calcium chloride; 1 – without glutaraldehyde, 2 – with glutaraldehyde, 3 - without glutaraldehyde but with NaOH.

Major Product Name	Primary Biopolymers	Cross-link Agent	Modified product name	Biopolymer Sand ratio	Additives			
					5% HCl	Glutar-aldehyde	1N NaOH	water
					mL	mL	mL	mL
CGB	Chitosan Guar gum	Borax	CGB1	0.05	475			500
			CGB2	0.05	200	5		300
			CGB3	0.05	200		20	400
GB	Guar gum	Borax	GB1	0.005	100			500
			GB2	0.005			20	600
			GB3	0.025		5	20	600
GX	Guar gum	Xanthan	GX1	0.05	100			500
			GX2	0.05			20	600
			GX3	0.05				500
XCc	Xanthan Chitosan	Calcium chloride	XCc	0.025	100	5		500
XC	Xanthan	Chitosan	XC					500
XG	Xanthan	Guar gum	XG					500

Table 2. Preparation Method for Biopolymer Coated Sand Materials. Materials selected for erosion tests in an Adjustable Shear Stress Erosion and Transport (ASSET) flume are marked by an asterisk; C-chitosan; G-guar gum, B-borax, X-xanthan; c- calcium chloride; 1 – without glutaraldehyde, 2 – with glutaraldehyde, 3 - without glutaraldehyde but with NaOH.

Product Number	Coated Sand	Biopolymers/ Cross-link Agent	Preparation Method
1	CGB3 – 5% acid added	Chitosan/ Guar Gum/Borax	<p>2 kg sand + 50 g guar gum + 50 g chitosan + 25 g borax + 300 mL 1N NOH + 5 L tap water + 1 L 5% HCl</p> <p>Sand, biopolymer powders, and cross-link agent were well mixed as solids. One N NaOH was added to create a basic pH for cross-linking of guar with borax. Water was added in small amounts under continuous shaking, followed by the addition of acid under continuous shaking. The prepared material was placed on a rotary shaker (at about 30-40 rpm) overnight (12 h), then neutralized by the addition of 1N NaOH. The coated sand (as slurry) was collected wet and stored wet for erosion testing.</p>

Table 2 (continued). Preparation Methods for Biopolymer Coated Sand Materials.

2*	CGB3 – 5% no acid added		2 kg sand + 50 g guar gum + 50 g chitosan + 25 g borax + 100 mL 1N NOH + 6 L tap water The same procedure as 1 except that an additional liter of water was added instead of HCl. A weak acid (acetic acid) was used for pH adjustment. The pH of the resulting mixture was slightly basic due to the initial addition of NaOH.
3	XCc – 2.5% no acid	Xanthan/ Chitosan / Calcium chloride/ glutaral- dehyde	2 kg sand + 25 g xanthan + 25 g chitosan + 7.5 g CaCl ₂ + 50 mL glutaraldehyde + 6 L tap water Sand, biopolymer powders, and cross-link agent CaCl ₂ were well mixed as solids, then 50 mL glutaraldehyde was added. Additional mixing was performed mechanically. Water was added in small amounts under continuous shaking. The prepared material was left on a rotary shaker (at about 30-40 rpm) overnight (12 h), after which the pH was adjusted to neutral and the mixture filtered through a sieve. The coated sand (as slurry) was collected wet and stored for erosion testing.
4*	XCc – 5% no acid		2 kg sand + 50 g xanthan + 50 g chitosan + 15 g CaCl ₂ + 75 mL glutaraldehyde + 6 L tap water The same procedure as 3.
5*	XG – 2.5% no acid	Guar Gum/ Xanthan	2 kg sand + 25 g guar gum + 25 g xanthan + 6 L tap water Sand and biopolymer powders were well mixed as solids. Water was then added under continuous shaking. The prepared material was placed on a rotary shaker (at about 30-40 rpm) overnight (12 h). The coated sand (as slurry) was collected wet and stored wet for erosion testing.
6*	XG – 5% no acid		2 kg sand + 50 g guar gum + 50 g xanthan + 6 L tap water The same procedure as product #5.
7*	AXG – 5% coated apatite, no acid	Guar Gum/ Xanthan/ NC apatite	1.75 kg sand + 0.25 kg apatite + 50 g guar gum + 50 g xanthan + 6 L tap water The same procedure as product #5.
8*	OXG – 5% coated organoclay no acid	Guar Gum/ Xanthan/ PM-199 organoclay	1.75 kg of sand + 0.25 kg of organoclay + 50 g guar gum + 50 g xanthan + 6 L tap water The same procedure as product #5.
9*	XG/AO – 5% coated amendments no acid added	Guar Gum/ Xanthan/ NC apatite/ PM-199 Organoclay	1.5 kg of sand + 0.25 apatite + 0.25 kg of organoclay + 50 g guar gum + 50 g xanthan + 6 L tap water The same procedure as product #5.

Sorption of Organic Contaminants on Cross-linked Biopolymers Coated Sand

In the first year of the study, coating sand grains with cross-linked biopolymers was identified as a useful method of delivering biopolymers to the sediment surface (see Task 2, Subtask 2.1). In this experiment the sorption capacities of five coated sand samples (three with chitosan/guar gum cross-linked with borax (CGB, CGB2, and CGB3), one with guar gum cross-linked with borax (GB2), and one with xanthan/chitosan cross-linked with calcium chloride (XCc)) were evaluated for organic contaminants. Sorption measurements were made in triplicate in 50 mL vials with a 48 hour equilibration time. Measurements were also made at shorter and longer times to demonstrate 48 hours were sufficient to achieve equilibrium. Typically 1 g of sorbent biopolymer was introduced to the vials with a known PAH initial concentration. We examined PAHs purchased from a commercial supplier (Sigma Aldrich, MO) including 5000 mg L⁻¹ phenanthrene in methanol, 1000 mg L⁻¹ pyrene in methanol, and 200 mg L⁻¹ benzo(a)pyrene in methylene chloride. These solutions were diluted in electrolyte solutions (0.01M NaCl, 0.01M CaCl₂·2H₂O) to prepare a mixture of 20 ppb phenanthrene and 100 ppb pyrene. Exact concentrations of these compounds were determined by HPLC, affiliated with a Waters 2475 Multi λ Fluorescence Detector and Waters 996 Photodiode Array Detector. Sodium azide (0.05M) was added to the electrolyte solution to inhibit bacterial degradation of the PAHs.

Sorption of Metals on Cross-linked Biopolymer Coated Sand

Five biopolymer coated sand products were selected for evaluation of metal sorption: two with chitosan/guar gum cross-linked with borax (CGB1 and CGB3), two with guar gum cross-linked with borax (GB2 and GB3), and one with xanthan/chitosan cross-linked with calcium chloride (XCc). The experiments were conducted in 50 mL centrifuge tubes for one week. Each treatment had three replicates, two for metal analysis by ICP-MS and a third for measurement of pH. The spike solution used in the experiment was obtained from Inorganic Ventures, Lakewood, NJ. The metal concentrations in the spike solution were 1 mg L⁻¹ of As, Cd, Cr, Co, Cu, Pb, Ni, Se, and Zn. Suspensions composed of 0.2 gram of solid (biopolymer coated sand or a control sand without biopolymers) and 15 mL of spike solution were shaken for one week, phase separated by centrifugation, and then analyzed for metals by ICP-MS.

SUBTASK 1.2. EFFECT OF SEQUESTERING AGENTS ON MOBILITY, BIOAVAILABILITY, AND RETENTION OF CONTAMINANTS IN SEDIMENTS

Kinetic Studies on Retention of Organic Contaminants

Sorption and desorption are both time sensitive processes. A kinetic study was conducted to ensure that equilibrium was reached before samples were taken for the measurement of sorption and desorption coefficients. Three materials were tested, with one from each of the three groups of amendments under investigation: apatite, organoclay and zeolite. Specifically, the three materials tested were clinoptilolite TSM 140 (8x14 mesh), PIMS biological apatite (ground fish bones), and clay 750 (Biomim). The kinetic studies were performed in 50mL centrifuge tubes. Sorbents (20 mg to 1g) were weighed into the centrifuge tubes followed by 50 mL of electrolyte solutions artificially contaminated with phenanthrene and pyrene. The tubes were then tumbled in a tumbler, and water samples were collected at 6 hrs, 24 hrs, 48 hrs, and 96 hrs. The tubes

were centrifuged for sample collection and 1 mL of liquid was taken for contaminant analysis by HPLC.

Effect of Sequestering Agents on Availability and Retention of Metals

Under this subtask experiments were conducted to determine the effects of amendments on metal speciation and retention in contaminated sediment. Sediment samples were treated with North Carolina apatite, zeolite (clinoptilolite), a mixture of North Carolina apatite with chitosan, a mixture of North Carolina apatite with organoclay (OCB-750), and a mixture of North Carolina apatite, chitosan and organoclay (OCB-750). The experiment was conducted under oxidized and reduced conditions. For the reduced treatments, 40 g of Anacostia River sediment, 2 g of amendment or amendment mixture, and 25-mL of pore water from the Anacostia River sediment was added to 50-mL tubes. The tubes were on a platform shaker for eight weeks before separating the solids and liquids for chemical characterization.

Disposable filtration units were used for the oxidized treatments. These 115 mL plexiglass containers consisted of two chambers separated by a 0.45 μm filter membrane. Forty g of the Anacostia River sediment, 2 g of amendment or amendment mixture, and 25 mL of pore water from the Anacostia River sediment were added to the treated sediment. The units were open to provide oxygen exchange with the atmosphere. After eight weeks the remaining water was suction vacuumed through the filter and measured for pH, Eh (a measure of the redox status), dissolved O_2 , DOC, and electrical conductivity (EC) (a measure of the total concentration of ions in solution). The collected water solutions were analyzed for metals by ICP-MS.

A sequential extraction scheme based on modified methods of Tessier et al. (1979) was used to evaluate the distribution of metals in sediments from the Anacostia River, DC and the Elizabeth River, VA that were untreated and treated with amendments (Table 3). The Anacostia sediment was amended with North Carolina apatite (NCA) at 2.5% of the sediment wet weight, and with a mixture of 50% NCA and 50% organoclay (OCB-750), also at 2.5% of the wet sediment weight. The Elizabeth River sediment was amended with NCA at three rates (2.5%, 5%, and 10%), with OCB-750 (2.5%), and with a mixture of 50% NCA and 50% OCB-750 (2.5 % of the sediment wet weight). The following fractions were extracted: 1) exchangeable, 2) carbonate, 3) amorphous Fe and Mn oxides, 4) crystalline Fe and Mn oxides, 5) organic, 6) sulfides, and 7) residual (Table 3). All extractions, except the final digestion, were conducted in 50 mL polypropylene centrifuge vials to minimize losses of solid material. Separation of extracts from sediments was achieved by centrifuging at 2400 rpm for 20 min between each successive extraction. The supernatant was removed with a pipette, filtered through a 0.45 μm filter, and stored for analysis. The residue was washed with 10 mL of nanopure water (resistivity greater than 18.0 $\text{M}\Omega\text{ cm}$, conductivity less than 0.055 $\mu\text{S cm}^{-1}$), centrifuged, and the supernatant was added to the sample extract. The nanopure water was obtained from a water purification system EASY II LF (model D738, Barnstead International, Dubuque, IA). The residual and total concentrations of elements were determined by a total microwave digestion of 1 g of sediment with aqua regia (mixture of concentrated acids HCl and HNO_3). The extract solutions from all fractions were analyzed by ICP-MS.

Table 3. Sequential Extraction Procedure for Geochemical Fractionation of Untreated and Amended Sediments.

Step	Operationally defined fraction	Reagents	Extraction time
1	exchangeable	1.0 M MgCl_2	1 h
2	carbonates	1.0 M CH_3COOHNa	6 h
3	amorphous oxides	0.25 M $\text{NH}_2\text{OH}\cdot\text{HCl}$ in 0.25 M HCl	2 h
4	crystalline oxides	1.0 M $\text{NH}_2\text{OH}\cdot\text{HCl}$ in 25% CH_3COOH	3 h
5	organic	0.1 M $\text{Na}_4\text{P}_2\text{O}_7$	24 h
6	sulfide	4.0N HNO_3	30 min
7	residual	HNO_3/HCl (agua regia)	

TASK 2. STUDIES FOR DETERMINATION OF THE BEST COMBINATION OF AMENDMENTS FOR PLACEMENT AND CONSTRUCTION OF ACTIVE SEDIMENT CAPS

The second task consisted of the laboratory studies to address the following five subtasks:

1. Evaluation of mechanical properties,
2. Evaluation of diffusive transport,
3. Evaluation of advective transport,
4. Evaluation of the potential toxicity of active cap materials, and
5. Evaluation of biodegradability of biopolymer products.

SUBTASK 2.1. EVALUATION OF MECHANICAL PROPERTIES

Physical Properties of Biopolymer Products and Other Amendments

Organic Carbon Content of Biopolymer Products

The organic carbon content of biopolymer/sand products was measured as an indication of the amount of biopolymer transferred to the sand by the coating process. The organic carbon content was measured by heating samples to 375°C overnight and comparing the combusted samples with the unburned samples to obtain the carbon fraction. Time of exposure to the atmosphere was minimized during this process to minimize moisture uptake.

Porosity

Porosity was measured using the water saturation method. Five mL of water was added to graduated cylinders followed by 2 mL of sorbent, which was slowly introduced over three hours to allow saturation. Free water was removed from the top of the graduated cylinder and measured. Pore space was the difference between the total volume of water (5 mL) and the decanted water. Porosity was then calculated as the ratio between unsaturated water and total volume of sorbent and water (approximately 2 mL). For materials that swelled such as ClayFloc, the swollen volume was used as the total volume.

Permeability

Permeability was assessed by measuring the drop in head as water passed through treated sand. Tap water was supplied with a 6-channel syringe pump through a 50 mL syringe (Cole Parmer, IL). The tested samples (organoclays and coated sand) were packed into a threaded 15x2.5 cm (LxD) chromaflex column (Kimble/Kontes, NJ). The column was held vertically to allow upward water flow. A low pressure and low vacuum gauge was placed between the pump and the column to measure the water pressure drop due to the resistance of the materials. The pressure in the gauge was read and the height of the water head in the column was recorded at different times throughout the experiment. Permeability was determined with equation 5:

$$q = -\frac{k}{\mu} \frac{dp}{dx} A \quad (5)$$

where:

q = rate of flow in units of cm^3/s
 k = permeability in the unit of “darcies”
 u = viscosity of the fluid (tap water) in units of centipoises
 p = pressure read from the gauge in the units of atmospheres
 x = position along the path of water flow in the units of cm
 A = cross-sectional area of the column in units of cm^2

SUBTASK 2.2. EVALUATION OF DIFFUSIVE TRANSPORT

Diffusion of Metals through Active Caps – Laboratory Experiment

The following amendments were tested in the diffusion experiment: sand, washed rock phosphate from NC, organoclay (OCB 750), sand coated with biopolymer xanthan cross-linked with chitosan and calcium chloride (XCc), sand coated with biopolymer chitosan cross-linked with guar gum and borax (CGB3), and acid washed sand. A 10 cm layer (421 grams) of dry sediment was placed at the bottom of each clear plastic tube (total 18 tubes). The sediment was taken from Tims Branch, a stream located on the Savannah River Site near Aiken, SC, and was spiked with metals (Cd, Cr, Co, As, Ni, Se, Zn, and Pb). Water samples were collected two days, one month, two months, four months, five months, and six months after the start of the study. The samples were collected from the center of the water column (about 10 cm from the surface), and one sample was collected from each tube. All sets of water samples were analyzed for pH, EC, and metals by ICP-MS. The last two sets were analyzed for total carbon (TC), total inorganic carbon (TIC), and total organic carbon (TOC).

The diffusion experiment was conducted for six months. On Feb 12, 2008 the experiment was terminated. The water was decanted, and analyzed for pH, EC, TC, TIC, TOC, and metals by ICP-MS. The solid was collected and separated into cap material, and sediment. The sediment was sliced into layers at depths of 1 cm, 1.5 cm, 2.5 cm, and 5 cm for further analysis including pH, and TOC and TIC. Relative microbial abundance and composition was determined for the cap materials and selected sediment samples.

TC and TIC were measured in the water column using an OI Analytical Combustion TOC Analyzer, model 1020A. The sample was first transferred to a vessel that would not contribute TC and then introduced to the TOC Analyzer through a sipper, which pulled a fixed volume for analysis. The aqueous sample was heated to approximately 900°C in a high oxygen environment, and the TC evolved as CO_2 was measured. TIC was determined by adding phosphoric acid to the sample and measuring the gas devolved. TOC was calculated from the difference in the TC and TIC measurements.

A Solids TOC Analyzer manufactured by OI Analytical was used to measure both TC and TOC in the sediment samples. Approximately 0.5 g of sample was added to a sample cup and then lifted into the TOC analyzer where it was exposed to a temperature and time regime appropriate for the parameter being measured. TC was determined by measuring the quantity of carbon

dioxide (CO₂) devolved when the sample was heated to approximately 900°C in an oxygen atmosphere, which removed all carbon present as CO₂ gas. TOC measurements required acidification of the sample with hydrochloric acid followed by heating at 250°C in an oxygen atmosphere to purge the sample of TIC. The sample was then heated to 950°C and the quantity of CO₂ released was measured, which came only from TOC as all of the inorganic carbon had been removed. TIC was determined by subtracting the TOC from the TC.

Diffusion of Metals through Active Caps – Modeling

A one-dimensional numerical model was used to qualitatively assess the diffusion of selected metals through the various cap materials as tested in the laboratory column diffusion experiments. The modeling exercise was not intended to exactly predict concentration as a function of time for each element and cap material. Rather, it was intended to provide general insight into the diffusive behavior of the metals for each cap material based on measured and assumed material and transport properties.

A total of four cases were modeled: three cases with cap materials and one case with no cap. The cases simulated were:

1. Contaminated sediment and water only (no cap)
2. Contaminated sediment, apatite (NCA) cap, and water
3. Contaminated sediment, sand cap, and water
4. Contaminated sediment, organoclay (OCB750) cap, and water.

The numerical simulations conducted for this analysis were performed using the PC-based PORFLOW code (ACRI, 2004). A 1-dimensional diffusive transport model was created to represent the laboratory column experiments. The 1-dimensional governing equation for mass transport of species k in the fluid phase is given by:

$$\frac{\partial C_k}{\partial t} + \frac{\partial}{\partial x} \left(\frac{V}{R_f} C_k \right) = \frac{\partial}{\partial x} \left(\frac{D_m}{R_f} \frac{\partial C_k}{\partial x} \right) \quad (6)$$

where:

C_k = concentration of species k , ppm

V = fluid velocity in the i^{th} direction, m/yr

D_m = molecular diffusion coefficient for the species, cm²/yr

R_f = retardation factor

t = time, yr

x = distance coordinate, cm

For this analysis, the advection term was disabled within PORFLOW and only the diffusive term was evaluated. For this analysis, the molecular diffusion coefficient of each element in open water was used for the water layer. As such, Equation 6 may be simplified as follows:

$$\frac{\partial C_k}{\partial t} = \frac{D_m}{R_f} \frac{\partial^2 C_k}{\partial x^2} \quad (7)$$

For the remaining material layers, an effective diffusion coefficient was used which takes into account the tortuosity of the material. For this case, Equation 7 may be simplified as follows.

$$\frac{\partial C_k}{\partial t} = \frac{D_e}{R_f} \frac{\partial^2 C_k}{\partial x^2} \quad (8)$$

Equations 7 and 8 were solved within PORFLOW to evaluate the transient diffusive transport of metals from the contaminated sediments through the cap material and into the overlying column of water.

The boundary conditions imposed on the entire model domain included:

- No-flux specified for all metals along sides, top, and bottom
($\partial C / \partial X = 0$ at $x=0$, $x=1$ and $\partial C / \partial Y = 0$ at $y=0$, $y=y_{\max}$)

The initial condition imposed on the domain, except for the waste zone, included:

- Species concentration set to 0 at time = 0
($C=0$ for $0 \leq x \leq 1$ at $t=0$ and $C=0$ for $0 \leq y \leq y_{\max}$ at $t=0$)

The initial conditions for the model assumed a concentration of 1 ppm of each metal uniformly spread through the pore water of the sediment layer. Simulations were conducted in transient mode for diffusive transport with results being obtained over 10,000 years.

The numerical grid for the diffusion model was constructed as a node mesh 3 nodes wide by 202 nodes high. This mesh creates a vertical stack of 200 model elements totaling 40 cm in length with each element having a uniform width of 0.2 cm. Three material layers were used in the model which included the sediment layer, the cap layer, and the water layer. The sediment layer consisted of 50 elements and totaled 10 cm in length. The cap layer consisted of 25 elements and totaled 5 cm in length. The water layer consisted of 125 elements and totaled 25 cm in length. A set of consistent units was employed in the simulations for length, mass and time, these being centimeters, grams and years, respectively.

SUBTASK 2.3. EVALUATION OF ADVECTIVE TRANSPORT

Advective Transport of Metals through Cap Materials – Laboratory Experiments

Laboratory column experiments were conducted to evaluate the effectiveness of sand and apatite in the sorption and retention of various metals (As, Cd, Co, Se, Cr, Cu, Ni, Pb, and Zn). Two columns were tested under saturated conditions, one packed with sand and one packed with apatite. The acrylic glass (Lucite) columns used in the experiments were 5 cm in diameter and 10 cm in length (Picture 1). The saturated hydraulic conductivity of both the sand and apatite was estimated using a constant head method (Mariotte tube) prior to the start of the leaching experiments.



Picture 1. Setting of the Experiment on Advective Transport of Metals through Cap Materials.

The sand column was initially leached with deionized (DI) water containing an ionic strength adjuster (ISA) necessary for ion-selective analysis. The column was then leached with a spike solution containing approximately 10 ppm of each metal and 100 ppm of bromide (NaBr). A peristaltic pump was used to maintain a 0.2 ml/min up-flow of influent spike solution through the column. The effluent bromide concentration was continuously monitored with an ion-selective electrode and recorded with a data logger. Samples of the effluent from the column were collected for ICP-MS analysis using an auto-sampler (5 ml per sample). A 1-dimensional numerical model of the sand column was created using the PORFLOW code for comparison to the laboratory measurements.

Like the sand column, the apatite column was leached with DI water containing an ISA necessary for ion-selective analysis. The apatite column was leached with a spike solution containing 100 ppm of bromide (NaBr), and the flow rate of the influent spike solution was maintained at 0.5 ml/min. The effluent bromide concentration was continuously monitored and recorded with an ion-selective electrode and data logger. The column was purged with DI water to eliminate bromide from the column once breakthrough of the bromide tracer was achieved. The column was then leached with a spike solution containing about 2 ppm of each metal at a rate of 0.5 ml/min with up-flow through the column. A 1-dimensional numerical model of the apatite column was created using the PORFLOW code for comparison to the laboratory measurements as done with the sand column. Predicted breakthrough times for the apatite column are shown in Table 4.

Table 4. Predicted Breakthrough ($C/C_0 = 0.5$) of Selected Metals for the Apatite Column.

Metal	Breakthrough ¹ (yrs)	Breakthrough ¹ (days)
As	0.06	23
Cd	11.02	4,022
Co	1.73	631
Cr	28.02	10,227
Cu	9.09	3,318
Pb	36.52	13,330
Ni	0.68	248
Se	0.51	186
Zn	3.107	1,134

¹Breakthrough defined as $C/C_0 = 0.5$ for apatite column 10 cm thick at $Q = 0.5$ ml/min.

Diffusive and Advective Transport of Organic Contaminants - Column Studies

Advection transient models can calculate the time required for the breakthrough of various contaminants in caps composed of different experimental materials (Choy and Reible, 1998). A key parameter in such models is the sorption related retardation factor, R_f . Advectively dominated column experiments are being used in this study to define effective sorption related retardation factors, R_f , in organoclays and biopolymer coated sand for various hydrophobic organic compounds. Point (single concentration) partition coefficient measurements suggested solid-water concentration ratios in the order of 10^5 L/kg for phenanthrene and 10^6 L/kg for pyrene (previously reported). With a dry bulk density in the order of 1 kg/L, this implies a retardation factor of 10^5 or 10^6 for phenanthrene and pyrene, respectively. Less hydrophobic organics, such as naphthalene, would exhibit smaller retardation factors and more hydrophobic organics, such as benzo(a)pyrene and most PCBs would exhibit larger retardation factors. Although these estimates of the retardation factor are based upon single concentration partitioning, they represent a good starting point for the design of experiments to better define effective retardation in column experiments.

This magnitude of these sorption-related retardation factors suggests that diffusion measurements for hydrophobic organic compounds would not be productive in the organoclay caps. The time required for significant diffusion is given by equation 9:

$$\text{diffusion time} \sim 0.1 L^2 * R_f / (D_w \varepsilon / \tau) \quad (9)$$

where:

D_w = molecular diffusivity in water ($\sim 5 * 10^{-5}$ cm²/s)

ε = porosity

τ = tortuosity

The ratio ε / τ , is typically around 0.2. Where R_f is on the order of 10^5 , then the time required to diffuse through a 1 cm layer is 10^9 s or decades.

Although advection is also retarded by sorption, the velocity in a column experiment can be adjusted to allow measurements of effective retardation within a reasonable time frame without using unrealistic velocities. The time required for significant advection is given by:

$$\text{Advection Time} \sim 0.1LR_f/U$$

If $R_f \sim 10^5$ and U is of the order of 100 cm/day ($\sim 10^{-3}$ cm/s), then the time required to migrate at measurable levels through a column 1 cm in length is of the order of 10^7 seconds or a few months. It is this basic design that was employed in the column experiments for organic contaminants in organoclay and biopolymer caps.

To achieve a 1 cm cap layer thickness, a conventional 15 cm long, 1 inch diameter column was filled with glass beads except for the last 1 cm length, which was filled with organoclay. A superficial (Darcy) velocity of 100 cm/day was passed through the column. Due to the high flow rates required (100 cm/day with a 1 inch diameter column corresponds to 500 cm³/day of feed solution), the column was operated in a closed loop with the effluent recycled back to the influent. Feed reservoirs supplied the influent and collect the effluent. To maintain a constant concentration in the feed reservoir, solid samples of the feed organic constituents was introduced to the feed reservoir, maintaining saturated water conditions in the column influent. Organic compounds (naphthalene and phenanthrene, chosen to minimize required column operation time) can be detected at concentrations far below saturation; therefore, only the earliest phases of the breakthrough time in the column were measured. Naphthalene was expected to be detectable in the effluent from the column within 30-60 days of initiation and the effective retardation factor was estimated from the observed breakthrough curve and compared to the single concentration partition coefficient measurement.

Column experiments were also used to estimate the effective retardation factor of hydrophobic organics in the biopolymer coated sand capping material and organoclay (PM-199). Only two types of biopolymer coated sand were used; sand coated with xanthan/chitosan and cross-linked with calcium chloride (XCc) and sand coated with chitosan/guar gum cross-linked with borax (CGB3). Because preliminary single concentration partition coefficient measurements indicated a far smaller partition coefficient for these materials, the column design was relaxed significantly. Three 15 cm long, 2.5 cm diameter glass columns from Kontes were used as reactors for the column experiments. After the columns were cleaned with solvent and water, they were packed to 12.5 cm with cleaned 3mm glass beads. A thin layer of glass wool (2.5 cm in diameter) was placed on top of the glass beads. Next, 2.5 cm of sample was added to complete the column packing.

Teflon tubing was used for the influent and effluent supply lines to minimize sorption to the walls of the tubing. Flow was re-circulated in a 2 L glass flask that was placed on a stir plate. A rubber cap was placed in the top of the flask to minimize volatilization losses. Holes were drilled in the cap to pass the influent and effluent tubing into the flask. The water solution that was used in the experiment was prepared to contain solubility concentrations of naphthalene and phenanthrene; 30 ppm and 1 ppm, respectively.

Flow was provided by an eight channel peristaltic pump from Cole Parmer (Istamec Model CP 78002-10, Head CP 78002-50). The tubing used for the pump was three-stop color coded analysis tubing from Cole Parmer. The tubing had an inside diameter of 0.76 mm, capable of providing flow rates in the range of 0.101 to 10 mL/min. Before commencing the column tests, the pump was calibrated to obtain the desired flow rate of 0.38 mL/min (Darcy velocity of 100 cm/day). The influent end of the tubing was placed in a small beaker filled with water, and a 10 mL graduated cylinder was used to collect the flow on the effluent end. The pump was set to a known speed, and allowed to run for long enough to collect a known volume of water. The volume of water collected was used to calculate a flow rate. After calibration, the tubing was hooked into the column tubing, and the tested material in each column was saturated with clean de-ionized water drawn from a beaker.

After saturation with water, the columns were hooked into the contaminated water supply and placed in a 25°C temperature controlled room. The 2 L flask was stirred often to maintain solubility concentrations and occasionally more solid naphthalene and phenanthrene were added to the flask as needed. A portion of the effluent tubing was spliced near the effluent end of each column in order to facilitate sampling. Influent solution water samples were taken at the same time as effluent samples with a syringe. Sampling was conducted every 2-3 days initially, but the frequency was increased to every other day or every day once significant breakthrough began. Fifty microliters of solution were collected from each effluent sampling port, and the solution concentrations were analyzed with HPLC.

Tracer Study for Column Experiments

A tracer test was conducted to examine the hydraulic characteristics of each column and to obtain the non-sorbing breakthrough curve. Bromide was selected as a tracer for this test instead of chloride since organoclay has shown in laboratory tests to have significant chloride content that is partially reduced by sequential washings, but still sufficient to cause interference. The bromide probe was purchased from Cole Parmer and used with a pH/ISE meter. ISA solution was prepared following the instructions given in the manual for the bromide probe. To make the ISA solution, 106.25 g of sodium nitrate was added to 250 mL of distilled water. Next, a 1000 ppm bromide stock solution was prepared using sodium bromide. Five additional standards, 100 ppm and 10 ppm bromide ion and 0.1 M, 0.01 M, 0.001 M sodium bromide were made from the 1000 ppm stock using the serial dilution method. A slope check was performed on the electrode by adding 1mL of ISA to 50 mL of distilled water in a beaker. The beaker was placed on a stir plate and then 0.5 mL of 0.1 M sodium bromide solution was added. An electrode reading was then taken. Next, 5 mL of 0.1 M sodium bromide solution was added to the beaker, and another reading taken. The electrode was calibrated by measuring the 1000 ppm, 100 ppm, and 10 ppm standards with the bromide probe.

Throughout the duration of the tracer test, a ratio of 2 mL of ISA per 100 mL of sample was maintained. A 500 ppm bromide ion solution was prepared for the test by adding 0.645 g of sodium bromide to 500 mL of distilled water. The solution was divided among three 250 mL beakers and an influent tube from the pump was placed in each beaker. The flow rate used in this test, 0.38 mL/min, was the same as used in the sorption column experiments. Effluent samples were collected from each column into 10 mL glass vials beginning at ten minute intervals, then

fifteen, thirty and one hour. Bromide ion concentration in the initial solution was checked as well.

SUBTASK 2.4. EVALUATION OF POTENTIAL AMENDMENT TOXICITY

Analysis of Extracts

Extracts from the amendments were analyzed to determine if they contained impurities that could affect aquatic organisms. Elements were extracted using water extractions and the EPA toxicity characteristic leaching procedure (TCLP). The water extraction procedure was conducted by mixing 0.15 g of each amendment (rock phosphate, organoclay, and biopolymer coated sand) with 30 ml of distilled water in 50 ml centrifuge tubes. The tubes were placed on a shaker for 24 hrs hours, after which the supernatant was decanted, acidified, and analyzed for metals by ICP-MS. Concentrations of metals in the water extracts were compared with EPA ambient water quality criteria, EPA final chronic values, ORNL lowest chronic values (Suter and Tsao, 1996), and CCME water quality guidelines (1998).

The TCLP is a regulatory test widely used to classify materials as hazardous or nonhazardous (U.S. EPA, 1992). Rock phosphates (NCA and TRP), organoclays (OCB750 and PM-199), biopolymer coated sand (with xanthan/chitosan cross-linked with calcium chloride) (CS), and sand (PS) were extracted using the TCLP. The TCLP leaching solution was comprised of 0.1M glacial acetic acid and 0.0643 M NaOH, with a final pH of 4.93. Forty milliliters of leaching solution was added to 2 g of tested material; the mixture was agitated on a shaker for 18h at 25°C, and then centrifuged. After centrifugation, the supernatants were filtered through 0.22 µm pore-size polycarbonate filters, acidified to 1% HNO₃, and analyzed for metals with ICP-MS for 20 elements.

Sediment Toxicity Tests for Fresh and Salt Water

Sediment toxicity tests were used to determine if the amendments have the potential to harm aquatic organisms. Both freshwater and brackish water (estuarine) sediment toxicity tests were conducted because the amendments may be used in both environments. The tests followed standard EPA protocols (EPA, 2000) and involved the exposure of laboratory cultured known-age *Hyallela* (freshwater) and *Leptocheirus* (brackish water) to sediments composed entirely of North Carolina apatite or biopolymer coated sand (with xanthan/chitosan cross-linked with calcium chloride). All tests were conducted for 10 days under controlled temperature and light conditions. Freshwater tests employed eight chambers with amendments and eight chambers with control sediments; each contained 10 organisms. Brackish water tests employed four chambers with amendments and four chambers with control sediments; each contained 20 organisms. Freshwater test chambers consisted of 500 ml beakers filled with 100 ml of sediment and 175 ml of overlying water, and brackish water test chambers consisted of 1000 ml beakers, each with 175 ml of sediment and 800 ml of overlying water. Control sediments for the freshwater tests were from an uncontaminated natural environment (Middle Tyger River at Jones Gap, SC) and control sediments for the brackish water tests were purchased from Aquatic Biosystems (Fort Collins, CO). Measured amounts of a standardized food supply were added to each chamber to prevent starvation, and the overlying water was renewed at consistent intervals

to maintain water quality. Conductivity, hardness, pH, alkalinity, and ammonia were measured at the beginning and end of each test, and dissolved oxygen was measured daily. Because the survival data were generally characterized by non-normal distributions and heterogeneous variances, Wilcoxon rank sum tests were used to determine the significance of differences in survival between chambers with control sediments and chambers with amendments.

Two additional bioassays were conducted on organoclay using procedures similar to those described above with a few modifications. In the first bioassay, organoclay was mixed with natural substrate (primarily sand) from Tinker Creek rather than with Tyger River sediment. This test was conducted to verify the results of the previously described tests. Tinker Creek is a medium-sized uncontaminated stream located on the Savannah River Site, an 800 km² Department of Energy reservation located near Aiken, SC (USA). In the second bioassay, organoclay was rinsed before testing. Organoclay released chloride causing chloride levels to rise to nearly 4500 mg L⁻¹ in freshwater toxicity tests. Chloride was removed from organoclay by successively rinsing until the chloride concentration in the final rinsate was about 200 mg L⁻¹ to see if this affected toxicity. Chloride concentrations were measured with a Dionex DX-500 ion chromatograph.

The California blackworm *Lumbriculus variegatus*, a readily available freshwater oligochaete, was used for additional toxicity testing. Changes in aggregate weight between the beginning and ends of the tests rather than counts of the numbers of surviving individuals were used to estimate toxicity because California blackworms reproduce asexually by fragmentation; therefore, counts are not a valid indicator of survival for this species. Changes in aggregate weight integrated survival and growth.

California blackworms were obtained from Aquatic Foods, a company that produces California blackworms in large quantities, primarily as a live food for tropical fish. Aquatic Foods uses commercial fish food to produce California blackworms in dedicated rearing ponds supplied with a combination of filtered river water and well water. The worms were thoroughly rinsed with chilled, chlorine free water upon receipt from Aquatic Foods and stored under refrigeration in shallow trays filled with dechlorinated tap water to a depth of about 2.0 cm. Worms were removed from the trays as required to conduct the experiments described below.

An acute sediment bioassay using *Lumbriculus variegatus* was conducted to assess organoclay (PM-199TM) toxicity. Four dilutions of organoclay mixed with reference sediment were tested in addition to a control consisting of 100% reference sediment (50% sand and 50% silt from Tinker Creek). Each dilution plus the control was represented by five 1 L beakers, each containing 100 mL of test material, 100 mL of overlying water, and about 1.0 g of *Lumbriculus*. The water overlying the test material was renewed daily with fresh water. Conductivity and pH were measured at day 1, 4, and 8, and dissolved oxygen was measured daily. The organisms were removed after eight days and weighed in aggregate. One-Way Analysis of Variance (ANOVA) was used to assess the significance of differences between amendments and controls.

Bioaccumulation Study

In addition to the previously described standard sediment toxicity tests, studies were conducted on the oligochaete worm *Ilyodrilus templetoni* to obtain information on survival, growth, and contaminant uptake in sediment mixed with organoclay. In these studies organoclay was mixed at rates of 15% and 50% with Anacostia River sediment contaminated with the PAHs phenanthrene, chrysene, and benzo[a]pyrene from industrial sources. Phenanthrene, chrysene, and benzo(a)pyrene were the primary PAHs in Anacostia River sediment. Uncontaminated sediment was used as a control. The experiment was conducted in 50 ml tubes, each with 20 organisms. There were seven replicates per treatment. The worms were analyzed for survival, growth, lipid content, and PAH concentration at the end of 28 days.

Recovering California Blackworms from Sediments and Amendments

To support the active biomonitoring studies in field, preliminary work was conducted in the laboratory to provide background information needed to accurately evaluate the field results. This work consisted of developing efficient methods of recovering California blackworms from the sediments and amendments placed in the cages. Simple and comparatively rapid techniques were developed in the laboratory for removing California blackworms from sediments and amendments. Sand, apatite, organoclay (PM 199), and silt were used in these experiments. The sand and silt were collected from Tinker Creek, an unpolluted and relatively undisturbed stream on the Savannah River Site. For the first three materials, the cage contents were poured into a rectangular plastic pan and the pan was shaken to separate the light worms from the relatively heavy sediments. Individual worms were removed from the pan with an eyedropper and placed in a beaker. The aggregated worms were then placed on a piece of plastic window screen, blotted on a paper towel to remove excess water, and weighed to determine the percent recovery efficiency ($\text{initial weight} / \text{final weight} \times 100$). For silt additional steps were needed to separate silt and fine sand from organic debris (e.g., leaf, twig, and root fragments) and worms. The contents of the pan were poured into soil sieves (#25, #30, #35) stacked from largest to smallest mesh size, with the worms removed from the debris in each sieve with an eyedropper. The smallest mesh sieve did not permit the passage of any worms. The worms were then weighed.

Complete recovery of the California blackworms was difficult because of the small size of some of the worms. Therefore, we conducted recovery efficiency experiments to determine what level of recovery to expect in the absence of mortality. For these experiments about one g of worms were removed from the holding trays, weighed in aggregate to the nearest hundredth of a gram and placed in a one liter beaker with 100 ml of test material and 75 ml of dechlorinated water. The worms were permitted to separate and burrow into the sediments for five minutes, after which they were recovered and weighed again to determine the recovery efficiency ($\text{final weight} / \text{initial weight} \times 100$).

Laboratory Survival Studies

Laboratory survival tests were conducted to provide preliminary indications of the ability of California blackworms to survive in the sediments they would be exposed to in the streams. The

sediments included silt and sand from Tinker Creek (the former collected from depositional areas in Tinker Creek). Ten one liter beakers were used in most tests with two beakers harvested every two or three days resulting in a total test duration of 17 days. About one gram of California blackworms were placed in each beaker along with 100 mL of test material and 100 mL of dechlorinated water. The water in the beakers was replaced daily to maintain water quality. The worms were collected and weighed when a beaker was harvested, with the difference between beginning and ending weights providing an integrated measure of survival and growth (or weight loss) over the test period.

SUBTASK 2.5. BIODEGRADABILITY OF BIOPOLYMER PRODUCTS

Biodegradability of Biopolymer Products

Biopolymer products were evaluated for biodegradability by microorganisms associated with the polymers. One gram of polymer material was mixed with and without 10 ml sterile basal salts medium (BSM) (Turick et al. 2002) and sealed in sterile test tubes with airtight butyl rubber stoppers. Uncoated sand was used as a control for comparison with the biopolymer coated sand. Static incubation in the dark was at 0°C and 35°C. Low temperature (0°C) and high temperature (35°C) and wet and dry moisture regimes simulated a broad range of environmental conditions and seasonal changes. Microbial activity (biopolymer degradation) was measured by CO₂ release with a Hewlett Packard 5890 series 2 gas chromatograph (GC) with a mass spectrometer. A 250 µL sample of the headspace gas was injected into the GC using a gas tight syringe with a side-hole needle. A carrier gas of helium was used to move the sample through the column into the mass spectrometer. An internal standard of argon was used to calculate CO₂ production in the samples. The release of CO₂ from the biopolymer products was measured for ten weeks. Additionally, metal concentrations for biopolymers from the sorption experiment were also evaluated (ICP-MS) upon termination of this experiment in an effort to correlate biopolymer breakdown with metal release. Microbial density on biopolymers was characterized at the termination of the study by direct microscopic counts. Filtered biopolymers and cells were stained with 496-diamidino-2-phenylindole (DAPI) and stained cells were detected using epifluorescent illumination (Lehman et al., 2001). The heterogeneous nature of the biopolymers did not permit quantitative enumeration of cells but results generally correlated with CO₂ evolution.

Microbial Effects on the Properties of Biopolymers

Microbial degradation of the biopolymers was further evaluated by sampling polymers that appear to be biodegradable (as indicated by increased CO₂ evolution) by soil microbes. This method included addition of sterile biopolymers to BSM or BSM solidified with 1.5% Noble agar, thus providing the biopolymers as the sole source of carbon for microbial isolates associated with the biopolymers (above). As a source of bacterial inocula, fresh sediment was treated following the methods of Lehman et al. (2001), which included addition of 0.1% sodium pyrophosphate, and blended followed by sedimentation (for 24 hrs) of sediment particles. Disorbed bacteria, in suspension, were used as inocula for degradation studies following washing in phosphate buffer. A 1% inoculum (wt/vol) was added to sterile biopolymers in gas tight vials as above. Carbon dioxide evolution and oxygen utilization were monitored over time to

determine the rate (if any) of degradation. Controls consisted of uninoculated biopolymers as well as inoculum without biopolymers. The samples were incubated statically in the dark for 2 weeks at 25°C to evaluate microbial growth resulting from biopolymer breakdown. Gas analyses were conducted either through periodic GC headspace analysis or via respirometry. Following the incubation period (when CO₂ concentrations level off) biopolymer material was dried and weighed to determine loss due to biodegradation, and a carbon balance was attempted with the CO₂ data. Microbial isolates were grown with specific polymers (i.e., guar gum, chitosan, glutaraldehyde, etc.) on BSM and Nobel agar plates to obtain a gross characterization of microbial community changes resulting from polymer biodegradation. Growth did not occur on Nobel agar plates without supplemental carbon. Biopolymers were also evaluated before and after degradation using electron microscopy to determine if biodegradation affected polymer size. Polymer breakdown products were evaluated by ion chromatography and/or GC/MS.

TASK 3. EVALUATION OF THE RESISTANCE OF CAPS TO PHYSICAL DISTURBANCE

Evaluation of Suspension by Shaker Tests

The biopolymer products tested for erosion resistance are described in Table 2. These products were prepared and kept wet (as slurry) for testing as a wet product. Large amounts of each product (2-5 kg) were produced. The main objective was to identify the best product for use in field deployment.

A standard shaker test (Tsai and Lick, 1986) was used to assess the ability of sand and amendments with and without biopolymers to resist physical disturbance. Methods for preparing biopolymer products are shown in Table 2. The shaker allowed a standardized assessment of the shear stress needed to suspend a sample. The shear stress needed to suspend a sample was measured using a sampling port (Picture 2; Figure 1). Seven cm of sample were placed inside of the cylindrical chamber, and sufficient amount of distilled water was added to the cylinder to bring the depth to 12.7 cm. Suspended sample particles were allowed to settle, the cylinder was reattached to the shaker, and the motor speed was recorded when the following conditions were visually observed: fine top particles disturbed, motion of top particles, cloudiness, full re-suspension of bottom layer, and full re-suspension of top layer. The motor speed of the shaker drive disc was measured with a tachometer in meters per minute. The circumference of the drive disc (17 cm) was measured and used to convert the m/min measurements into revolutions per minute (0.17 rpm), which was further converted to oscillations by equation 10:

$$\text{oscillation period} = \frac{1}{60 \times \text{RPM}} \quad (10)$$

Tsai and Lick (1986) determined equivalent shear stresses by calibrating the shaker with a laboratory flume, based on the premise that when the flume and the shaker produce the same amount of suspended particles under the same environmental conditions, the stresses needed to induce the suspension of particles are equivalent. Their paper presents a chart of oscillation period versus equivalent shear stress (Figure 2).

The chart was used with the calculated oscillations to estimate the equivalent shear stresses; however, the two slowest oscillation periods could not be read directly from the chart (Table 5). Therefore, a linear regression was calculated from the data in the chart (Figure 3) and used to estimate equivalent shear stresses of these oscillation periods. Estimated values for other higher oscillation periods were within ± 0.1 dynes/cm² of the chart values indicating the accuracy of the regression.

The critical shear stress is recognized as the threshold of shear stress at which particle motion will occur, and it depends entirely on the diameter of the particle described in the following equations below:

$$\tau_c = \tau^* (\gamma_s - \gamma) d \quad (11)$$

$$\beta = \left(\frac{1}{\gamma} \sqrt{\frac{(\gamma_s - \gamma)}{\gamma}} g d^3 \right)^{-0.6} \quad (12)$$

$$\tau^* = 0.22\beta + 0.06 \times 10^{-7.1\beta} \quad (13)$$

where:

γ_s = particle specific weight,

γ = specific weight of water, and

d = particle diameter.

Table 5. Estimated Shear Stresses for the Shaker Test.

Erosion Threshold	Oscillation Period (s)	Equiv. Shear Stress (dynes/cm ²) from Chart	Equiv. Shear Stress (dynes/cm ²) from Regression
Fine Top Particles Disturbed	0.23	-	0.29
Motion of Top Particles	0.18	-	1.36
Cloudiness	0.16	2	1.95
Full Re-suspension of Top Layer	0.11	3.4	3.56
Maximum Re-suspension	0.09	4.3	4.31



Picture 2. Shaker for Simulating Erosion.

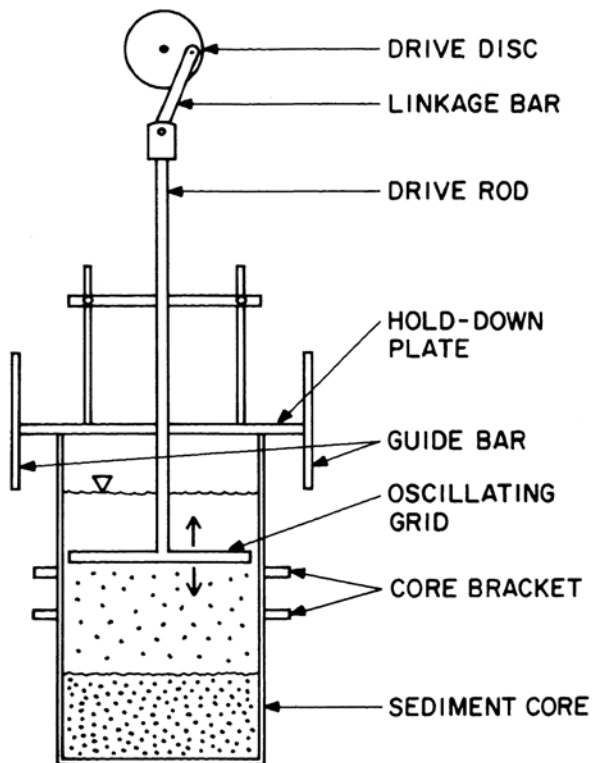


Figure 1. Shaker Test Experimental Design (after Tsai and Lick, 1986)

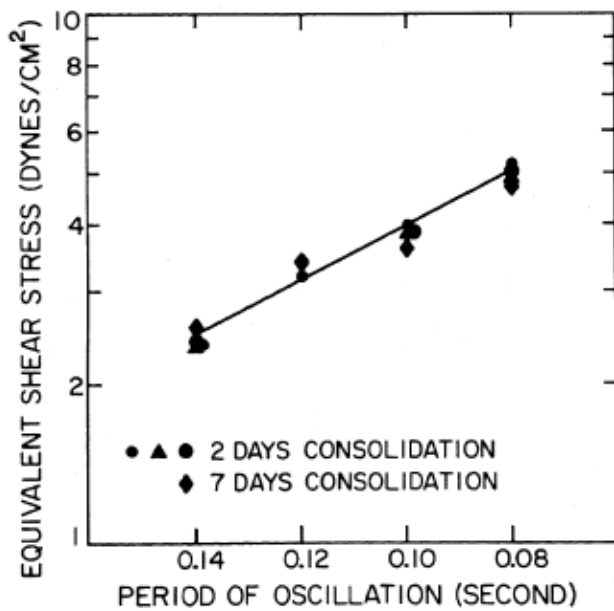


Figure 2. Shear Stress as a Function of Oscillation Period (Tsai and Lick, 1986)

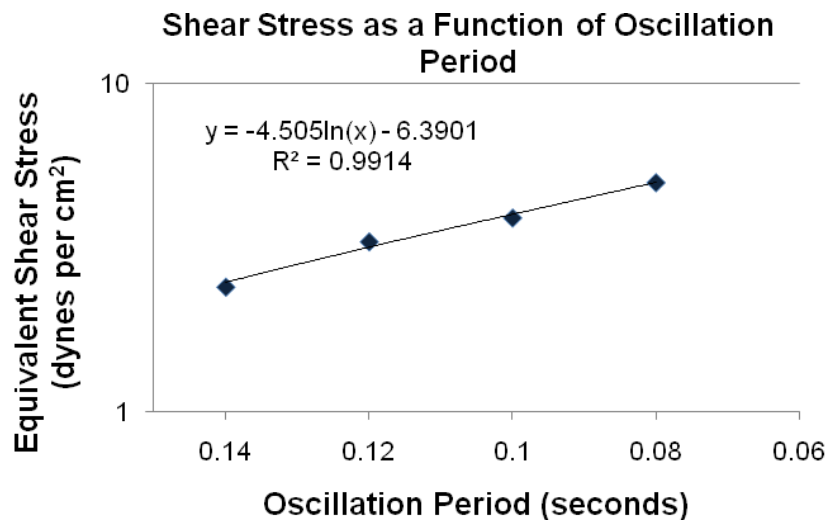


Figure 3. Fitting of Tsai and Lick's (1986) data

Evaluation of Cap Resistance to Physical Disturbance by Adjustable Shear Stress Erosion and Transport (ASSET) Flume

Description of the ASSET Flume

The ASSET flume is considered a next generation SEDflume in that it maintains all capabilities of its predecessor while also quantifying the transport modes of the sediments after erosion. The erosion test section of the ASSET flume is similar in design, with a slightly taller channel height, and identical in erosion testing operation to the SEDflume, which has been described extensively in the literature (McNeil et al., 1996; Jepsen et al., 1996; Jepsen et al., 1997; Roberts et al., 1998; Roberts and Jepsen, 2001). It consists of eight primary components (Figure 4): a 120 gallon reservoir, a 200 gpm centrifugal pump, a motor controlled screw jack, an erosion channel including erosion test section, a transport channel including bedload traps, a three way valve, a magnetic flow meter, and connective plumbing. Water is pumped from the reservoir through the three-way valve, which either sends water directly back to the reservoir or through the flow meter to the erosion and transport channels (and then back to the reservoir). A manually controlled screw jack is used to push the sediments through the core tube to keep the sediment surface flush with the channel floor such that, as closely as possible, the sediments are exposed only to an applied shear stress. The ASSET Flume's enclosed (internal flow) erosion and transport channels are 5 cm tall and 10.5 cm wide (Figure 4). The erosion test section is preceded by 180 cm of enclosed rectangular channel to ensure fully developed turbulent flow over the sediment core. The cylindrical sediment core tube is 10 cm in diameter. The first bedload trap is located 1 m from the center of the erosion test section, and the center of each successive trap is 1 m from the center of the preceding one. Based on the theoretical definition of bedload in combination with fluid velocities and particle/aggregate settling speeds, a bedload particle/aggregate should contact the flume floor at least once every 15 cm of downstream travel. Consequently, the traps are 15 cm long and span the width of the channel (10.5 cm). Capture basins that are 10 cm deep and have a 2 L volume are located below the traps, each with a baffle system that reduces recirculation and minimizes the resuspension of trapped sediments. As the sediment core is eroded upstream, some of the material is suspended and some is transported as bedload. All sediment that falls into the traps is considered bedload.

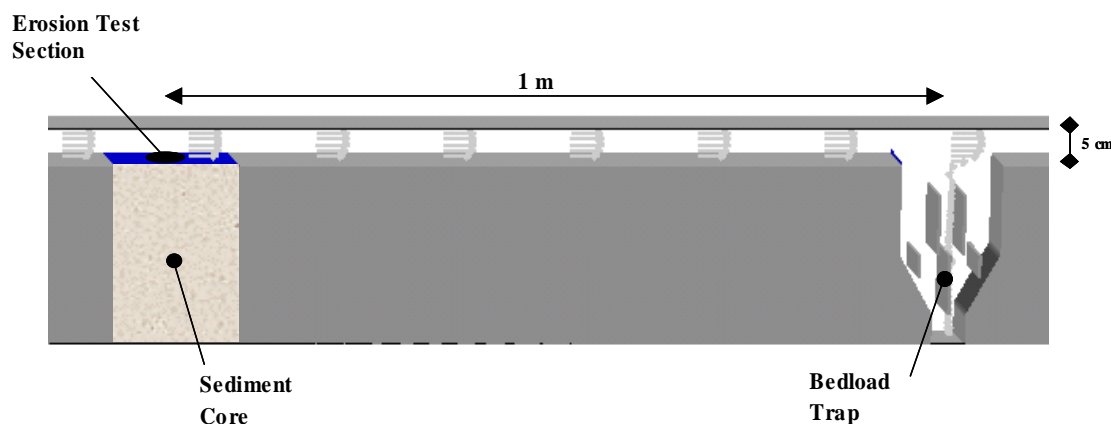


Figure 4. Schematic Illustration of the ASSET Flume.

Hydrodynamics

The hydrodynamics within the flow channel of the ASSET Flume are equivalent to those of the SEDflume (McNeil et al., 1996); however, the increase in duct height necessitated a change to the system inlet. To achieve fully developed turbulent flow over the sediment core, the flume inlet was lengthened to 180 cm and preceded by a 20 cm circular-to-rectangular flow converter and several meters of inlet pipe. Turbulent flow through pipes has been studied extensively, and empirical functions have been developed that relate the mean flow rate to the boundary shear stress. In general, flow in circular cross-section pipes has been investigated. However, the relations developed for flow through circular pipes can be extended to non-circular cross-sections by means of a shape factor. An implicit formula relating the boundary shear stress to the mean flow in a pipe of arbitrary cross-section can be obtained from Prandtl's Universal Law of Friction (Schlichting, 1979). For a pipe with a smooth surface, this formula is

$$\frac{1}{\sqrt{\lambda}} = 2.0 \log \left[\frac{UD\sqrt{\lambda}}{\nu} \right] - 0.8 \quad (14)$$

where:

- U = mean flow speed
- ν = kinematic viscosity
- λ = friction factor
- D = hydraulic diameter

For a duct with a rectangular cross-section the hydraulic diameter is

$$D = 2hw/(h + w) \quad (15)$$

where:

- w = duct width
- h = duct height

The friction factor is defined as

$$\lambda = \frac{8\tau}{\rho U^2} \quad (16)$$

where:

- ρ = density of water and
- τ = wall shear stress.

Substituting Equations 15 and 16 into Equation 14 yields the boundary shear stress as an implicit function of the mean flow speed. The mean flow speed and hence the boundary shear stress are controlled by the pump speed. For flow in a circular pipe, turbulent flow theory suggests that the transition from laminar to fully turbulent flow occurs within 25 to 40 diameters from the entrance to the pipe. Because the hydraulic diameter of the duct is 6.8 cm, this indicates a necessary entry length between 170 and 270 cm, which is supplied by the inlet piping, converter, and ducting. Furthermore, for shear stresses in the range of 0.1 to 10 N/m², the Reynolds numbers, UD/ν , are on the order of 10⁴ to 10⁵ implying that turbulent flow existed in all

experiments performed for this study. These arguments along with direct observations indicate that the flow is fully turbulent in the test section.

Sample Collection and Preparation for the ASSET Flume Test

Samples tested in the ASSET flume were prepared following the method described in Table 2. All materials were stored in a refrigerator at 4°C. The samples were stirred and poured into erosion core tubes to a depth of 10 cm. Five cm of water was gently poured on top of each material, which was returned to a refrigerator. Each sample remained in the refrigerator until the day of the erosion test for consolidation times of 2, 5, 10, and 175 days.

Measurements of Sediment Erosion Rates and Critical Shear Stress

To measure the erosion rates of the samples as a function of shear stress and depth, the samples were placed upward into the test section until the sample surface was even with the bottom of the test section. A measurement was made of the depth to the bottom of the sample in the tube. The flume was then run at a specific flow rate corresponding to a particular shear stress. Erosion rates were obtained by measuring the remaining sample depth at different time intervals, taking the difference between each successive measurement, and dividing by the time interval. To measure erosion rates at several different shear stresses using only one sample, the flume was run sequentially at higher shear stresses with each succeeding shear stress being 1.33, 1.5 or 2 times the previous one. Generally between three and five shear stresses were run sequentially. Each shear stress was run until at least 0.5 mm but no more than 10 mm were eroded. The time interval was recorded for each run with a stop watch. The flow was then increased to the next shear stress, and so on until the highest shear stress was run.

A critical shear stress can be quantitatively defined as the shear stress at which a very small, but accurately measurable rate of erosion occurs. In the present study, this rate of erosion was chosen to be 10^{-4} cm/s; this represents 1 mm of erosion in approximately 15 minutes. Since it would be difficult to measure all critical shear stresses at exactly 10^{-4} cm/s, erosion rates were generally measured above and below 10^{-4} cm/s at shear stresses which differ by a factor of 1.33, 1.5 or 2. The critical shear stress was then linearly interpolated to an erosion rate of 10^{-4} cm/s. This gave results with 20% accuracy for determination of critical shear stress.

Erosion Rate Ratio Analysis

The erosion rate data collected for each sample is generally plotted as erosion rate as a function of depth from the sediment surface and applied shear stress. The non-linear relationship between erosion rate and bed shear stress can make it difficult to quantify variability in the erosion behavior within a single core and between many cores. In order to overcome this limitation, the data can be analyzed to determine an erosion rate ratio that produces a single numerical value for a particular erosion rate data series that accounts for this non-linear relationship (Jones et al., 2008). The erosion rate ratio is used to make direct comparisons between erodibility within a single core (i.e., to identify changes with depth), between similar cores, and between all tested cores to aid in the identification of the most erosion resistant cap material. In this analysis, each core was sub-sampled into separate depth intervals. Following the methods of Roberts et al.

(1998), the erosion rate for each depth interval can be approximated by a power law function of sediment density and applied shear stress. For a particular depth interval, density is assumed to remain relatively constant; therefore the density term is dropped. For each depth interval, the measured erosion rates (E) and applied shear stresses (τ) are used to develop the following equation:

$$E = A\tau^n \quad (17)$$

where:

E = erosion rate (cm/s) and

τ = shear stress (Pa).

The parameters A and n are determined using a log-linear regression analysis. From this analysis an average erosion rate for the entire core can also be determined, and the erosion rate at each depth interval can be directly compared to this average. The result is an erosion rate ratio which provides an estimation of the erosion susceptibility of each depth interval relative to the core average. In addition, an average erosion rate of similar cores and for all cores can be determined. The erosion rate for each depth interval within a core as well as each core average erosion rate can be compared to the specified average and a graph of the erosion rate ratios for all of the cores can be created and compared to the average erosion behavior of all cores.

TASK 4. GENERATION OF CONCEPTUAL AND MATHEMATICAL MODELS FOR CONTAMINANTS ATTENUATION

1-D Metal Transport Modeling

A one-dimensional numerical model was used to qualitatively assess transport of selected metals through the various cap materials as tested in the laboratory column experiments. This exercise was not intended to exactly predict concentration as a function of time for each element and cap material. Rather, it was intended to provide general insight into the advective and diffusive behavior of the metals for each cap material based on measured and assumed material and transport properties.

A total of four cases were modeled: three cases with cap materials and one case with no cap. The cases simulated were:

1. contaminated sediment and water only (no cap)
2. contaminated sediment, apatite cap, and water
3. contaminated sediment, sand cap, and water
4. contaminated sediment, organoclay cap, and water.

The numerical simulations conducted for this analysis were performed using the PC-based PORFLOW code (ACRI, 2004). A 1-dimensional advective/diffusive transport model was created to represent the laboratory column experiments.

For this analysis, a steady state advective flux of 1 ml/hr (8760 cm/yr assuming a fluid density of 1 g/cm³) was applied to the model domain. For this analysis, the molecular diffusion coefficient of each element in open water was used for the water layer. For the remaining material layers, an effective diffusion coefficient was used which takes into account the tortuosity of the material. A no-flux boundary condition was imposed along the sides and bottom of the model domain. For the top boundary, the concentration gradient normal to the boundary was set to zero ($\partial C / \partial Y = 0$). The initial conditions for the model assumed a concentration of 1 ppm of each metal uniformly spread through the pore water of the sediment layer. Elsewhere in the domain, the initial concentration of each metal was set to zero. Simulations were conducted in transient mode for advective and diffusive transport with results being obtained over 100 years.

Model Grid Construction

The numerical grid for the model was constructed as a node mesh 3 nodes wide by 202 nodes high. This mesh creates a vertical stack of 200 model elements totaling 40 cm in length with each element having a uniform width of 0.2 cm. Three material layers were used in the model which included the sediment layer, the cap layer, and the water layer. The sediment layer consisted of 50 elements and totaled 10 cm in length. The cap layer consisted of 25 elements and totaled 5 cm in length. The water layer consisted of 125 elements and totaled 25 cm in length. A set of consistent units was employed in the simulations for length, mass and time, these being centimeters, grams and years, respectively.

Material Properties and Other Input Parameters

Material properties utilized within the 1-D numerical model were specified by material layer for each case simulated. Each material zone was assigned values of particle density, total porosity, saturation, and tortuosity. The bulk density and porosity of each material type except the sediment were previously measured. These values were used to calculate particle density. The properties assigned to each material type are given in Table 6.

The sediment used in the experiment and simulated in the modeling exercise originated from Tims Branch at the SRS. The sediments along Tims Branch belong to the soil series named Fluvaquents (Rogers, 1990). The Fluvaquents soil series consists of poorly drained, permeable soils which occur along the flood plain of small streams and drainages in the sandy sediments of the Atlantic Coastal Plain. Surficial sediments from this soil series typically grade from sand to loamy sand. Material properties of these sediments were not measured for this experiment. However, properties for similar sediments at SRS have been previously measured. Thus, average property values for the sediment were determined based on existing data for sediments classified as sand, loamy sand, and sandy loam.

An effective diffusion coefficient was used for each metal and material layer (except the water layer). Molecular diffusion coefficients for each metal were taken from Li and Gregory (1974). Effective diffusion coefficients for each metal and material type were calculated using the molecular diffusion coefficient and the material tortuosity. The diffusion coefficients used in the model are given in Table 7.

The partitioning coefficient K_d was determined from earlier sorption studies for each metal and cap material. These values were used in the model to account for partitioning of the metals in the cap materials. Values of K_d were not available for the sediment and K_d was set to zero in this material layer. This was a conservative assumption for this modeling exercise as it allowed for maximum advection and diffusion into the overlying cap material. The partitioning coefficients assigned to each metal and material type are given in Table 8.

Table 6. Material Properties Used in Transport Modeling.

Layer	Particle Density (g/cm³)	Total Porosity (fraction)	Average Saturation (fraction)	Tortuosity (unitless)
Sediment layer	2.66	0.360	1.00	2
Apatite layer	2.57	0.412	1.00	4
Sand layer	2.44	0.378	1.00	2
Organoclay Layer	2.71	0.857	1.00	4

Table 7. Diffusion Coefficients Used in Transport Modeling.

Metal	Water¹ (cm²/yr)	Sediment (cm²/yr)	Apatite (cm²/yr)	Sand (cm²/yr)	Organoclay (cm²/yr)
Cd	2.261E+02	1.131E+02	5.653E+01	1.131E+02	5.653E+01
Cr	1.873E+02	9.366E+01	4.683E+01	9.366E+01	4.683E+01
Co	2.204E+02	1.102E+02	5.511E+01	1.102E+02	5.511E+01
Cu	2.312E+02	1.156E+02	5.779E+01	1.156E+02	5.779E+01
Pb	2.980E+02	1.490E+02	7.450E+01	1.490E+02	7.450E+01
Ni	2.141E+02	1.071E+02	5.353E+01	1.071E+02	5.353E+01
Se	2.983E+02	1.492E+02	7.458E+01	1.492E+02	7.458E+01
Zn	2.693E+02	1.347E+02	6.733E+01	1.347E+02	6.733E+01

¹From Li and Gregory, 1974**Table 8. Partitioning Coefficients Used in Transport Modeling.**

Metal	Water (cm²/yr)	Sediment (cm²/yr)	Apatite (cm²/yr)	Sand (cm²/yr)	Organoclay (cm²/yr)
Cd	0.000E+00	0.000E+00	7.696E+03	0.000E+00	2.073E+05
Cr	0.000E+00	0.000E+00	1.928E+04	0.000E+00	1.135E+04
Co	0.000E+00	0.000E+00	1.161E+03	0.000E+00	2.471E+04
Cu	0.000E+00	0.000E+00	6.237E+03	0.000E+00	1.146E+04
Pb	0.000E+00	0.000E+00	2.494E+04	0.000E+00	1.622E+03
Ni	0.000E+00	0.000E+00	4.760E+02	0.000E+00	3.058E+03
Se	0.000E+00	0.000E+00	3.520E+02	0.000E+00	7.141E+03
Zn	0.000E+00	0.000E+00	2.157E+03	0.000E+00	2.744E+03

TASK 5. FIELD DEPLOYMENT

SUBTASK 5.1. SELECTION AND CHARACTERIZATION OF A STUDY SITE FOR A PLOT STUDY

Selection of a Study Site

Task 5 of this research consisted of a small-scale field deployment and evaluation of the capping technologies developed in the laboratory during earlier phases of the project. The first step in this process (Subtask 5.1) was to identify a suitable site for the field study. Sediment contaminant levels have been measured at numerous locations on the 800 km² Savannah River Site near Aiken, SC. These data were examined for candidate locations, which were subsequently surveyed in the field to identify a site that was suitable for evaluating the effects of the experimental caps on contaminant mobility and toxicity, cap durability and resistance to erosion, and cap acceptability to benthic organisms. Two potential study sites on the Savannah River Site were selected for field investigation following preliminary surveys of maps and sediment contaminant records; the sites were located on Tims Branch and Steel Creek (Figure 5). Of these, the site on Steel Creek was chosen for the field deployment because of its greater width and depth, which provide more realistic conditions and permit larger experimental plots.

Characterization of a Study Site

Figure 6 shows the configuration of the experimental caps in Steel Creek. Samples of surface water, pore water and sediment were collected from each plot before cap construction to characterize the study site.

Sample Collection and Analysis before Cap Construction

Surface Water

Surface (water column) water quality was recorded in each plot with a portable environmental sampler (Model 7518-02, Cole-Parmer Instrument Company) before cap construction (Picture 3). The following parameters were recorded: temperature, electrical conductivity (EC), dissolved oxygen (DO), pH, and redox potential (ORP). Total carbon (TC), total organic carbon (TOC), and total inorganic carbon (TIC) in the water samples were measured with an OI Analytical Combustion TOC Analyzer, Model 1020A. The sample was first transferred to a vessel that would not contribute TC and then introduced to the TOC Analyzer through a sipper, which pulled a fixed volume for analysis. The aqueous sample was heated to approximately 900°C in a high oxygen environment, and the TC evolved as CO₂ was measured. TIC was determined by adding phosphoric acid to the sample and measuring the gas devolved. TOC was calculated from the difference in the TC and TIC measurements. Current velocity was recorded using a portable water flow meter (Marsh-McBirney, Inc., Model 201) (Picture 4).

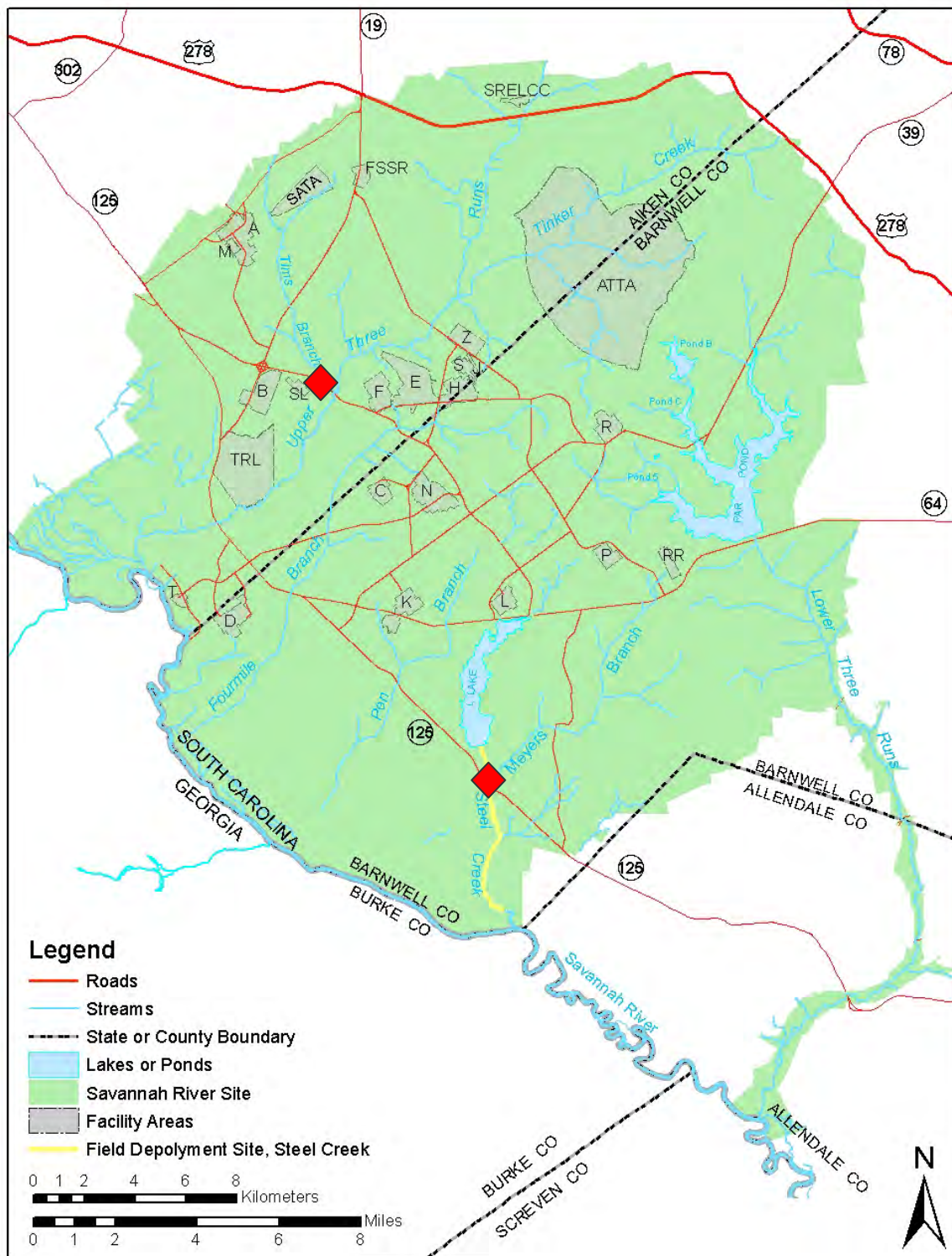


Figure 5. Map of the Savannah River Site showing Potential Field Study Locations on Steel Creek and Tims Branch (red diamonds).

Scheme of Field Deployment

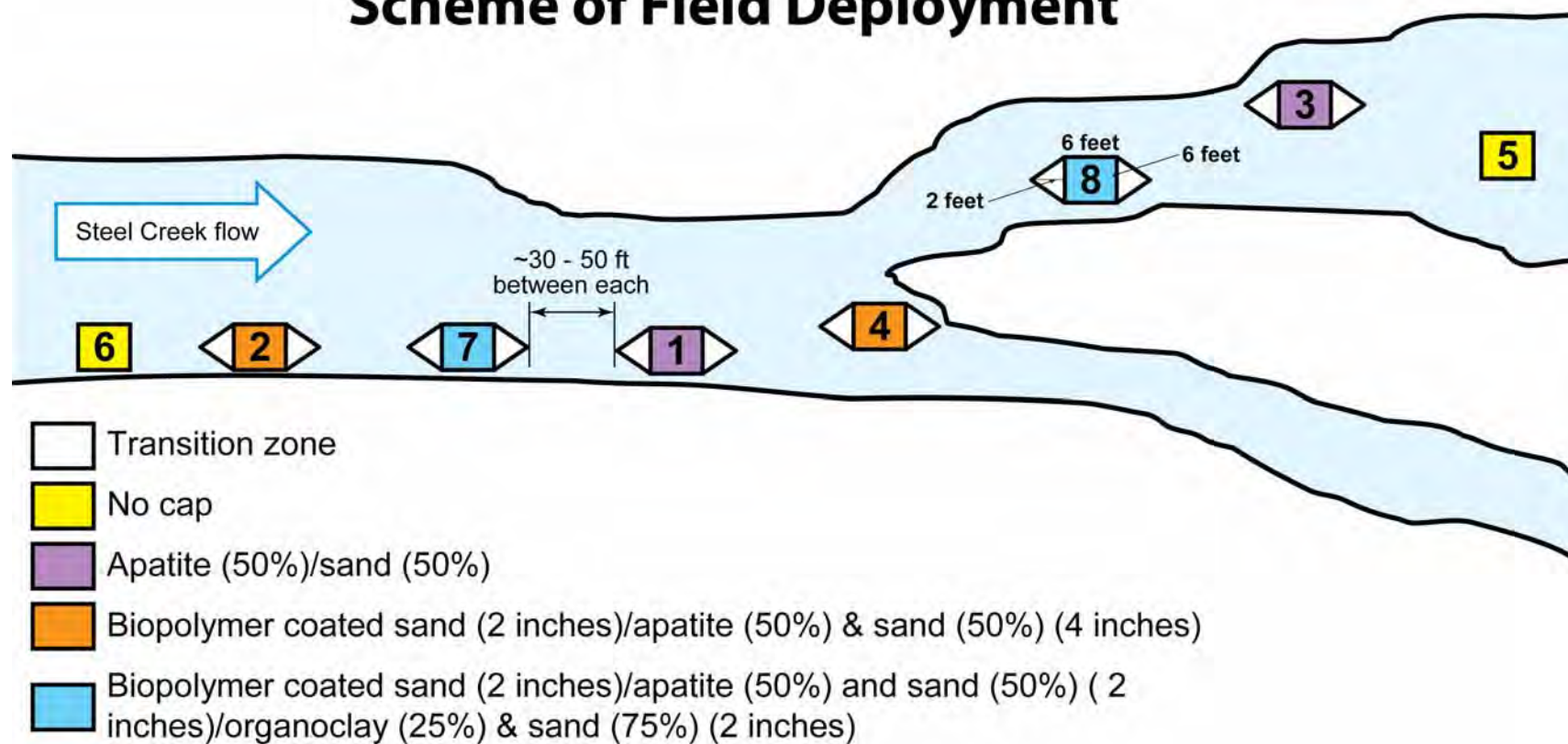


Figure 6. Scheme of Field Deployment.



Picture 3. In-situ Measurement of Pore Water Properties.



Picture 4. Measurement of Water Flow with Portable Water Flow Meter (Marsh-McBirney, Inc., Model 201).

Pore Water

Pore water samplers were constructed using a stainless steel wire mesh screen connected to nylon tubing. Different colored tubing was used for each depth interval to avoid confusion in the field during subsequent sampling events. Two pore water samplers were buried in the stream sediment underneath each cap to a depth of about two inches, and two pore water samplers were buried to a depth of about two inches within each cap (Figure 7). Additionally, two pore water samplers were located downstream of each plot (6 feet apart) to help determine if cap materials were transported downstream (P concentrations served as an indicator of apatite transport, and C concentrations served as an indicator of biopolymer transport) (Figure 7). The tubes leading from the sediment pore water samplers were white, and the tubes leading from the cap pore water samplers were black. Pore water was collected before cap construction from all sediment pore water samplers. Pore water samples were analyzed for metal concentrations and TC and TIC content. Measurements of temperature, EC, DO, pH, and ORP were conducted in-situ in the field with an Environmental Sampler (Model 7518-02, Cole-Parmer Instrument Company).

The pore water samples were analyzed for TC, TIC, TOC, and metals in the lab. The TC and TIC concentrations were measured using an OI Analytical Combustion TOC Analyzer, model 1020A and metals were analyzed by ICP-MS.

Sediment Characterization before Treatment

Two sediment core samples were collected from each plot to characterize the sediments before cap construction. Sediment cores were collected with a push-tube coring device. The first sediment core was split into two parts: 0-2 inches and 2-4 inches. The sediment from the 2-4 inch portion was analyzed for acid volatile sulfide (AVS) and simultaneously extracted metals (SEM) (Allen et al., 1991). The second sediment core from each plot was split into three parts: A (0-2 inches), B (2-4 inches), and C (below 4 inches). All three parts of this sediment core were analyzed for metal concentrations, pH, Eh, organic content in the solid phase, and speciation.

A solid TOC Analyzer manufactured by OI Analytical was used to measure both TC and TOC in the sediment samples.

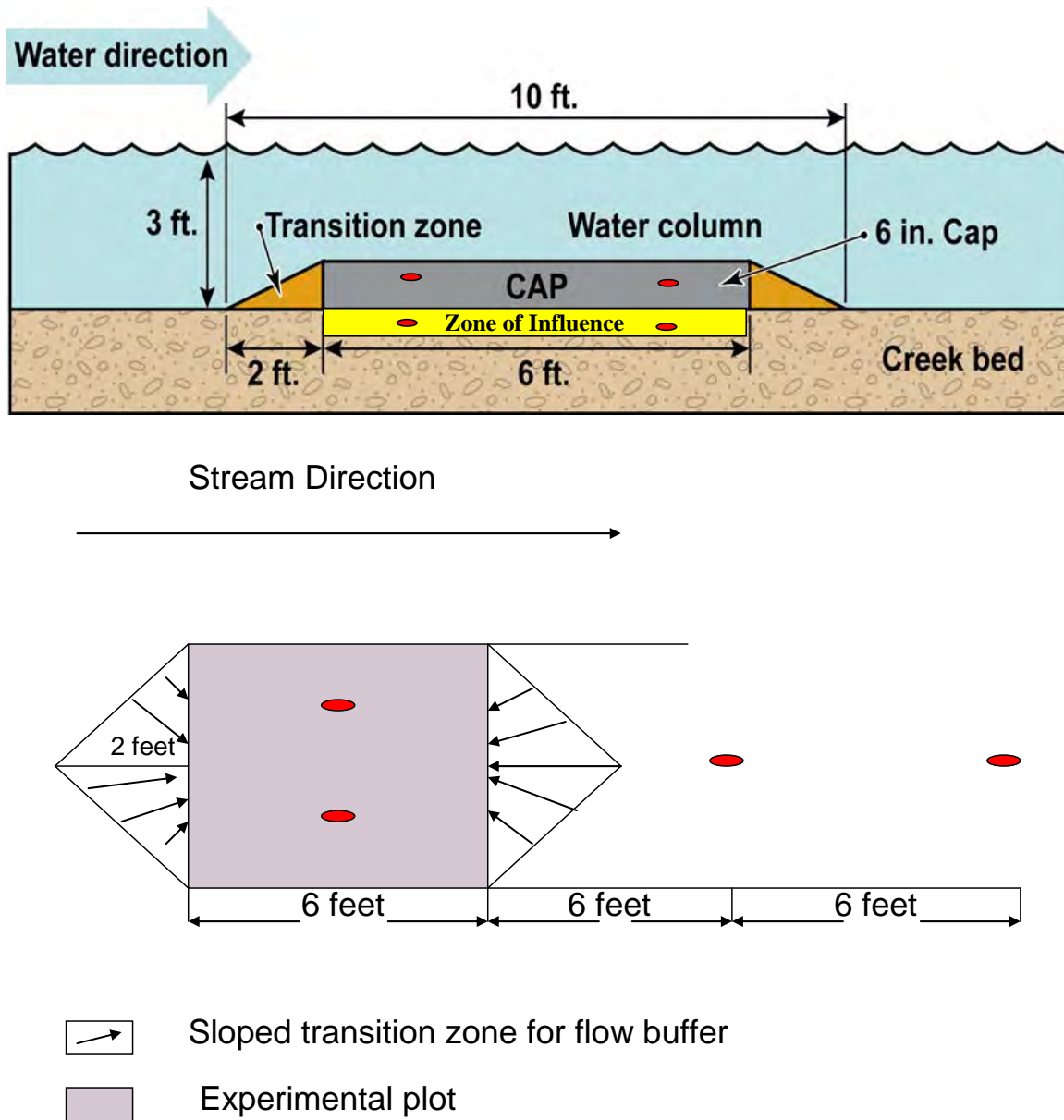


Figure 7. Top and Cross-section Views of Cap and Locations of the Sippers.

SUBTASK 5.2. CAP CONSTRUCTION

Cap Construction

Materials for each cap were premixed accordingly to the experimental plan (Table 9) in a multi-use portable mixer (Picture 5). The mixed amendments were transported to the plot locations by an eight wheel, amphibious, all-terrain vehicle (Picture 6). Construction materials were moved from the all-terrain vehicle to each experimental plot (Figure 7) and manually deposited within an aluminum frame. The four-wall aluminum frame, with dimensions corresponding to the cap length and width, was erected in each plot prior to cap construction (Picture 8). Wedge-shaped flow deflectors were present at the leading and trailing edges of the frame to deflect downstream flow, stabilize the frame, and reduce turbulence (Picture 8). The frame and deflectors were driven two to three inches into the stream bottom to prevent undercutting and were anchored at the corners with metal stakes driven into the sediment. The frame extended above the top of the cap by a few inches to facilitate material settlement and prevent the downstream transport of cap materials during construction. The frame was carefully removed wall-by-wall when construction was completed and all cap materials had settled (Picture 9). The top cap layers that contained low density materials, such as biopolymers, were applied as a slurry to prevent material separation and differential settling.

The plots were permanently marked with 4 foot long PVC pipes in the plot corners and with one PVC pipe on the stream bank which served as an additional reference point for locating the plots using simple surveying methods. The reference point on the stream bank ensured that plots could be located even if buried by sediments displaced by flood flows.

Table 9. Material Composition of Experimental Caps in Steel Creek; plot numbers correspond with numbers on the field deployment scheme (Figure 6).

Plot No.	Cap Description	Layer No.	Layer Thickness (in.)	Sand (lb.)	Apatite (lb.)	Organo-clay (lb.)	Guar Gum (lb.)	Xanthan (Kelzan brand) (lb.)
6	No cap (control plot)							
5	No cap (control plot)							
3	50% apatite and 50% sand in one layer (applied dry)	1	6	850	850			
1	50% apatite and 50% sand in one layer (applied dry)	1	6	850	850			
2	2.5% cross-linked biopolymer and 97.5 % sand layer (top layer; applied as slurry)	1	2	570			15	15
	50% apatite and 50% sand in layer (bottom) (applied dry)	2	4	570	570			
4	2.5% cross-linked biopolymer and 97.5 % sand layer (top layer; applied as slurry)	1	2	570			15	15
	50% apatite and 50% sand in layer (bottom) (applied dry)	2	4	570	570			

Table 9 (continued). Material Composition of Experimental Caps in Steel Creek

7	2.5% cross-linked biopolymer and 97.5 % sand layer (top layer; applied as slurry)	1	2	570			15	15
	50% apatite and 50% sand (middle layer; applied dry)	2	2	285	285			
	25% organoclay and 75% sand (bottom layer; applied dry)	3	2	425		100		
8	2.5% cross-linked biopolymer and 97.5 % sand layer (top layer; applied as slurry)	1	2	570			15	15
	50% apatite and 50% sand (middle layer; applied dry)	2	2	285	285			
	25% organoclay and 75% sand (bottom layer; applied dry)	3	2	425		100		



Picture 5. Amendments were Mixed in a Multi-Use Portable Mixer (Kobalt™)



Picture 6. Mixed Amendments were Transported in All-Terrain Vehicle.



Picture 7. All Terrain Vehicle in Use.



Picture 8. Cap Frame during Deployment.



Picture 9. Cap Frame was Removed in Sections after Cap Construction was Completed.

SUBTASK 5.3. POST - CAP MONITORING

In this study the effects of active caps on metal bioavailability, erosion resistance, and toxicity were evaluated in pilot-scale experimental active caps in Steel Creek, at the Savannah River Site near Aiken SC, USA (Figure 5). There were eight plots with four treatments: two controls consisting of uncapped sediments; two caps composed of apatite and sand; two caps composed of a layer of biopolymer/sand slurry over a layer of apatite and sand; and two caps composed of a top layer of biopolymer/sand slurry, a middle layer of apatite and sand, and a bottom layer of organoclay and sand (Figures 6 and 8).

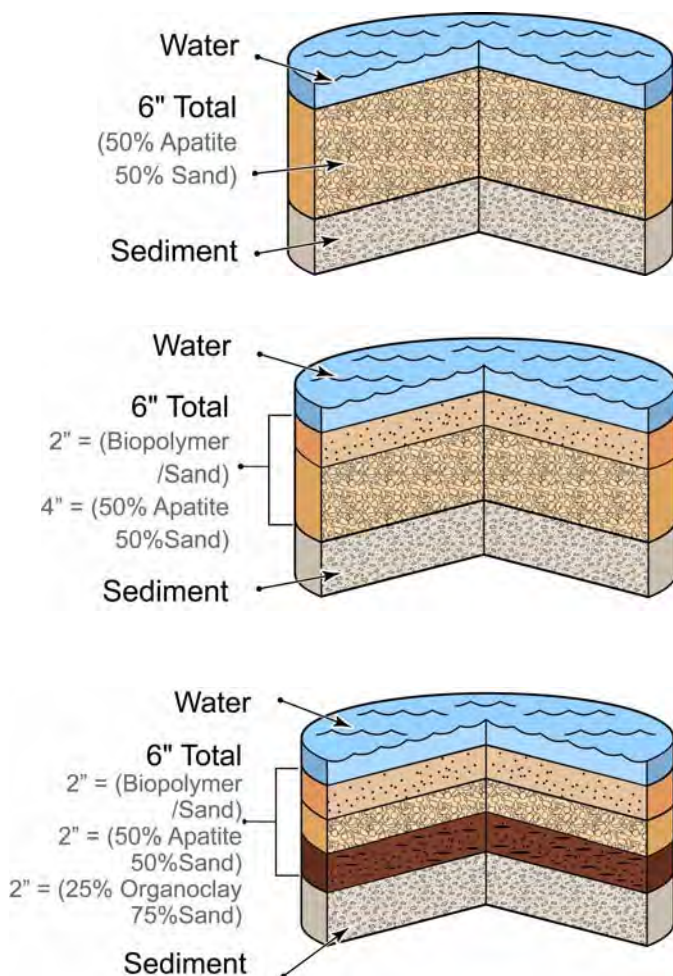


Figure 8. Three Types of Caps were Tested in the Field Deployment.

The monitoring of active caps in Steel Creek was conducted for twelve months. The effectiveness of the active caps was determined based on evaluation of contaminant availability in sediment, amendment impact on benthic organisms (toxicity tests), and cap resistance to erosion.

The effect of the active caps on metal bioavailability was evaluated by metal concentrations in surface and pore water, acid volatile sulfide (AVS), simultaneously extracted metals (SEM), SEM/AVS ratio, zone of influence (ZOI), and diffusive gradients in thin films (DGT) probes.

The impact of the amendments that were used in the active caps on benthic organisms was evaluated by active biomonitoring using caged organisms held in-situ. The following organisms were tested: *Lumbriculus variegatus* (California blackworm), *Corbicula fluminea* (Asiatic clam), and *Hyaella azteca* (amphipod).

The erosion evaluation was based on visual observations, sediment core characterization for integrity of the cap layers, and measurements of erosion rates and critical shear stresses by an ASSET flume.

Sample Collection and Analysis after Cap Construction

Surface Water

Surface (water column) water quality was recorded in each plot with a portable environmental sampler (Model 7518-02, Cole-Parmer Instrument Company) every month for the first two months and every three months thereafter. The following parameters were recorded: temperature, EC, DO, pH, and ORP. Total carbon, TOC, and TIC in the water samples were measured with an OI Analytical Combustion TOC Analyzer, Model 1020A. Stream velocity was recorded using a portable water flow meter (Marsh-McBirney Inc., Model 201).

Pore Water

Two pore water samplers were buried in the stream sediment underneath each cap to a depth of about two inches, and two pore water samplers were buried to a depth of about two inches within each cap (Figure 7). Additionally, two pore water samplers were located downstream of each plot (6 feet apart) to help determine if cap materials were transported downstream (Figure 7). Pore water was collected from all pore water samplers monthly for the first two months after cap construction and every three months thereafter. Pore water samples were analyzed for metal concentrations and TC and TIC content. Measurements of temperature, EC, DO, pH, and ORP were conducted in-situ in the field with an Environmental Sampler (Model 7518-02, Cole-Parmer Instrument Company). The pore water samples were analyzed for TC, TIC, TOC, and metals in the lab. The TC and TIC concentrations were measured using an OI Analytical Combustion TOC Analyzer, Model 1020A.

Sediment Characterization after Treatment

Six and twelve months after field deployment of the caps, sediment core samples were collected from plots located in depositional areas of Steel Creek [control (plot #5), apatite cap (plot #3), biopolymer/apatite cap (plot #4), and biopolymer/apatite/organoclay cap (plot #8)] to characterize sediment chemistry. Four sediment cores were collected with a push-tube coring device from the native sediment beneath each plot. The sediment cores were split into three parts: 0-2.5 cm and 2.5-5 cm. The sediment from the 5-10 cm portion was analyzed for AVS and SEM (Allen et al., 1991).

The sediment samples were also analyzed for pH, TC, and TOC. Both TC and TOC concentrations were measured by a solid TOC Analyzer manufactured by OI Analytical.

Quality control for samples analyzed by SEM/AVS and double acid methods included replicate analysis, blanks, matrix spike recovery, and blank spike recovery.

Evaluation of Zone of Influence (ZOI)

Laboratory Study

Contaminated sediment from Tims Branch, a stream located on the Savannah River Site near Aiken, SC, was used for an experiment that investigated the ZOI created by the diffusion of active cap materials into the sediment beneath the active caps. The sediment was contaminated with Cd, Cr, Co, As, Ni, Se, Pb, Zn, and possibly other metals. Four simulated caps (each 5 cm thick) were tested: sand; North Carolina apatite; organoclay (OCB 750 from Biomin, Inc.); and a three layer cap composed of sand coated with biopolymer (guar gum cross linked with chitosan), apatite, and organoclay. Each cap was replicated twice. The caps were placed over 10 cm (421 grams) of sediment at the bottom of clear plastic tubes. The simulated caps and underlying sediment were gently saturated with DI water, after which 500 ml of DI water was added to each tube. After the six month experiment was terminated, the water was decanted and analyzed for pH, EC, TC, TIC, TOC, and metals by ICP-MS. The solids were separated into cap material and sediment. The sediment was sliced into four layers: A (0- 1.5 cm), B (1.5 - 2.5 cm), C (2.5 - 5 cm), and D (5 – 10 cm). Two grams of sediment from each layer were extracted with 10 ml of DI water and analyzed for metal concentrations by ICP-MS.

Field Study

To determine the effects of active reagents in deployed caps on sediment and to determine the ZOI of the tested amendments, sediment cores were collected twice: six and 12 months after cap placement. Two replicate cores were collected from the control (plot #5), apatite cap (plot #3), biopolymer/apatite cap (plot #4), and biopolymer/apatite/organoclay cap (plot #8). The cores were divided into cap material and sediment. The sediment was split into two layers: 0-2.5 cm and 2.5-5 cm. Sub-samples from each layer were extracted with double acids (0.05 n HCl and 0.25 n H₂SO₄) for evaluation of available P and other elements. Phosphorous and metals in the double acid extracts were analyzed by ICP-MS. Double acid extraction was conducted on five grams of sediment from each sub-sample. Each sediment sample was put into a 50 ml centrifuge

tube with 40 ml of the double acid extracting solution (0.05 n HCl and 0.25 n H₂SO₄). The tubes were shaken for 30 minutes and then centrifuged for 10 minutes. The supernatant was filtered through Whatman filters (#41) into plastic bottles. These extract solutions were analyzed for P and other elements by ICP-MS.

DGT Probes for Assessment of Active Cap Effectiveness

Sediment DGT probes were placed in-situ in untreated sediment and an apatite/sand cap plot to determine their ability to measure metal bioavailability. Additional sediment and cap samples were returned to the laboratory where DGT performance was evaluated under laboratory conditions. Comparison of DGT performance between the laboratory and field could be important because the configuration of DGT probes generally limits their use to shallow sediments. Metal concentrations in deep sediment cores could be measured ex-situ in the laboratory using DGT methods providing that laboratory and field measurements with DGT are in agreement. Successful results could expand the usefulness of DGT methods to deeper sediments including sediments located below active caps.

Sediment DGT Probes - Method

DGT sediment probes were sealed and refrigerated in a plastic bag with a few drops of 0.01 M NaNO₃, added as necessary over time to keep the units moist. The DGT sediment probes were deoxygenated before deployment. A 0.01 M NaCl solution was created with 10 grams of Chelex-100 in order to remove any trace metals in the NaCl solution. The NaCl solution was added to a container with enough space to cover the open windows of the DGT sediment probes with solution and accommodate plastic tubing for degassing. Nitrogen was then bubbled through the solution for 30 minutes. Immediately following the degassing, the container was placed in an anaerobic chamber to further deoxygenate the solution. The solution with probes was removed from the anaerobic chamber after 12 hrs, and the probes were transported to the field.

The probes were deployed by inserting them vertically into the sediment until a previously made mark 2 cm below the window was in line with the sediment/water interface. The sediment temperature at the time of the deployment was recorded as well as 24 hr later when the unit was retrieved. Upon removal from the sediment, the unit was rinsed with deionized water to remove any particles left on the window area. The unit was then sealed in a clean plastic bag and stored in a refrigerator until analysis.

Prior to analysis, the internal portions of the sediment probes were retrieved by cutting through the window at the sediment/water interface and below using a Teflon coated blade. The gel and filter layers were then placed on a clean flat surface, and the filter and diffusive gel layers peeled away so that the bottom resin-gel layer could be removed. The resin-gel was then placed in a small sample tube with enough 1 M HNO₃ to fully immerse the resin-gel. The tube was sealed and the solution allowed to sit for 24 hr, after which an aliquot of the solution was removed and diluted at least 5 times with deionized water prior to analysis by ICP-MS.

The resulting concentration from the diluted aliquot was adjusted for dilution to determine the concentration of metals in the 1M HNO₃ elution, C_e . The mass of metal accumulated in the resin gel layer (M) was calculated using equation 18 for each metal:

$$M = \frac{C_e * (V_{NO_3} + V_{gel})}{f_e} \quad (18)$$

where:

V_{NO_3} = amount of nitrate added (750 μ L for sediment probes, based on the amount of nitric acid required to submerge the resin-gel layer)

V_{gel} = volume of the resin gel (810 μ L)

f_e = elution factor of 0.8 (Zhang and Davison, 1995 and 2001)

The concentration of metal measured by the DGT unit (C_{DGT}) was calculated using equation 19:

$$C_{DGT} = \frac{M * \Delta g}{D * t * A} \quad (19)$$

where

Δg = thickness of the diffusive layer and filter layer (0.096 cm) (Zhang and Davison, 1995 and 2001)

D = diffusion coefficient each metal at the retrieval temperature

t = deployment time (24 hr = 86400s)

A = exposed area of the DGT unit (23.4 cm²)

Statistical Analysis

The experimental results were analyzed using ANOVA. Two separate ANOVAs were performed. The first included only DGT data and assessed the significance of three factors: treatment (apatite cap vs. control plot), location (i.e., location of the sediment samples during 24 hour exposure period – laboratory vs. field), and metal (Cd, Co, Cr, Cu, and Ni) plus all interactions. The second ANOVA compared DGT data with sediment pore water data collected using sippers. It included three factors: treatment (apatite cap vs. control plot), method (DGT vs. pore water collected with sippers), and metal (Cd, Co, Cr, Cu, and Ni) plus all interactions. The dependent variable in both ANOVAs was the measured metal concentration (ppm), which was log₁₀ transformed to better meet the assumptions of analysis of variance.

Cap Monitoring for Erosion

Monitoring after cap placement was designed to characterize the effectiveness of cap construction and resistance to erosion. Sediment cores were collected weekly for the first month and monthly thereafter to characterize the integrity of the cap-layers. The sediment surface downstream from the tests plots was visually examined for displaced cap materials.

On May 7, 2009, eight sediment cores were collected for evaluation of erosion from the following plots: three cores from the apatite cap (plot #3), three cores from the biopolymer/apatite/organoclay cap (plot #8), and two cores from the untreated control area (plot #5) (Picture 10). Core samples were collected by pushing thin-walled, polycarbonate,

circular core tubes (~10 cm in diameter) into the sediment. The distance of penetration into the sediment varied with the characteristics of the sediment (i.e., greater penetration occurred in softer sediment than in more compacted sediment). When maximum penetration was reached a large rubber stopper was used to create a seal at the top of the tube. The tube was withdrawn from the sediment, and a plug was placed in the bottom of the tube to prevent loss of sediment. The core was then removed from the water, the bottom plug was pushed into the tube to consolidate the core and remove excess water, and an additional plug was placed at the top of the tube and sealed with tape. The sediment strata and density profiles remained intact during this process resulting in a relatively undisturbed core. Sediment cores varying in length from 13.1 to 16.2 cm were obtained from the Steel Creek plots by this method. The cores were packed with ice in an insulated cooler and shipped to Sandia National Laboratories (SNL) in Carlsbad, NM for erosion testing. At SNL, the core samples were analyzed in an ASSET flume.



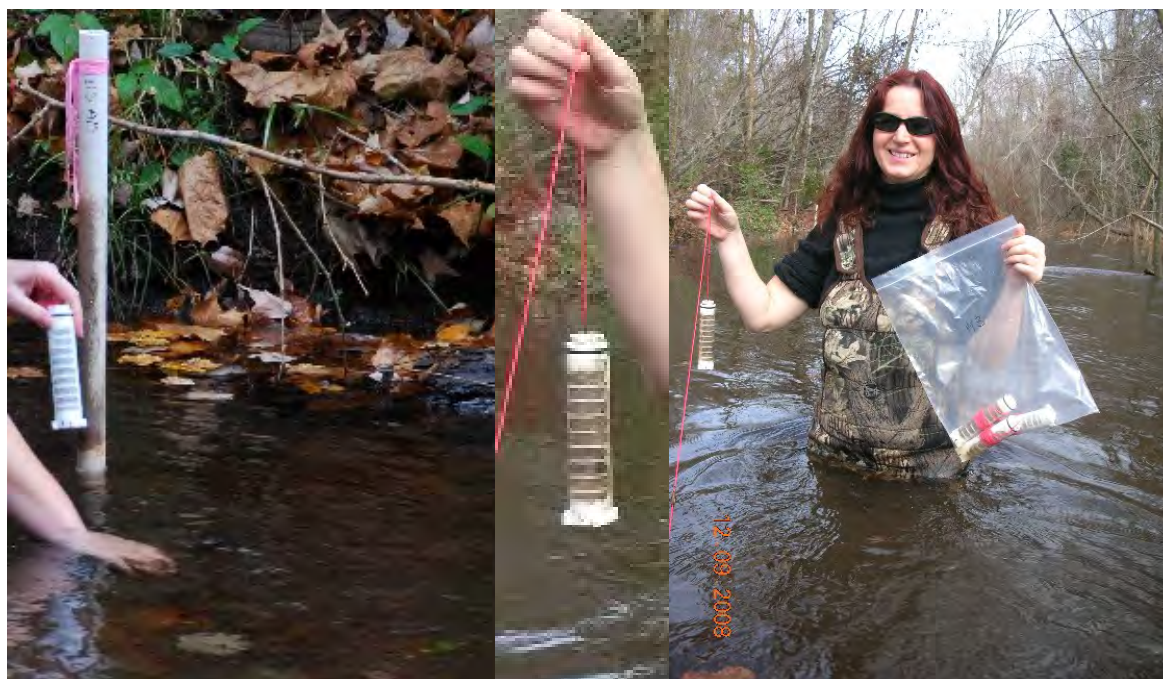
Picture 10. Coring Tubes and Sediment Cores used for Evaluation of Erosion Resistance by an ASSET Flume.

Active Biomonitoring

Active biomonitoring was used in the field deployment to assess the acceptability of different types of experimental caps to benthic organisms. Active biomonitoring consists of translocating organisms from clean reference sites or laboratory cultures to cages within contaminated sites where they can be maintained for the in-situ study of environmental toxicity and contaminant uptake. This procedure has numerous advantages over the collection of indigenous sediment organisms including the ability to provide adequate quantities of the same organisms for defensible comparisons among sites, definite knowledge of exposure periods, and more control of potentially confounding variables such as life stage. Active biomonitoring can encompass many of the complex environmental factors (e.g., temporal fluctuations, organism behavior) that influence the toxicity and availability of sediment contaminants. Three types of benthic organisms were used for active biomonitoring including the amphipod *Hyaella azteca*, the California blackworm *Lumbriculus variegates*, and the Asiatic clam *Corbicula fluminea*.

Active biomonitoring started on November 13th, 2008 to assess the survival of California blackworms in the amendments used in the experimental caps (Picture 11). California blackworms were placed in small screened cages that contained the cap amendments or native

sediment in case of controls. The cages with California blackworms and cap materials were placed in the following plots: apatite/sand (plot #3), biopolymer/apatite/sand (plot #4), biopolymer/apatite/ organoclay/sand (plot #8), and control (plot #5; cage with only native sediment). Four cages were placed in each plot except for the plot with the biopolymer/apatite/organoclay/sand cap. Eight cages were placed in the latter: four cages with biopolymer/apatite/sand layer, and four cages with organoclay/sand layer. The screened (300 μ mesh) 15 cm long and 2.5 cm diameter cages were made of plastic (Picture 11). Amendments or native sediment were placed in the cages before adding pre-weighed worms (about 2.0 g per cage). The cages were then placed in a horizontal position within the substrate in each plot. Most were partly buried so that about 25% of the cage was exposed; however, those within the organoclay sand layer in plot 8 were buried more deeply (about 7-8 cm). The cages were retrieved on 12/9/2008 after 28 days of exposure (Picture 11). The substrate was removed from the cages, and the California blackworms were recovered from the substrate and weighed as a measure of survival and growth. ANOVA followed by Holm-Sidak multiple comparison tests were used to assess the significance of differences among groups.



Picture 11. Installation of Cages with California Blackworms on November 13, 2008 and Collection of Cages after 28 days in the Field (December 9, 2008).

The California blackworm is a freshwater oligochaete commonly found in shallow ponds, lakes, and marshes throughout North America and Europe. California blackworms are aerobic organisms that use their anterior end to burrow into shallow sediment and extend their posterior end above the sediment surface for oxygen and carbon dioxide exchange. They survive well in the laboratory, can be kept alive for extended periods at low temperatures, are easily cultured, and are readily available from commercial sources at low cost. Commercially available worms are generally from 2.5 to 5.0 cm long, although they can reach larger sizes. Live worms can be easily distinguished from dead worms on the basis of color and motility.

California blackworms were obtained from Aquatic Foods, a company that produces these organisms in large quantities, primarily as a live food for tropical fish. Aquatic Foods uses commercial fish food to produce California blackworms in dedicated rearing ponds supplied with a combination of filtered river water and well water. The worms were thoroughly rinsed with chilled, chlorine free water upon receipt from Aquatic Foods and stored under refrigeration in shallow trays filled with dechlorinated tap water to a depth of about 2.0 cm. Worms were removed from the trays as required to conduct the experiments described below.

A second active biomonitoring experiment in Steel Creek was initiated on March 5th, 2009 to assess the survival of the Asiatic clam *Corbicula fluminea* in the amendments used in the experimental caps (Picture 12). *Corbicula fluminea* is a common organism in many of the streams on the SRS. Clams were collected from Steel Creek and placed in small screened cages that contained the cap amendments or native sediment in the case of controls. The cages with clams and cap materials were placed within the following plots: apatite/sand (plot # 3), biopolymer/apatite/sand (plot # 4), biopolymer/apatite/organoclay/sand (plot # 8), and control (plot # 5; cage with native sediment). Four cages were placed in each plot except for the biopolymer/apatite/organoclay/sand cap, which consisted of three layers. Eight cages were placed in the latter: four cages within the biopolymer/apatite/sand layer and four cages within the organoclay/sand layer. The cages were made of plastic with 1 to 2 mm openings for water circulation (Picture 12). Amendments or native sediment were placed in the cages before adding 10 clams (pre-weighed in aggregate). The cages were then placed horizontally within the substrate in each plot and partly buried so that about 25% of the cage was exposed. Cages within the organoclay sand layer within plot 8 were buried more deeply (about 7-8 cm). The cages were retrieved on April 3rd, 2009 after four weeks of exposure (Picture 13). The clams were recovered from the substrate, examined to determine if they were alive (Picture 13) and weighed in aggregate. The Kruskal-Wallis test was used to assess the significance of differences among groups.



Picture 12. Installation of Cages with Clams on March 5, 2009.



Picture 13. Collection of Clam Cages after 4 weeks in the Field (April 3, 2009).

A third active biomonitoring experiment was initiated on May 14th, 2009 to assess the survival of the amphipod *Hyaella azteca* in the amendments used in the experimental caps. The amphipod *Hyaella azteca* is commonly used to assess sediment toxicity. Amphipods were placed in small cages that contained the cap amendments or native sediment in the case of controls. Openings in the cylindrical plastic cages were covered with fine mesh screen to retain the organisms and permit water circulation (Picture 14). Amendments or native sediment were placed in the cages before adding 10 amphipods to each cage. The cages were placed within the following plots: apatite/sand (plot # 3), biopolymer/apatite/sand (plot # 4), biopolymer/apatite/organoclay/sand (plot # 8), and control (plot # 5; cage with native sediment). Four cages were placed in each plot except for plot 8 which contained biopolymer/apatite/organoclay/sand cap with three layers. Eight cages were placed in this cap: four cages within the biopolymer/apatite/sand layer and four cages within the organoclay/sand layer. The cages were situated horizontally and partially buried within the substrate in each plot; however, four cages in the organoclay sand layer (plot 8) were completely buried to a depth of 7-8 cm. The cages were retrieved on May 22nd, 2009 after nine days of exposure. The amphipods were recovered from the substrate and counted. ANOVA was used to assess the significance of differences in percent survival among groups.



Picture 14. Installation of Cages with *Hyaella azteca*.

RESULTS AND DISCUSSION

TASK 1. EFFECT OF AMENDMENTS ON CONTAMINANT MOBILITY AND BIOAVAILABILITY – LABORATORY STUDY

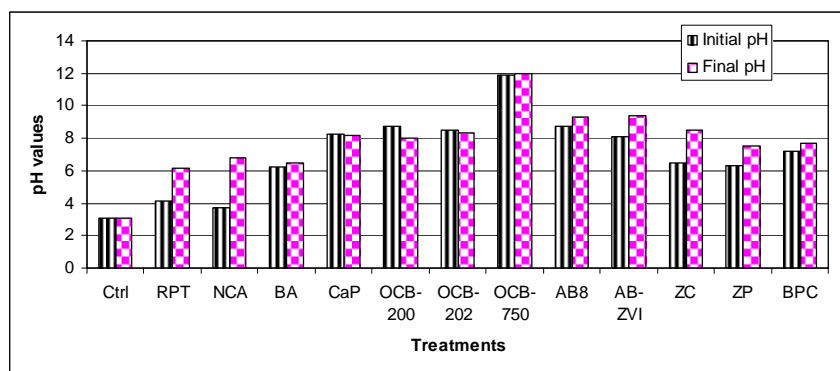
SUBTASK 1.1. SORPTION AND DESORPTION OF CONTAMINANTS BY SEQUESTERING AGENTS

Effect of Sequestering Agents on pH

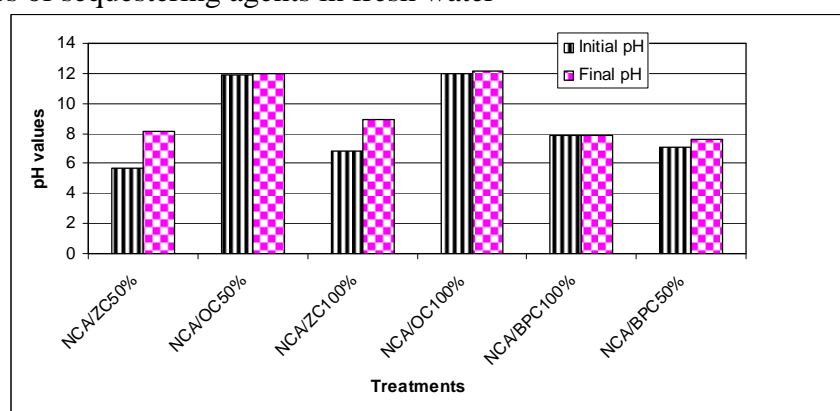
Changes in pH resulting from the application of amendments can be important because of the potential effects of pH on aquatic organisms. Most freshwater lakes, streams, and ponds have a natural pH in the range of 6 to 8, and extreme pH can harm invertebrates and fish. When the pH of freshwater becomes highly alkaline (e.g. 9.6), the effects on fish may include death, damage to outer surfaces like gills, eyes, and skin, and an inability to dispose of metabolic wastes. High pH may also increase the toxicity of other substances. For example, the toxicity of ammonia is ten times more severe at pH 8 than at pH 7, and the mobility of potentially toxic metals including As, Mo, Se, and Cr increases with pH. Harmful effects can also occur when the pH falls below 6 and especially below 5. As the pH approaches 5, non-desirable species of plankton may begin to predominate in some aquatic systems and populations of desirable fish may diminish. Calcium levels in female fish may decline to the point that egg production fails or eggs and/or larvae develop abnormally. Acidity can also result in the release of aluminum ions (Al^{3+}) attached to minerals in nearby sediment, resulting in excessive mucus formation by fish that can cause asphyxiation by clogging their gills. Therefore, it is important to carefully monitor the effects of potential amendments on pH. Identification of amendments or combinations of amendments that avoid large and/or rapid changes in pH may be an important factor in the development of an active capping system that results in minimal environmental impact.

Figure 9 shows the effect of the sequestering agents on the spike solution pH in fresh water. The pH measurements were taken after one hour (initial pH) and after one week of contact of the spike solution with the amendments. The addition of some amendments to the spike solution resulted in large changes in pH. Organoclays increased the pH of the spike solution the most; for example, Clayfloc™ 750 (OCB-750) increased the pH of the spike solution (control) from 3.09 to 11.9 (Figure 9 - A). In some cases, mixtures of amendments were associated with smaller pH shifts than were individual amendments (Figure 9 - B). The initial pH of the salt water spike solution was 7.2. Amendments such as rock phosphate from Tennessee, North Carolina apatite, calcium phytate, Aquablok™ -ZVI, and zeolite did not result in large pH changes in the salt water spike solution (Figure 9-C). The greatest changes were observed for OCB-750, which raised pH from 7.2 to 9.6 (Figure 9-C).

A Individual sequestering agents in fresh water



B Mixtures of sequestering agents in fresh water



C Salt water

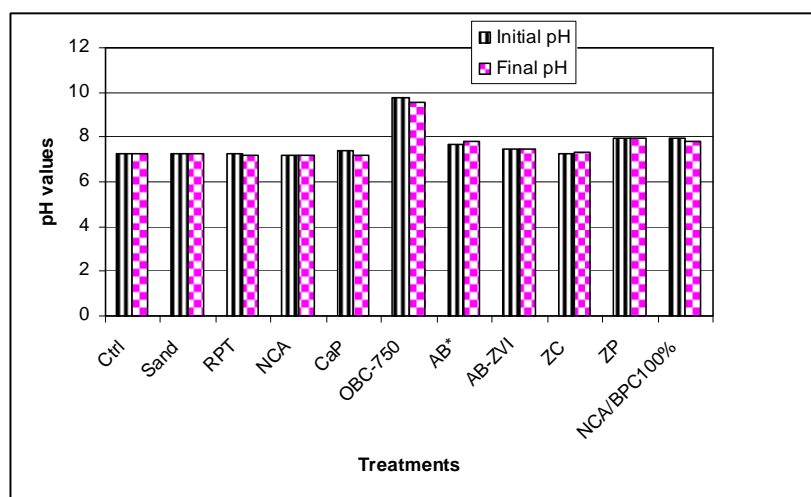


Figure 9. Effect of Sequestering Agents on Spike Solution pH. Ctrl – control (spike solution), RPT – rock phosphate from Tennessee, NCA- North Carolina apatite, BA- biological apatite, CaP – calcium phytate, OC or OCB – organoclays from Biomin Inc., AB8 – aquablok with clay coating, AB-ZVI aquablok with zero valent iron, ZC – clinoptilolite zeolite, ZP – phillipsite zeolite, BPC – chitosan biopolymer.

Sorption and Desorption of Metals in Fresh and Salt Water

The evaluation of the ability of sequestering materials (in different combinations) to stabilize a broad range of contaminants was evaluated in controlled laboratory sorption and desorption experiments. It is important to note that the interpretation of results from laboratory batch sorption tests generally allows no distinction to be made on how the sorbate (i.e., contaminant) is associated with the sorbent (i.e., sediment or sequestering agent). The sorbate may be adsorbed by ion exchange, chemisorption, bound to complexes that are themselves sorbed on the solid, and/or precipitated. Dissolution/ precipitation and adsorption/ desorption are considered the most important processes affecting metal and radionuclide interactions with sediments. In this study the sequestering agents (phosphates, organoclays, zeolites, aquablok, and biopolymers) were tested for As, Cd, Cr, Co, Cu, Pb, Ni, Se, and Zn sorption (removal) and retention in fresh and salt water. The sorption results were used to calculate partition coefficient (K_d) values and percent removal. Presenting the sorption data as percent removal instead of concentrations (mg L^{-1}) facilitated comparisons among amendments.

The K_d values in fresh water were highly variable, differing by an order of magnitude among replicates (Table 10 and Figure 10), but were useful in identifying effective amendments. Phosphates (especially rock phosphate from North Carolina and calcium phytate), organoclay (OCB-750), and biopolymer (BPC) had relatively high K_d values for Cd, Cr, Cu, Pb, Ni, and Zn (Table 10 and Figure 10). Only OCB-750 and the mixture of NCA and OCB-750 produced relatively high K_d values for As and Se. Even though OCB-750 had very high K_d values for all metals, it may not be effective by itself in sediment caps due to high alkalinity, light weight, and cost. Therefore, mixtures such as OCB-750 and apatite might be promising and were evaluated further.

Table 10. Average K_d Values (standard deviation) for Nine Elements for each Tested Amendment (in mL g⁻¹).

Amendments	Cr	Co	Ni	Cu	Zn	As	Se	Cd	Pb
Rock phosphate (RPT) ^a	172 (10) 19,278	827 (166)	205 (25)	6,187 (205)	1,784 (213)	45 (2)	0 (1)	2,787 (470)	13,504 (5,438)
Apatite (NCA)	(2,662)	1,161 (12)	476 (3)	6,237 (202)	2,157 (289)	43 (0)	352 (17)	7,696 (667)	24,942 (11,146)
Biological apatite (BA)	4,333 (551)	3,404 (2,574)	469 (478)	1,717 (494)	2,152 (348)	8 (8)	484 (54)	1,362 (953)	1,980 (1,189)
Calcium phytate (CaP)	23,722 (2,218)	17,302 (1,074)	7,886 (169)	9,106 (1,559)	4,215 (93)	0 (0)	0 (0)	33,077 (2,163)	35,049 (28,003)
Clayfloc TM 200 (OCB-200)	492 (95)	1,314 (65)	918 (26)	802 (23)	520 (2)	1 (9)	0 (8)	514 (28)	385 (17)
Clayfloc TM 202 (OCB-202)	376 (184)	1,411 (178)	919 (64)	800 (62)	539 (39)	1 (2)	1 (0)	442 (9)	428 (50)
Clayfloc TM 750 (OCB-750)	11,348 (28)	24,711 (2,277)	3,058 (140)	11,457 (2,012)	2,744 (132)	33,864 (9,012)	7,141 (1,100)	207,270 (13,2054)	1,622 (240)
Aqua Blok 8 (AB8)	282 (37)	607 (38)	487 (15)	474 (3)	287 (26)	31 (2)	13 (4)	244 (4)	359 (9)
Aqua Blok ZVI (ABZVI)	143 (9)	742 (86)	441 (6)	504 (50)	373 (19)	153 (10)	23 (3)	539 (37)	238 (7)
Clinoptilolite (ZC)	855 (157)	899 (114)	810 (132)	711 (53)	415 (43)	0 (0)	0 (4)	1,184 (156)	2,529 (950)
Phillipsite (ZP)	509 (90)	1,303 (99)	1,012 (134)	948 (128)	477 (28)	11 (5)	1 (4)	3,127 (461)	1436 (203)
Chitosan (BPC)	9,115 (1,250)	16,870 (928)	16,831 (2460)	8,466 (216)	1,926 (193)	23 (6)	0 (3)	20,829 (3,825)	9,536 (4361)
NCA/ZC50% ^b	809 (28)	1,455 (13)	1,122 (24)	822 (66)	498 (12)	5 (7)	69 (2)	728 (41)	378 (29)
NCA/OCB-750-50%	3,937 (1,762)	42,570 (19,491)	5,251 (2442)	5,628 (432)	1,648 (388)	12,818 (4,835)	3,334 (1,093)	42,205 (16,025)	6,374 (7,483)
NCA/ZC100%	352 (1)	643 (16)	548 (22)	490 (7)	284 (30)	0 (0)	43 (2)	538 (53)	316 (9)
NCA/OCB750-100%	3,814 (438)	15,866 (5,439)	1,714 (807)	4,597 (325)	1,589 (82)	4,823 (948)	2,847 (325)	27,560 (34,926)	9,400 (11,792)
NCA/BPC 100%	3,691 (1,276)	3,665 (1,000)	4,676 (560)	5,241 (670)	1,482 (309)	62 (18)	180 (11)	7,263 (1,759)	1,220,795 (10,246)
NCA/BPC50%	3,501 (12)	1,722 (82)	5,026 (540)	7,435 (1,145)	2,165 (174)	138 (61)	221 (65)	5,190 (875)	7,376 (1,143)

^a Weight of an individual amendment was 0.2 g (100%).^b 50% is equivalent to 0.1 g.

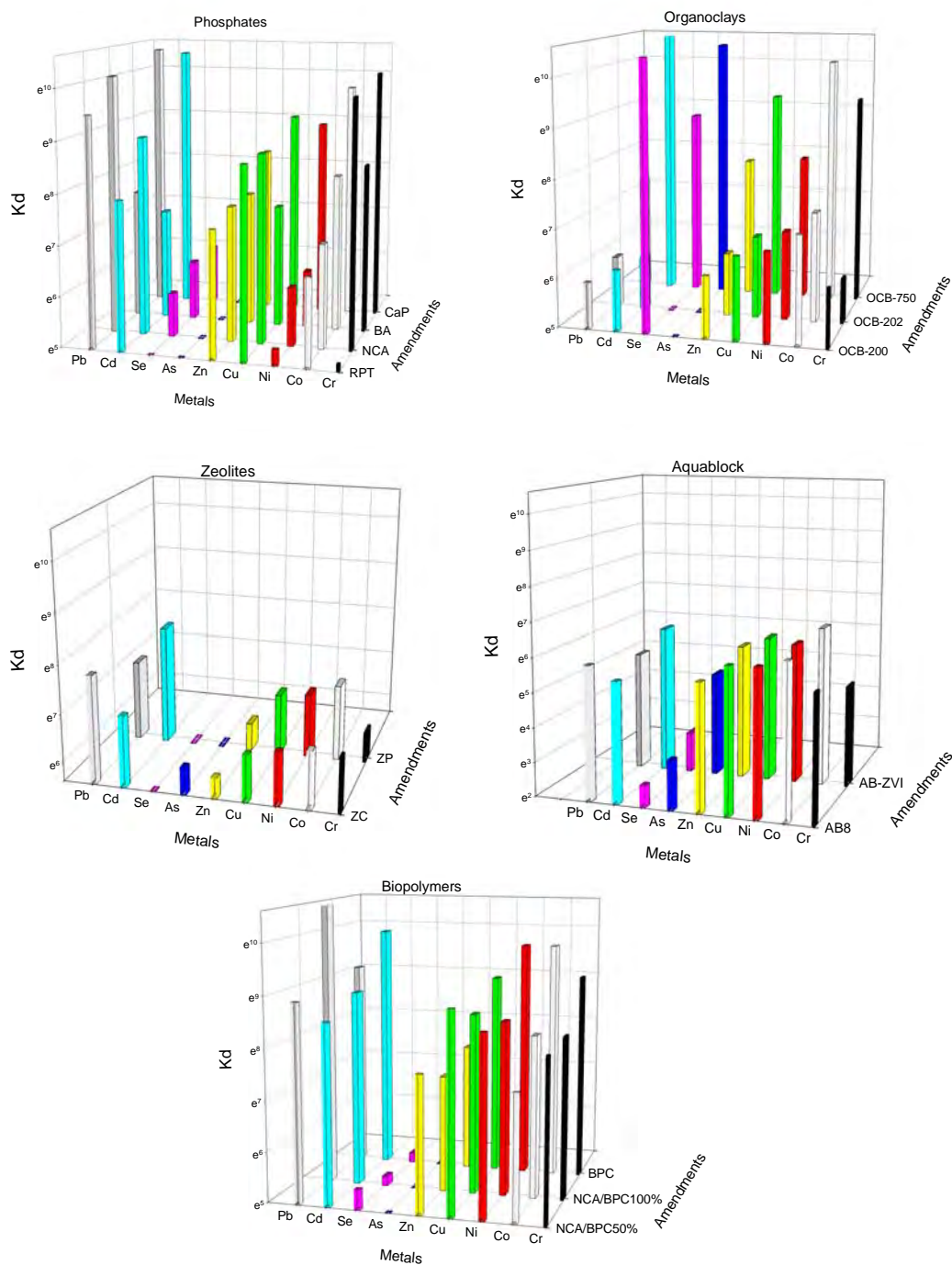


Figure 10. Partition Coefficients (K_d) (mL g^{-1}) for As, Cd, Cr, Co, Cu, Ni, Pb, Se, and Zn in Fresh Water; RPT – rock phosphate from Tennessee, NCA- North Carolina apatite, BA- biological apatite, CaP – calcium phytate, OCB – organoclays from Biomin Inc., AB8 – aquablok with clay coating, AB-ZVI aquablok with zero valent iron, ZC – clinoptilolite zeolite, ZP – phillipsite zeolite, BPC – chitosan biopolymer.

The removal (sorption) of Cd, Co, Cr, Cu, Pb, and Zn from spike solutions in fresh water was very high for almost all tested amendments (Table 11, Figure 11), but removal of As and Se was only effective (greater than 50%) for organoclay-750 (OCB-750), AquablokTM-ZVI (AB-ZVI), and mixtures of North Carolina Apatite (NCA) with OCB-750 or chitosan (BPC) (Table 12). Removal in salt water (3.5% salinity, room temperature, alkaline pH) was very high for most metals, especially Cr, Co, Cu, Pb, and Zn (Figure 12). However, the removal of Cd, Co, Ni, and some other elements by phosphates in salt water was lower than in fresh water (Figure 12). Clinoptilolite zeolite effectively removed only Cr, Cu, Pb, and Zn in both fresh and salt water (Figure 13). Other researchers have reported that sorption by clinoptilolite is not affected by increased Ca^{2+} , Na^{+} , and K^{+} in solution (Ponizovsky and Tsadilas, 2003); however, in this study sorption by clinoptilolite was substantially lower in salt water than in fresh water (Figure 13). A study by Leppert (1990) reported that zeolite, especially clinoptilolite, demonstrates strong affinity for Pb, Cr and Cd.

Organoclay (OCB-750) sorbed (removed) the tested metals about equally from metal spiked fresh and salt water (Figure 13), with lower performance only for Se in fresh water. AquablokTM with zero valent iron coating removed As and Se more efficiently in salt water than fresh water (Figure 12). Chitosan, the only biopolymer tested so far, was very promising as a stand-alone amendment and when mixed with phosphate amendments (Figure 11, 12 and 13). Chitosan can be produced chemically from chitin and is found naturally in some fungal cell walls. Not only is chitosan inexpensive and abundant, it is a strong adsorbent for heavy metals (Berkeley, 1979; Yang and Zall, 1984). Our results showed that chitosan was very effective in fresh and salt water at sorbing Cd, Co, Cu, Ni, Pb, and Zn (Figure 13). Mixing it with North Carolina apatite increased its effectiveness for As and Se (Table 12). Other researchers also reported high adsorption capacities of chitosan for Cd, Cr, Hg, and Pb (Yang and Zall, 1984).

A sand treatment served as a control treatment in all experiments. The sand was collected at the Savannah River Site, Aiken, SC, and was not pure; for example, it had 0.6% of organic matter. Using this sand made the experiments more realistic because quarried sand would be expected to have a small amount of clay or organic matter. Sorption of all metals on the sand was very low (near zero) in fresh and salt water (Figure 11, 12, and 13).

Table 11. Metal Sorption (%) by the Tested Amendments in Fresh Water^a.

Amendment	Average Sorption								
	As	Cd	Co	Cr	Cu	Ni	Pb	Se	Zn
RPT ^b	43	95	76	70	98	50	98	0	93
NCA	43	98	83	100	98	75	99	83	94
BA	18	88	98	98	92	59	85	87	94
CaP	0	100	99	100	98	98	99	0	97
OCB-200	9	77	84	87	84	86	44	0	78
OCB-202	10	74	85	82	84	86	49	1	79
OCB-750	100	100	99	99	99	96	85	99	95
AB8	35	58	68	79	74	75	41	16	64
AB-ZVI	70	78	74	66	75	73	18	24	71
ZC	0	89	78	92	82	84	89	0	74
ZP	20	96	85	87	86	87	83	2	77
BPC	31	99	99	99	98	99	97	0	94
NCA/ZC50%	14	84	86	92	84	89	44	49	78
NCA/OCB-750-50%	99	100	99	98	98	97	88	98	92
NCA/ZC100%	5	89	84	91	87	88	64	54	80
NCA/OCB750-100%	99	99	99	99	98	96	94	99	96
NCA/BPC100%	65	99	97	99	99	99	100	83	96
NCA/BPC50%	67	98	88	98	98	97	97	75	94

The concentration of each metal in the spike solution was 1 mg L⁻¹.

^a % Sorption = $[(C_{\text{spike}} - C_{\text{final}})/C_{\text{spike}}] \times 100$

C_{spike} - metal concentration ($\mu\text{g L}^{-1}$) in spike solution before a contact with the amendment

C_{final} - metal concentration ($\mu\text{g L}^{-1}$) in spike solution after one week of contact with the amendment

^b Same acronyms as in Table 1.

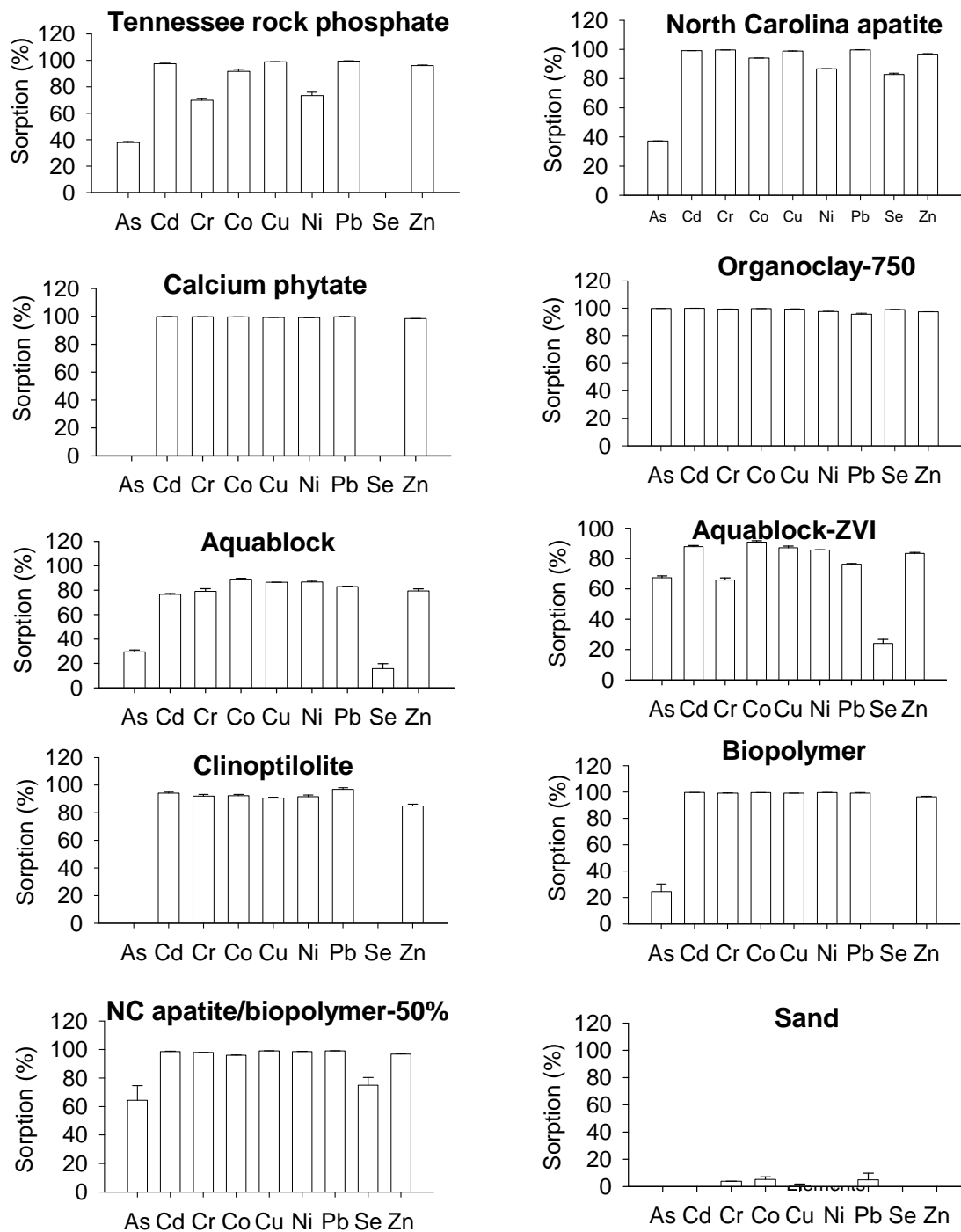


Figure 11. Sorption of As, Cd, Cr, Co, Cu, Ni, Pb, Se, and Zn in Fresh Water (concentration of each metal in the spike solution was $\sim 1 \text{ mg L}^{-1}$).

Table 12. Evaluation of Amendment Effectiveness for the Removal of Metals from Fresh Water Based on Sorption Data^a.

Amendment	As	Cd	Co	Cr	Cu	Ni	Pb	Se	Zn
RPT ^b	X	XXX	XX	XX	XXX	X	XXX		XXX
NCA	X	XXX	XXX	XXX	XXX	XX	XXX	XXX	XXX
BA		XXX	XXX	XXX	XXX	XX	XXX	XXX	XXX
CaP		XXX	XXX	XXX	XXX	XXX	XXX		XXX
OCB-200		XX	XXX	XXX	XXX	XXX	X		XX
OCB-202		XX	XXX	XXX	XXX	XXX	X		XX
OCB-750	XXX	XXX	XXX	XXX	XXX	XXX	XXX	XXX	XXX
AB8	X	XX	XX	XX	XX	XX	X		XX
AB-ZVI	XX	XX	XX	XX	XX	XX			XX
ZC		XXX	XX	XXX	XXX	XXX	XXX		XX
ZP		XXX	XXX	XXX	XXX	XXX	XXX		XX
BPC	X	XXX	XXX	XXX	XXX	XXX	XXX		XXX
NCA/ZC50%		XXX	XXX	XXX	XXX	XXX	X	X	XX
NCA/OCB-750-50%	XXX	XXX	XXX	XXX	XXX	XXX	XXX	XXX	XXX
NCA/ZC100%		XXX	XXX	XXX	XXX	XXX	XX	XX	XXX
NCA/OCB750-100%	XXX	XXX	XXX	XXX	XXX	XXX	XXX	XXX	XXX
NCA/BPC100%	XX	XXX	XXX	XXX	XXX	XXX	XXX	XXX	XXX
NCA/BPC50%	XX	XXX	XXX	XXX	XXX	XXX	XXX	XX	XXX

^aX - sorption at 30 - 50%

XX – sorption at 50 - 80%

XXX – sorption at 80 - 100%

^b the same acronyms as in Table 1.

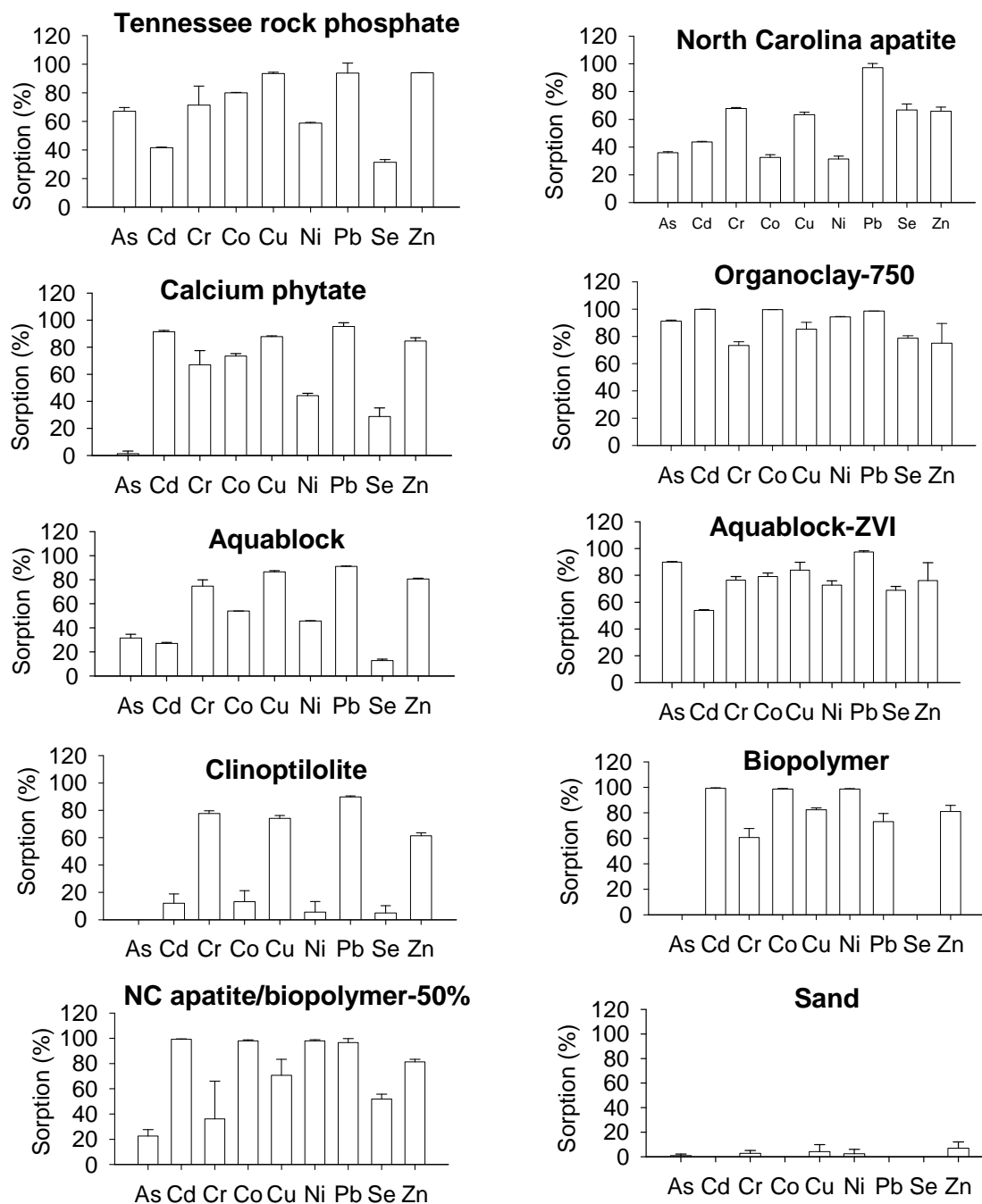


Figure 12. Sorption of As, Cd, Cr, Co, Cu, Ni, Pb, Se, and Zn in Salt Water (concentration of each metal in the spike solution was $\sim 1 \text{ mg L}^{-1}$).

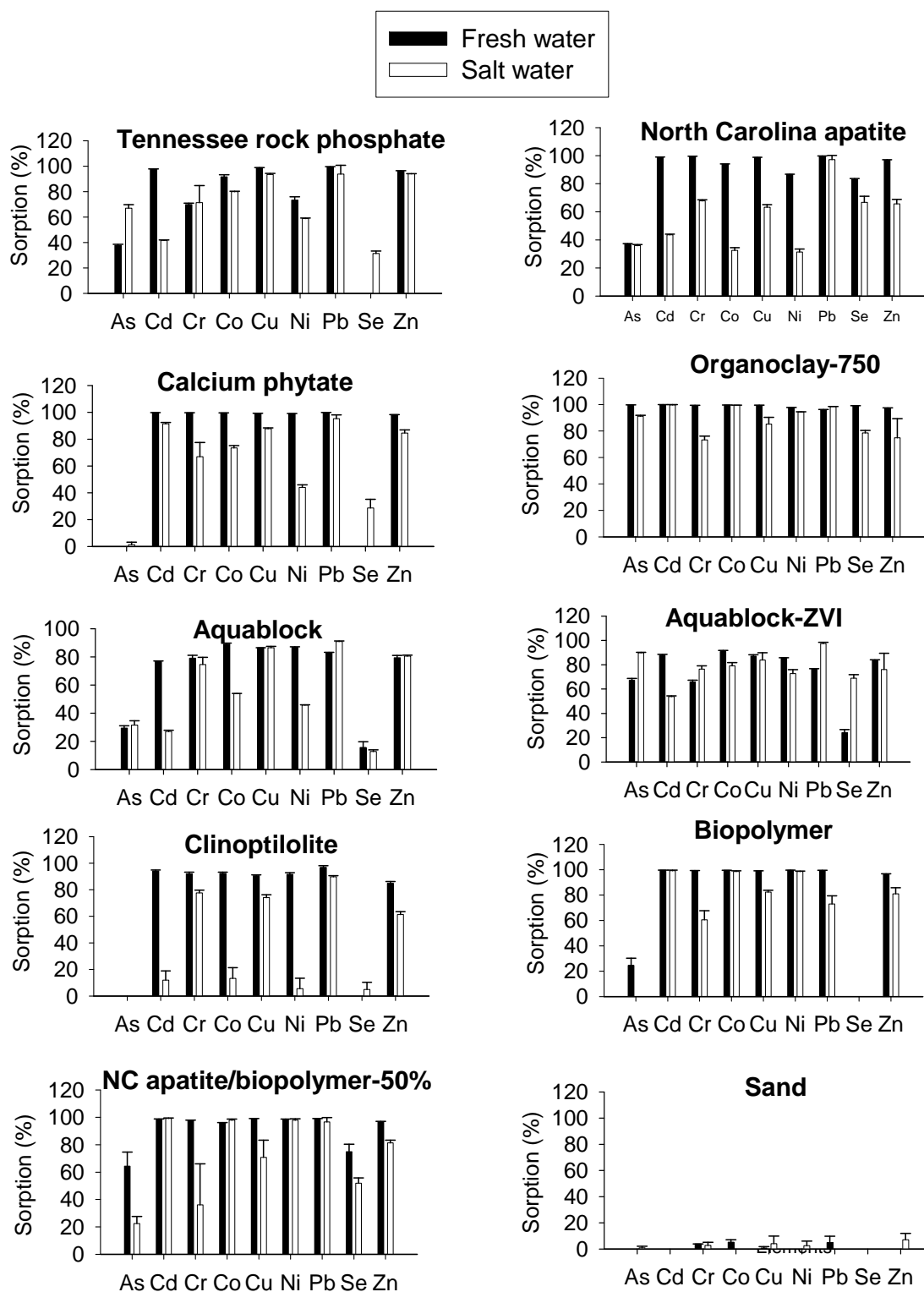


Figure 13. Comparison of Sorption of As, Cd, Cr, Co, Cu, Ni, Pb, Se, and Zn in Fresh and Salt Water (concentration of each metal in the spike solution was $\sim 1 \text{ mg L}^{-1}$).

Retention of removed metals by the amendments was evaluated in a series of desorption experiments, where the residue from the sorption studies was extracted with 1 *M* MgCl₂ solution, which is commonly used to determine the bioavailable and mobile pool of metals (Tessier et al., 1979). The data from the sorption and desorption studies were used to calculate metal retention in percent to facilitate comparisons among amendments. The desorption studies determined how strongly metals were bound to the amendments in fresh and salt water. Scientific understanding of binding strength and the irreversibility of reactions is essential to obtain regulator approval of in-situ immobilization as an acceptable remediation strategy because these variables have a direct effect on bioavailability and mobility. Although amendments remove contaminants from water very efficiently, subsequent contaminant remobilization from the amendments can release contaminants back to the water or treated sediments. The manner in which an amendment desorbs contaminants depends on its binding capacity and retention. Choosing the most appropriate treatment requires an understanding of how amendments bind contaminants and the conditions under which they could release the removed metals back into the water column.

Table 13 and Figure 14 show retention under fresh water conditions. Retention was calculated following equation number 2. Almost all tested amendments showed high retention (80% or more) for Cr, Cu, Pb, and Zn (Table 14). The best Cd retention was for organoclay (OCB-750), chitosan, and the mixture of North Carolina apatite and chitosan (Table 14). The highest retention (80% or more) for As was by organoclay (OCB-750) and Aquablok™ with zero valent iron coating (AB-ZVI) (Table 14). In fresh water only NC apatite and the mixture of NC apatite and chitosan had Se retention higher than 80% or 50%, respectively (Table 14).

Retention of sorbed metals on the tested amendments in salt water is presented in Tables 15 and 16 and Figure 15. Retention of Se in salt water (50% to 80%) was shown not only for NC apatite and OCB-750 but also for AB-ZVI and a mixture of NC apatite and chitosan (Table 17). Retention in fresh and salt water was similar for Cu, Cr, Ni, Pb, and Zn, mostly 80% or higher (Table 16).

Table 13. Average Metal Retention by Amendments (%) in Fresh Water^a.

Amendment	As %	Cd %	Co %	Cr %	Cu %	Ni %	Pb %	Se %	Zn %
RPT	38	0	75	70	85	30	99	0	47
NCA	37	23	61	100	86	53	100	82	62
CaP	0	29	75	100	99	64	98	0	98
OCB-750	100	86	100	99	99	98	96	7	97
AB 8	29	0	67	75	80	62	55	14	63
AB-ZVI	67	0	65	62	84	57	76	21	77
ZC	0	0	42	86	75	24	97	0	39
BPC	15	83	87	70	81	100	87	0	76
NCA/BPC50%	48	92	94	80	91	99	99	55	87

^a % retention = $[(C_{\text{adsorbed}} - C_{\text{desorbed}})/C_{\text{spike}}] \times 100$

C_{adsorbed} - concentration of metal adsorbed at the end of the adsorption experiment

C_{desorbed} - concentration of metal desorbed at the end of the desorption experiment

C_{spike} - concentration of metal in spike solution

^b The same acronyms as in Table 1.

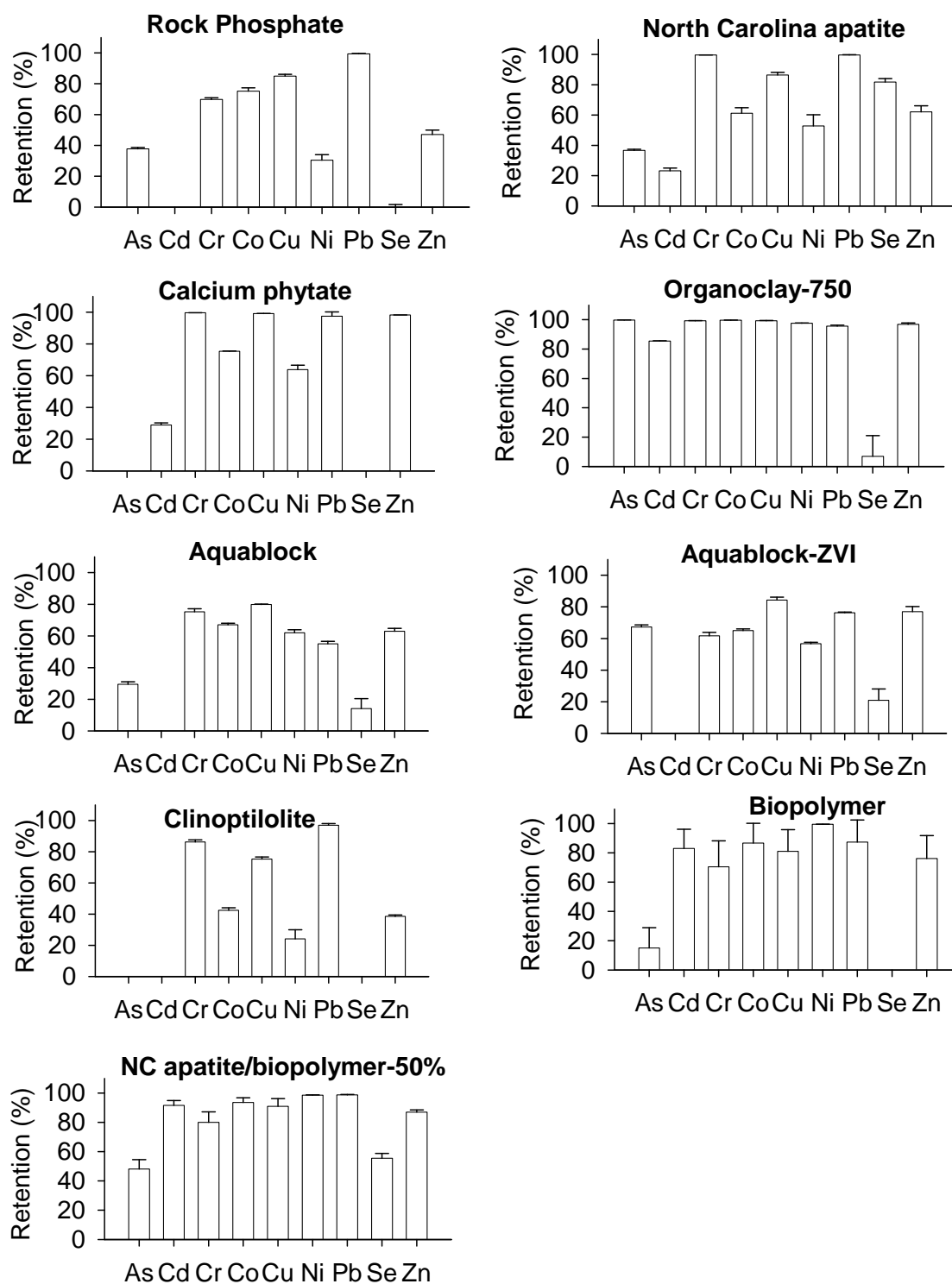


Figure 14. Retention of Metals by Amendments in Fresh Water.

Table 14. Evaluation of Amendment Effectiveness in Fresh Water Based on Retention Data.

Amendment	As %	Cd %	Co %	Cr %	Cu %	Ni %	Pb %	Se %	Zn %
RPT ^b	X		XX	XX	XXX	X	XXX		X
NCA	X		XX	XXX	XXX	XX	XXX	XXX	XX
CaP			XX	XXX	XXX	XX	XXX		XXX
OCB-750	XXX	XXX	XXX	XXX	XXX	XXX	XXX		XXX
AB 8			XX	XX	XXX	XX	XX		XX
AB-ZVI	XX		XX	XX	XXX	XX	XX		XX
ZC			X	XXX	XX		XXX		X
BPC		XXX	XXX	XX	XXX	XXX	XXX		XX
NCA/BPC50%	X	XXX	XXX	XXX	XXX	XXX	XXX	XX	XXX

^a X - retention at 30 - 50%

XX - retention at 50 - 80%

XXX - retention at 80 - 100%

^b same acronyms as in Table 1.

Table 15. Average Metal Retention by Amendments (in %) in Salt Water.

Amendments	As	Cd	Cr	Co	Cu	Ni	Pb	Se	Zn
	%	%	%	%	%	%	%	%	%
RPT	67	0	72	77	93	59	94	27	94
NCA	35	17	68	22	63	28	97	65	54
CaP	0	41	67	25	88	0	95	20	85
OCB-750	91	98	74	100	85	94	99	76	75
AB*	32	0	75	40	86	46	64	13	81
AB-ZVI	90	3	77	66	84	73	98	64	76
ZC	0	1	78	10	74	3	90	5	61
BPC	0	97	0	99	82	99	58	0	81
NCA/BPC50%	22	98	0	98	60	98	97	52	81

$$^a \% \text{ retention} = [(C_{\text{adsorbed}} - C_{\text{desorbed}})/C_{\text{spike}}] \times 100$$

C_{adsorbed} - concentration of metal adsorbed at the end of the adsorption experiment

C_{desorbed} - concentration of metal desorbed at the end of the desorption experiment

C_{spike} - concentration of metal in spike solution

^b The same acronyms as in Table 1.

Table 16. Evaluation of Amendment Effectiveness in Salt Water Based on Retention Data^a.

Amendment	As %	Cd %	Cr %	Co %	Cu %	Ni %	Pb %	Se %	Zn %
RPT	XX		XX	XX	XXX	XX	XXX		XXX
NCA	X		XX		XX		XXX	XX	XX
CaP		X	XX		XXX		XXX		XXX
OCB-750	XXX	XXX	XX	XXX	XXX	XXX	XXX	XX	XX
AB*	X		XX	X	XXX	X	XX		XXX
AB-ZVI	XXX		XX	XX	XXX	XX	XXX	XX	XX
ZC			XX		XX		XXX		XX
BPC		XXX		XXX	XXX	XXX	XX		XXX
NCA/BPC50%		XXX		XXX	XX	XXX	XXX	XX	XXX

^a X - retention at 30 - 50%

XX - retention at 50 - 80%

XXX - retention at 80 - 100%

^b same acronyms as in Table 1.

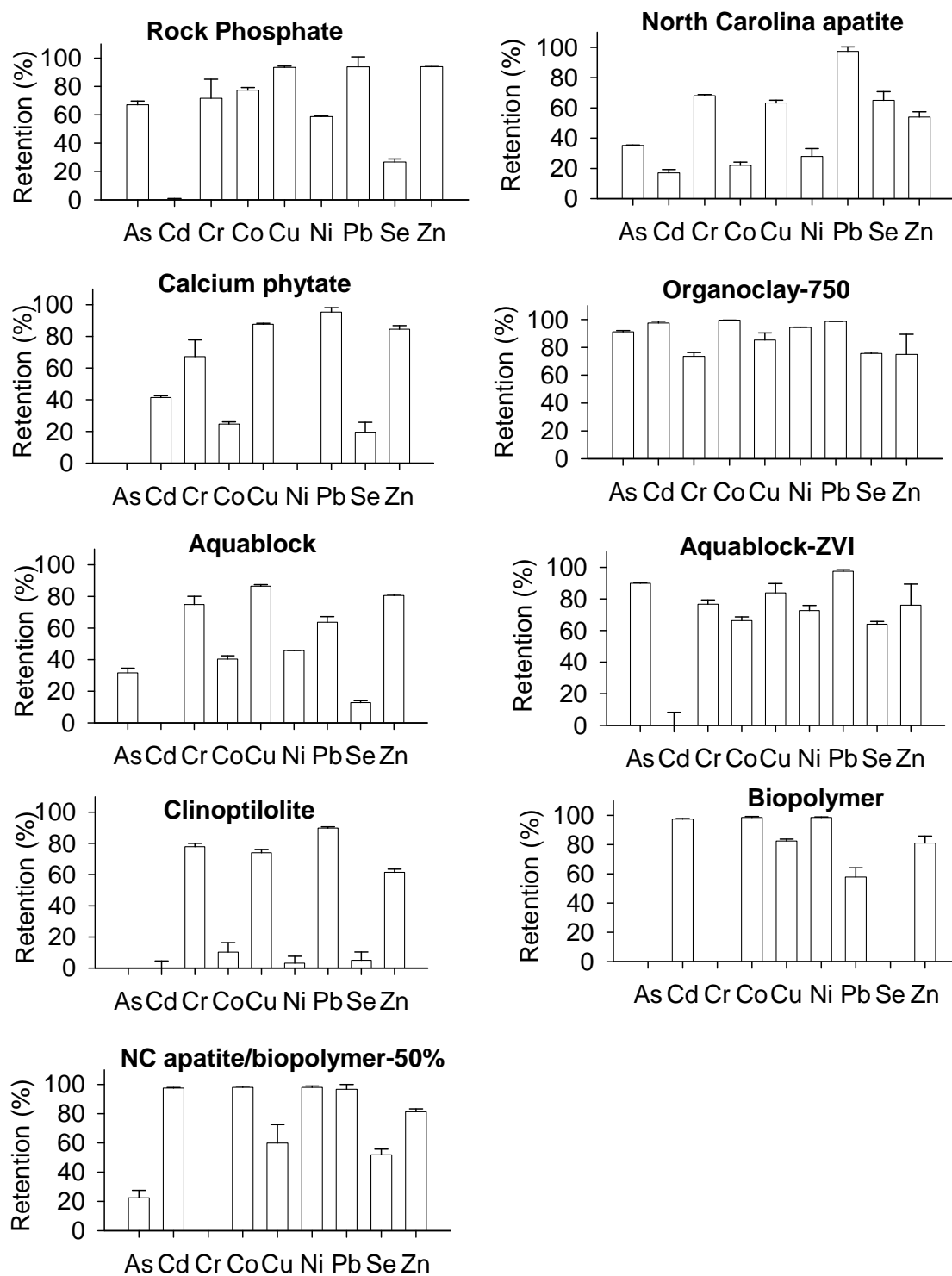


Figure 15. Retention of Metals by Amendments in Salt Water.

Sorption of Organic Contaminants by Sequestering Agents

Two organoclays, Clayfloc 750 and PM-199, exhibited relatively high sorption capacities for phenanthrene, pyrene, and benzo(a)pyrene as indicated by a comparison of K_d values among the 12 amendments under study. Partitioning coefficients for these two organoclays ranged from about 3000-3500 ml g^{-1} for benzo(a)pyrene, 400-450 ml g^{-1} for pyrene, and 50-70 ml g^{-1} for phenanthrene (Table 17). Biological apatite followed the organoclays with K_{ds} of about 500 ml/g for benzo(a)pyrene, 20 ml g^{-1} for pyrene, and 4 ml g^{-1} for phenanthrene (Table 17). The sorption capacities of the other amendments were substantially lower; usually under 100 for benzo(a)pyrene, five ml g^{-1} for pyrene, and one ml g^{-1} for phenanthrene. These results suggest the potential utility of some organoclays and, to a lesser extent, biological apatite for controlling organic contaminants.

Table 17. Partitioning Coefficients (ml g⁻¹) for Sorption of Organic Compounds on Various Amendments

Solid phase	Phenanthrene	Pyrene	Benzo(a)pyrene
Sediment	0.7116* (0.1186 ^o)	2.52 (-)	38.75 (-)
Clay 200	0.459 (0.0186)	3.828 (0.6162)	48.12 (9.336)
Clay 202	0.356 (0.0267)	1.380 (0.1814)	24.24 (11.42)
Clay 750	55.63 (10.68)	413.5 (71.97)	3016 (324.1)
PM-199, CETGO	68.02 (8.423)	454.2 (104.9)	3505 (441.9)
Clinoptilolite Zeolite powder	0.1303 (0.0088)	0.1577 (0.0153)	12.25 (5.386)
Clinoptilolite zeolite - 4mesh	0.1865 (0.0320)	0.5152 (0.1113)	19.34 (6.405)
Clinoptilolite zeolite 8x14	0.2606 (0.0065)	0.3111 (0.03)	27.15 (4.838)
Phili Zeolite	0.1775 (0.0828)	0.4656 (0.1017)	38.67 (3.2617)
Apatite NC	0.5567 (0.1893)	1.658 (0.0062)	50.39 (7.489)
PIMS biological apatite	4.151 (1.326)	20.19 (6.012)	512.3 (20.69)
Washed phosphate Ore, Tennessee	0.986 (0.1203)	5.038 (1.243)	105.5 (10.66)
Calcium Phytate	0.1937 (0.0587)	0.3215 (0.0197)	12.84 (2.152)

* The average of three to four replicates

o Standard deviation

Development of Biopolymer Products

The pH of all biopolymer solutions except chitosan was close to neutral or slightly acidic and was not substantially changed by cross-linking (Table 18). Viscosity measurements (at different shear rates and using different spindles) are presented in Figures 16 and 17. A clear increase in viscosity was recorded for each cross-linked product compared with the initial biopolymer solution, which confirmed that cross-linking occurred. An exception was the cross-linked product of chitosan with guar and borax (with or without addition of glutaraldehyde). This product decreased in viscosity following attempted cross-linking, indicating that cross-linking

probably did not occur. A possible explanation is that the chitosan solution was neutralized by the addition of NaOH.

The viscosity measurements showed that some of the biopolymers exhibited pseudoplasticity (Picture 15). A pseudoplastic liquid has different viscosities at different shear rates (the higher the shear rate, the lower the viscosity). Such liquids are of potential interest for environmental applications, since they can be easily added to porous media by pressure (high shear rate), while forming stable gels when the pressure ceases. Only the xanthan solution was pseudoplastic before cross-linking.

Table 18. Development of Cross-linked Biopolymer Products – Procedures and Characteristics

Biopolymer 1	Biopolymer 2	Cross Linking agents	Solution batches	Procedure	pHi / pHf ^a	Viscosity (i/f) (cP)
Experiment 1.1						
Guar gum (GG)		Sodium borate (Borax) (SB)	GG 3 g/L	0.75 g of borax mixed with 1L of 3g/L guar gum, solution mixed with a magnetic stirrer overnight (about 12 hours) at room temperature.	4.42 / 7.50	53 / 19600
Experiment 1.2						
Xanthan (X)	Guar (GG)	Gum (guar gum)	X 2 g/L GG 2 g/L	500 mL of 2g/L xanthan solution mixed (under continuous stirring) with 500 mL of 2g/L guar gum solution, resulting solution mixed with a magnetic stirrer over night (about 12 hours) at room temperature.	5.37 (X); 5.78 (GG) / 6.50	72.2 (X); 30 (GG) / 330
Experiment 1.3						
Xanthan (X)		Calcium phytate (CaP)	X 2 g/L	0.5 g of CaP mixed with 1L of 2g/L xanthan, solution mixed with a magnetic stirrer overnight (about 12 hours) at room temperature.	5.37 /	72.2 /

Table 18 (continued). Development of Cross-linked Biopolymer Products – Procedures and Characteristics

Biopolymer 1	Biopolymer 2	Cross Linking agents	Solution batches	Procedure	pHi / pHf ^a	Viscosity (i/f) (cP)
Experiment 1.4						
Alginate (A)		Ca Cl ₂	A3 g/L	0.75 g of calcium chloride mixed with 1L of 3g/L alginate, solution mixed with a magnetic stirrer overnight (about 12 hours) at room temperature.	7.00 / 5.00	46.6 / 64.2
Experiment 1.5						
Chitosan (C)	Alginate (A)	(alginate)	C 2 g/L; A 2 g/L		2.37 /	28.2 (C); 45 (A) /
Experiment 1.6a						
Chitosan (C)	Guar (GG)	Gum Borax (SB)	C 2 g/L; GG 2 g/L	500 ml of 2g/L chitosan mixed with 500 mL 2g/L guar gum under continuous stirring, 0.25g of borax added to the resulting solution and mixed (chitosan solution initially neutralized with NaOH (about 100mL) to PH 5)	2.37(C); 5.37 (GG) / 12.00	28.2 (C); 30 (GG)/ 13.6
Experiment 1.6b						
Chitosan (C)	Guar (GG)	Gum Borax (SB)+glutaraldehyde		Same as 1.6.a but with the addition of 1mL of glutaraldehyde after the addition of borax.	2.37(C); 5.37 (GG) / 4.50	28.2 (C); 30 (GG) / 23.7
Experiment 1.7						
Chitosan (C)	Xanthan (X)	(xanthan)	C 2 g/L; X 2 g/L			
Experiment 1.8						
Chitosan (C)		Calcium phytate (CaP)	C 2 g/L	Same as 1.3. but with chitosan instead of xanthan.	2.38 /	

^a pHi / pHf = pH of initial solution (biopolymer) / pH of final solution (cross- linked biopolymer)

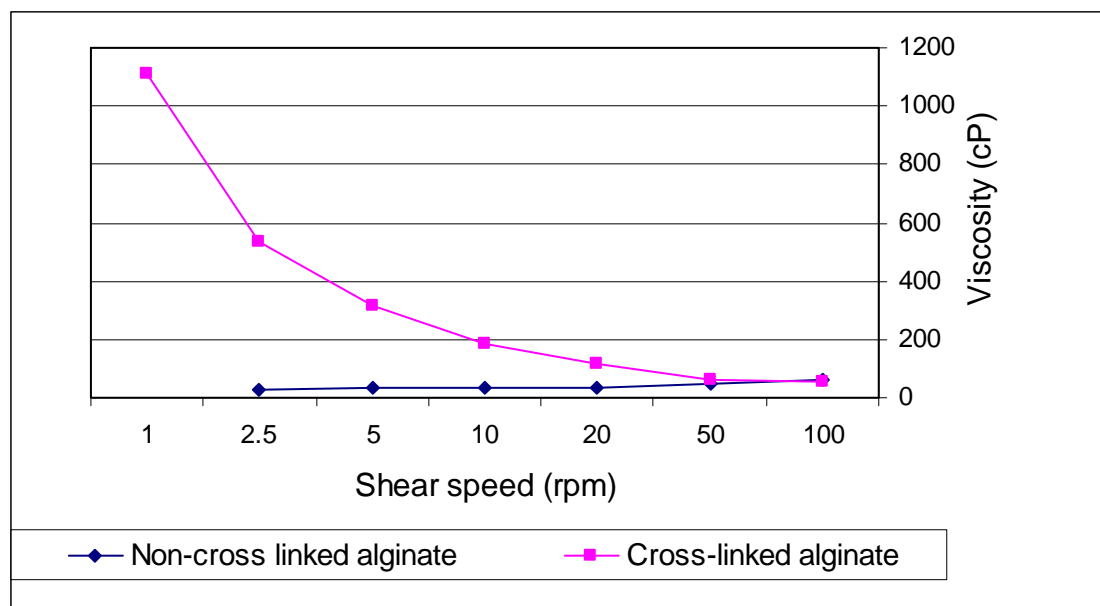


Figure 16. Viscosity of Alginate before and after Cross-linking with CaCl_2 .

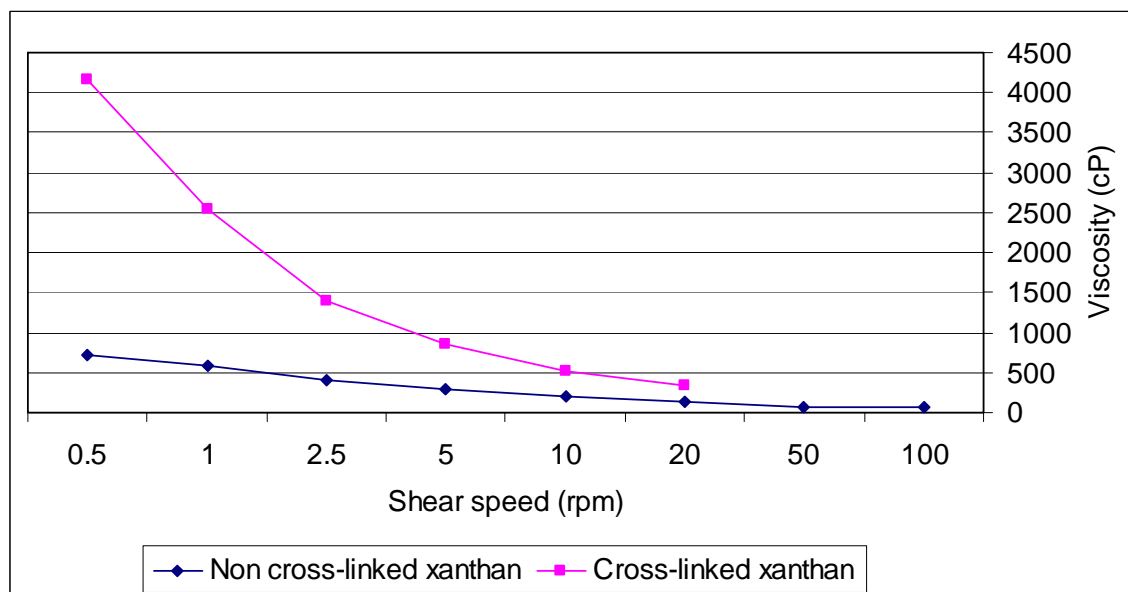


Figure 17. Viscosity of Xanthan before and after Cross-linking.



Picture 15. Adhesive Product of Sand Coated with Guar Gum Cross-linked by Borax.

Sorption of Metals and Organic Contaminants by Biopolymers

The most promising materials for metal removal were xanthan cross linked with guar gum and xanthan cross-linked with chitosan (Figure 18). These cross-linked biopolymers sequestered a variety of metals from a spike solution; e.g., As, Cd, Co, Cr, Cu, Ni, Pb, and Zn (Figure 18). Removal of most metals by xanthan cross linked with guar gum and xanthan cross-linked with chitosan exceeded 90% (Figure 18). The tested biopolymers were as effective at removing metals from the spike solution as apatite (rock phosphate from North Carolina), which has proven ability to immobilize metals such as Pb, Cd, and Zn in soils and sediments (Knox et al., 2008 a) (Figure 18).

Various processes such as adsorption, ion exchange, and chelation dominate the mechanisms responsible for complex formation between biopolymers and metal ions. The interactions of metal ions with biopolymers (e.g., chitosan) are influenced by the degree of polymerization and deacetylation, as well as by the distribution of acetyl groups along the polymer chains (Bassi et al., 1999). The evidence currently available supports the concept that chitosan-metal ion complex formation occurs primarily through the amino groups functioning as ligands (Randall et al., 1979; Udaybhaskar et al., 1990).

Organic carbon content was measured as an indicator of the efficiency of the procedure for coating the sand with biopolymers and as an indicator of the potential for the sorption of organic contaminants on the coated sand. The measured carbon fractions are presented in Figure 19. The carbon fractions of coated sand with one wash, two washes and three washes did not differ substantially from the unwashed sand, indicating that the coated sand was resistant to washing.

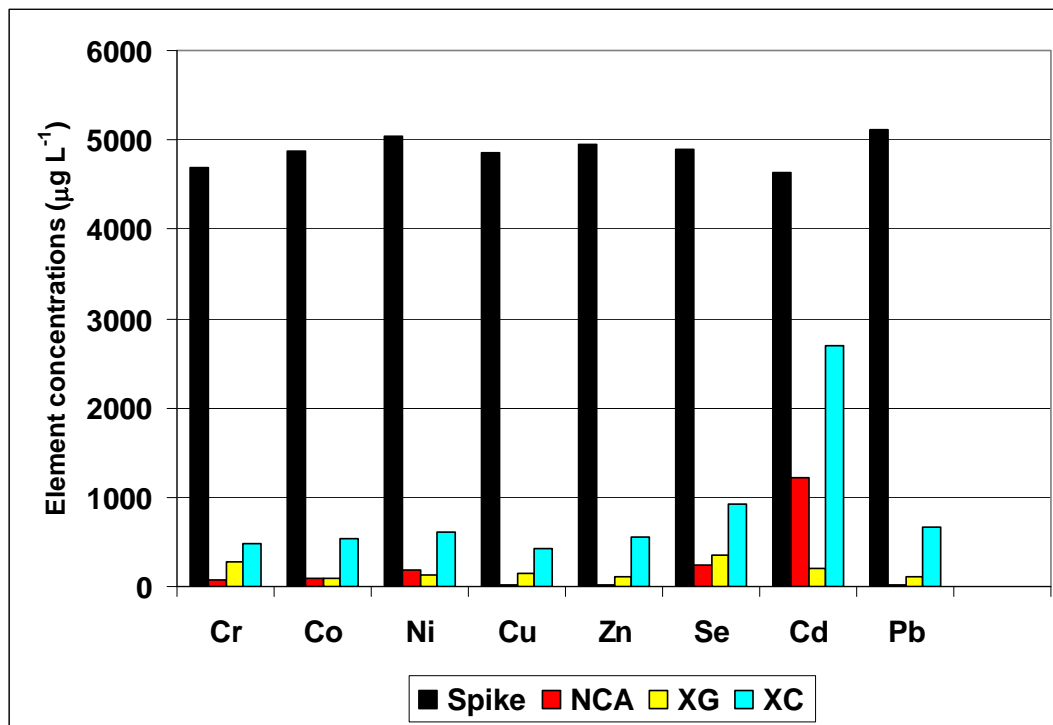


Figure 18. Removal of Metals by Biopolymers from a Spike Solution with an Initial Concentration of 5000 mg L⁻¹ of Cd, Co, Cr, Cu, Ni, Pb, Se, and Zn; NCA - North Carolina apatite, XG - xanthan cross-linked with guar gum, XC - xanthan cross-linked with chitosan.

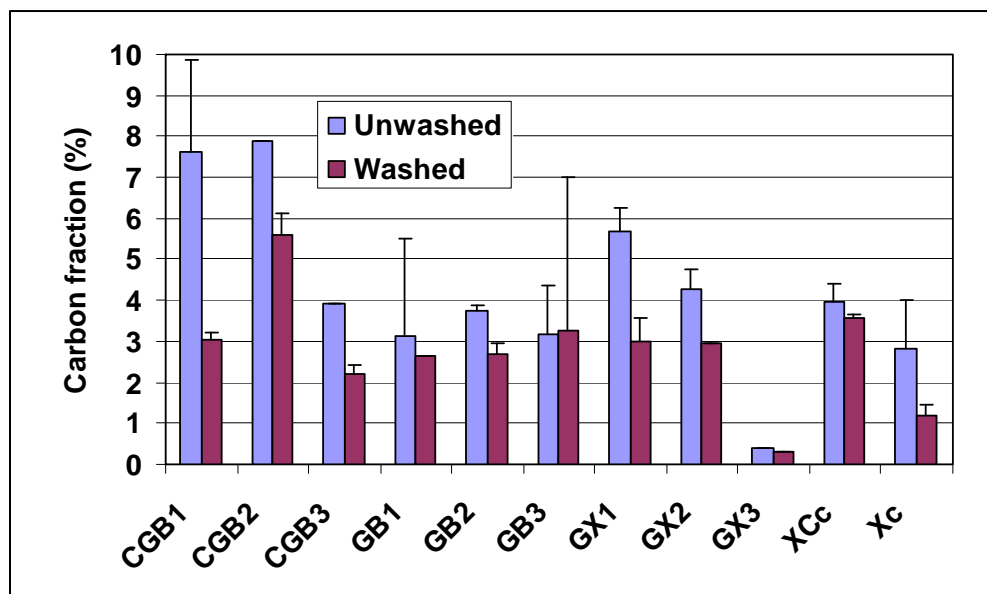


Figure 19. Carbon Fraction of Biopolymer Coated Sand; C – chitosan, G – guar gum, B – borax, X – xanthan, c – calcium chloride.

Sorption capacities of sand samples coated with chitosan/guar gum cross-linked with borax (CGB) and with xanthan/chitosan cross-linked with calcium chloride (XCc) for organic contaminants are presented in Table 19. Both biopolymer coated sand materials had a significantly higher sorption capability than sand for pyrene (Table 19).

Table 19. Average Sorption Coefficients of Sand and Sand Coated by Biopolymers (standard deviation in parentheses); B - borax, C - chitosan, G - guar gum, X - xanthan, c - calcium chloride; 1 – without glutaraldehyde, 2 – with glutaraldehyde, 3 - without glutaraldehyde but with NaOH.

	Phenanthrene L kg⁻¹	Pyrene L kg⁻¹
Sand	3.19 (1.87)	27.01 (5.34)
CGB1	0.4 (-)	29.54 (4.19)
CGB2	27.72 (3.07)	127.1 (23.26)
CGB3	40.64 (24.32)	118.3 (17.15)
GB2	13.18 (2.32)	68.82 (14.4)
XCc	12.8 (3.42)	106.7 (15.08)

SUBTASK 1.2. EFFECT OF SEQUESTERING AGENTS ON THE MOBILITY, BIOAVAILABILITY, AND RETENTION OF CONTAMINANTS IN SEDIMENT

Removal and Retention of Organic Contaminants

Organoclay has the potential to contain both nonaqueous phase liquids (NAPL) and dissolved phase contaminants, although containment of dissolved contaminants is less well understood. This study evaluated the separate phase sorption capacity of two commercial organoclays for weathered creosote mixtures collected from a former waste deposit area (FWDA) and a tank farm area (TFA) near Portland, OR (Table 20). Organoclays were obtained from AquaTechnologies (ET1, Casper, WY) and CETCO (PM-200, Arlington, IL). Sorption capacities varied, but both organoclays could absorb more than their own weight in contaminants.

Column breakthrough of dissolved contaminants (indicated by naphthalene and phenanthrene) generally occurred only just before breakthrough of NAPL (Figure 20). That is, the organoclay appeared to effectively contain dissolved contaminants until saturation by NAPL. It was not possible, however, to determine the capacity of the organoclay for dissolved constituents from these experiments.

Table 20. Sorption Capacities of Two Commercial Organoclays for LNAPLs and DNAPLs from Different Weathered Creosote Mixtures.

	Aqua Technologies (Casper, WY) ET-1			CETCO (Arlington, IL) PM-200		
	Sorption Capacity g/g (std dev)	NAPL Balance %	Water Balance %	Sorption Capacity g/g (std dev)	NAPL Balance %	Water Balance %
FWDA LNAPL	1.36 (0.08)	101(10)	106 (17)	4.60 (0.04)	97 (2)	120 (6)
FWDA DNAPL	1.25 (0.12)	89 (8)	110 (14)	4.82 (0.06)	82 (1)	126 (4)
TFA LNAPL	1.35 (0.03)	86 (3)	111 (1)	4.41 (0.03)	75 (3)	124 (3)
TFA DNAPL	1.39(0.10)	82(4)	107(8)	4.50(0.11)	84(4)	115(5)

The potential effectiveness of organoclay for containment of phenanthrene during gas release is shown in Figure 21. Gas was injected continuously at rates typical of microbial generation in contaminated areas (1 L/m²/day); and containment effectiveness of no cap, a thin sand cap and a thin organoclay cap was monitored by measuring the mass of contaminants captured in a solvent (hexane) layer at the top of apparatus. This experiment showed that organoclay can effectively reduce contaminant release due to gas movement over both uncapped and sand capped sediments.

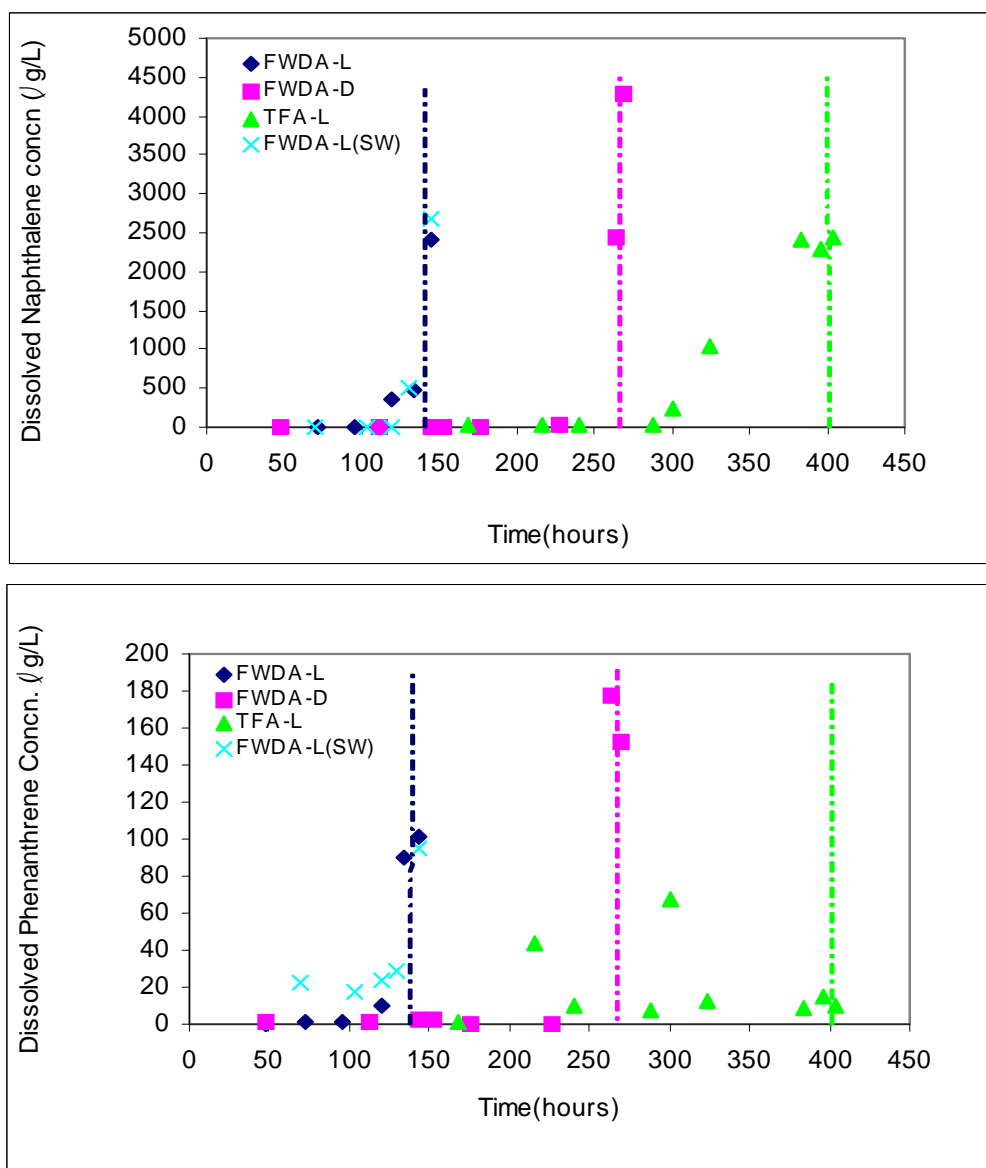


Figure 20. Dissolved Naphthalene and Phenanthrene Release from Columns in which Creosote Mixtures were Continuously Injected. Vertical lines indicate NAPL breakthrough

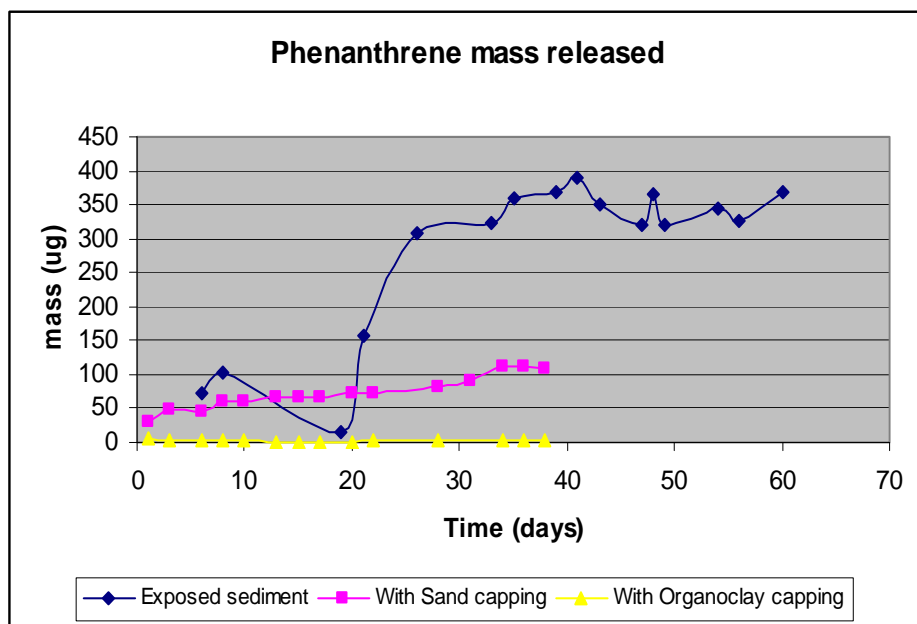


Figure 21. Phenanthrene Released by Gas Migration from a Weathered Creosote Mixture Showing the Effectiveness of an Organoclay Layer.

Kinetic Study and Sorption/ Desorption of Organic Contaminants by Selected Amendments

Sorption and desorption are both time sensitive processes. Sorption measurements were made in triplicate in 50 mL vials with a 48 hour equilibration time. Measurements were also made at shorter and longer times to demonstrate 48 hours were sufficient to achieve equilibrium. Typically 1 g of sorbent material was introduced to the vials with a known PAH initial concentration. Three materials were tested, with one from each of three groups of amendments: apatite, organoclay and zeolite. Specifically, the three materials were clinoptilolite TSM 140 (8x14 mesh), PIMS biological apatite (ground fish bones) and organoclay 750 (Biomim, Inc.).

Equilibrium for sorption was reached after 24 to 48 hours (Figures 22 through 24). Therefore, 48 hours was used as the equilibrium time, and all sorption coefficients were measured at 48 hours. The measured sorption coefficients differed significantly among materials; the most sorptive materials for PAHs were CETCO-199, CETCO-200, and organoclay 750 (Table 21).

The desorption kinetics studies indicated that desorption reached equilibrium within 48 hours for all four materials chosen as potential capping amendments. The desorption kinetics for NC apatite and organoclay materials are shown in Figures 25, 26, and 27. PM199 and PM 200 were the same organoclays but with different particle sizes; therefore, only results for PM 200 are shown (Figure 27).

The measured desorption coefficients are listed in Table 21. In general, the desorption coefficients were several times higher than the sorption coefficients, meaning that some of the phenanthrene and pyrene adsorbed to the sorbents will not be released at the same environmental

conditions. This is advantageous because only contaminants dissolved in pore water are available to benthic organisms (Lu et al., 2006).

The partition coefficients in Table 21 were used to estimate model-generated penetration times through a cap using an analytical advection-diffusion model. The penetration time is the time until concentrations at the top of the active cap layer are 50% of what they would be under steady state conditions (or 50% of the concentration at the bottom of the active cap layer). This time is given by

$$\tau_{adv/diff} \approx \left(\frac{1}{1/\tau_{diff} + 1/\tau_{adv}} \right) \approx \left(\frac{1}{D_1/(\varepsilon R_f h_{eff}^2) + U/(\varepsilon R_f h_{eff})} \right) \approx \frac{\varepsilon R_f h_{eff}^2}{D_1 + U h_{eff}} \quad (20)$$

where:

D_1 = effective diffusion/dispersion coefficient

h_{eff} = effective cap thickness

U = Darcy upwelling velocity

ε = active cap layer porosity

R_f = effective sorption-related retardation factor in the cap

Assuming a velocity of 100 cm/yr as an upper bound for upwelling (which typically causes diffusion and dispersion to be negligible), Table 22 contains estimates of the penetration time in years. Clearly, the active cap amendments can be extremely effective for the containment of the contaminants.

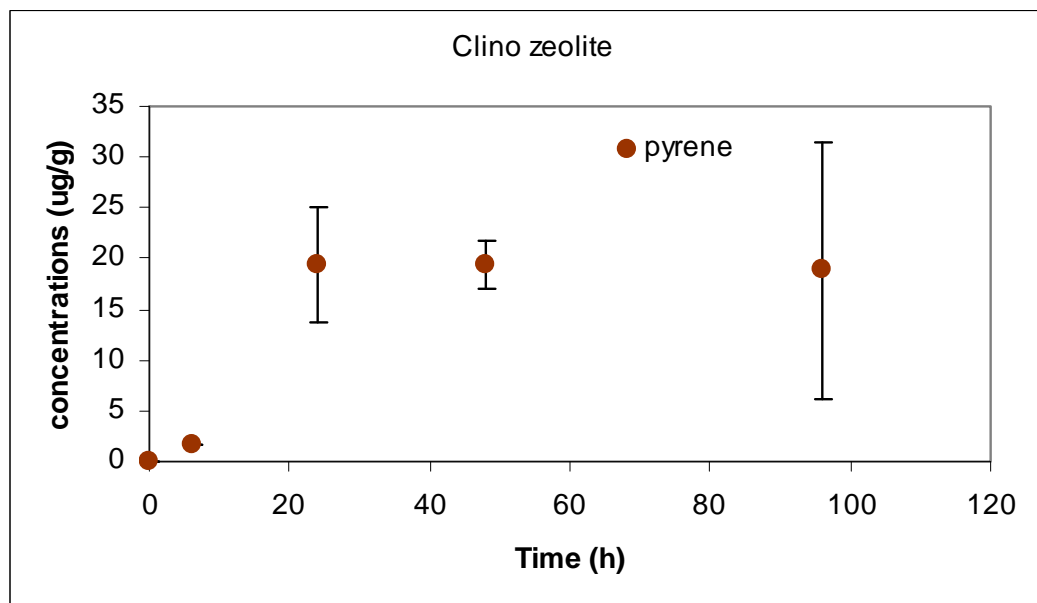
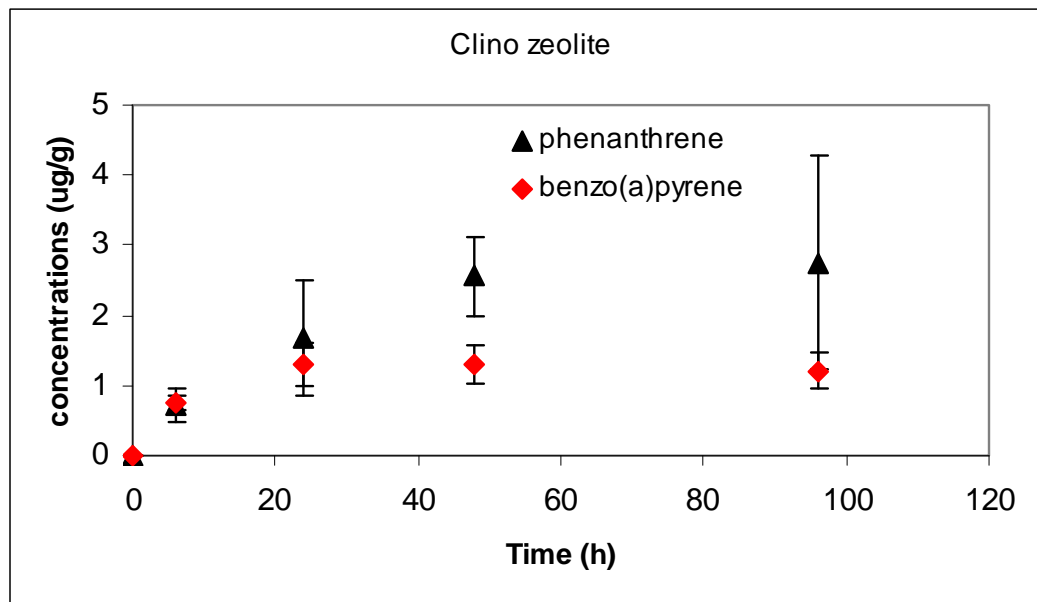


Figure 22. Sorption of Three PAHs to Zeolite (Clinoptilolite).

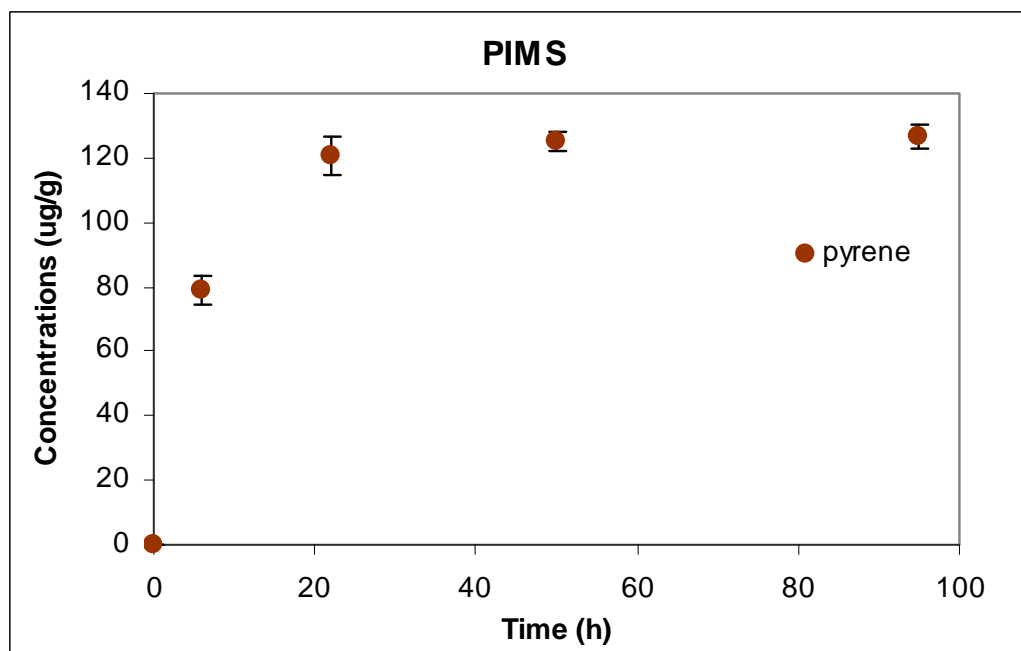
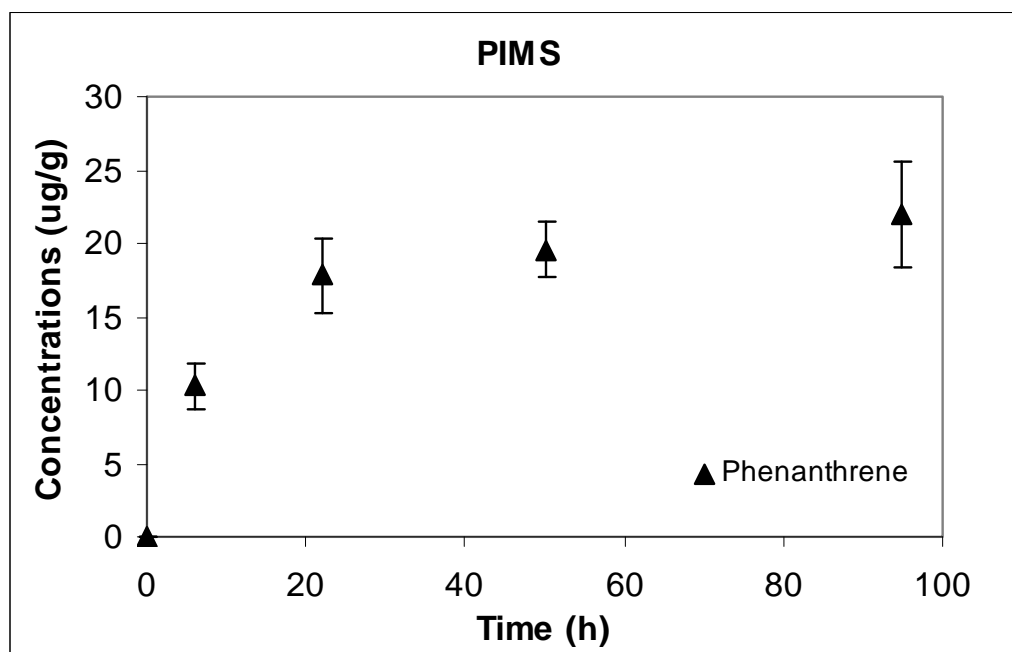


Figure 23. Sorption of Two PAHs to PIMS (Biological Apatite).

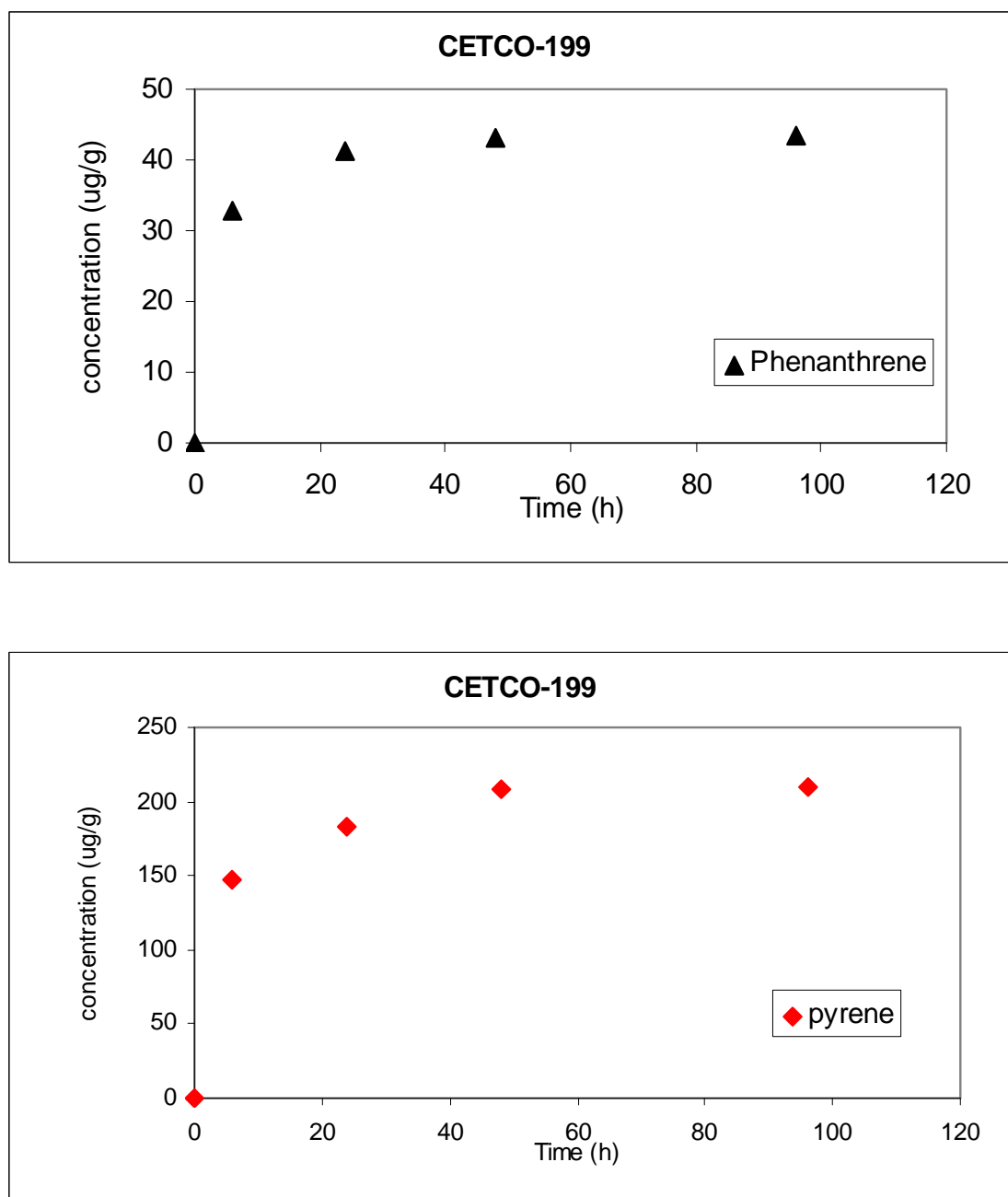


Figure 24. Sorption of Phenanthrene and Pyrene to CETCO-199.

Table 21. Sorption and Desorption Coefficients for Selected Amendments (L kg⁻¹)

	Sorption (std dev)		Desorption (std dev)	
	Phenanthrene	Pyrene	Phenanthrene	Pyrene
Clay 750	55,600 (10,700)	414,000 (72,000)	95,300 (25,600)	304,000 (88,800)
PM-199	68,000 (8,400)	454,000 (105,000)	126,000 (22,300)	-
PM-200	36,500 (5,800)	98,700 (31,000)	94,400 (15,100)	377,000 (50,100)
NC Apatite	220 (8.9)	695 (131)	428 (127)	1,060 (319)

Table 22. Estimation of Cap Penetration Time (in years) for 15 and 2.5 cm Active Layers Subject to a 100 cm yr⁻¹ Groundwater Upwelling Velocity.

	K_d (L kg⁻¹)	τ 15 cm	τ 2.5 cm		K_d (L kg⁻¹)	τ 15 cm	τ 2.5 cm
	Phenanthrene				Pyrene		
Clay 750	55,600	11,000	1,800		414,000	79,000	13,000
PM-199	68,000	13,000	2,200		454,000	87,000	15,000
PM-200	36,500	7,100	1,200		98,700	19,000	3,200
NC Apatite	220	43	7.1		695	140	22

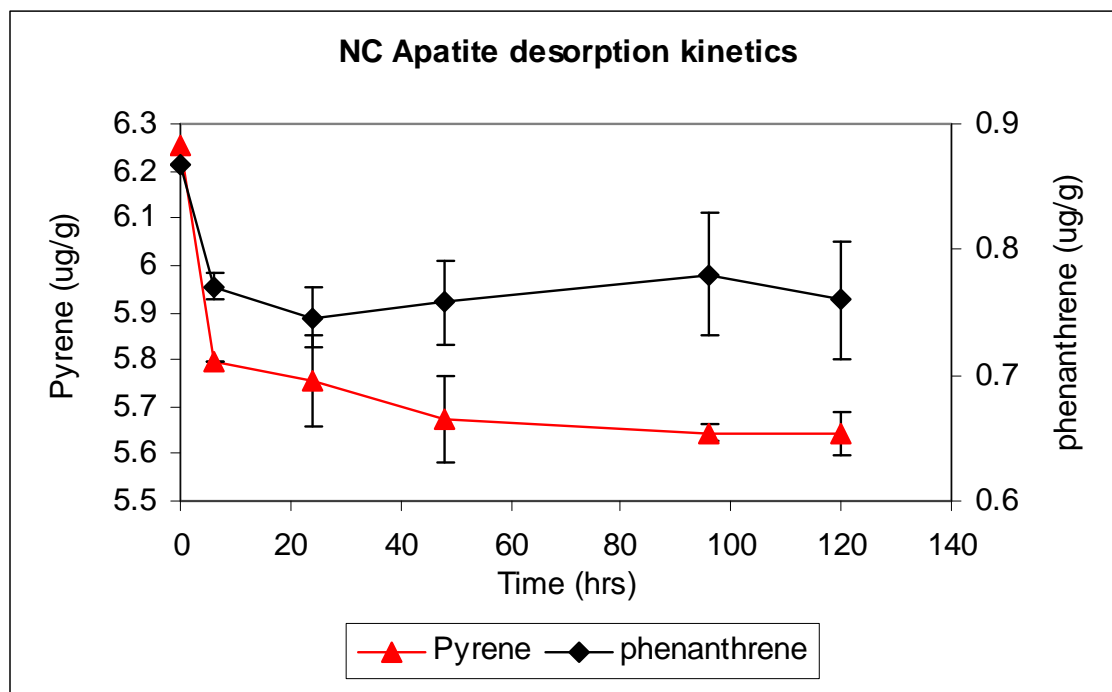


Figure 25. North Carolina Apatite Desorption Kinetics. Reported data were the average of three replicates. The error bars are standard deviations.

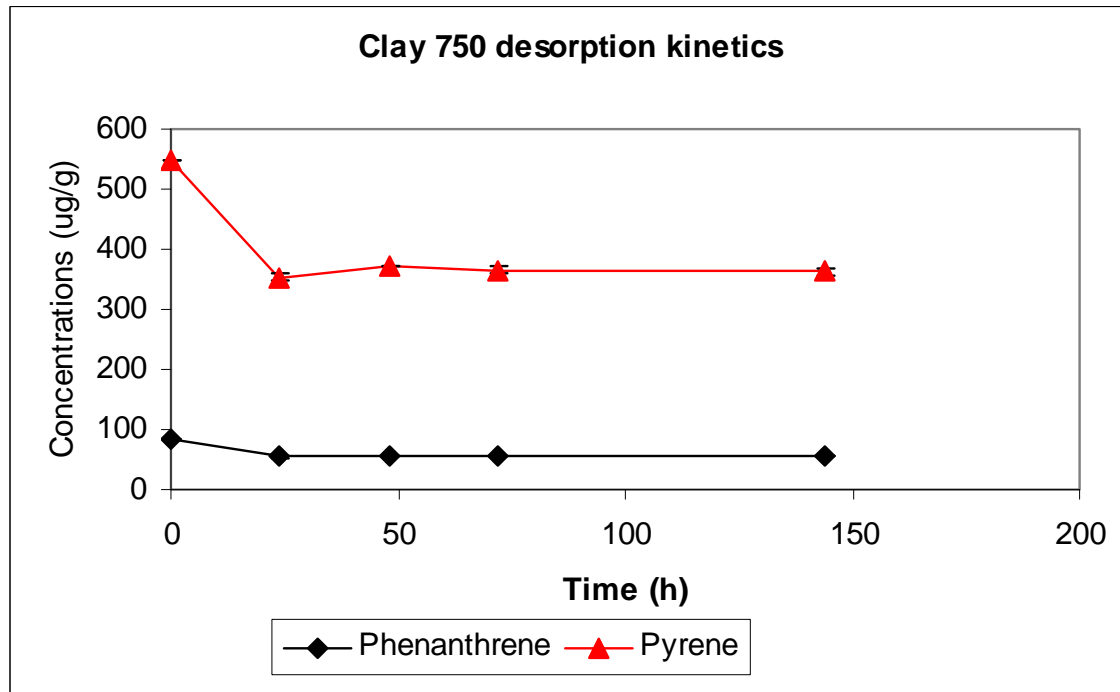


Figure 26. Organoclay (OCB750) Desorption Kinetics. Reported data were the average of three replicates. The error bars are standard deviations.

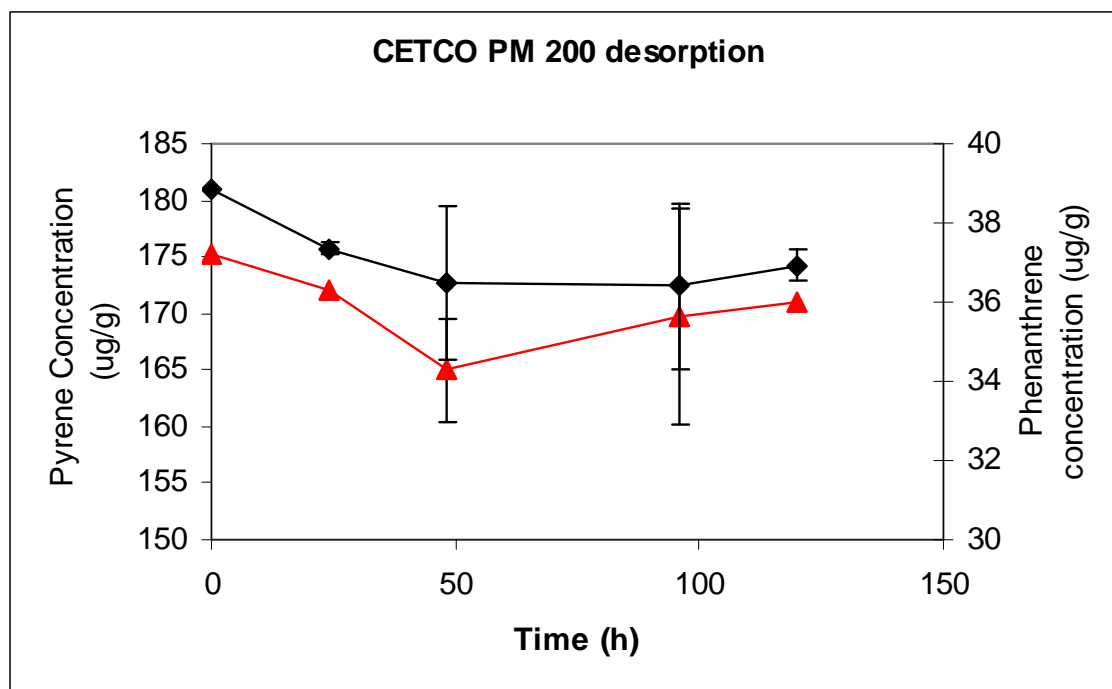


Figure 27. Organoclay (CETCO PM 200) Desorption Kinetics. Reported data were the average of three replicates. The error bars are standard deviations.

Cap Effectiveness for Organics

Measured partitioning coefficients were used to indicate the effectiveness of a one inch (2.54 cm) layer of the material as a sediment cap by estimating the time required for a contaminant to penetrate the cap. The time was estimated assuming that the underlying concentration remained constant and that no degradation or transformation processes were operative. The time was estimated by the methods recommended by the standard EPA guidance on capping (US EPA, Appendix B, 1998).

A one inch layer of active capping material simulates the placement of the material in thin layers. Such a placement might be considered for high value materials that might be cost-prohibitive if placed in bulk. If placed in bulk, an alternative placement might be six inches (15 cm) of active sorbent. If the time to penetrate a six inch active capping layer is required, the times in Table 23 should simply be multiplied by six. The active layer would likely be overlain by biopolymer coated sand or a similar inert material. For purposes of the current estimates, the sand cover is conservatively assumed to provide no additional contribution to the time required for contaminants to migrate through the cap. Two scenarios were considered:

- A cap layer in which migration is dominated by upwelling at an average rate of 1 cm/ day
- A cap layer in which migration is dominated by molecular diffusion

Table 23 summarizes the time, in years, before a significant flux might be observed at the top of the one inch active cap layer. As indicated previously, the time required for penetration of a six inch layer is simply six times these values.

An examination of the predicted times before the measurement of a flux through the cap shows that the highly sorptive cap materials can lead to very long migration times perhaps longer than the expected lifetime of the contaminant in the sediment environment. If the predicted time is longer than the expected lifetime of the contaminant it should be expected that no significant flux will ever be detected.

Table 23. Breakthrough Times under Upwelling (1 cm yr⁻¹) and Diffusion (0.124 cm² day⁻¹) Conditions for a Thin Cap Layer.

Active Media 1 inch layer	Phenanthrene Breakthrough (years)	Pyrene Breakthrough (years)	Benzo[a]pyrene Breakthrough (years)	Transport Condition
Sediment	7	26	404	Upwelling
	8	29	442	Diffusion
Clay200	5	40	502	Upwelling
	5	44	548	Diffusion
Clay 202	4	14	253	Upwelling
	4	16	276	Diffusion
Clay 750	581	4,316	31,482	Upwelling
	634	4,711	34,363	Diffusion
PM-199, CETCO	710	4,741	36,586	Upwelling
	775	5,175	39,935	Diffusion
Clinoptilolite zeolite powder	1	2	128	Upwelling
	1	2	140	Diffusion
Clinoptilolite zeolite -4 mesh	5	13	505	Upwelling
	2	6	220	Diffusion
Clinoptilolite zeolite 8x14	3	3	283	Upwelling
	3	4	309	Diffusion
Phili Zeolite	2	5	404	Upwelling
	2	5	441	Diffusion
Apatite NC	6	17	526	Upwelling
	6	19	574	Diffusion
PIMS biological apatite	43	211	5,348	Upwelling
	47	230	5,837	Diffusion
Washed phosphate Ore, Tennessee	10	53	1,101	Upwelling
	11	57	1,202	Diffusion
Calcium phytate	2	3	134	Upwelling
	2	4	146	Diffusion

Effect of Selected Sequestering Agents on Mobility and Retention of Metals

Water Extraction under Reduced and Oxidized Conditions

The bioavailable pool of contaminants could be indicated by several methods; water extraction is one method that is often used in sequence with stronger reagents. Water extraction, by itself, can identify the portion of the contaminant pool that is loosely bound with sediments and may enter the aqueous phase. Generally, metals are transferred from sediments to pore water and then to the overlying water and into suspended plankton or directly into e.g., mussels or clams. Quantification of metal bioaccumulation in aquatic organisms has relied on determinations of metal uptake from diet and directly from the aqueous phase. Metal bioaccumulation models have incorporated coefficients of metal uptake from these two sources and have also incorporated the efflux rate constants of the metals in the animal (Luoma and Rainbow, 2005).

The chemistry of water extracts from the oxidized and reduced treatments differed (Figure 28). The redox potential was about -200mV in the reduced treatments and about -15mV in the oxidized treatments. Dissolved oxygen concentrations were about 1 mg L⁻¹ or less in the reduced treatments and about 7 mg L⁻¹ in the oxidized treatments. Differences in pH and EC between treatments were smaller but still substantial (Figure 28). Generally, addition of apatite and biopolymer or their mixture to the Anacostia River sediment did not influence EC values, especially in reduced treatments. However, addition of zeolite and organoclay increased EC values in both oxidized and reduced treatments (Figure 28).

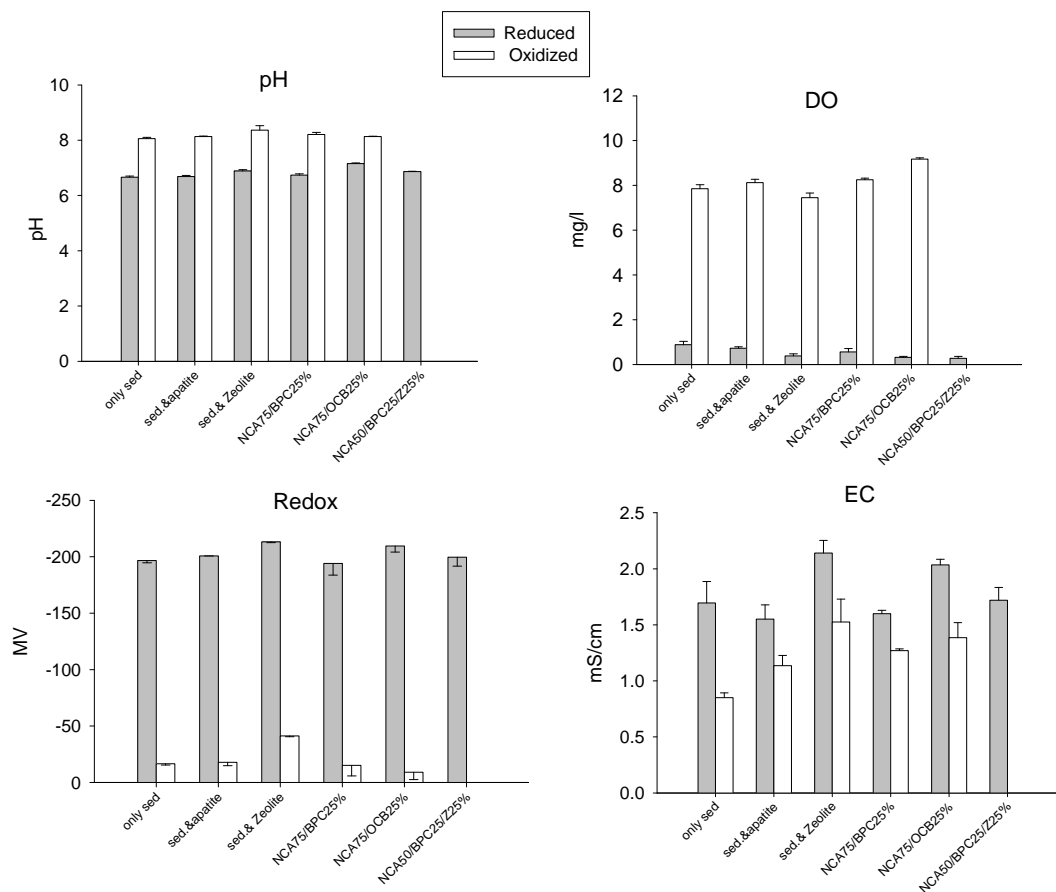


Figure 28. Effect of Amendments on Anacostia River Sediment Properties under Oxidized and Reduced Conditions; NCA – North Carolina apatite, OCB – organoclay 750 from Biomim, Inc., BPC – biopolymer chitosan, Z- zeolite.

Metal concentrations were generally higher under reduced conditions than under oxidized conditions (Table 24). The addition of 2% (dry weight) of apatite, zeolite, biopolymer, and organoclay, by itself or as a mixture influenced concentrations of elements in water extracts from both reduced and oxidized treatments (Table 24, Figures 29 and 30). Generally, all amendments reduced Fe and Mn concentration under reduced condition (Table 25). However, addition of North Carolina apatite increased P concentration from 2.5 to 3.3 mg L⁻¹ and from 0.8 to 1.4 mg L⁻¹; under reduced and oxidized conditions, respectively. Addition of NCA increased the Ca concentration under oxidized conditions (Table 25). Addition of other amendments generally reduced Ca concentration under oxidized condition.

The concentrations of most metals in water extracts from both reduced and oxidized Anacostia River sediments were lower than typical of contaminated sediments (Table 24). The concentrations of some elements, especially under oxidized conditions, approached method

detection limits making it difficult to accurately assess treatment effects. Therefore, only a few elements are presented for oxidized treatments in this report. In the reduced sediments North Carolina apatite (NCA), a mixture of NCA with chitosan (biopolymer) and zeolite (clinoptilolite), and a mixture of NCA with organoclay (OCB 750 from Biomin Inc.) substantially reduced Cr, Co, Ni, and Pb (Figure 30). In the oxidized treatments, element concentrations were very low and often near the detection limit for ICP-MS; therefore, we only present data for Pb and Cd in this report. The addition of 2% NCA, zeolite or a mixture of NCA with biopolymer, zeolite, or organoclays reduced Cd concentrations in the water extracts from the oxidized treatments (Figure 30). Lead concentrations were reduced by all tested amendments or mixtures of amendments under oxidized conditions (Figure 30).

The effectiveness of active amendments on stabilization of metals is based on several factors; eg., pool of available metal concentration, pH, redox potential, and other competing ions and anions. If the mobile/bioavailable pool of metals under specific conditions is substantial (e.g., about 50% of a total pool of metal) addition of active amendments could be clearly effective. However, if a metal is strongly bound to sediment (most of it is in the non-label fractions), then addition of active amendment would not be successful. In our experiments, amendments show some effectiveness for Co, Cr, Ni, and Pb. But, for Cu, As, and Se there was no benefit from the addition of active amendments to the sediments under the experimental setting because these elements were strongly bound to the mineral phases in the tested sediment. Research of Viana et al, (2008) showed similar results; e.g., performance of apatite was the best for Cd, Cr, and Pb; but not for As.

Table 24. Comparison of Element Concentrations in Water Extracts from Anacostia River Sediment under Reduced and Oxidized Conditions.

Elements	Units	Reduced		Oxidized	
		Avg	Stdev	Avg	Stdev
Cr	$\mu\text{g L}^{-1}$	77.0	5.2	28.4	1.4
Co	$\mu\text{g L}^{-1}$	16.9	1.2	3.6	0.2
Ni	$\mu\text{g L}^{-1}$	56.9	0.9	11.3	0.6
Cu	$\mu\text{g L}^{-1}$	33.1	15.5	25.7	0.4
Zn	$\mu\text{g L}^{-1}$	137.5	10.6	85.1	6.5
As	$\mu\text{g L}^{-1}$	23.1	2.8	3.3	0.2
Se	$\mu\text{g L}^{-1}$	7.1	0.2	2.0	0.1
Cd	$\mu\text{g L}^{-1}$	0.40	0.08	0.12	0.05
Pb	$\mu\text{g L}^{-1}$	22.8	0.4	4.6	0.4
Ca	mg L^{-1}	310.8	8.3	126.0	8.3
Fe	mg L^{-1}	88.3	3.0	0.4	0.1
Mn	mg L^{-1}	12.0	0.2	3.4	0.3
P	mg L^{-1}	2.5	0.1	0.8	0.1

Table 25. Effect of Amendments on Ca, Fe, Mn, and P Concentrations in Water Extracts from Reduced and Oxidized Treatments of Anacostia River Sediment.

Treatments		Unit	Reduced				Oxidized			
			Ca	Fe	Mn	P	Ca	Fe	Mn	P
Ctrl	Avg	mg L ⁻¹	310.8	88.3	12.0	2.5	126	0.37	3.39	0.76
NCA	Avg	mg L ⁻¹	265.5	68.0	8.6	2.5	215.4	0.39	4.83	1.40
ZC	Avg	mg L ⁻¹	137.8	36.8	5.4	3.3	61.4	0.71	1.81	0.80
NCA/BPC	Avg	mg L ⁻¹	236.9	48.8	6.8	1.5	181.3	0.22	4.24	0.80
NCA/OCB	Avg	mg L ⁻¹	385.9	8.2	2.6	2.0	225.7	0.29	2.56	1.56
NCA/BPC/Z	Avg	mg L ⁻¹	195.5	39.3	5.8	1.6	111.3	0.19	3.33	0.52
Ctrl	Stdev		8.3	3.0	0.2	0.1	22.1	0.05	0.29	0.11
NCA	Stdev		30.6	5.8	1.1	0.1	47.5	0.27	1.81	0.35
ZC	Stdev		3.0	0.6	0.1	0.1	17.7	0.30	0.54	0.68
NCA/BPC	Stdev		8.6	5.0	0.4	0.1	28.8	0.03	0.25	0.04
NCA/OCB	Stdev		50.6	0.8	0.1	0.2	7.7	0.01	0.10	0.74
NCA/BPC/Z	Stdev		8.5	0.6	0.2	0.2	89.4	0.08	4.42	0.09

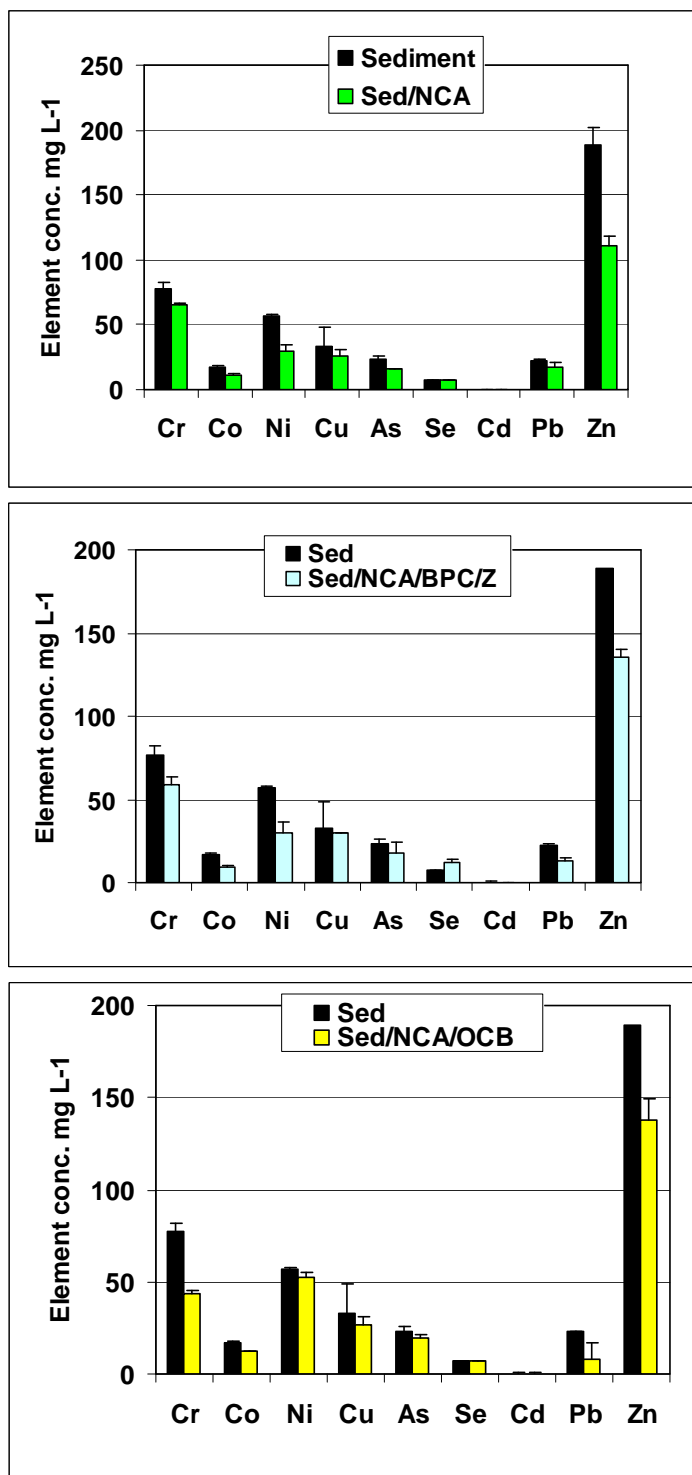


Figure 29. Effect of Amendments on Metal Concentrations in the Water Extracted from the Anacostia Sediment after Eight Weeks of Contact with Amendments under Reduced Conditions ($\sim 200\text{mV}$); the amount of added amendments - 2 % by dry weight.

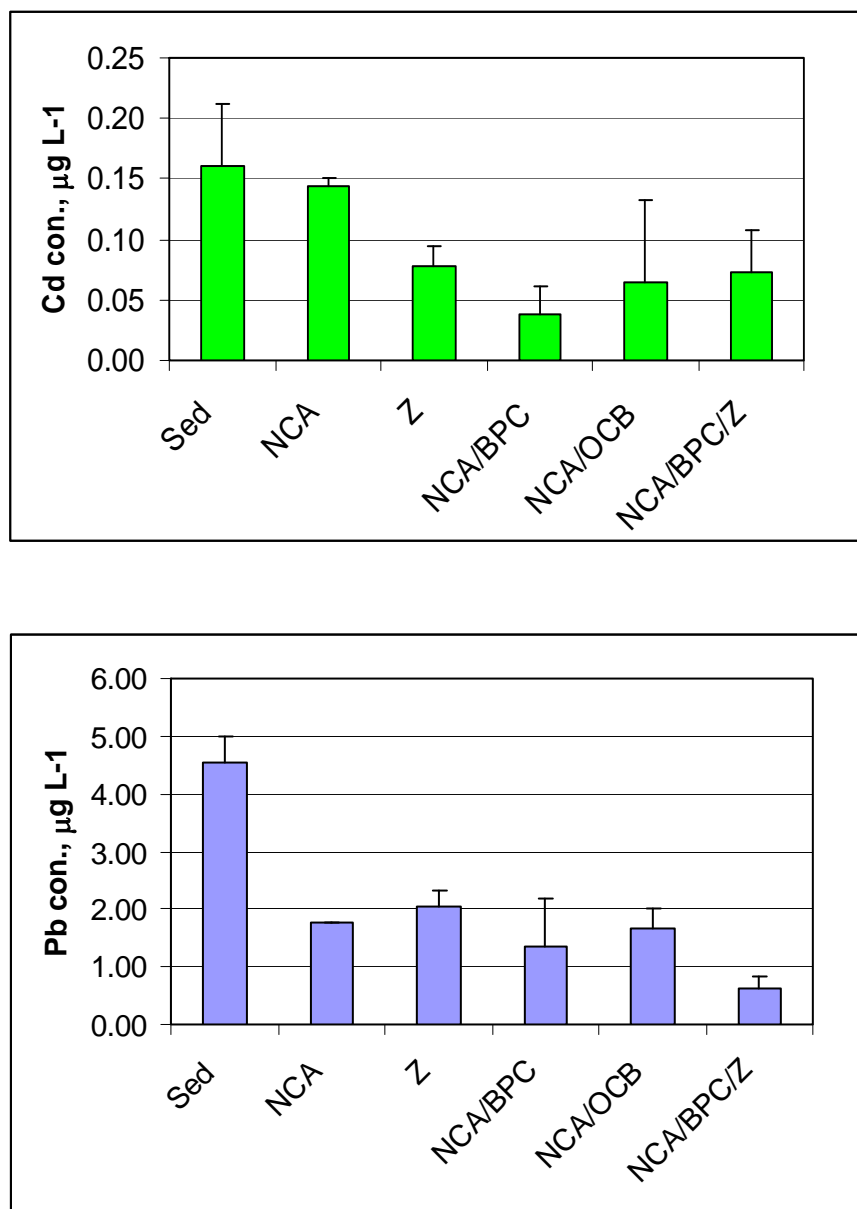


Figure 30. Effect of Amendments on Metal Concentrations in the Water Extracted from the Anacostia Sediment after Eight Weeks of Contact with Amendments under Oxidized Conditions ($\sim 200\text{mV}$); the amount of added amendments - 2 % by dry weight.

Sequential Extractions

The mobility and retention of metals in sediments strongly depends on their specific chemical and mineralogical forms and their binding characteristics. This implies that these forms and characteristics should be studied in addition to total metal concentrations. Since the early 1980s, single and sequential extraction schemes have been designed for the speciation of metals in soils and sediments (Tessier et al., 1979; Quevauviller et al., 1997). The technique developed by Tessier et al (1979) is one of the most frequently employed sequential extraction schemes. However, to obtain a greater understanding of potential metal mobility and retention in sediments, the method was modified. The original single extraction targeting Fe and Mn oxides as described by Tessier et al (1979) was replaced with two separate extractions (Amacher, 1996). Additionally, the sulfide fraction was included as an individual step to address the effect of reduced conditions that are typical for sediments.

The total concentration of a sedimentary metal could have little relevance to its bioavailability. The bioavailability of different metals in contaminated sediments is likely to be a function of a metal's characteristics – for example charge, ionic radius, and oxidation state, its chemical form and phase speciation in the sediment (Luoma and Bryan 1982; Tessier et al., 1993; Lee et al 2000; Griscom et al. 2000). Addition of amendments to sediments results in changes of sediment chemistry, for example amendments will change sediment pH, redox and chemical phases of elements and minerals. One way to evaluate these changes is a sequential extraction. Several studies showed that related phase speciation with bioavailability, metals bound to more refractory fractions would be expected to be less available for animals than metals loosely bound to sediment particle surface in exchangeable and carbonate fractions (Griscom et al., 2000). However, if a metal is strongly bound to sediment (most of it is in the non-label fractions), then the addition of active amendment will not be successful. In our experiments, amendments were not effective for As, Cd, Ni likely because these elements were strongly bound to the mineral phases in the tested sediment.

The data presented below are for the Elizabeth River sediment.

Sequential Extraction of Arsenic (As)

Many arsenic compound sorb strongly to hydrous oxides and sulfides in sediments and therefore are not very mobile. Rather a small portion of the As is detected in the exchangeable and carbonate fractions. Exchangeable and carbonate fractions include metals weakly sorbed via specific adsorption and precipitation reactions as well as those sorbed via outer-sphere reactions (Tessier et al., 1979) that are readily exchanged with other cations.

The partitioning of As in treated sediment was similar to the control sediment (untreated); however, more mobile fractions such as exchangeable and carbonates were higher in the untreated sediment than in the sediment treated with NCA or OCB-750 (Figure 31). In the sediment with the highest addition of NCA (10%), sulfide and residual fractions increased substantially compared with the control sediment (Figure 31).

Sequential Extraction of Cadmium (Cd)

In soils and sediments, Cd may be adsorbed by clay minerals (e.g., illite), carbonates or hydrous oxides of iron and manganese or it may be precipitated as Cd carbonate, hydroxide, or phosphate phase. Dudley et al. (1988 and 1991) suggested that adsorption mechanisms may be dominant for the deposition of Cd in soil and sediment. In the sequential extraction of sediments contaminated with Cd, the greatest proportion of the total Cd is typically associated with the exchangeable fraction (Hickey and Kittrick, 1984). Under strongly reducing conditions, precipitation as CdS controls the mobility of Cd (Smith et al., 1995).

Apatite is known to effectively remove soluble Cd (Ma et al, 1994 a and b; Wright 1995). From results for short-term contact studies with the use of fossil apatite mineral, Ma et al. (1997) concluded that minor octavite (CdCO_3) precipitation does occur, but that sorption mechanisms (such as surface complexation, ion exchange, or the formation of amorphous solids) are primarily responsible for the removal of soluble Cd. Cadmium phosphate, if formed, should be more stable than otavite under acidic conditions (Bodek et al., 1988; Chen et al., 1997).

The partitioning of Cd within the various fractions of the untreated and treated Elizabeth River sediment is illustrated in Figure 32. The distribution patterns are similar for the sediment with and without amendments, except that the proportion of Cd in exchangeable, carbonate, and amorphous oxides is substantially greater in the untreated sediments (Figure 32). The greatest increase in the Cd sulfide fraction was observed for the addition of 10% NCA. The residual fraction increased proportionally to the increased dose of NCA, with the highest values for the 10% addition of NCA (Figure 32). Similar patterns of Cd distribution among the fractions were observed for the addition of OCB and the mixture of OCB and NCA (Figure 32).

Sequential Extraction of Cobalt (Co)

Various investigators have found that Co accumulates in hydrous oxides of Fe and Mn in soils and sediments (Adriano, 2001). However, the sorption mechanism of Co by crystalline Fe and Mn oxides apparently differs at different pH values and generally is based on the interchange of Co^{2+} with Mn^{2+} and on the formation of the hydroxyl species, $\text{Co}(\text{OH})_2$, precipitated at the oxide surface. Different redox mechanisms have been proposed for Co sorption by Mn oxides (Kabata-Pendias, 2001). These include: (1) oxidation of Co^{2+} to Co^{3+} at the oxide interface, (2) reduction of Mn^{4+} to Mn^{3+} in the oxide crystal lattice, and (3) replacement of Mn^{3+} or Mn^{4+} by Co^{3+} . Generally, the sorption of Co by Mn oxides increases greatly with pH, however, mobility of Co in sediments is influenced by Mn oxides and by Eh-pH sediment intensities. Also, sediment organic matter and clay content are important factors that govern Co distribution and behavior (Kabata-Pendias, 2001). Under very reducing conditions in the presence of dissolved sulfide, Co(II) bisulfide species, such as $\text{Co}(\text{HS})_2$ likely dominate (Krupka and Serne, 2002).

Figure 33 illustrates the effect of apatite and organoclay on Co distribution in the Elizabeth River sediment. In the untreated sediment Co mainly associated with the amorphous Fe, Mn oxide, and sulfide fractions. The carbonate and crystalline oxide fractions were the second most predominant fractions. The exchangeable pool of Co in the untreated sediment was even higher

than the residual Co pool; i.e., 1.3 mg kg^{-1} and 0.4 mg kg^{-1} , respectively (Figure 33). Addition of 2.5, 5.0, and 10% by weight of NCA reduced substantially the exchangeable fraction of Co, and increased the residual fraction. A similar pattern was observed for the addition of organoclay and the mixture of NCA with organoclay (Figure 33).

Sequential Extraction of Chromium (Cr)

Chromium sorbs to many sediment mineral phases, such as clays and oxides of Fe and Mn, but this is pH dependent and is competitive with common anions such as sulfate, sulfide, and carbonate (Zachara et al., 1987). Thus, chromate generally remains relatively mobile. Reduced Cr^{3+} is readily hydrolyzed to form $\text{Cr}(\text{OH})_3$ hydrates, which also may form a solid intermixed with Fe oxyhydroxide. The solubility and mobility of reduced Cr is typically very low. The existence of minerals such as embreyite (hydrated lead chromate phosphate) suggests that it is possible for Cr^{6+} (as chromate) to be co-precipitated into crystalline structures along with phosphate phases.

Data summarized in Figure 34 indicate that there was substantial interaction between the highest dose of NCA (10%) and Cr in the Elizabeth River sediment, which resulted in a substantial increase of Cr in the residual fraction (Figure 34). Also, a 2.5% dose of organoclay and organoclay mixed with NCA provided similar results (Figure 34).

Sequential Extraction of Nickel (Ni)

Suzuki et al. (1981 and 1982) studied the removal of selected metals from solutions passed through columns packed with synthetic hydroxyapatite; very limited data suggests that appreciable Ni (II) could be removed. The authors assumed a cation exchange mechanism, and ranking in terms of the amount exchangeable was $\text{Cd(II)}, \text{Zn(II)} > \text{Ni(II)}, \text{Ba(II)}, \text{Mg(II)}$. Sowder et al. (1999) also suggested that hydroxyapatite may be effective for reducing Ni availability in sediment. Nickel forms an insoluble phosphate salt ($\text{Ni}_3(\text{PO}_4)_2 \cdot 7\text{H}_2\text{O}$) and should be amenable to precipitation by the phosphate released by the dissolving apatite phase. In addition, the existence of mixed nickel-containing phosphate minerals (e.g., cassidyite, hydrated calcium nickel magnesium phosphate) suggests that synergistic co-precipitation may occur (Bostick et al., 2003).

The data on the effect of apatite and organoclay on Ni distribution among mineral phases extracted from the Elizabeth River sediment are presented in Figure 35. Addition of NCA or OCB, or OCB/NCA resulted in a reduction of the mobile pool of Ni and an increase in the residual pool of Ni in the sediment (Figure 35).

Sequential Extraction of Lead (Pb)

Most Pb salts (e.g., phosphates, sulfates, sulfides, carbonates, hydroxides) are either sparingly soluble or almost completely insoluble. Lead interacts strongly with clay minerals, oxides of Fe and Mn, and with organic matter such as humic acids (Bodek, 1988; McLean and Bledsoe, 1992). As a result, Pb solubility and mobility is low in most subsurface systems. In natural

waters at $\text{pH} > 7$, Pb is either adsorbed on clay surfaces or forms Pb-carbonate precipitate. Lead has a strong affinity for organic ligands, and the formation of such complexes may greatly increase Pb mobility in sediments. The long-term stability of Pb-compounds in the sediments depends upon differences in the nearly insoluble phases, e.g., pyromorphite-type phosphate minerals versus carbonate or hydroxide phases. Lead phosphates, especially pyromorphite minerals, demonstrate minimal solubility and bioassessability (Ruby, 1994; Chen 1997; Zhang 1998).

The partitioning of Pb within the various fractions of the Elizabeth River sediment with and without amendments is illustrated in Figure 36. For the untreated Elizabeth sediment, the Pb was predominantly associated with the amorphous Fe and Me oxide fraction, presumably by sorption to these oxides (Barnett et al., 2002). The next most abundant fractions were the residual and sulfite fractions, with the exchangeable fraction being the least abundant (Figure 36). As expected, the additions of NCA (2.5%, 5.0%, and 10% by weight) shifted Pb from amorphous oxide, carbonate, and exchangeable fractions to the sulfide and residual fractions. The largest shift was observed with the addition of 10% NCA (Figure 36).

Sequential Extraction of Zinc (Zn)

Zinc in dilute solution hydrolyzes negligibly below pH 6, but at pH values > 7.5 , the neutral species $\text{Zn}(\text{OH})_2$ typically becomes the predominant soluble species in aqueous systems (Bodek et al., 1988). As its species formed with common ligands in surface waters are soluble in neutral and acidic solution, zinc is readily transported in most natural waters and is one of the most mobile heavy metals (Bodek et al., 1988).

Zinc may be sequestered by reaction with apatite, as demonstrated by Wright et al. (1995), Moody and Wright (1995), and Chen et al. (1997). Chen et al. (1997) reported that sorptive removal of Zn(II) by apatite is pH dependent, with a sharp increase in the removal of soluble Zn when the final solution pH value is > 6.5 . Chen et al. (1997) also reported that hopeite [$\text{Zn}_3(\text{PO}_4)_2 \cdot 4\text{H}_2\text{O}$] is the principal mineral phase formed by interaction of Zn(II) and apatite at near-neutral pH values.

The partitioning of Zn within the various fractions of the untreated and treated Elizabeth River sediment is illustrated in Figure 37. For the untreated sediment, the Zn was predominantly associated with the amorphous oxide and carbonate fractions, which are relatively mobile fractions (Figure 37). Oxyhydroxide (oxide) minerals, along with organic matter, have been recognized as the predominant metal sorbents in aquatic systems. In comparison with carbonate minerals, amorphous oxide minerals have a surface site density that is three to four orders of magnitude greater and a larger surface area (oxides up to $300 \text{ m}^2 \text{ g}^{-1}$, organic matter up to $1900 \text{ m}^2 \text{ g}^{-1}$, and carbonates usually $< 1 \text{ m}^2 \text{ g}^{-1}$) (Forstner and Wittmann, 1979; Benjamin and Leckie, 1981; Bilinski et al., 1991). The addition of only 2.5% (by dry weight) of NCA or OCB reduced by 90% the exchangeable pool of zinc. Also, carbonate and amorphous oxide fractions were substantially reduced in the Elizabeth River sediment when treated with NCA or OCB (Figure 38). The reduction of relatively mobile fractions such as the exchangeable, carbonate, and

amorphous resulted in new mineral phases associated with the crystalline, sulfide, and residual fractions (Figure 37).

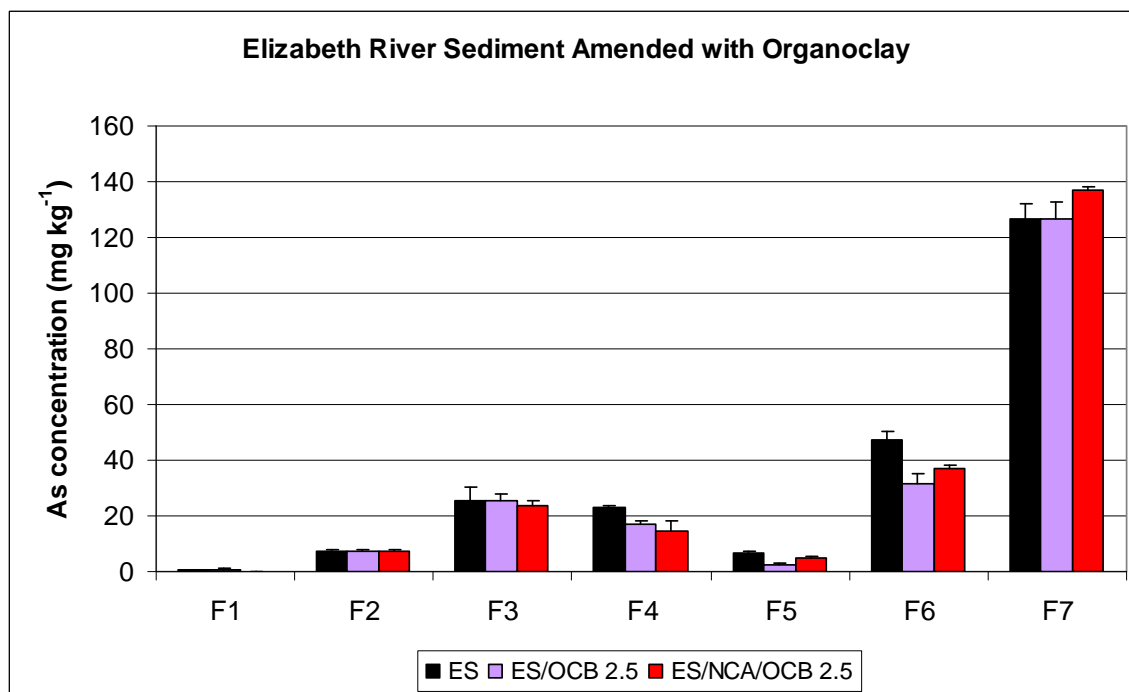
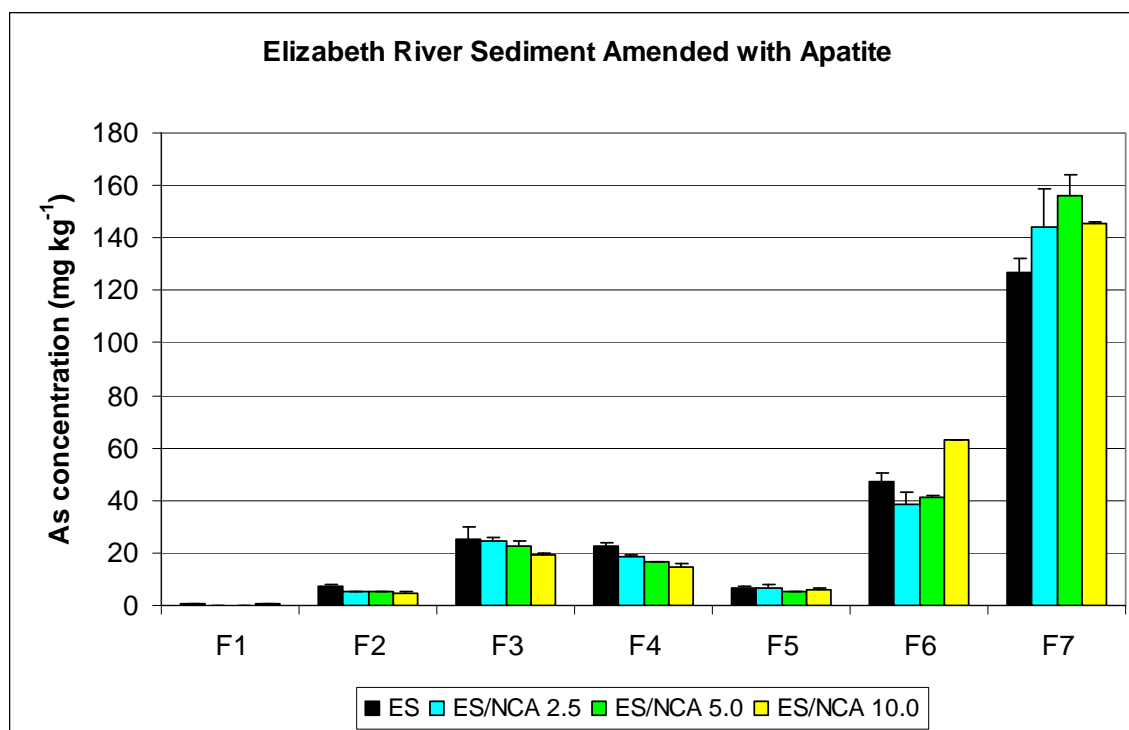


Figure 31. Effect of North Carolina Apatite (NCA) and Organoclay (OCB) on Partitioning of As in Elizabeth River Sediment (ES); F1 - exchangeable fraction, F2 - carbonate fraction, F3 - amorphous fraction, F4 - crystalline oxide, F5 - organic, F6 - sulfide, and F7 - residual; doses of amendments in % by dry weight: 2.5, 5, and 10.

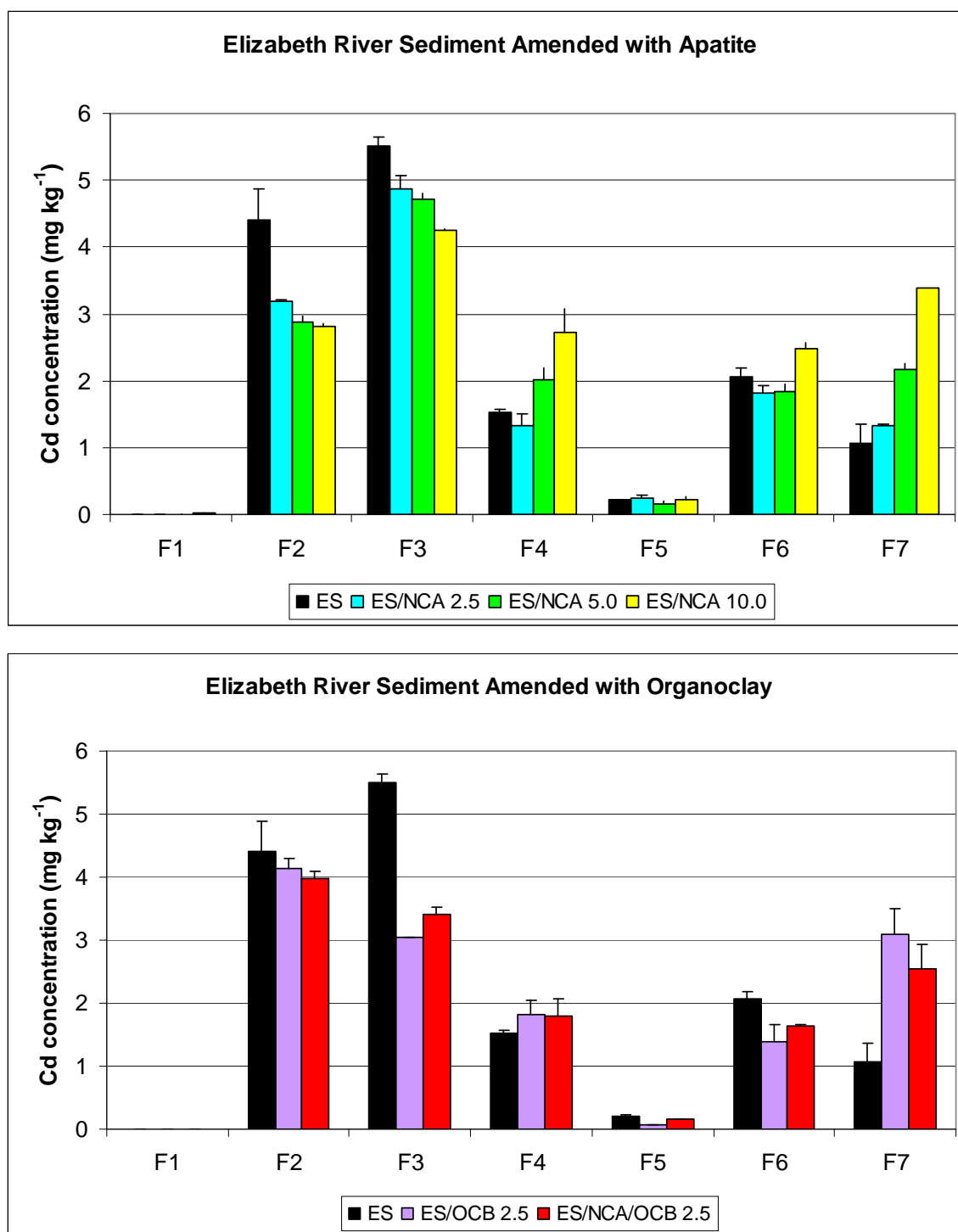


Figure 32. Effect of NCA and OCB on Partitioning of Cd in Elizabeth River Sediment (ES); F1 - exchangeable fraction, F2 - carbonate fraction, F3 - amorphous fraction, F4 – crystalline oxide, F5 – organic, F6 – sulfide, and F7 – residual; doses of amendments in % by dry weight: 2.5, 5, and 10.

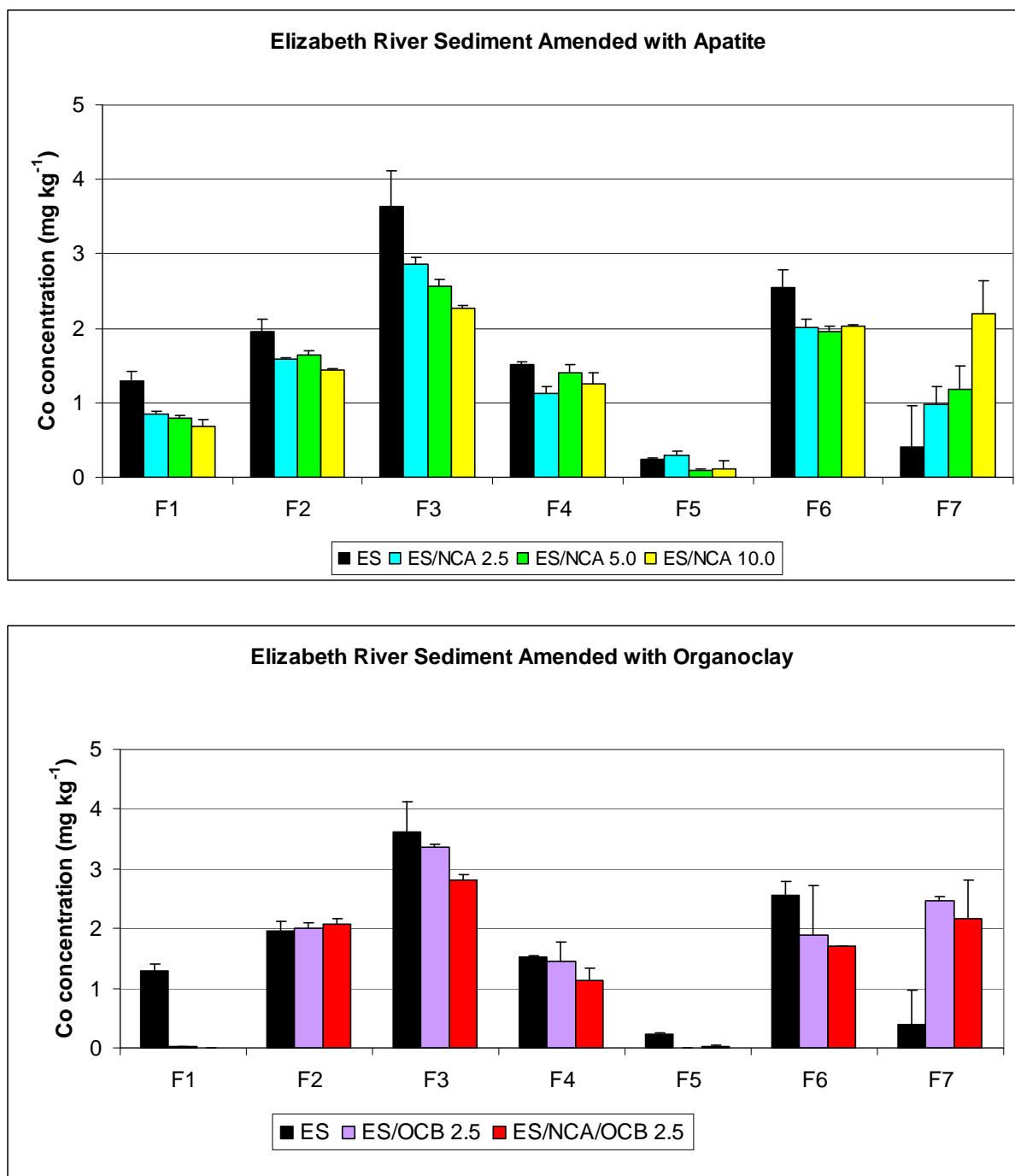


Figure 33. Effect of NCA and OCB on Partitioning of Co in Elizabeth River Sediment (ES); F1 - exchangeable fraction, F2 - carbonate fraction, F3 - amorphous fraction, F4 – crystalline oxide, F5 – organic, F6 – sulfide, and F7 – residual; doses of amendments in % by dry weight: 2.5, 5, and 10.

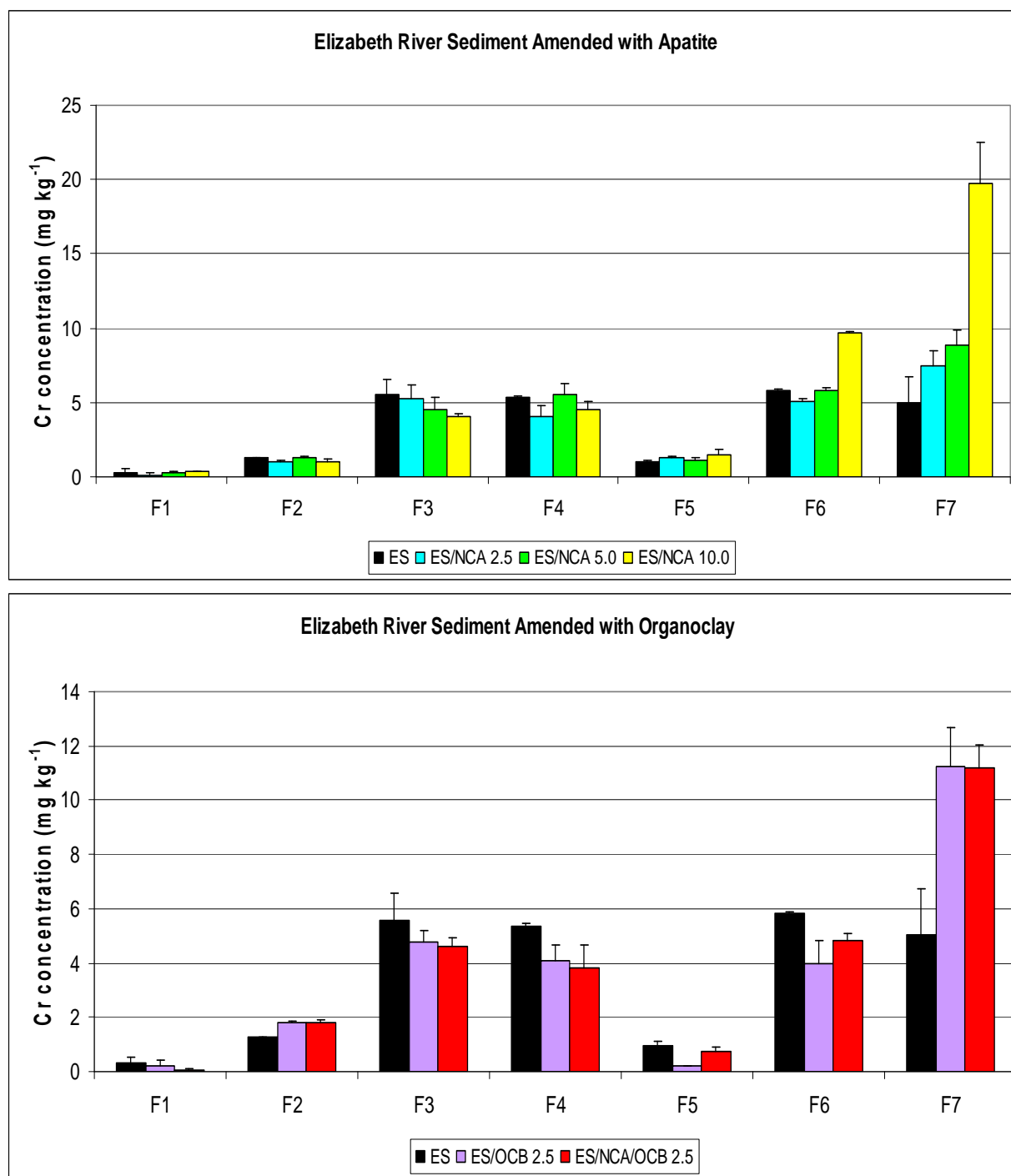


Figure 34. Effect of NCA and OCB on Partitioning of Cr in Elizabeth River Sediment (ES); F1 - exchangeable fraction, F2 - carbonate fraction, F3 - amorphous fraction, F4 – crystalline oxide, F5 – organic, F6 – sulfide, and F7 – residual; doses of amendments in % by dry weight: 2.5, 5, and 10.

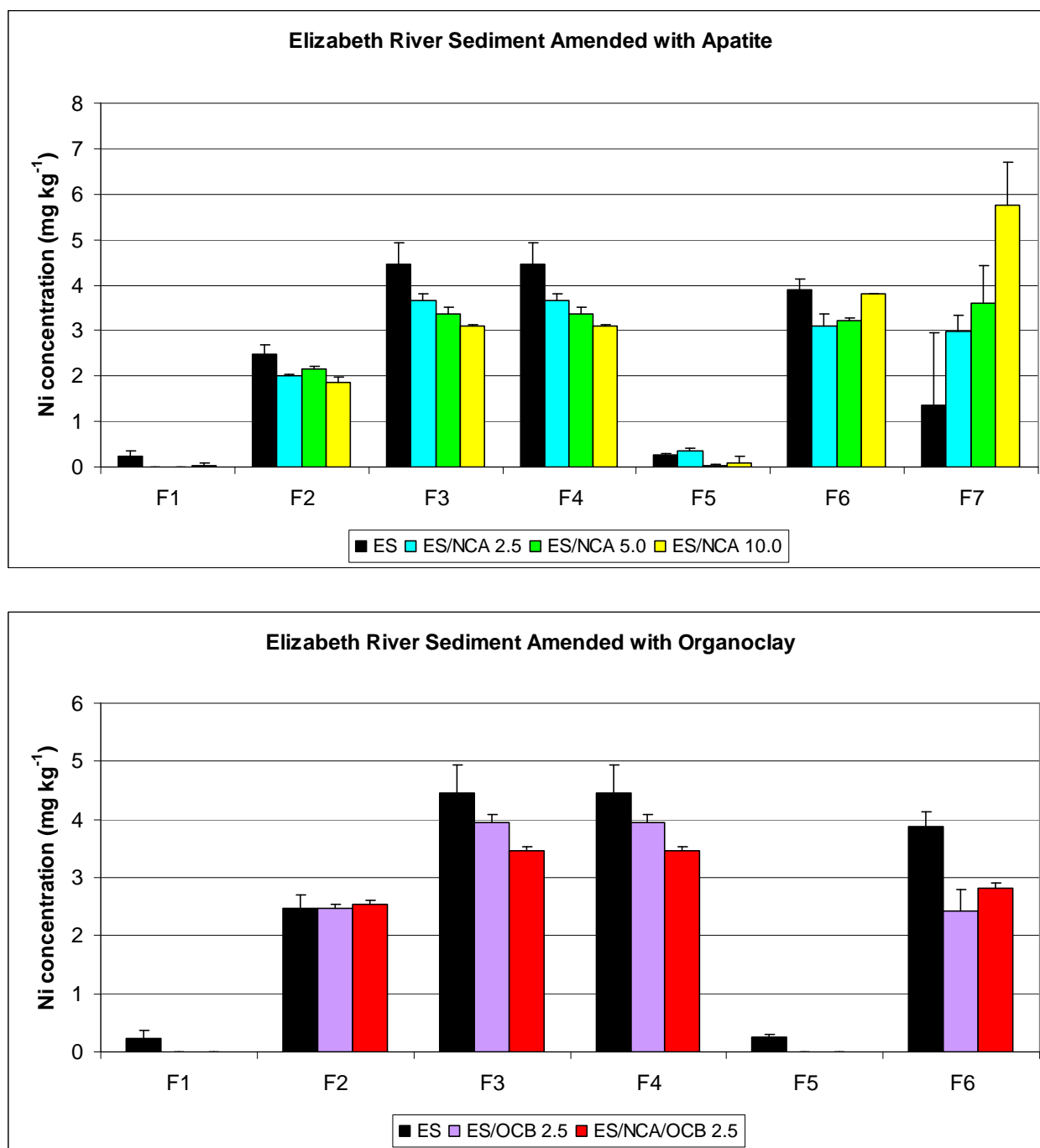


Figure 35. Effect of NCA and OCB on Partitioning of Ni in Elizabeth River Sediment (ES); F1 - exchangeable fraction, F2 - carbonate fraction, F3 - amorphous fraction, F4 – crystalline oxide, F5 – organic, F6 – sulfide, and F7 – residual; doses of amendments in % by dry weight: 2.5, 5, and 10.

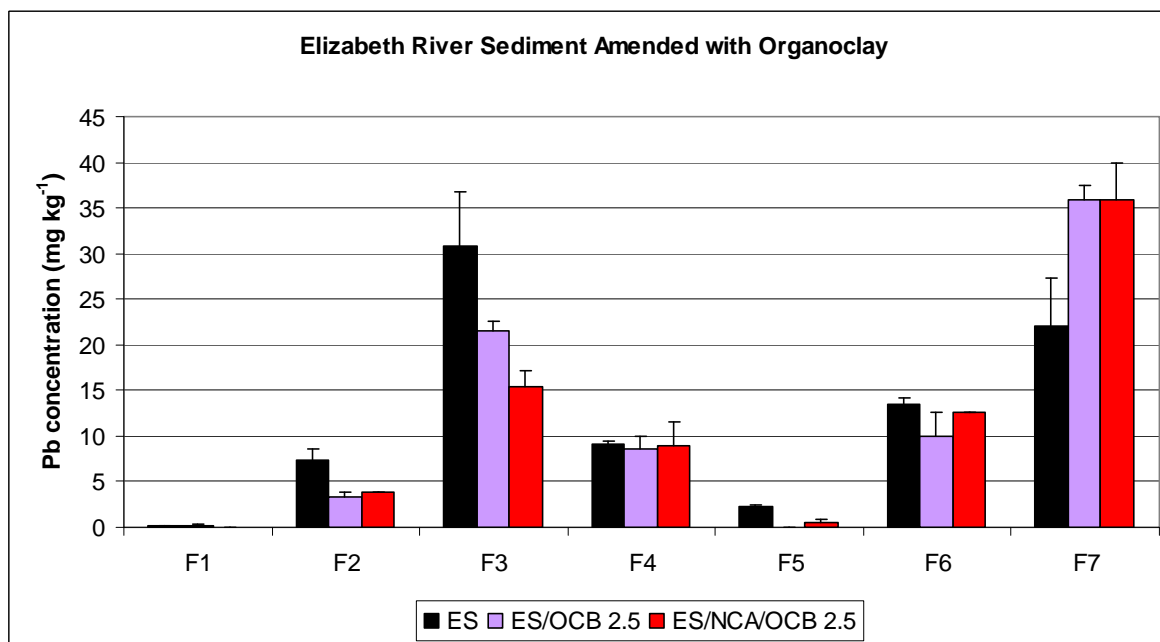
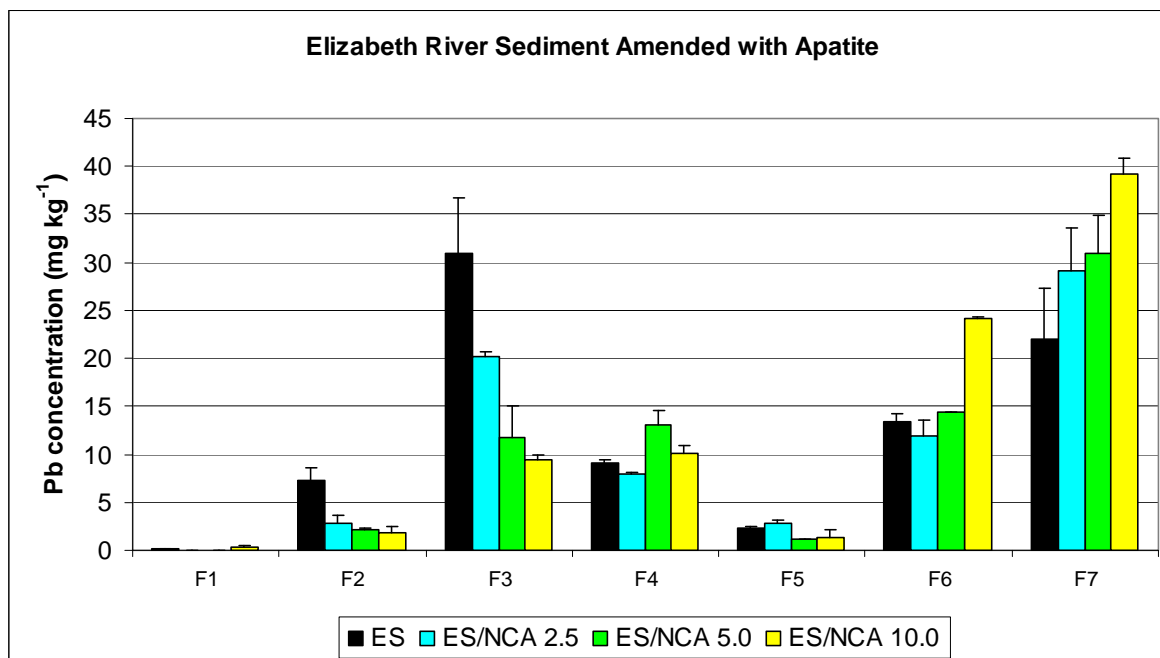


Figure 36. Effect of NCA and OCB on Partitioning of Pb in Elizabeth River Sediment (ES); F1 - exchangeable fraction, F2 - carbonate fraction, F3 - amorphous fraction, F4 – crystalline oxide, F5 – organic, F6 – sulfide, and F7 – residual; doses of amendments in % by dry weight: 2.5, 5, and 10.

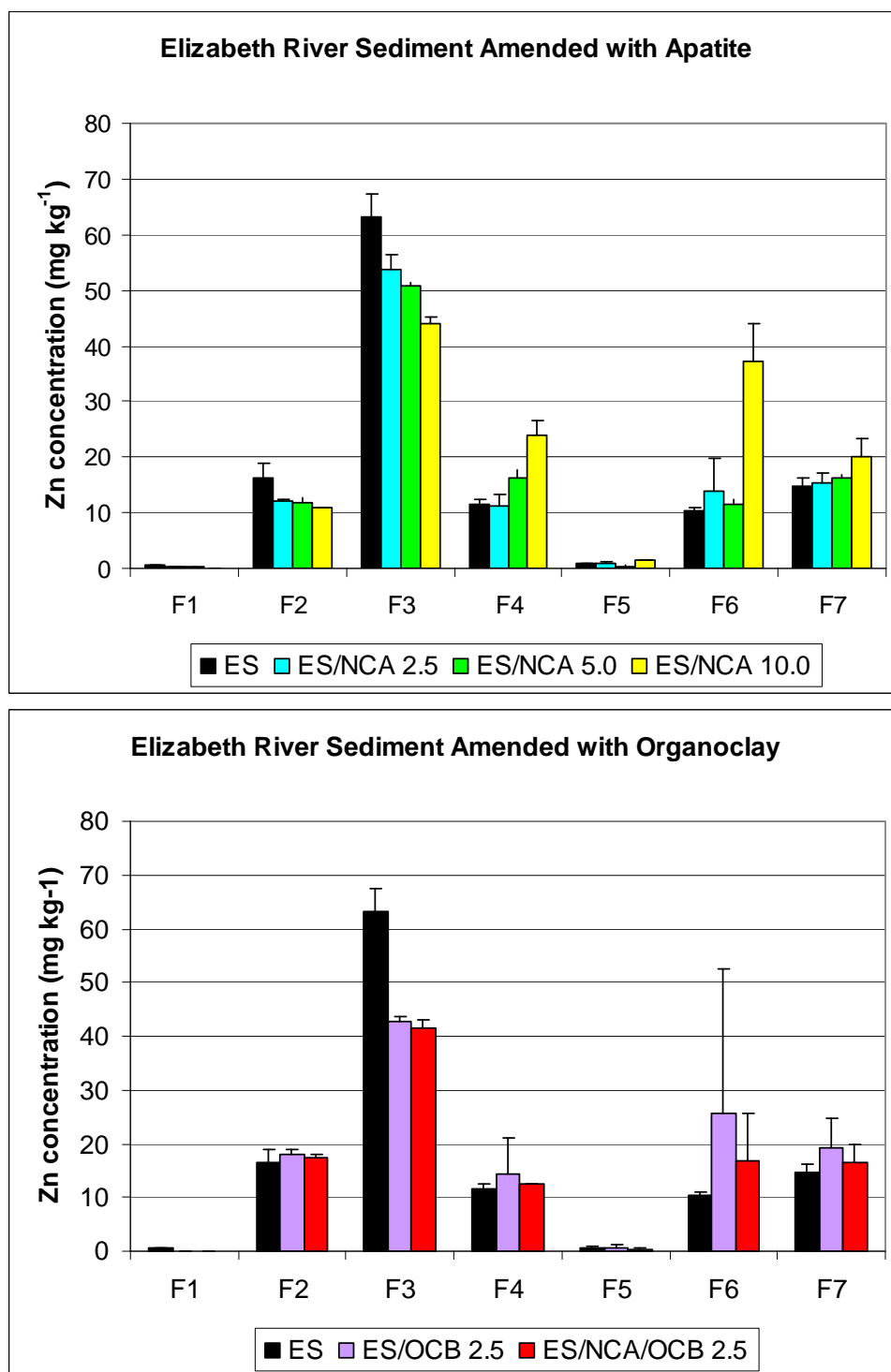


Figure 37. Effect of NCA and OCB on Partitioning of Zn in Elizabeth River Sediment (ES); F1 - exchangeable fraction, F2 - carbonate fraction, F3 - amorphous fraction, F4 – crystalline oxide, F5 – organic, F6 – sulfide, and F7 – residual; doses of amendments in % by dry weight: 2.5, 5, and 10.

Potentially mobile fraction and recalcitrant factor

Sequential extraction results can be summarized using the concepts of the Potentially Mobile Fraction (PMF) and Recalcitrant Factor (RF) (Knox et al., 2006a). Early extraction steps (exchangeable, carbonate, amorphous oxides, and organic fractions) tend to recover metal fractions that are less strongly bound than the fractions collected in the later extraction steps (crystalline oxides, sulfides, and residue fractions). The less strongly bound fractions can be termed the PMF because they constitute the contaminant fraction that has the potential to enter into the mobile aqueous phase in response to changing environmental conditions, such as pH, Eh, temperature, etc. The PMF for the untreated and treated Elizabeth River sediment was calculated using equation 21 shown below:

$$\text{Potentially Mobile Fraction} = 100 - (F_{\text{Cry. oxides}} + F_{\text{Sulfide}} + F_{\text{Residual}}) \quad (21)$$

where:

$F_{\text{Cry. oxides}}$ = crystalline Fe oxide fraction (wt-%)

F_{Sulfide} = sulfide fraction (wt-%)

F_{Residual} = residual fraction (wt-%)

Fractions of the contaminant pool that are very strongly bound by the sediment include crystalline oxides, sulfides or silicates, and aluminosilicates. These strongly bound fractions were used to calculate the RF. The RF is the ratio of strongly bound fractions to the total concentration of the element (i.e., sum of all fractions) in the sediment. The meaning of the RF is opposite to the PMF; i.e., the RF indicates the virtually irreversible retention of metals by the solid phase. For this study the RF was calculated using equation shown below:

$$\text{Recalcitrant Factor} = \left[\frac{C_{\text{cry.oxides}} + C_s + C_{\text{residual}}}{C_{\text{exch}} + C_c + C_{\text{org}} + C_{\text{oxides}} + C_s + C_{\text{residual}}} \right] \times 100 \quad (22)$$

where:

C = concentration

Subscripts *crystalline oxides* (*cry. oxides*), *sulfides* (*s*) and *residual*, represent the three final fractions of the sequential extractions. The subscripts *exch*, *c*, *org*, and *oxides* stand for water soluble and exchangeable metals, carbonates, organically bound metals, and metals bound to amorphous and crystalline oxides, respectively. This construct provides an estimate of the percentage of a contaminant in the sediment that is resistant to remobilization; i.e., retention of contaminants in sediments.

Results for the untreated and treated Elizabeth sediment are presented in Figure 38. Of the seven tested elements, Cd, Zn, Co, and Pb showed the highest PMF values in the untreated sediment, more than 50% (Figure 38). Addition of amendments such as apatite or organoclay to the sediment reduced substantially the PMF values of all tested elements, with the greatest reductions for Pb, Zn, Cd, and Co (Figure 38). For example, the addition of 10% NCA to the sediment resulted in about a 40% reduction in the PMF values for Co, Cd, Pb, and Zn (Figure

38). Of all tested elements, As had the highest RF value in the untreated sediment: 84% (Figure 38). When the mobile fraction is very limited, like for As, the addition of amendments reduces the PMF and increases the RF less substantially (Figure 38).

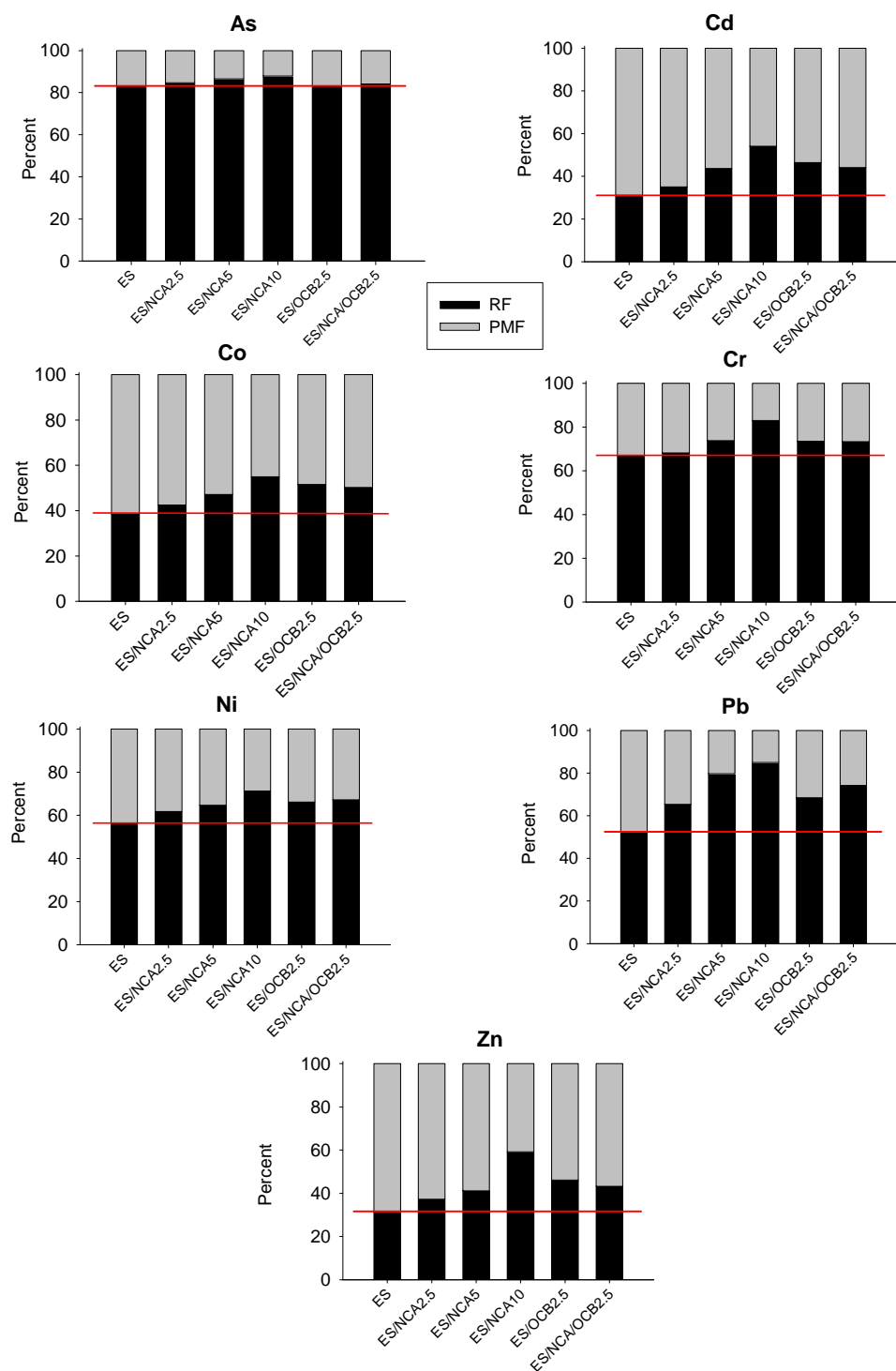


Figure 38. Average Potentially Mobile Fraction (PMF) and Recalcitrant Factor (RF) for As, Cd, Co, Cr, Ni, Pb, and Zn in Untreated and Treated Elizabeth River Sediment (ES). The red line represents the partitioning of untreated sediment; doses of amendments in % by dry weight: 2.5, 5, and 10.

TASK 2. STUDIES FOR DETERMINATION OF THE BEST COMBINATION OF AMENDMENTS FOR PLACEMENT AND CONSTRUCTION OF ACTIVE SEDIMENT CAPS

SUBTASK 2.1. EVALUATION OF MECHANICAL PROPERTIES

Physical Properties of Biopolymer Materials and Other Amendments

Organic carbon content was measured as an indicator of the efficiency of the procedure for coating the sand with biopolymers and as an indicator of the potential for the sorption of organic contaminants on the coated sand. The acid washed sand was successfully coated with cross-linked biopolymers. The carbon fraction of the acid washed coated sand was similar to with the carbon fraction of the coated play sand indicating that the coating procedure was equally effective with both types of sand. The measured carbon fractions are listed in Table 26. The carbon fractions of coated sand with one wash, two washes and three washes did not differ substantially from the unwashed sand, indicating that the coated sand was resistant to washing.

Table 26. Carbon Fractions of Biopolymer Materials.

Samples	Unwashed (%)		Washed (%)	
	Replicate 1	Replicate 2	Replicate 1	Replicate 2
CGB1	9.210	6.009	2.932	3.180
CGB2	7.893	-	5.197	5.964
CGB3	3.938	-	2.366	2.062
GB1	1.482	4.809	2.653	2.615
GB2	3.670	3.828	2.515	2.877
GB3	4.000	2.329	5.919	0.607
GX1	6.072	5.267	3.395	2.618
GX2	4.634	3.941	2.97	-
GX3	0.385	0.369	0.301	0.306
XCc	3.660	4.282	3.631	3.490
Xc	3.645	1.964	1.361	1.018
Ac	1.207	2.049	0.332	0.277
CGB*	1.050	1.058	0.774	1.042
XCc*	1.297	1.888	0.953	1.352
GX1*	1.197	2.267	0.482	0.966
GX2*	1.781	0.415	0.064	0.174
C*	5.287	5.576	3.336	3.996
C*	1.622	1.322	1.097	1.190

* Sand used in these batch studies is unwashed; C-chitosan; G-guar gum, B-borax, X-xanthan; c-calcium chloride; 1 – without glutaraldehyde, 2 – with glutaraldehyde, 3 - without glutaraldehyde but with NaOH.

Other properties such as bulk density and porosity of amendments and coated sands are presented in Tables 27-30. The coated sands had lower density than regular sand (Table 27). On the other hand, the porosity of the coated sand was higher than the regular sand (Table 30).

Table 27. Bulk Density of Sequestering Agents (g mL⁻¹).

Sorbents	Density (g mL⁻¹)	Standard deviation
PIMS biological appetite	0.7835	0.0134
Clino zeolite 8x14	0.7646	0.0182
Clino zeolite -4 mesh	0.9335	0.0246
Clino zeolite powder	0.6538	0.0365
Phili Zeolite	0.7779	0.0179
CETCO TM-199	0.7618	0.0272
Washed phosphate	1.2631	0.0133
Clay 750	0.3875	0.0128
Clay 202	1.1303	0.0331
Clay 200	1.1637	0.0185
North Carolina apatite	1.5138	0.0294
Calcium phytate	0.4418	0.0243
CETCO TM-200	0.6885	0.0338

Table 28. Bulk Density of Coated Sand (g mL⁻¹).

Coated Sand	Density (g mL⁻¹)	Standard deviation
CGB1	0.741	0.074
CGB2	0.909	0.024
CGB3	1.061	0.004
GB2	1.287	0.009
XCc	1.182	0.081
GX1	1.182	0.048
Sand	1.515	0.069

C-chitosan; G-guar gum, B-borax, X-xanthan; c- calcium chloride; 1 – without glutaraldehyde, 2 – with glutaraldehyde, 3 - without glutaraldehyde but with NaOH.

Table 29. Porosity of Sorbents.

Sorbents	Porosity	Standard deviation
PIMS biological appetite	0.791	0.013
Clino zeolite 8x14	0.486	0.009
Clino zeolite -4 mesh	0.435	0.050
Clino zeolite powder	0.516	0.022
Phili Zeolite	0.544	0.009
CETCO TM-199	0.557	0.053
Washed phosphate	0.479	0.035
Clay 750	0.857	0.024
Clay 202	0.861	0.076
Clay 200	0.805	0.056
North Carolina apatite	0.412	0.068
Calcium phytate	0.567	0.047
CETCO TM-200	0.550	0.001

Table 30. Porosity of Biopolymer Materials.

Sorbents	Porosity	Standard deviation
CGB1	0.646	0.005
CGB2	0.650	0.008
CGB3	0.629	0.054
GB2	0.561	0.056
XCc	0.546	0.001
GX1	0.388	0.017
Sand	0.378	0.031

C-chitosan; G-guar gum, B-borax, X-xanthan; c- calcium chloride; 1 – without glutaraldehyde, 2 – with glutaraldehyde, 3 - without glutaraldehyde but with NaOH.

SUBTASK 2.2. EVALUATION OF DIFFUSIVE TRANSPORT

Diffusion of Metals through Active Caps – Laboratory Experiment

Diffusion is a spontaneous process that results in the movement of a solute. It is caused by the random thermal motion of a solute in solution and is driven by concentration gradients. Solutes move from high concentration areas to low concentration areas.

In the diffusion experiment, water samples were collected 48 hrs, one, two, four, and six months after the experiment was initiated (Picture 16). The water samples were analyzed for metal content. The water from the control treatment (i.e., sediment without cap material) showed the highest metal concentrations (average of 5 samplings) (Figure 39). As was expected, all cap materials prevented desorption of metals from the underlying sediment over the short period represented by the study. Therefore, metal concentrations in solution were near zero or background DI water levels (Figure 39) for all treatments employing sediment caps. These data are in agreement with model predictions, which show that even sand will retain metals in sediment for one year.

For almost all amendments the pH stabilized after two months and remained fairly constant until the end of the experiment (Figure 40). Amendments such as North Carolina apatite, coated sand (XCc), sand, and mixtures of amendments were associated with the smallest pH shifts, and pH in these treatments did not exceed 8.

Electrical conductivity (EC) after six months decreased for almost all amendments (Figure 41). The highest shift in EC values were observed for organoclay (Figure 41).

Total organic carbon (TOC) and TIC were measured in water, sediment, and in selected cap materials at the end of the six month diffusion experiment. The aqueous TOC concentration was elevated in experimental columns containing caps with the biopolymer CGB, the biopolymer XCc, and organoclay (Figure 42). Elevated aqueous TOC in the columns with biopolymer caps may reflect the release of carbon from the biopolymers. The reason for elevated TOC in the columns with organoclay caps is unknown. Total organic carbon (TOC) in the sediments underlying the caps did not differ substantially among most treatments but was somewhat higher in the sediment beneath the cap with biopolymer CGB (Figure 43). However, the diffusion of carbon in the sediment beneath the biopolymer CGB occurred only in the first layer of the sediment (0-1.5 cm). The deeper layers had TC content similar to the control sediment (Figure 43). This pattern was not observed with the biopolymer XCc suggesting that it may be more stable over time (Figure 43).

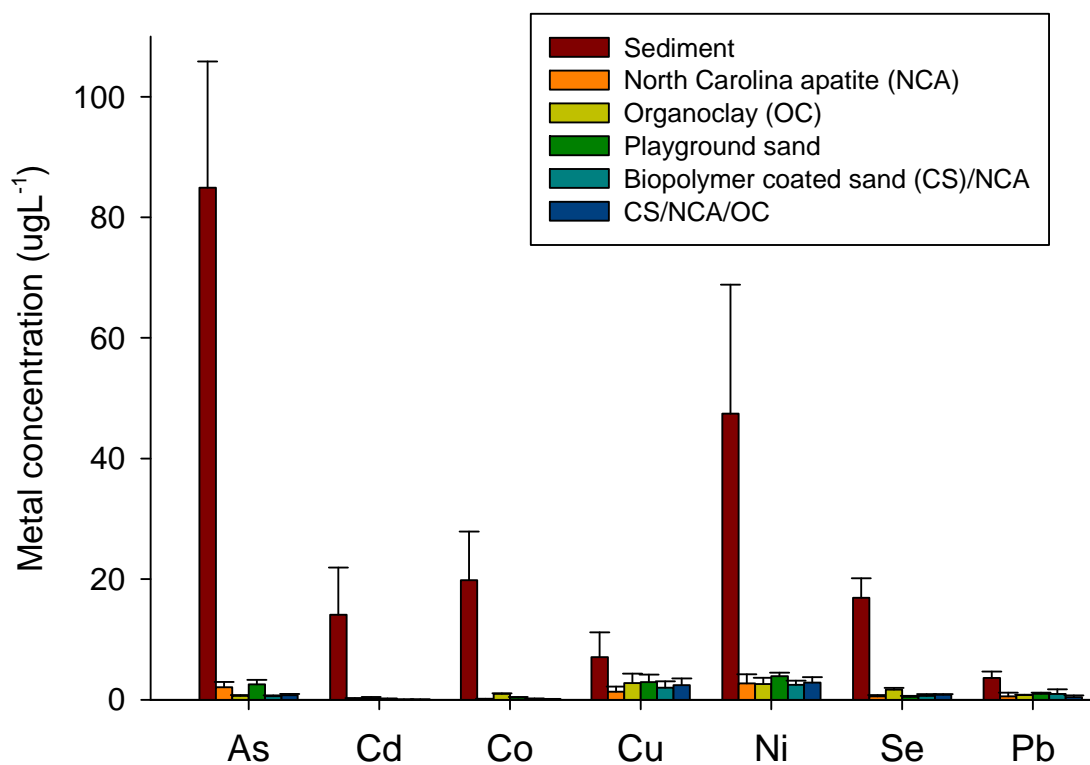


Figure 39. Metal Release in Diffusion Experiment after Six Months; average of five samplings.

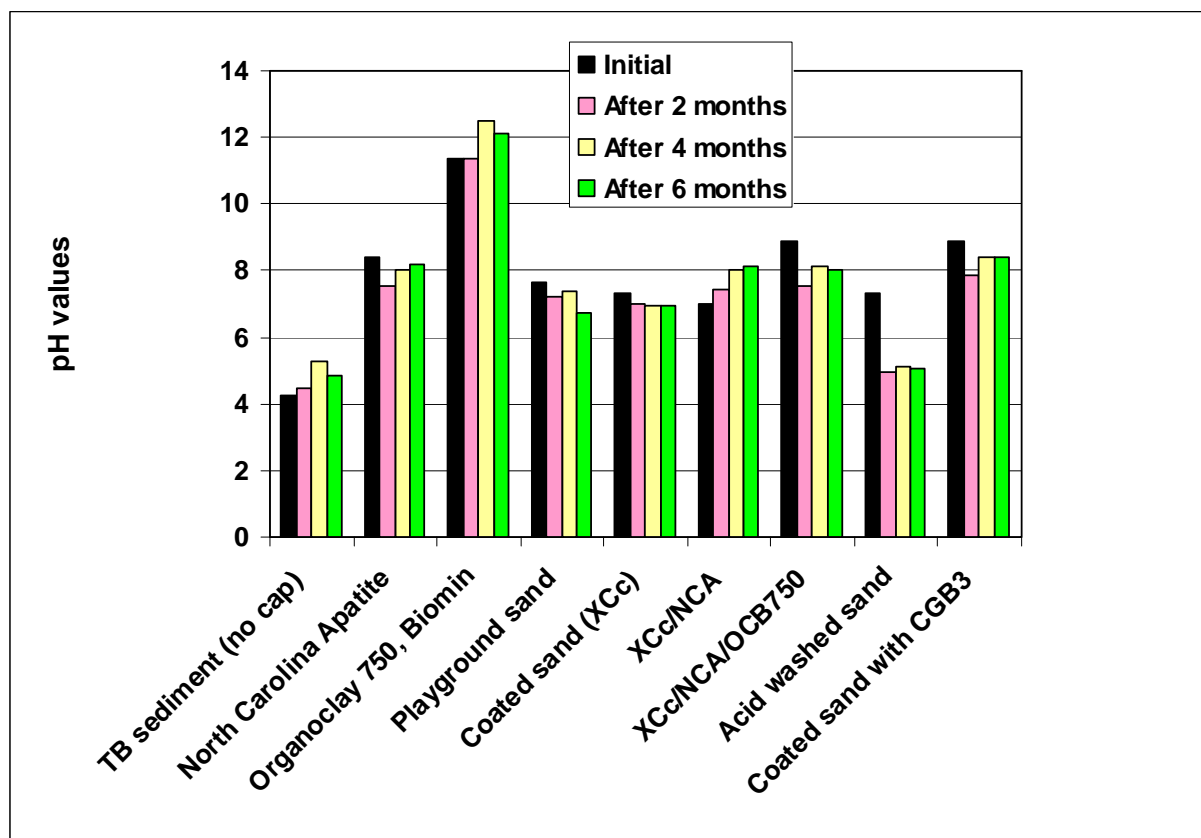


Figure 40. pH Changes with Time in Diffusion Experiment.

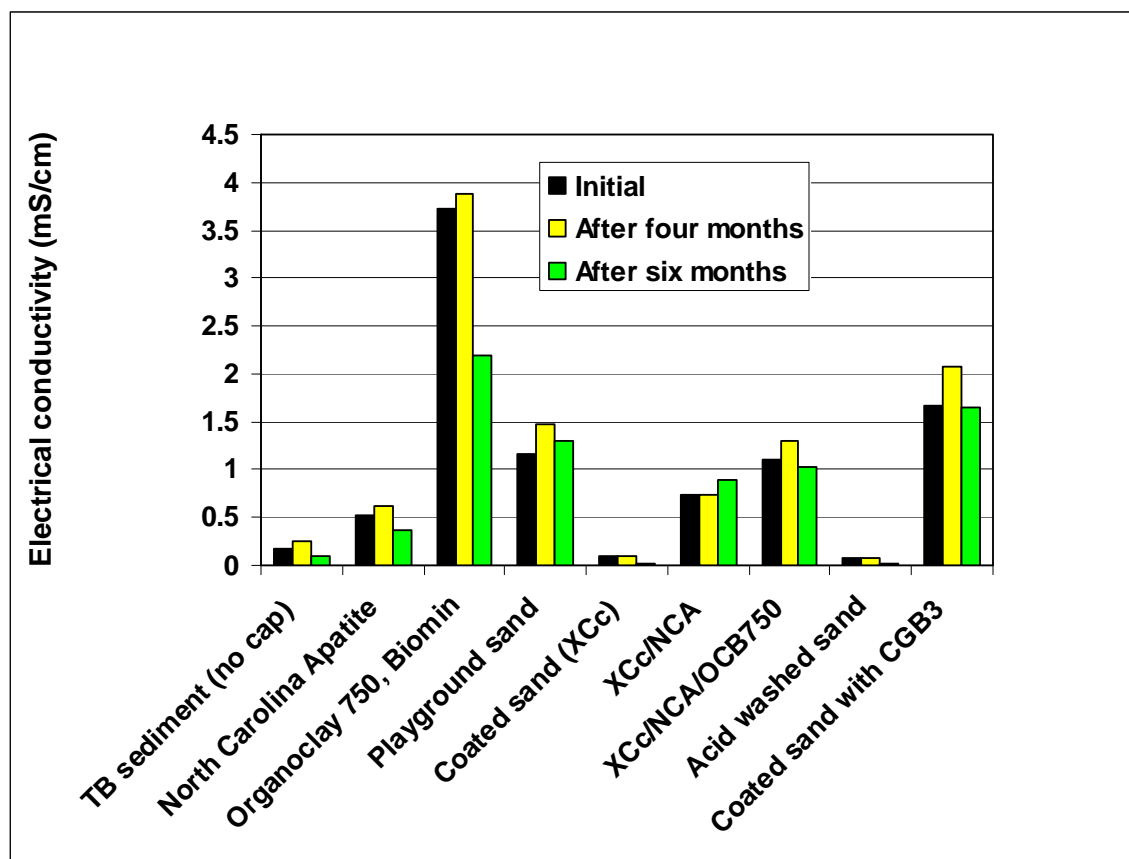


Figure 41. Electrical Conductivity in Diffusion Experiment.

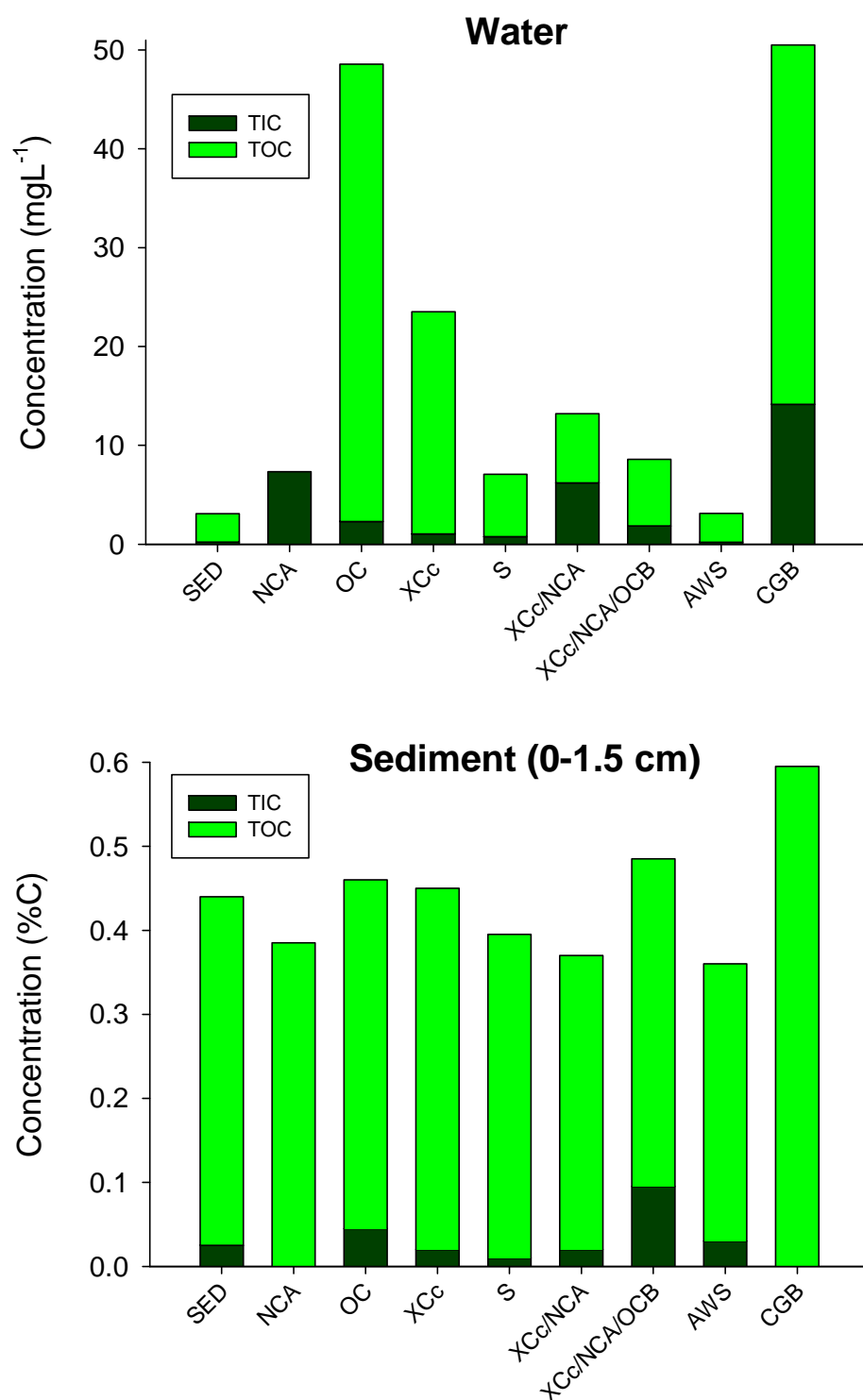


Figure 42. Total Inorganic (TIC) and Total Organic (TOC) Carbon in Water and Sediment after Six Month Diffusion Experiment.

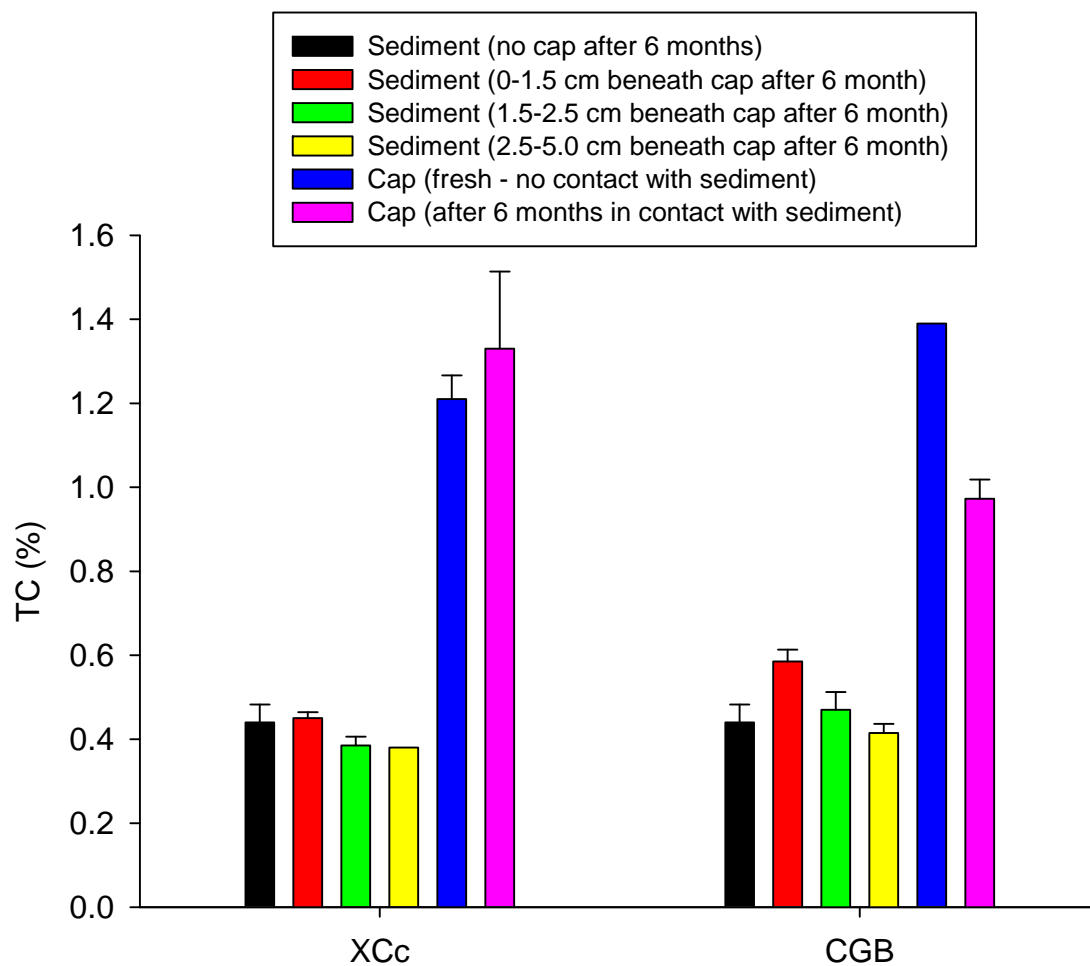
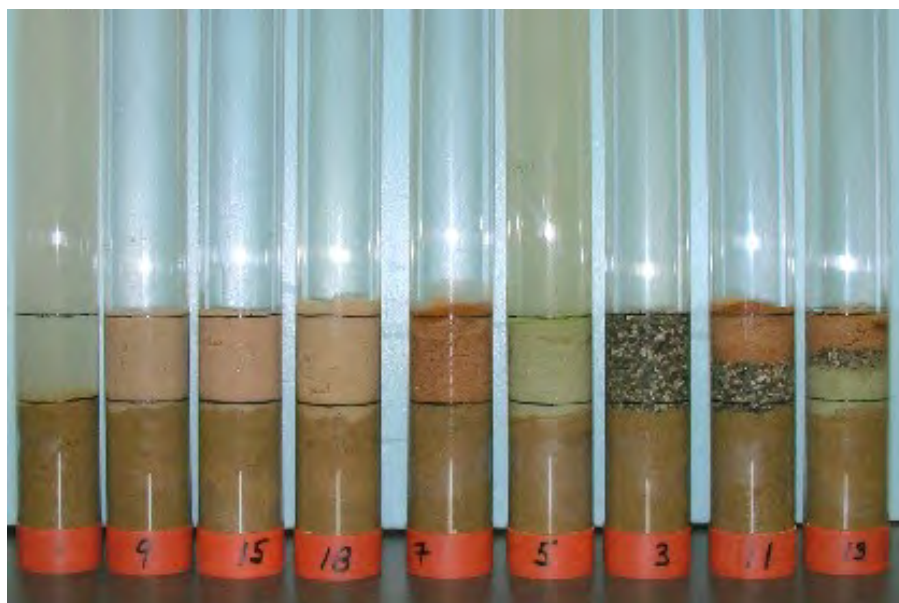
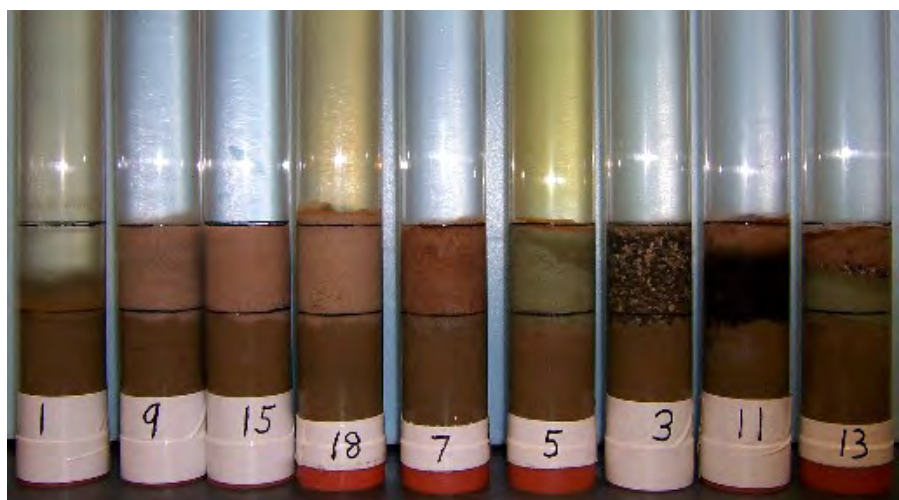


Figure 43. Carbon Content in Water and Sediment Layers under Two Biopolymer Caps and in Biopolymer Caps at Start and End of Diffusion Experiment.



9/28/2007



2/14/2008

Picture 16. Diffusion Experiment at Start (9/28/07) and after Six Months (2/14/2008); cap compositions: 1- no cap (control - only sediment), 9- sand, 15 – acid washed sand, 18 – biopolymer coated sand (chitosan and guar gum cross-linked with borax), 7 - biopolymer coated sand (xanthan and chitosan cross-linked with calcium chloride), 5 – organoclay 750 from Biomin Inc., 3 – NC apatite, 11- biopolymer coated sand (xanthan and chitosan cross-linked with calcium chloride) with NC apatite (50% of each), 13 - biopolymer coated sand (xanthan and chitosan cross-linked with calcium chloride) with NC apatite, and organoclay 750 (33.3% of each).

Diffusive Transport of Metals through Active Caps – Modeling

The results of the modeling are shown in Figures 44 through 51. Each figure shows the sediment pore water concentration and subsequent depletion due to diffusion into the overlying materials. Figures 44 and 45 show the results for Case 1 where there is no cap and, contaminants are allowed to diffuse out of the sediment into the overlying water column. These graphs show that the sediment and water concentration for each metal reach equilibrium in about 2 to 3 years. Slight differences in the time to equilibrium is a function of the effective diffusion coefficient used for each metal. Because there is no sorption processes involved with this simulation, the equilibrium concentration of each metal is identical.

Figures 46 and 47 show the results for Case 2 where there is a sand cap overlying the contaminated sediments. Since there is no sorption in the sand cap, this case is similar to Case 1. The concentration of contaminants in the pore water of the sediment and sand reach equilibrium with the overlying water column in 3 to 5 years. The equilibrium concentration of each metal is identical.

Figures 48 and 49 show the results for Case 3 where there is an apatite cap overlying the contaminated sediments. Compared to Case 2 (sand cap), these figures clearly show the apatite cap delayed contaminant breakthrough. Except for nickel and selenium, equilibrium is delayed for a minimum of 1000 years. Therefore, due primarily to sorption processes, the apatite cap appears to be an effective barrier against diffusive transport of the contaminants to the overlying water column.

Figures 50 and 51 show the results for Case 4 where there is an organoclay cap overlying the contaminated sediments. These figures show the organoclay cap delayed contaminant breakthrough. Contaminant equilibrium was reached between 100 and 1000 years for each contaminant except cadmium and cobalt which were delayed past 1000 years. As with the apatite cap, due primarily to sorption processes, the organoclay cap appears to be an effective barrier against diffusive transport of the contaminants to the overlying water column.

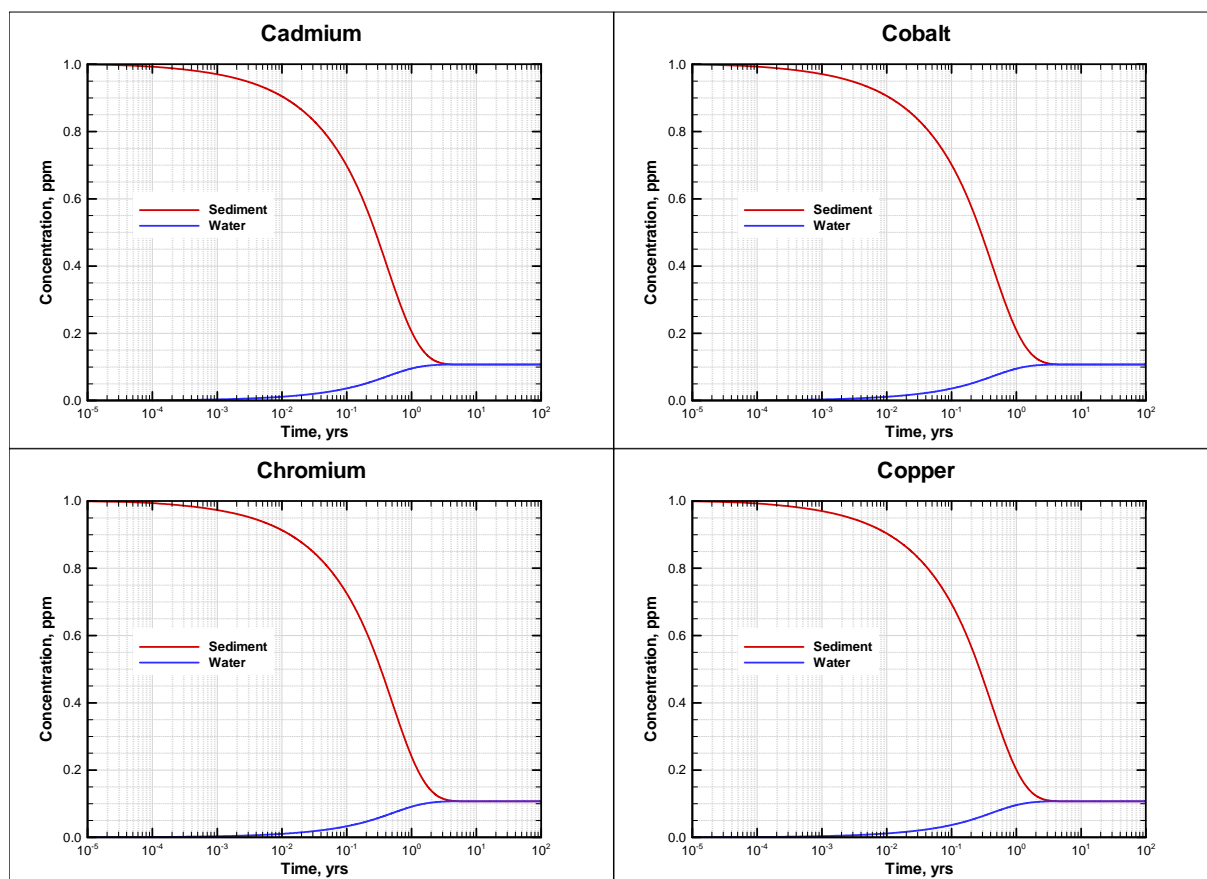


Figure 44. Predicted Breakthrough Curves for Cd, Co, Cr, and Cu for the no cap case.

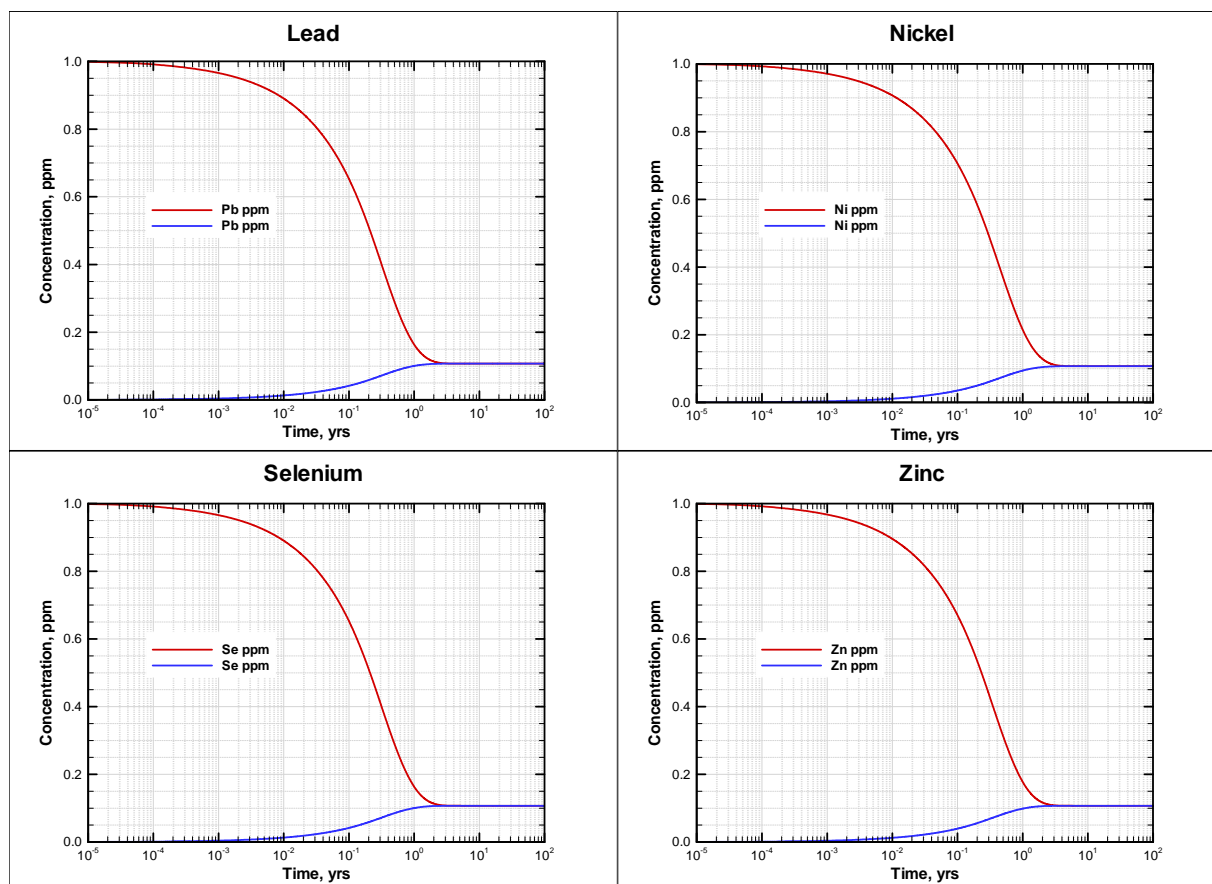


Figure 45. Predicted Breakthrough Curves for Pb, Ni, Se, and Zn for the no cap case.

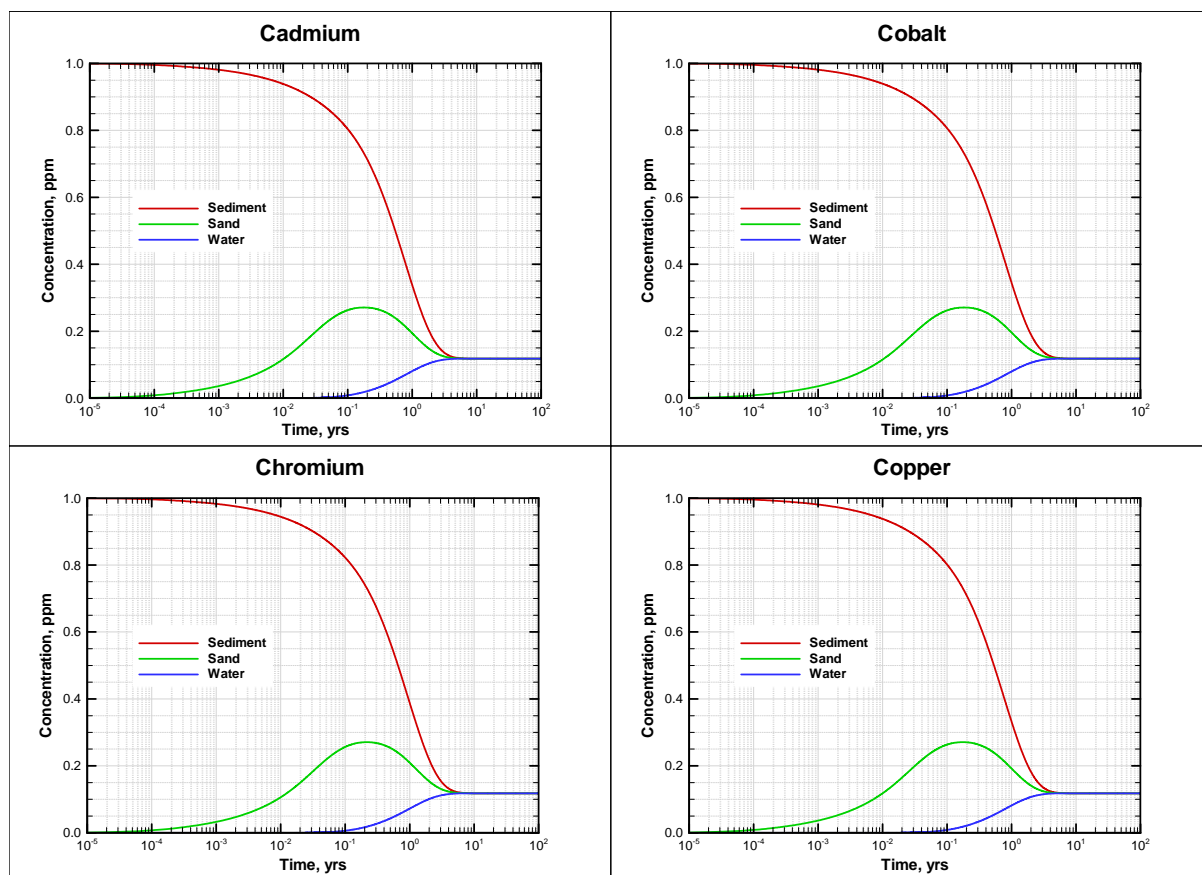


Figure 46. Predicted Breakthrough Curves for Cd, Co, Cr, and Cu for the sand cap case.

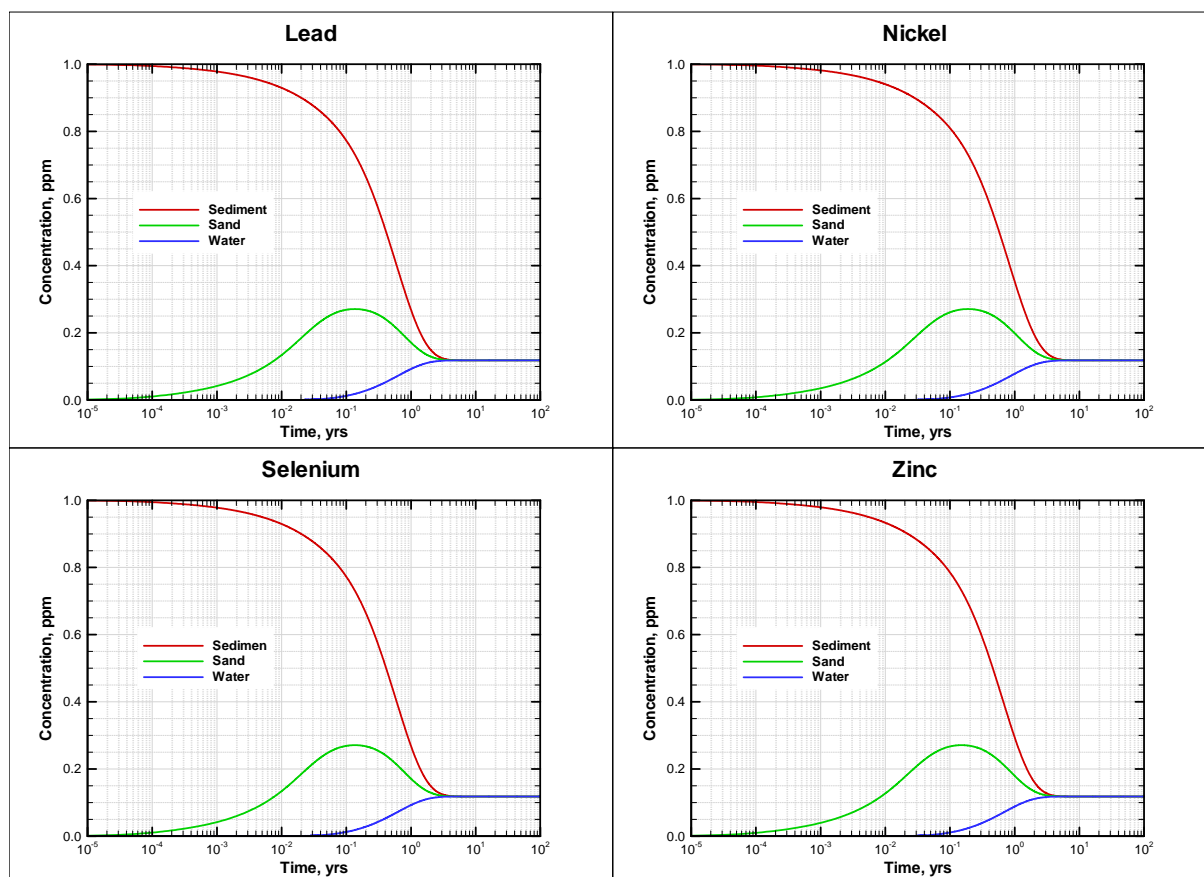


Figure 47. Predicted Breakthrough Curves for Pb, Ni, Se, and Zn for the sand cap case.

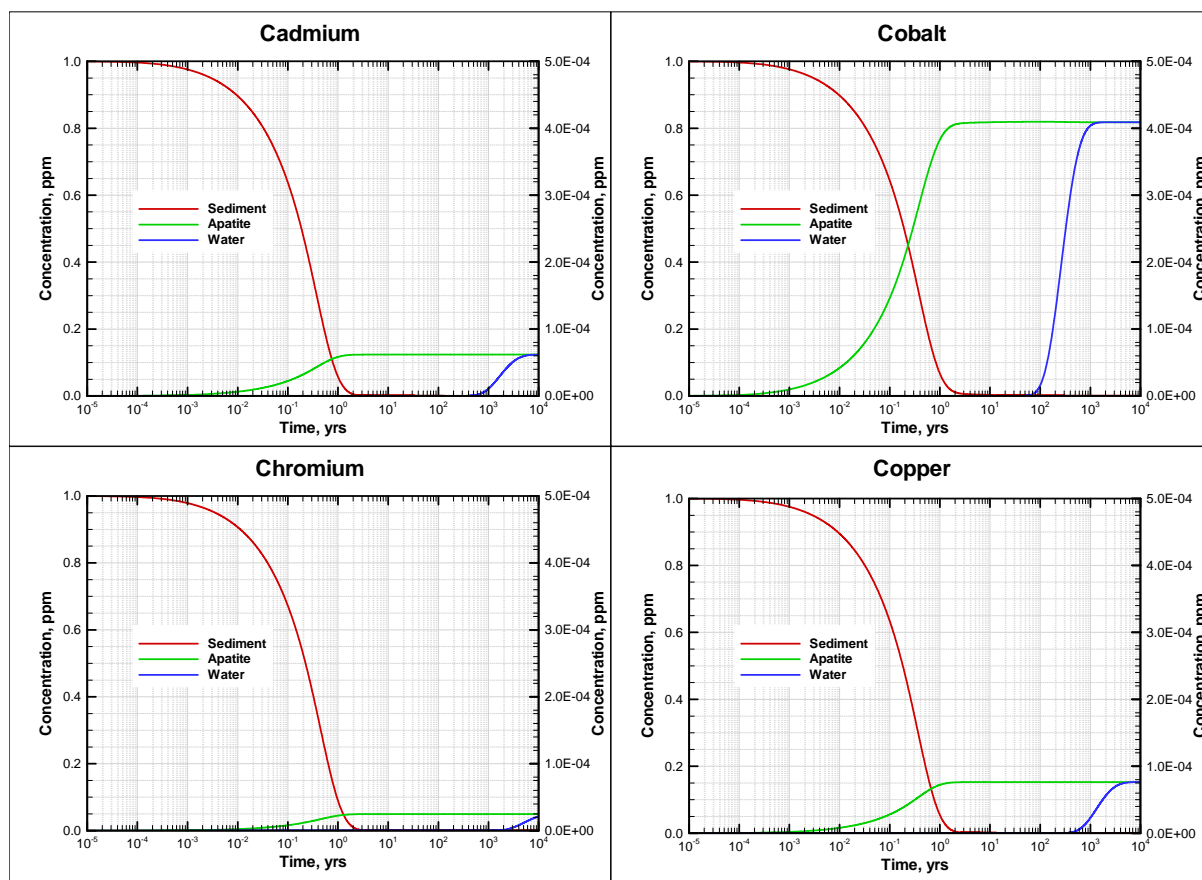


Figure 48. Predicted Breakthrough Curves for Cd, Co, Cr, and Cu for Apatite (NCA) Cap Case. The sediment concentration curves are plotted against the left y-axis and all others against the right y-axis.

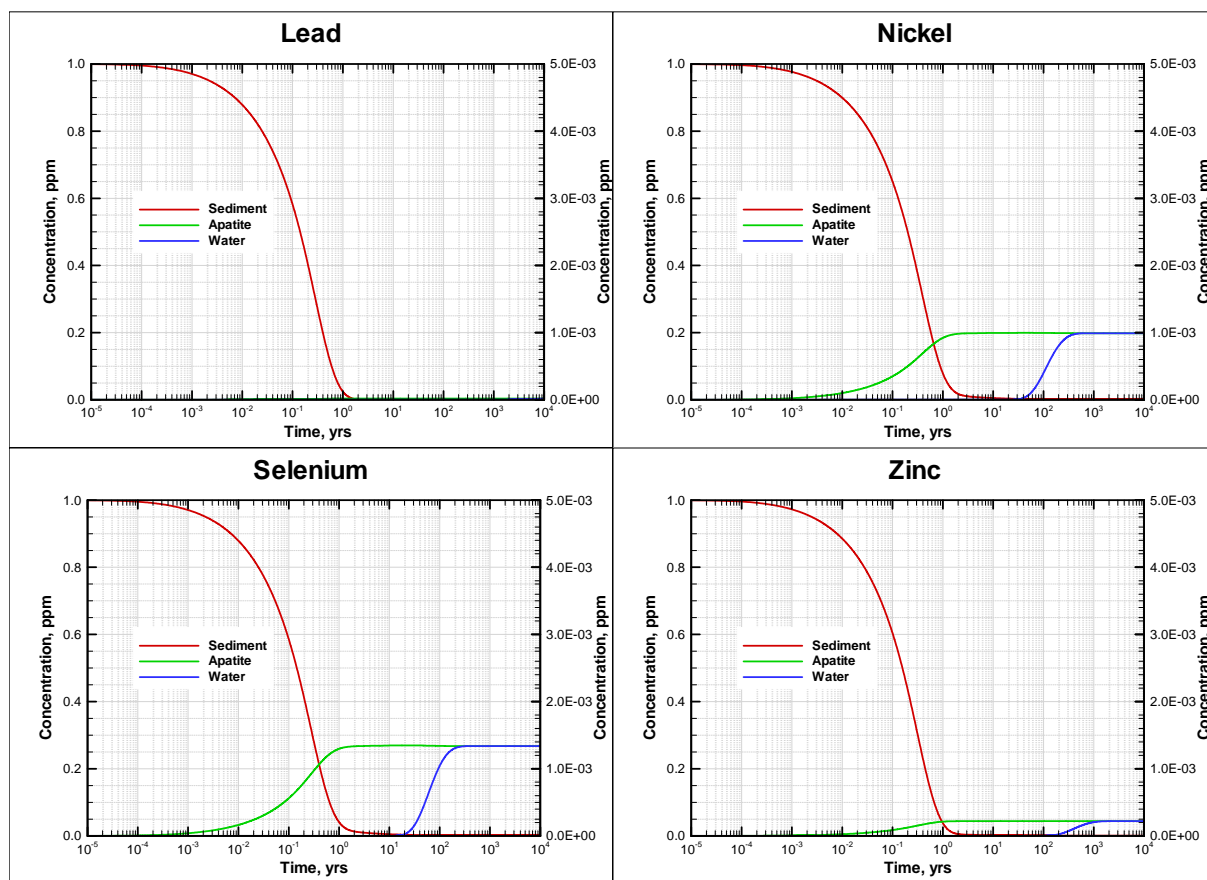


Figure 49. Predicted Breakthrough Curves for Pb, Ni, Se, and Zn for Apatite (NCA) Cap Case. The sediment concentration curves are plotted against the left y-axis and all others against the right y-axis.

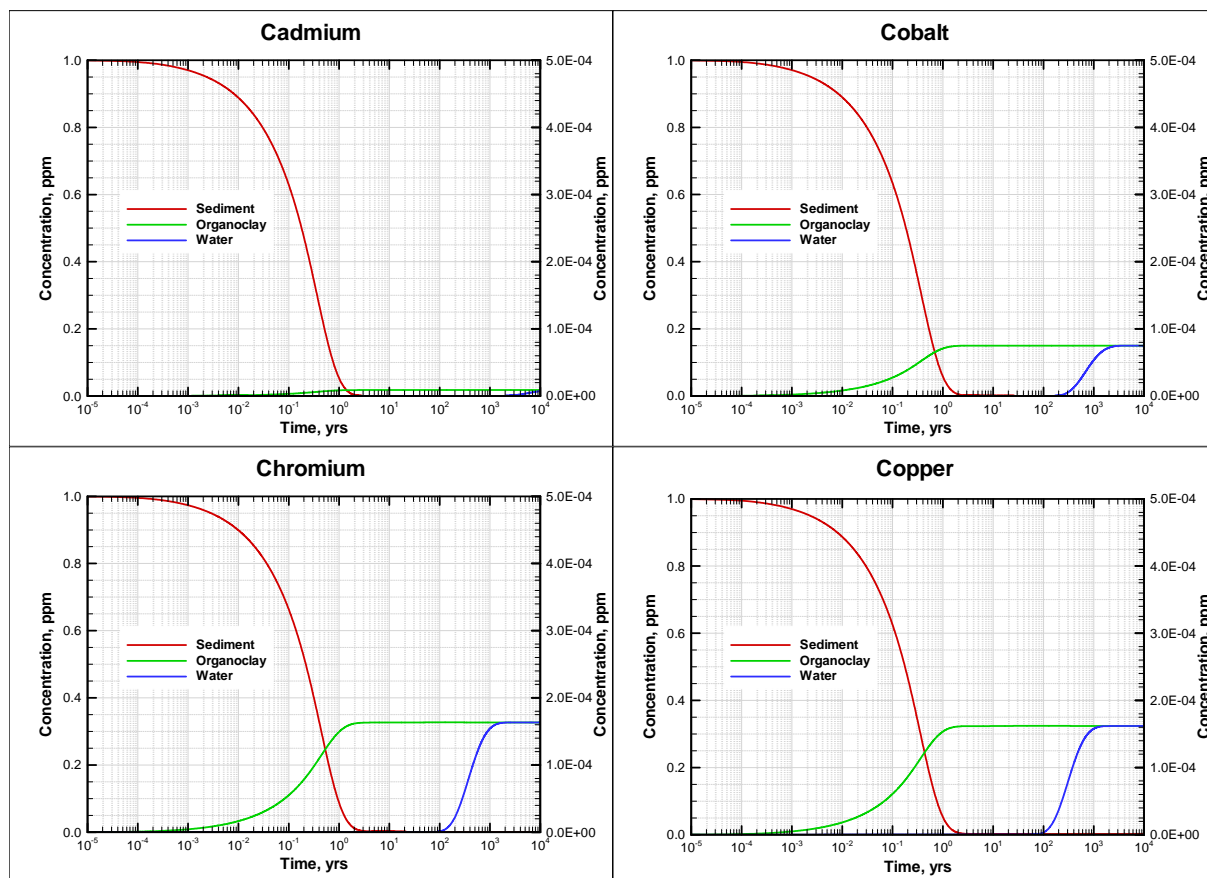


Figure 50. Predicted Breakthrough Curves for Cd, Co, Cr, and Cu for the organoclay (OCB750) cap case. The sediment concentration curves are plotted against the left y-axis and all others against the right y-axis.

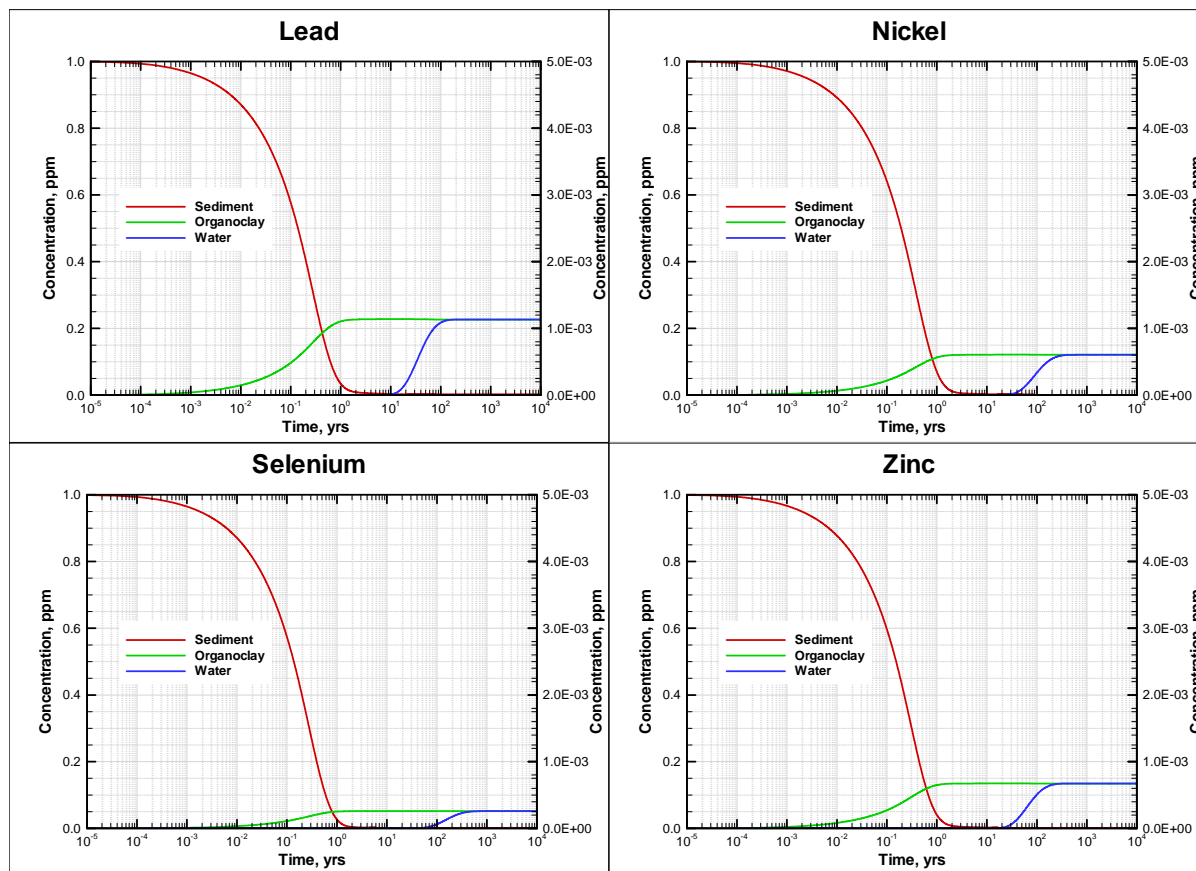


Figure 51. Predicted Breakthrough Curves for Pb, Ni, Se, and Zn for Organoclay (OCB750) Cap Case. The sediment concentration curves are plotted against the left y-axis and all others against the right y-axis.

SUBTASK 2.3. EVALUATION OF ADVECTIVE TRANSPORT

Advective Transport of Metals through Active Caps – Laboratory Evaluation

The breakthrough curves for the sand column are shown in Figure 52. Based on the breakthrough of the Br^- tracer, the porosity of the play ground sand was estimated to be 0.42 with a pore volume of 84.6 ml. The saturated hydraulic conductivity of the sand was estimated to be $5.23 \times 10^{-3} \text{ cm sec}^{-1}$.

Figure 52 shows that the movement of the metals through the column was similar to the non-adsorbed Br^- tracer. Initial breakthrough was almost identical for all species. However, differences noticed at later time intervals may be attributed to analytical interferences associated with the ICP-MS method. Good agreement is noted between the predicted and observed contaminant breakthrough which validates the numerical model.

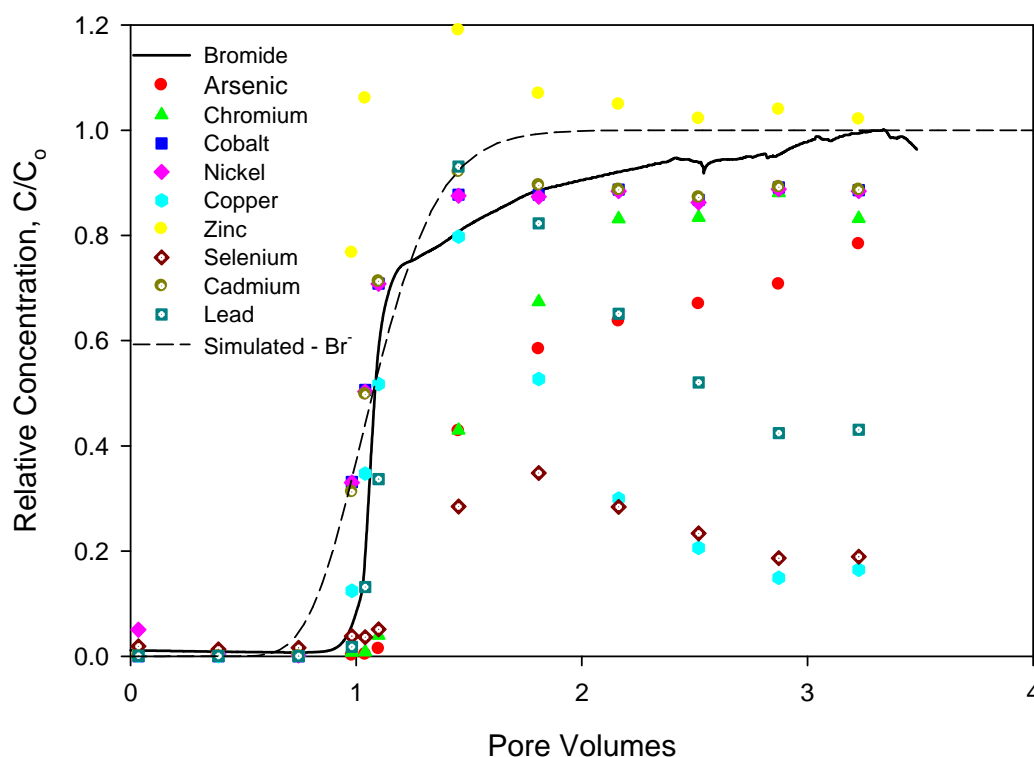


Figure 52. Breakthrough Curves as a Function of Pore Volume for Sand Column.

The breakthrough curves for the apatite column are shown in Figure 53. Based on the breakthrough of the bromide tracer, the porosity of the apatite was estimated to be 0.27 with a pore volume of 54.0 ml. The saturated hydraulic conductivity of the apatite was estimated to be $7.82 \times 10^{-5} \text{ cm sec}^{-1}$.

Figure 53 shows that each metal was sorbed by the apatite and delayed in breakthrough for several pore volumes. Further, the breakthrough of each metal was significantly delayed

compared to the Br^- tracer. Arsenic, cobalt, and selenium are the first metals to appear in the column effluent. Compared to the other metals in the spike solution, these metals should breakthrough the apatite column first based on the empirically determined partitioning coefficients.

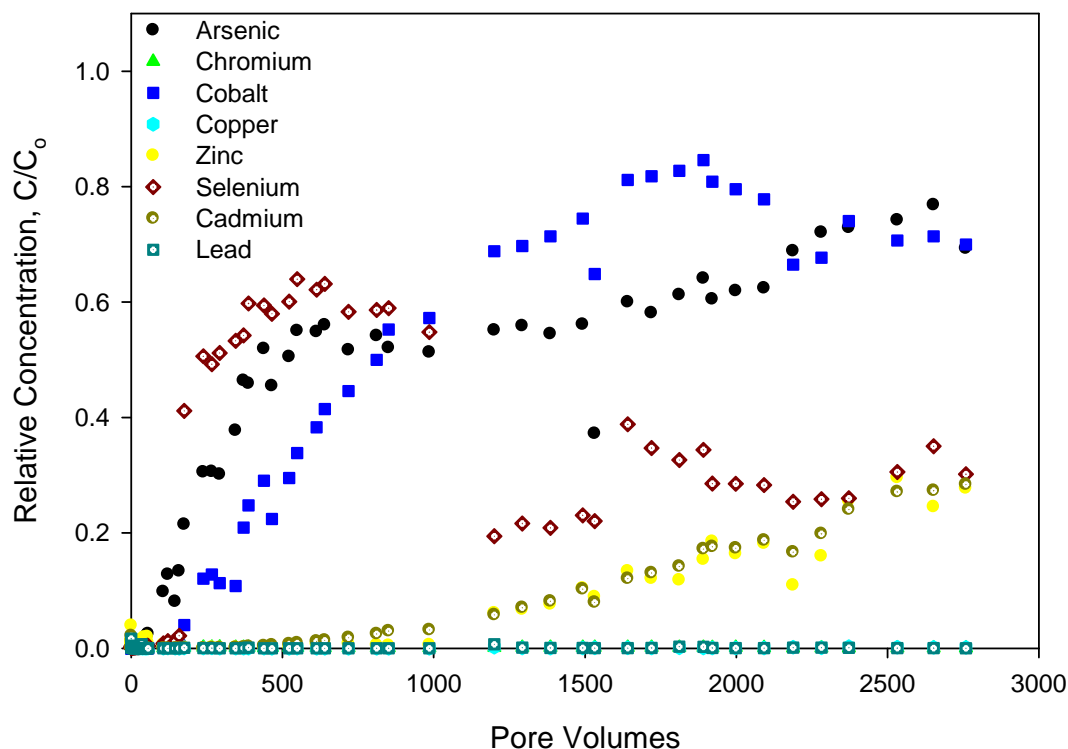


Figure 53. Breakthrough Curves for Apatite Column as a Function of Pore Volume.

Evaluation of Advective Transport of Organic Contaminants

Data was collected to parameterize diffusion advection transient models for two types of cross-linked biopolymer coated sand (one coated with xanthan/chitosan cross-linked with calcium chloride (XCc) and the other coated with chitosan/guar gum cross-linked with borax (CGB3) and for organoclay (PM-199) (Tables 31 and 32 and Figures 54 and 55). The model suggested that organoclay was successful in retarding organic contaminant breakthrough for long periods (Figure 55). The model was also used to generate theoretical depth profiles and breakthrough times for naphthalene and phenanthrene in caps composed of biopolymer coated sand (Figure 54).

Table 31. Model Inputs and Parameters for Diffusion Advection Transient Models for Biopolymer Coated Sand.

Model Inputs			
Contaminant Pore Water Concentration	C_o (ug/L)	Napthalene	100
		Phenanthrene	40
		Pyrene	60
Organic Carbon Partition Coefficient	$\log K_{oc}$ (log L/kg)	Napthalene	3.0406
		Phenanthrene	4.270865
		Pyrene	4.827
Water Diffusivity	D_w (cm ² /s)		6.00E-06
Porosity	ϵ		0.625
Particle Density	ρ_p (g/cm ³)		2.67
fraction organic carbon	$(f_{oc})_{cap}$	Napthalene	0.001094
		Phenanthrene	0.0023
		Pyrene	0.00158
Cap Depth	h_{cap} (cm)		2.5
Darcy Velocity	U (cm/yr)		1825
Cap Decay Rate	λ_{cap} (s ⁻¹)		3.00E-08
time scale (yr)	τ_{ss}		
Parameters			
Interstitial velocity	v	$v = U/\epsilon$	
Sorption-related retardation factor	R_f	$R_f = 1 + \frac{1-\epsilon}{\epsilon} \rho_p f_{oc} K_{oc}$	
Effective Cap Layer Diffusion Coeff.	D_{diff}	$D_{diff} = D_w \epsilon^{4/3}$	
Effective Cap Layer Dispersion Coeff.	D_{disp}	$D_{disp} = \alpha U$	
Dispersivity	α	$\alpha = 0.0169 h_{cap}^{1.53}$	

Table 32. Diffusion Advection Transient Model and Parameters for Modeling Breakthrough Time Curve for Organoclay as an Active Cap Component.

$$C_{pw}(z, t) = \frac{C_o}{2} \left[\operatorname{erfc} \left(\frac{R_f z - Ut}{2\sqrt{R_f Dt}} \right) + \exp \left(\frac{Uz}{D} \right) \operatorname{erfc} \left(\frac{R_f z + Ut}{2\sqrt{R_f Dt}} \right) \right]$$

Parameters			
ρ_b	bulk density of cap material (1-n)* ρ_b	1.272	g/cm ³
ε	Porosity	0.52	
v	Porewater Velocity (U/ ε)	70192.3	cm/yr
U	Darcy Velocity (measured through upwelling work or $v*\varepsilon$)	36500.00	cm/yr
C_o	Initial porewater concentration	430.00	μg/L
α	dispersivity (1/2 grain size diameter)	0.1000	
D_w	Molecular diffusion coefficient (1*10 ⁻⁵ cm ² /s)	1.00E-05	cm ² /sec
D_{eff}	(=diffusivity of compound* $\varepsilon^{4/3}$ +dispersivity*U)	3782.0	cm ² /yr
f_{oc}	fraction of organic carbon	365.00%	
K_{oc}	organic carbon partition coeff	18660	mL/g
K_d^{obs}	Mercury (organics= $f_{oc}*K_{oc}$, metals=literature value))	68109	L/kg
z	Chemical Isolation Layer Thickness	2.5	cm
t	time (end of simulation)	100	yr
R_f	Retardation Factor (formula specific to model) $R_f = \varepsilon + \rho_b * K_d^{obs}$	86635	

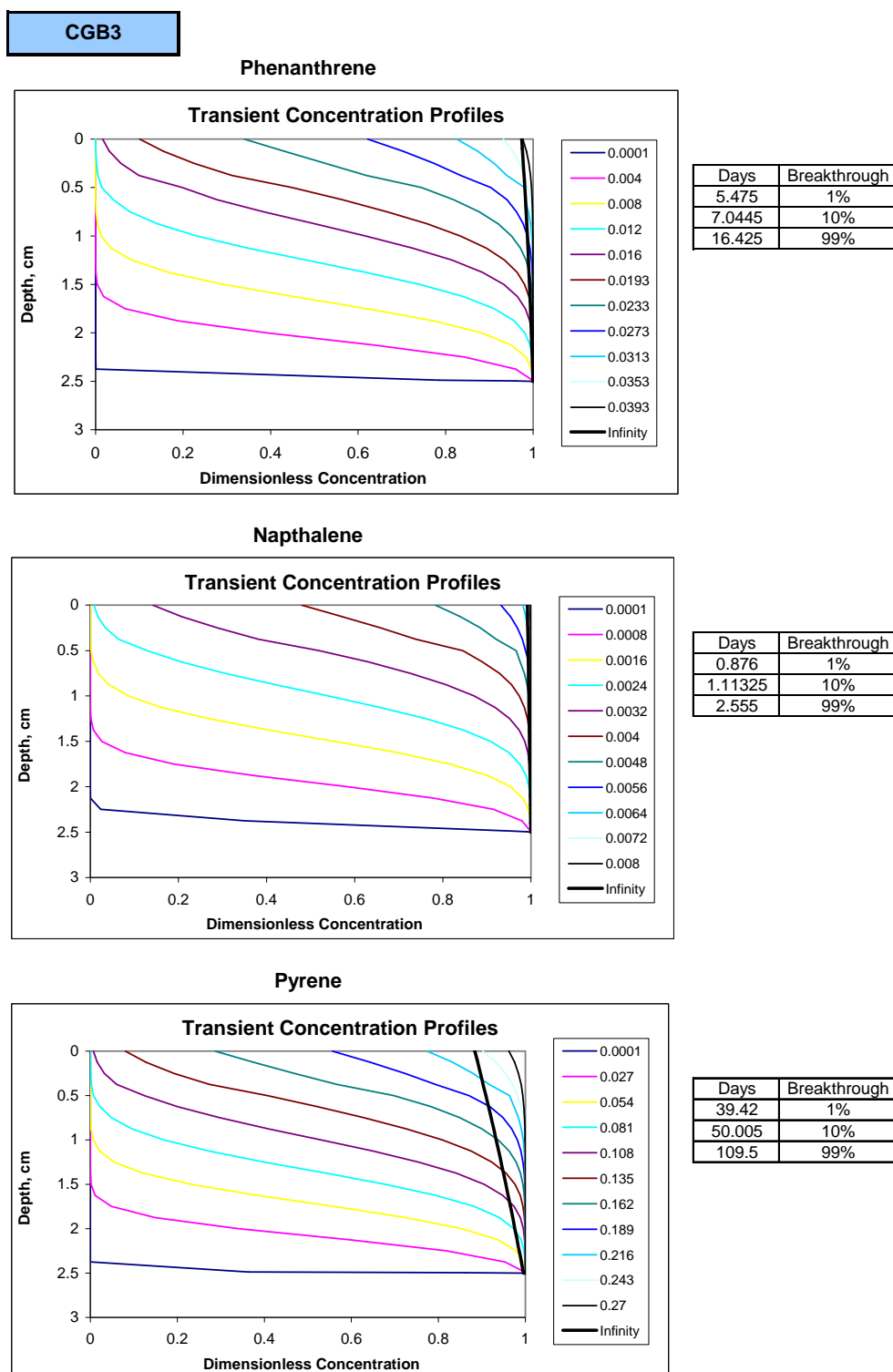


Figure 54. Predicted Breakthrough Curves for Biopolymer Coated Sand (CGB3) for Phenanthrene, Napthalene, and Pyrene.

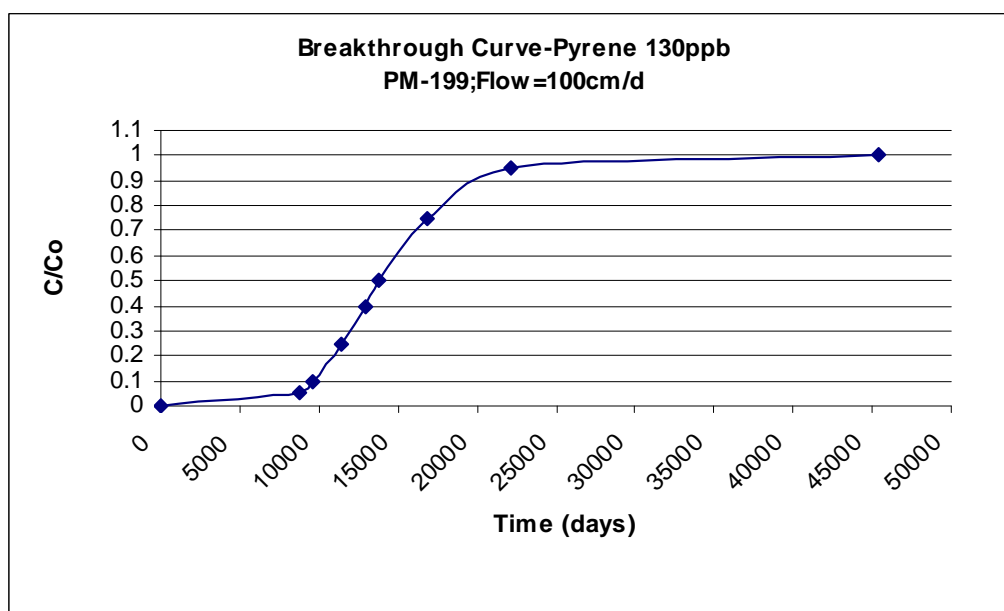
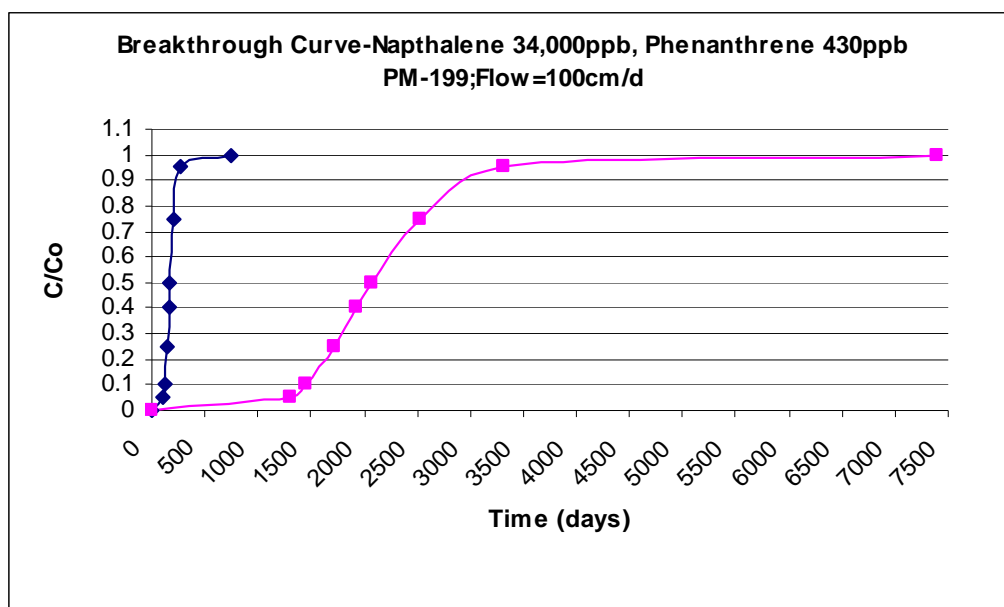


Figure 55. Predicted Breakthrough Curves for Organoclay PM-199 for Phenanthrene and Napthalene.

Diffusive and Advective Transport of Organic Contaminants -Measured Breakthrough and Model Comparison

Organoclay (PM-199)

Raw data obtained from measuring effluent concentrations from the columns was non-dimensionalized with the measured influent concentration fed to the column. The data was then fit with a 1D diffusion advection transport model (Equation 23) with the solution given by Equation 24. Only naphthalene data was fit to the model since the effluent concentrations of phenanthrene were too low to fit. This is due to the more sorptive nature of phenanthrene which slowed migration through the column.

$$R_f \frac{\partial C}{\partial t} + U \frac{\partial C}{\partial z} = D_{eff} \frac{\partial^2 C}{\partial z^2} \quad (23)$$

$$C_{pw}(z, t) = \frac{C_o}{2} \left[\operatorname{erfc} \left(\frac{R_f z - Ut}{2\sqrt{R_f D t}} \right) + \exp \left(\frac{Uz}{D} \right) \operatorname{erfc} \left(\frac{R_f z + Ut}{2\sqrt{R_f D t}} \right) \right] \quad (24)$$

The model was used to compare three different cases. First, the calculated dispersivity value and the laboratory measured K_d for naphthalene were used to obtain a predicted retardation factor. Second, the calculated dispersion value was used in the model and K_d was changed to fit the data and get a new retardation factor. Third, the laboratory determined value of K_d was used in the model and the dispersion value was changed to fit the data. Model fits and parameters that were varied are given in Figure 56 and Table 33.

Throughout the test period, the dimensionless breakthrough based on initial concentrations did not exceed $C/C_o = 0.04$. In order to obtain direct measurement of the retardation factor upon fitting the column data, the tests should have been allowed to run until $C/C_o = 0.5$ was achieved; at this point the dispersion is known and $\tau = \frac{L}{U R_f}$, (τ being the retention time) and the retardation factor can be calculated. This would have required nearly a year long experiment because of the strongly sorbing nature of the organoclay. It is difficult to get an accurate value for R_f at the bottom end of the breakthrough curve because the breakthrough concentration is influenced more by dispersion at values less than $C/C_o = 0.5$.

However, the measured dispersion coefficient and predicting breakthrough using the observed equilibrium partition provides a reasonable, if not optimal, fit to the data. This suggests that the equilibrium sorption measurements provide a good estimate of the actual retardation under dynamic conditions and no mass transfer resistances are expected to degrade the performance of an organoclay cap relative to that suggested by equilibrium at a darcy velocity of 100 cm/day.

Since actual groundwater upwelling rates are typically much lower than this, no kinetic limitations are expected that would limit the performance of the organoclay.

In Figure 56, the experimental data is extremely limited, and could take the shape of any of the three cases given above, demonstrating the importance of running the test until $C/C_0 = 0.5$ is reached. Still, the values for dispersivity and K_d are within an order of magnitude of each other, and the dispersivity value of 0.33 cm can be assumed valid and the retardation factor is taken as 4200, so it is likely that the data would best fit the model for Case 1 (Figure 57).

Biopolymer Coated Sands

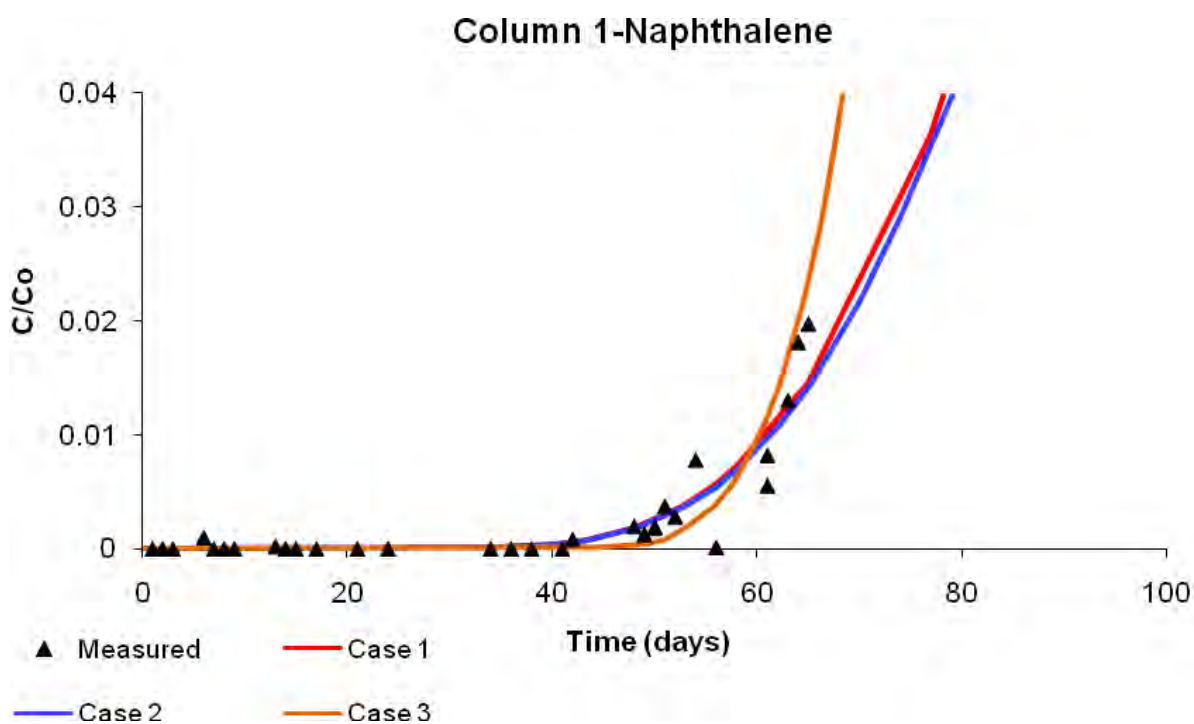
Column studies were performed to test the ability of dried biopolymer coated sands XCc and CGB3 to function as a cap in a flowing water environment. These experiments were specifically designed to identify if groundwater upwelling would lead to kinetic limitations in sorption onto the coated sands. Water contaminated with naphthalene and phenanthrene was pumped through 15 cm layers of the coated sand products, and the effluent concentrations of the contaminants were monitored. Column results were compared to the output generated by the model to evaluate the effectiveness of the model as a prediction tool. Figures 58 - 61 display the experimental results plotted against the model output.

Overall the model output tracked the measured experimental concentrations very well. The concentrations of phenanthrene flowing from CGB3 emerged more rapidly than the model predicted but this is most likely due to a discrepancy in the calculated dispersivity of the column.

Breakthrough of the organic contaminants occurred rapidly at the high flow rate the coated sand products were subjected in this experiment. In the field, contaminants would have a thicker cap depth to migrate through as well as a much slower upwelling velocity which would result in much longer breakthrough times than measured in the lab. The biopolymer coated sand would sequester contaminants from sediment longer than placement of a plain sand cap, but results from the column tests indicate that the coated sand would be only a short term buffer against organic contaminant flux into an overlying water column. The coated sands appear more appropriate as an armoring layer to prevent erosion than as an absorbent. They could be used alone over sediments with minimal contaminant risks or in addition with other amendments when risks are more severe.

Table 33. Model Results.

	Dispersivity, α (cm)	K_d (L/kg)	R_f
Case 1 Predicted	0.33	3,284	4,184
Case 2 Best Fit Kd/Rf adjusted	0.33	6,490	8,256
Case 3 Best Fit α adjusted	0.05	3,284	4,184

**Figure 56. Measured Effluent Concentrations and Comparison to Model.**

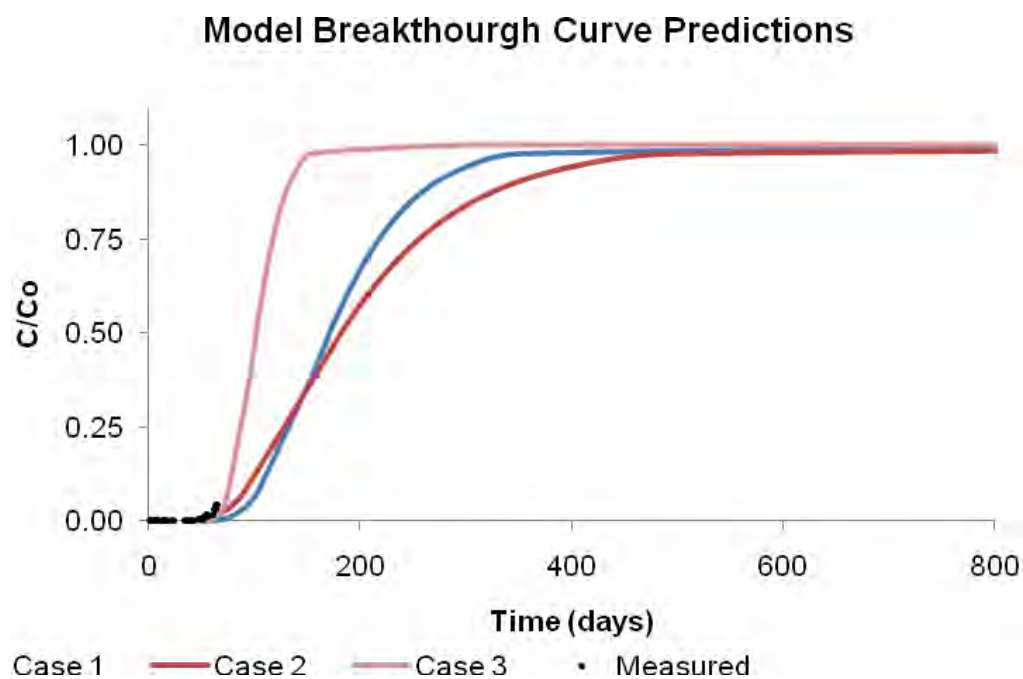


Figure 57. Total Breakthrough Curve Predictions.

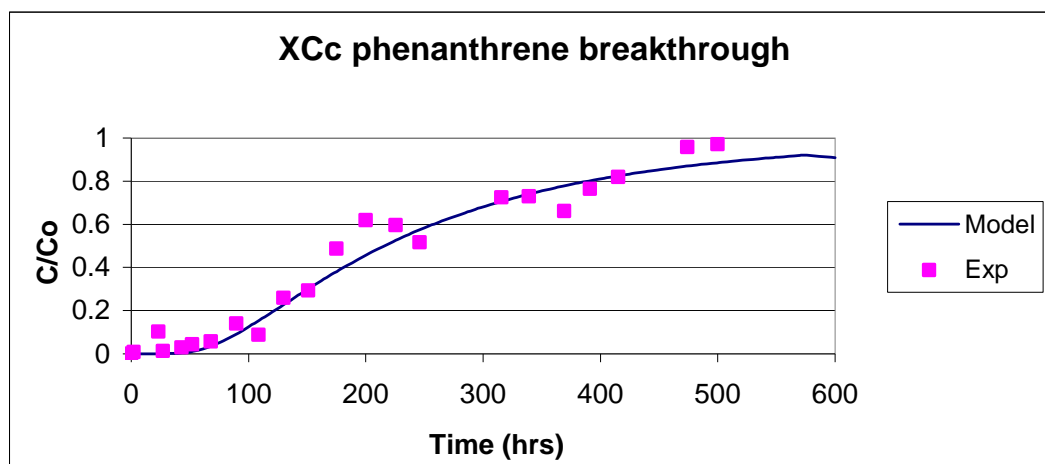


Figure 58. Comparison of Experimental and Model Data of Phenanthrene Breakthrough of 15 cm XCc Cap.

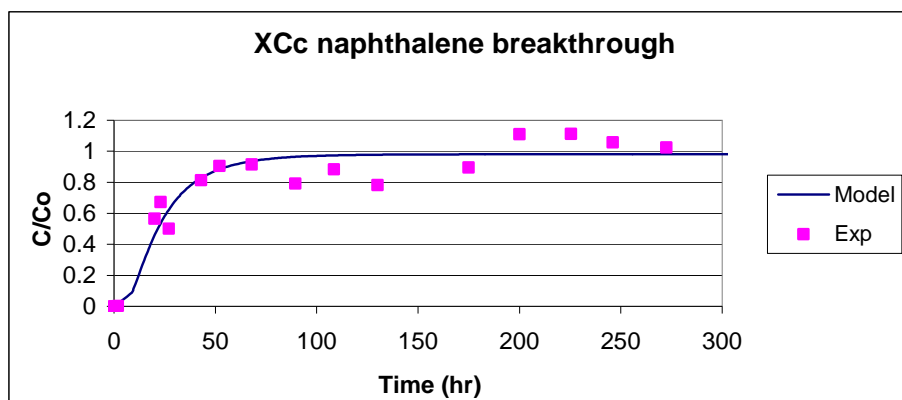


Figure 59. Comparison of Experimental and Model Data of Naphthalene Breakthrough of 15 cm XCc Cap.

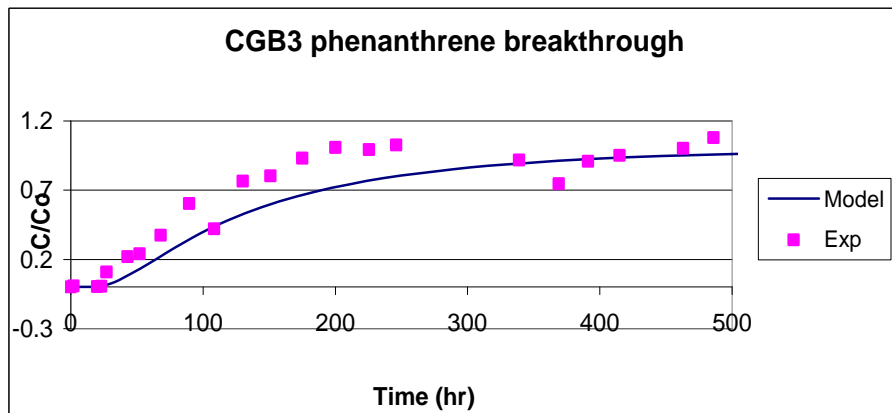


Figure 60. Comparison of Experimental and Model Data of Phenanthrene Breakthrough of 15 cm CGB3 Cap.

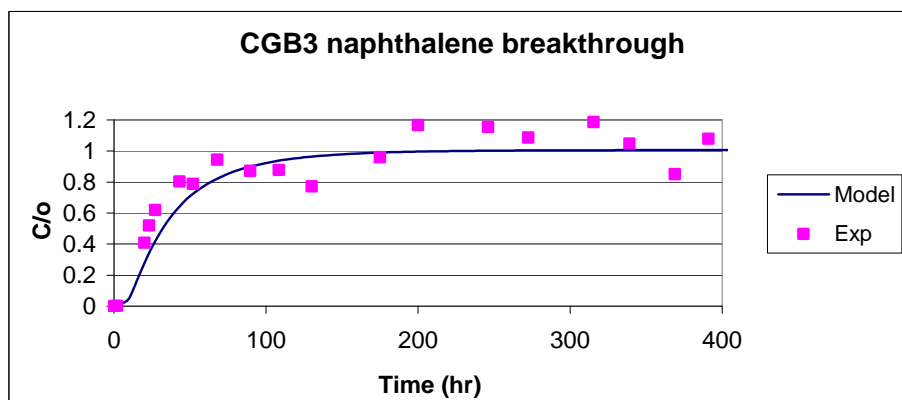


Figure 61. Comparison of Experimental and Model Data of Naphthalene Breakthrough of 15 cm CGB3 Cap.

SUBTASK 2.4. EVALUATION OF POTENTIAL AMENDMENT TOXICITY

Analysis of extracts

Metal concentrations in aqueous extracts from the amendments remained well below EPA ambient water quality criteria and other ecological screening values (Table 34). The results of these tests showed that amendment extracts do not contain heavy metals; therefore, will not contaminate sediment pore water or enter the water column.

For this project it was important to determine the TCLP concentration since this is one of the regulatory requirement at the Savannah River Site, where the field deployment of this project took place. Comparing the extracts to the regulatory levels indicated that all metal concentrations were well below the regulatory TCLP limits (Figure 62 and Table 35). Organoclays had higher concentrations of Ba, Cr, Ni, and Pb than the other tested amendments; however, these concentrations were still lower than TCLP limits (Table 35). Also, mixtures of amendments such as apatite with organoclay or apatite with coated sand (50% by dry mass) had lower concentrations of metals in the TCLP extracts than individual amendments (100%) (Table 35). These data show that the individual amendments and mixtures of amendments do not pose an environmental hazard due to metal leaching.

Table 34. Metal Concentrations ($\mu\text{g L}^{-1}$) in Water Extracts from Amendments. These metal concentrations are compared with ecological screening values (ESVs¹).

Element	North Carolina		Biopolymer coated sand	Sand	ESV
	apatite	Organoclay			
Al	30	43	0	<1	87
As	0.9	0.1	0	0.4	2.2
B	7.4	7.0	7.8	1.1	750
Cd	0.2	<0.1	<0.1	0.0	0.25
Co	<0.1	<0.1	<0.1	0.0	3
Cr	<0.1	0.0	0.2	0	11
Cu	1.3	0.4	1.4	0.0	6.5
K	337	980	406	104	53,000
Mn	0.2	46.3	3.7	0.5	80
Mo	4.0	0.8	0.2	0.3	240
Na	515	48,690	21,495	<1	680,000
Ni	<0.1	1	2	<0.1	52
Pb	1.2	0.1	0.0	0.2	2.5
Sb	0.1	<0.1	<0.1	<0.1	160
Se	0.8	1.2	0	0.8	5
Zn	2.3	0.5	1.9	1.5	59

¹ESVs are the lowest of EPA National Recommended Water Quality Criteria chronic values (USEPA, 2009), ORNL lowest chronic values (Suter and Tsao, 1996), CCME water quality guidelines (CCME, 2005), or ERD ecological screening values for surface water (ERD, 1999).

Table 35. Evaluation of Amendments for Toxicity Characteristic Leaching Procedure (TCLP) (data in ppb).

Amedments		Cap composition % of dry weight of each amedment	As ppb	Ba ppb	Cd ppb	Cr ppb	Ni ppb	Sb ppb	Se ppb	Pb ppb
North Carolina Apatite (NCA)	Avg	100	237.5	482.4	17.1	431.0	579.7	15.8	41.8	17.7
	Stdev		1.1	53.3	0.5	2.7	1.0	2.0	3.7	1.3
Tennessee brown Rock (TRP)	Avg	100	47.2	1067.2	2.5	292.4	61.5	3.0	0.0	22.6
	Stdev		0.3	69.0	0.0	11.7	2.0	0.3	0.0	0.7
Organoclay (PM-199)	Avg	100	26.8	2590.5	71.4	260.8	839.7	23.2	80.1	461.1
	Stdev		0.3	26.6	0.0	21.2	41.7	3.1	3.1	2.3
Organoclay 750, Biomin	Avg	100	29.1	3012.9	0.7	357.6	793.0	0.5	11.6	90.4
	Stdev		0.3	117.3	0.1	33.6	146.5	0.0	0.8	0.8
Coated sand (CS)	Avg	100	8.8	2335.5	6.2	386.6	94.7	2.6	19.0	57.8
	Stdev		0.8	129.4	0.1	6.8	0.1	0.1	3.1	24.3
Playground sand (PS)	Avg	100	13.2	169.8	0.9	290.6	39.6	5.3	10.6	178.9
	Stdev		0.1	18.7	0.0	1.7	0.4	0.6	0.7	32.9
TRP/sand	Avg	50/50	41.3	942.5	2.6	276.4	82.5	2.9	9.5	16.8
	Stdev		0.3	53.8	0.1	6.9	0.4	0.0	1.4	3.8
TRP/sand	Avg	75/25	37.1	856.2	2.5	253.3	76.1	7.3	10.2	33.2
	Stdev		0.2	36.9	0.0	20.9	2.2	1.3	4.6	46.9
PM-199/sand	Avg	50/50	12.9	2810.9	41.8	280.3	693.6	11.5	35.1	381.9
	Stdev		0.3	154.6	1.1	4.1	5.1	0.4	0.8	8.5
PM-199/sand	Avg	75/25	20.0	2447.2	60.7	291.4	898.4	14.7	60.6	394.4
	Stdev		1.1	3.5	0.3	9.2	1.5	0.3	0.7	8.6
TRP/CS	Avg	50/50	35.3	1084.1	3.6	273.8	85.2	6.2	17.1	0.0
	Stdev		0.8	58.2	0.0	14.1	2.0	0.2	0.7	0.0
TRP/CS	Avg	75/25	36.2	1899.2	5.6	371.6	147.5	4.5	22.9	0.0
	Stdev		7.6	190.5	2.2	70.4	32.5	0.2	3.0	0.0
CS/OCB750	Avg	50/50	25.3	2744.1	0.6	297.0	632.2	9.1	33.9	3.9
	Stdev		nd	nd	nd	nd	nd	nd	nd	nd
CS/TRP/OCB750	Avg	25/33.5/33.5	23.5	1119.4	0.0	276.0	481.3	12.7	25.9	0.0
	Stdev		0.4	98.8	0.0	3.5	0.7	2.8	4.6	0.0
TRP/PM_199	Avg	50/50	39.4	2006.2	18.9	369.7	474.4	8.6	40.1	0.0
	Stdev		7.9	123.8	0.9	14.2	16.8	0.1	7.7	0.0
TRP/PM_199	Avg	25/75	34.9	2449.7	39.5	373.1	799.3	12.7	67.0	1.8
	Stdev		0.8	106.7	0.2	6.0	12.2	0.2	2.5	2.5
TRP/PM_199	Avg	75/25	47.2	1516.4	6.7	249.5	228.0	9.1	31.6	0.0
	Stdev		5.0	90.8	0.1	17.0	1.0	0.9	3.3	0.0
TCLP Limit			5000	100000	1000	5000	70000	1000	1000	5000

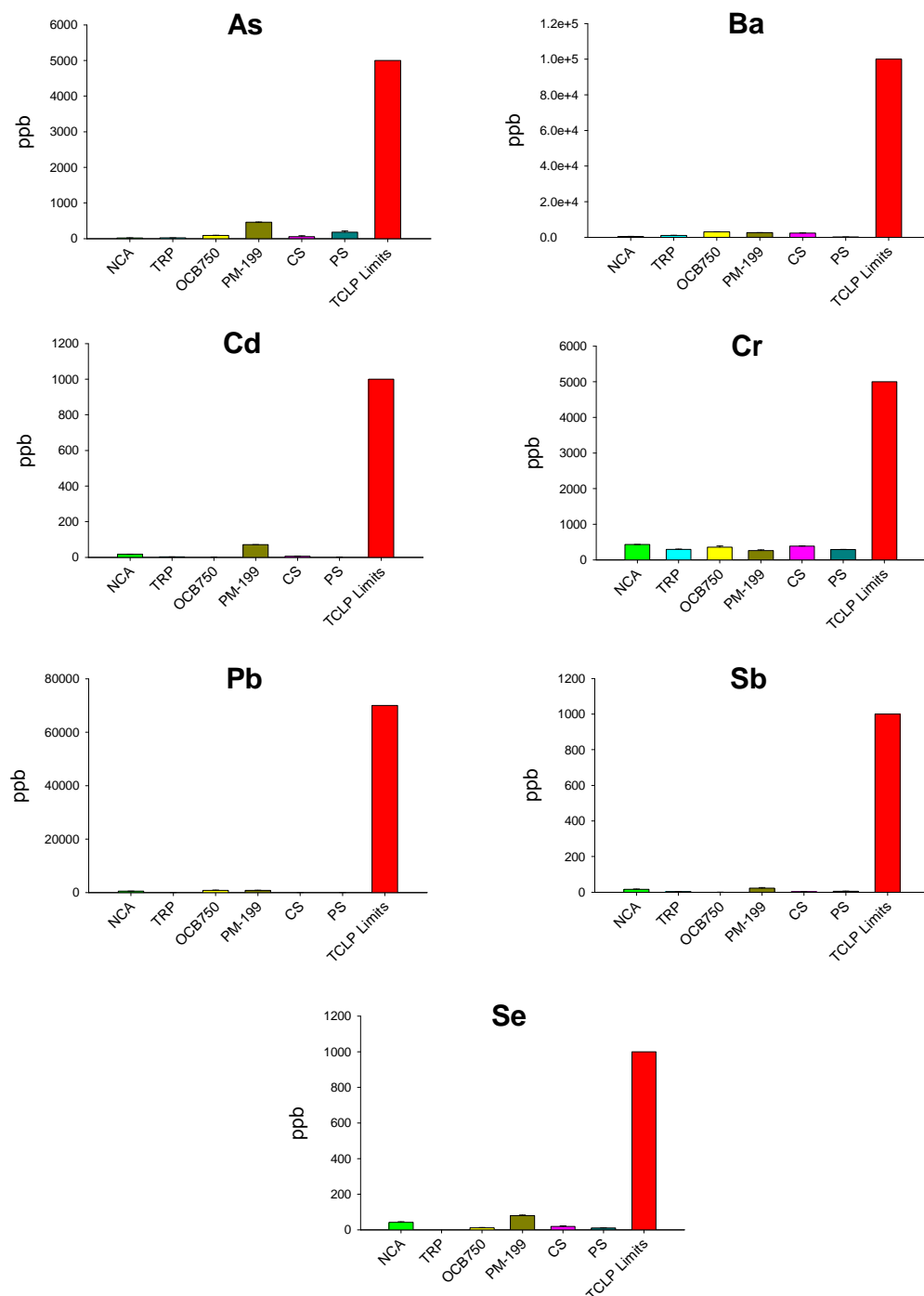


Figure 62. Comparison of the Concentrations of As, Ba, Cd, Cr, Pb, Sb, and Se in the TCLP Extract Solution to TCLP Limits (in ppb); NCA = North Carolina Apatite, TRP = rock phosphate from TN, OCB750 = organoclay 750 from Biomin Inc., PM-199 organoclay from CETCO, CS = coated sand with xanthan, chitosan and cross-linked with calcium chloride, PS = sand.

Sediment Toxicity Tests for Fresh and Salt Water

Before they are used in aquatic environments, potential sediment amendments must be assessed for possible side-effects that could stem from the presence of impurities or other properties that could directly or indirectly harm aquatic life. The objective of this portion of the project was to determine whether several amendments that hold promise for the construction of active caps have detrimental side-effects; and, if such is the case, to develop strategies for their use that minimize potential problems.

Substrates consisting of 100% apatite slightly reduced the survival of *Hyalella* in freshwater (Table 36). In contrast, *Hyalella* survival was markedly reduced in substrates consisting of 100% organoclay and in mixtures of organoclay and reference sediment. Concentrations of organoclay as small as 5% (by volume) in reference sediment had slight but significant effects ($P \leq 0.05$) on survival. The survival of *Hyalella* decreased as the proportion of organoclay increased showing a clear dose-response relationship in the freshwater tests (Figure 63). Unlike *Hyalella*, the survival of *Leptocheirus* in brackish water bioassays was not affected by mixtures of up to 25% organoclay and sediment (Table 36). Higher concentrations of organoclay were not tested.

Relatively high conductivities in some of the freshwater test chambers indicated that organoclay released high concentrations of chloride. Chloride was removed from organoclay by successive washings to see if this reduced its toxicity to *Hyalella*. However, a bioassay on washed organoclay indicated that toxicity was unaffected by chloride removal (Figure 63).

An additional bioassay was conducted on organoclay using procedures comparable to those used in the other bioassays, except that organoclay was mixed with natural substrate (mostly sand) from Tinker Creek. Survival of *Hyalella* in a mixture of 25% (by volume) organoclay and 75% Tinker Creek substrate averaged 84% compared with 80% in control beakers containing 100% Tinker Creek substrate. This absence of toxicity differed from the results of the previously described bioassays, which indicated that 25% organoclay significantly reduced survival. Neither conductivity, hardness, pH, alkalinity, dissolved oxygen, nor ammonia differed substantially between the two bioassays indicating that these factors were unrelated to the difference in results.

Recovery efficiency of *Lumbriculus* averaged 90% (SD=5.9) from sand, 87% (SD=12.1) from apatite, and 90% (SD=7.0) from organoclay. Recovery efficiency from silt was slightly lower (mean=82, SD=6.4) because silt typically contained decaying plant material that was difficult to separate from the worms. Recovery of *Lumbriculus* from sand, silt, and apatite was accomplished in 5 m or less, while recovery from silt took as long as 15-20 m. These results provided baseline expectations for recovery of *Lumbriculus* from different substrates in the absence of mortality.

The survival studies in sand showed that percent recovery based on weight slowly declined to about 65% over the 17 day test period. Expected percent recovery from sand in the absence of mortality or weight loss was 90%. In contrast, percent recovery did not decline in silt and

averaged 85% on day 17. Expected recovery from silt in the absence of any mortality or weight loss was 82%. These results provide baseline estimates of expected recovery over a 17 day period in natural sediments that were helpful in interpreting the results of the active biomonitoring studies described below. Better recovery in silt may have resulted from the presence of more organic matter that constituted a source of nutrition in these experiments (in which food was not provided).

Results of the 8 day acute toxicity bioassay with different ratios of organoclay and sediment showed that recovery of *Lumbriculus* declined slightly but not significantly ($P < 0.05$) as the proportion of organoclay increased from 1% to 20%. Percent recovery of *Lumbriculus* from organoclay percentages of 0%, 1%, 5%, 10%, and 20% were 87.0%, 86.5%, 84.6%, 80.4%, and 74.6%, respectively. It is possible that higher concentrations of organoclay would affect recovery, but such concentrations were not used in the active cap configurations under study.

Ilyodrilus, another annelid, was less sensitive than *Hyalella* to organoclay. Survival was not affected by up to 50% organoclay in sediment, although growth decreased and behavior was abnormal at this concentration, indicating sublethal effects (Figure 64). Bioaccumulation of PAHs (lipid normalized) by *Ilyodrilus* decreased significantly in the presence of 50% organoclay (Figure 65), a not unexpected result considering the ability of organoclay to sequester these contaminants in sediment and reduce their bioavailability. However, the mechanism underpinning the decrease in PAH concentrations in *Ilyodrilus* is uncertain. Reduced growth in 50% organoclay indicates a reduction in food intake which could contribute to a reduction in PAH uptake. Conversely, reduction in food intake would be expected to cause a reduction in whole body PAH levels but not necessarily lipid normalized PAH concentrations unless it was associated with physiological changes that resulted in PAH depuration from lipid-containing tissues. More detailed physiological studies will be needed to definitively resolve these questions.

The results of the laboratory sediment toxicity tests support the following conclusions:

- NC apatite and biopolymer coated sand are unlikely to adversely affect freshwater benthic organisms, even when used in high concentrations
- Organoclay may be harmful to sensitive freshwater benthic organisms, such as *Hyalella*, under some conditions but not brackish water benthic organisms. Laboratory tests on *Hyalella* produced variable results suggesting that the toxicity of organoclay to this organism may be partly dependent upon sediment characteristics or other unknown factors. Organoclay did not reduce the survival of annelid worms at concentrations useful for sediment remediation
- Amendment extracts do not contain metals that could contaminate sediment porewater or enter the water column

Table 36. Sediment Toxicity Test Results for Amendments and Mixtures of Amendments and Sediment.

Amendment	Test type	Amendment survival (%)	Control Sediment survival (%)	Significant difference (rank-sum test)	Amendment*			
					pH	DO (mg/l)	Conductivity umhos/cm	NH ₃
Apatite								
North Carolina Apatite (100%)	freshwater	72.5	81.3	marginal	8	8.6	249	2.2
NC Apatite (50%) / sand (50%)	freshwater	76.3	88.8	marginal	7.83	8.22	240	1.9
Organoclay								
Organoclay (100%)	freshwater	0	92.5	yes	6.98	7.8	2,420	0.65
Organoclay (50%) / sand (50%)	freshwater	0	87.5	yes	7.07	8.07	4,600	0.6
Organoclay (25%) / sediment (75%)	freshwater	32.5	86.3	yes	6.93	8.67	328	0.5
Organoclay (10%) / sediment (90%)	freshwater	67.5	86.3	yes	7.09	9.31	803	0.2
Organoclay (5%) / sediment (95%)	freshwater	73.8	86.3	yes	7.42	9.31	472	0.3
Organoclay (10%) /sediment (90%)	estuarine	87.5	87.5	no	7.77	8.84	37,000	0.2
Organoclay (25%) / sediment (75%)	estuarine	78.7	87.5	no	7.77	8.26	37,000	0.2
Biopolymer coated sand								
Biopolymer coated sand (100%)	freshwater	78.8	88.8	no	7.04	6.49	895	0.3

*Comparable values for the controls were: pH, 7.1- 8.0; DO, 7.7-8.6; Conductivity, 29 – 46; NH₃, <0.1 – 0.2 in freshwater and pH 7.7, DO 8.2, Conductivity 37000, NH₃ 0.2 in brackish water.

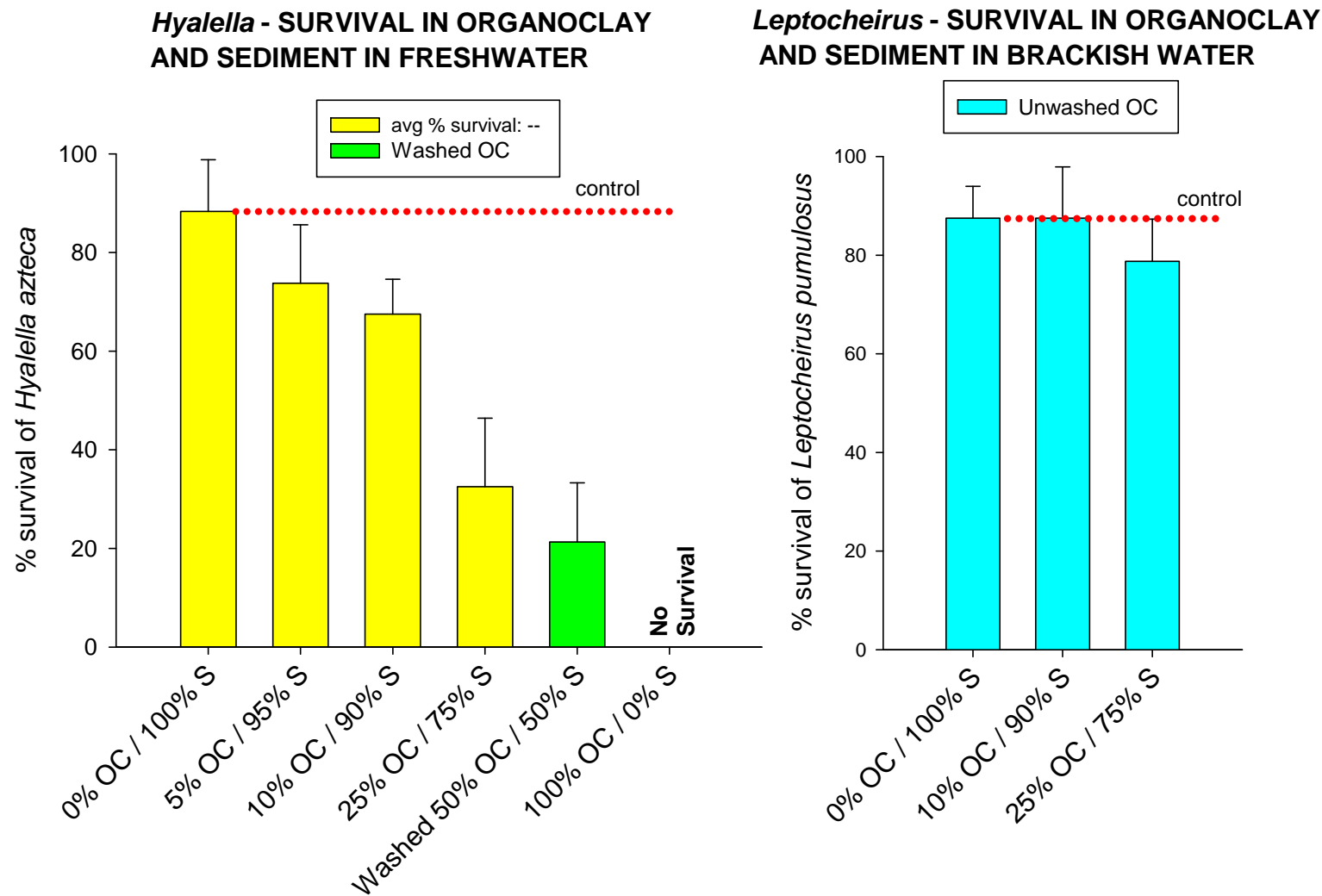


Figure 63. Effects of Organoclay on Survival of *Hyalella* and *Leptocheirus*; S – sediment, OC – Organoclay

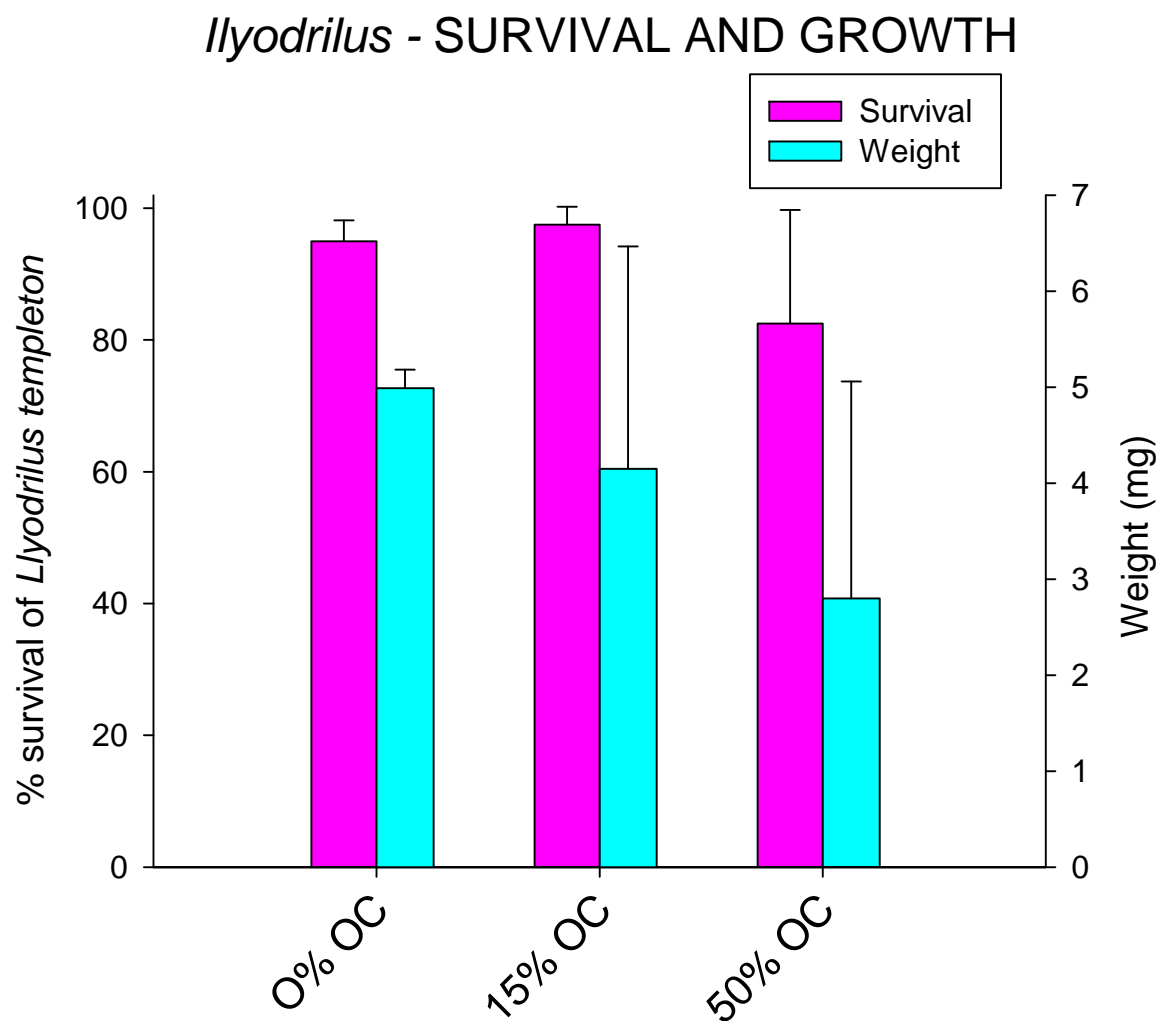


Figure 64. Effects of Organoclay on Survival and Growth of *Ilyodrilus*.

Ilyodrilus - BIOACCUMULATION OF PAHs

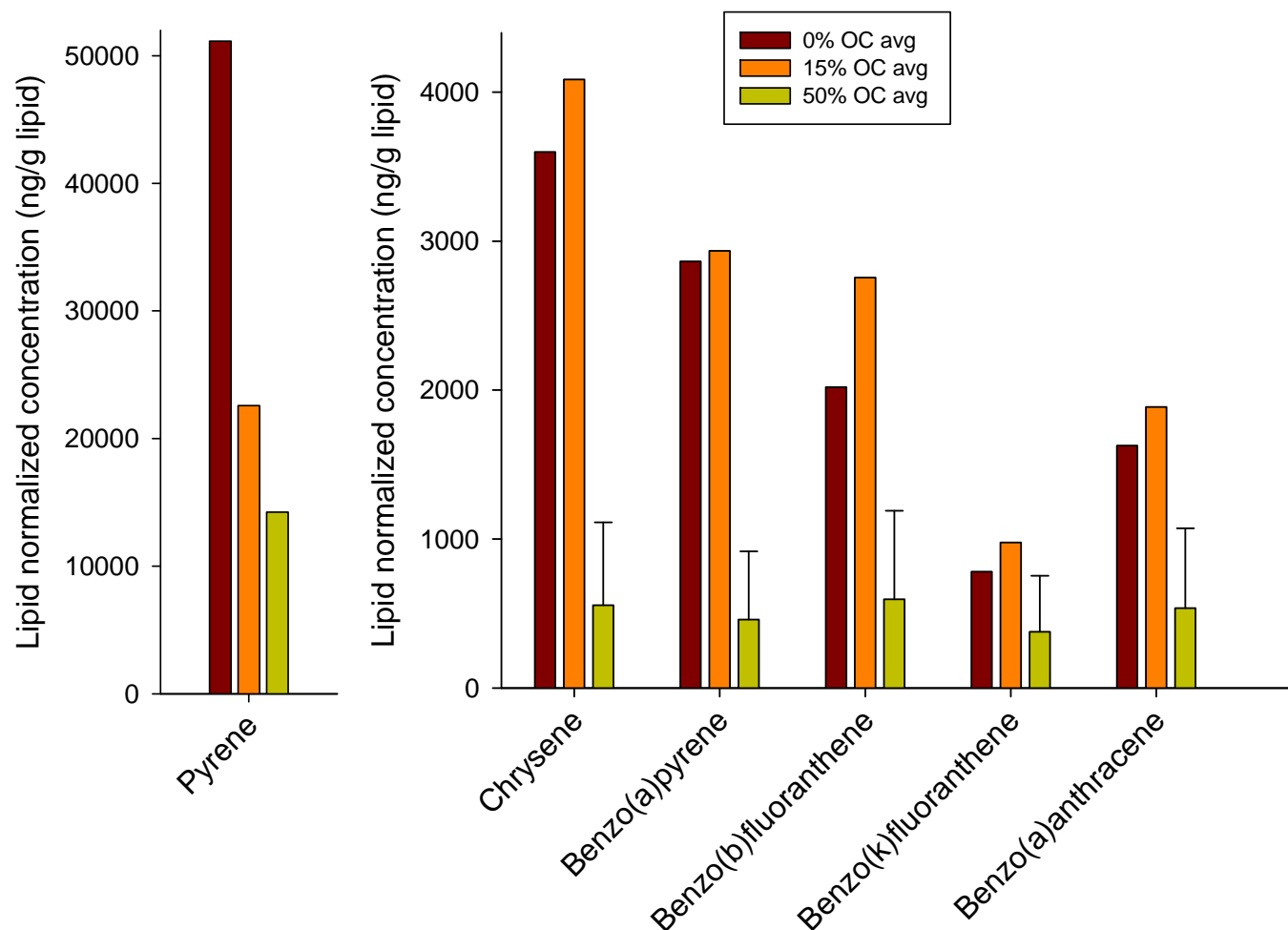


Figure 65. Effect of Organoclay on Lipid Normalized Bioaccumulation of PAHs in *Ilyodrilus*; OC - Organoclay.

Development of Biomonitoring Method for the Field Study

Several monitoring methods were used to assess the environmental effects of the experimental active caps in Steel Creek. Methods such as SEM-AVS and pore water measurements provide useful indications of the potential impacts of contaminated sediments, but do not necessarily encompass all of the environmental factors that influence the toxicity and availability of sediment contaminants. It is possible to directly measure the ecological effects of sediment contaminants by assessing the health and contaminant burdens of indigenous sediment organisms; however, this methodology is often hindered by lack of sufficient organisms of the same type (needed for valid comparative measures) at all sites. An alternative method is active biomonitoring, which consists of translocating organisms from clean reference sites or laboratory cultures to screened cages within contaminated sites where they can be maintained for the in situ study of environmental toxicity and contaminant uptake (Bervoets et al., 2004). Advantages of active biomonitoring include the ability to provide adequate sample sizes for defensible results, definite knowledge of exposure periods, and more control of potentially confounding variables such as life stage.

Active biomonitoring in Steel Creek was conducted with the California blackworm (*Lumbriculus variegates*), a freshwater oligochaete found in the shallow waters of streams, ponds, lakes, and marshes throughout North America and Europe. California blackworms are about 25 - 50 mm in length. They are aerobic and burrow into the sediments although they may extend their posterior end above the sediment surface for exchange of oxygen and carbon dioxide. California blackworms present several advantages for sediment biomonitoring: they survive well in the laboratory, individuals reared in uncontaminated environments are commercially available (which eliminates the need to maintain laboratory cultures), they are directly exposed to sediment pore water, and they have high potential for amassing bioaccumulative chemicals because they feed on organic matter in the sediments.

Recovery Methods and Efficiency

Recovery of California blackworms from depositional sediment (silt) was slightly lower (mean=82, SD=6.4) than from the other materials such sand, apatite, and organoclay (mean=90, SD=5.9 for sand; mean =87, SD=12.1 for apatite; and mean=90, SD=7.0 for organoclay). These results provide baseline expectations for recovery of California blackworms from different substrates in the absence of mortality and were helpful in interpreting the results of the field studies in Steel Creek.

Survival

Percent recovery based on weight slowly declined in sand to about 65% over the 17 day test period (Figure 66). Expected percent recovery from sand in the absence of mortality or weight loss was 90% (preceding section). In contrast, percent recovery based on weight did not decline in silt and averaged 85% on day 17. Expected recovery from silt in the absence of any mortality or weight loss was 82%. These results provide baseline estimates of expected recovery over a 17 day period in natural sediments. Better recovery in silt likely resulted from the presence of

greater amounts of organic matter that constituted a source of nutrition. These results were helpful to interpret the results of the Steel Creek field studies.

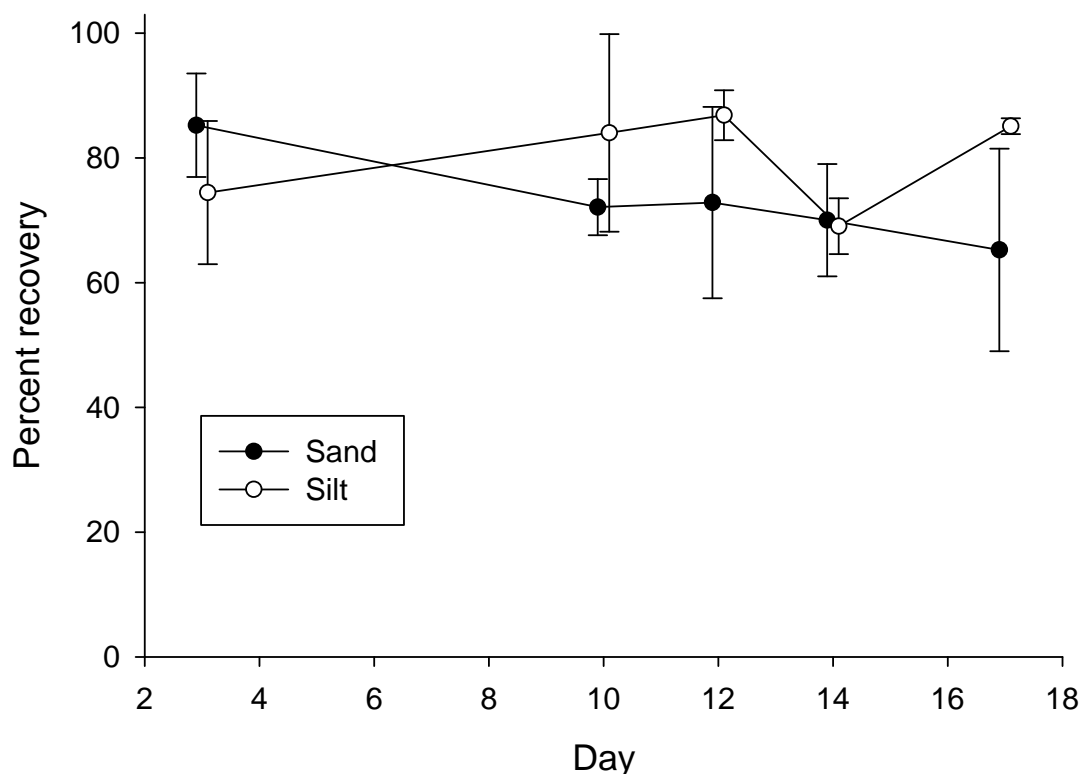


Figure 66. Recovery of California Blackworms (based on aggregate worm weight) from Silt and Sand over 17 Days. Recovery was a combined function of survival and growth.

SUBTASK 2.5. BIODEGRADABILITY OF BIOPOLYMER PRODUCTS

A ten week evaluation of several biopolymers (Figure 67) showed that chitosan cross-linked with guar gum and borax (CGB) and xanthan cross-linked with chitosan and calcium chloride (XCc) had the lowest evolution of CO₂; i.e., the lowest degradability. Biopolymers, especially xanthan cross-linked by guar gum, degraded faster under wet conditions and high temperatures (35°C) than under dry conditions (Figure 68).

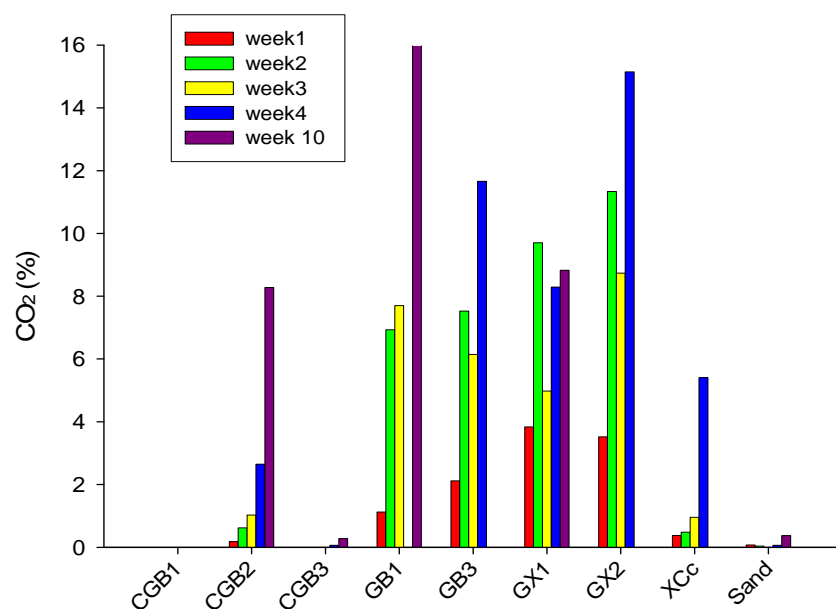


Figure 67. Release of CO₂ (measured by GC-MS) from Several Cross-linked Biopolymers: B - borax, C - chitosan, G - guar gum, X - xanthan, c - calcium chloride, 1 & 3 - without glutaraldehyde, 2 - with glutaraldehyde, 3 – with NaOH

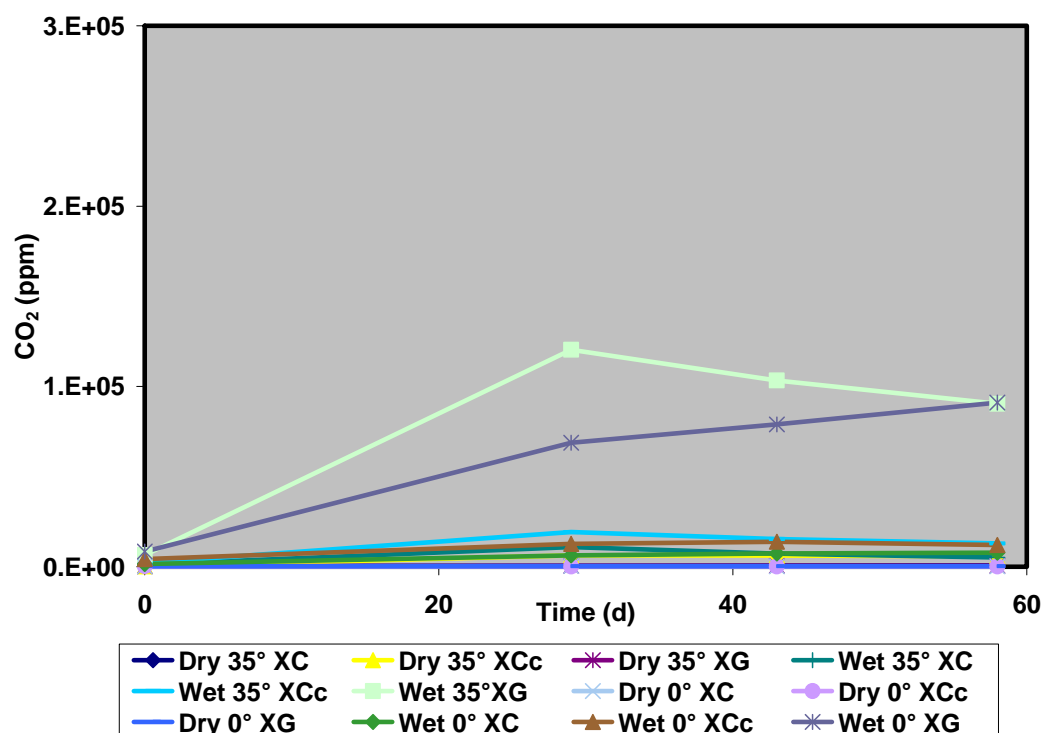


Figure 68. Evaluation of Biopolymer Degradation under Wet/Dry Conditions and Different Temperatures; X - xanthan, G - guar gum, C- chitosan, c- calcium chloride.

Microbial densities associated with the biopolymers likely were a result of bacteria present during manufacture of the biopolymers. Minimal increases in bacterial densities and CO₂ release over 6 months and under various conditions indicated that biopolymer-associated microbes did not contribute significantly to the degradation of some biopolymers (Figure 69).

Biopolymers with sorbed metals demonstrated decreased CO₂ release and likely minimal biodegradation compared to biopolymers without sorbed metals (Figures 70 and 71). Obvious morphological differences in bacteria isolated from biopolymers further indicated that different microbial consortia were associated with biopolymers as a function of metal concentration. Biodegradation of biopolymers resulted in minimal release of metal contaminants (Figure 72).

This study showed that cross-linked biopolymers have the potential to remove contaminants from the aqueous phase and to stabilize contaminants in soils/sediments. Cross-linked biopolymers vary in their susceptibility to biodegradation, with some being resistant for several months. Biopolymer degradation did not result in contaminant release during the test period. Our research showed that cross-linked biopolymers are promising for remediation, but longer periods of evaluation under field conditions are still needed.

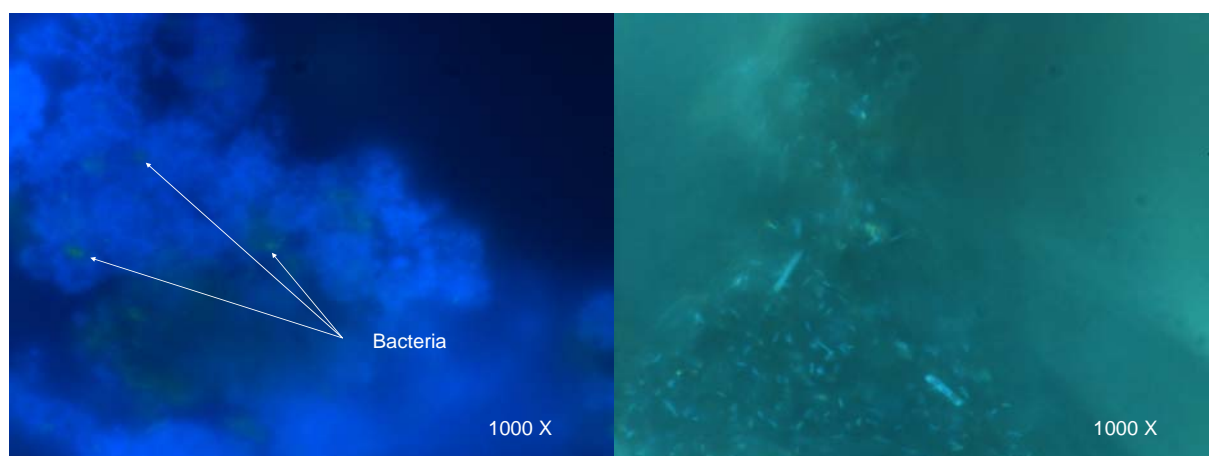


Figure 69. Microscopic Analyses of Biopolymer Surfaces using 4',6-Diamidino-2-Phenylindole (DAPI) and Epifluorescence Microscopy. Biopolymer XCc (left) contained fewer bacteria than CGB after 6 months of contact with sediment suggesting limited biodegradation.

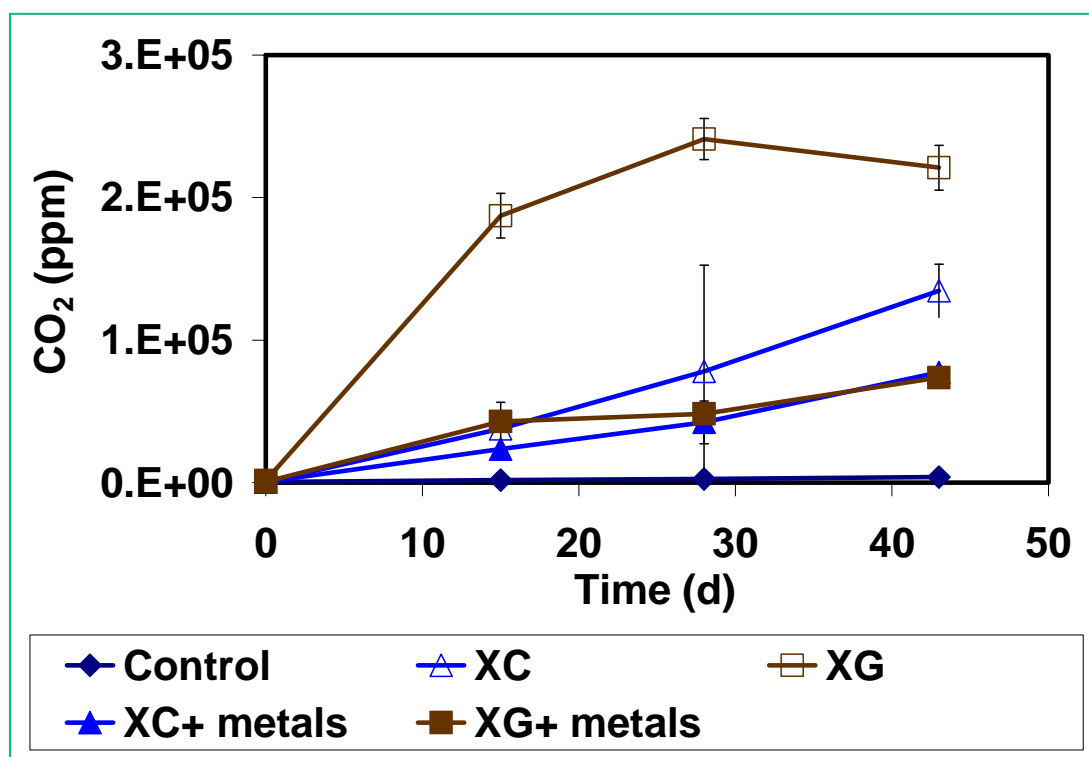


Figure 70. Evaluation of Biopolymer Degradation for 45 Days; X - xanthan, G - guar gum, and C- chitosan. Metal sorption of biopolymers inhibited bacterial activity.

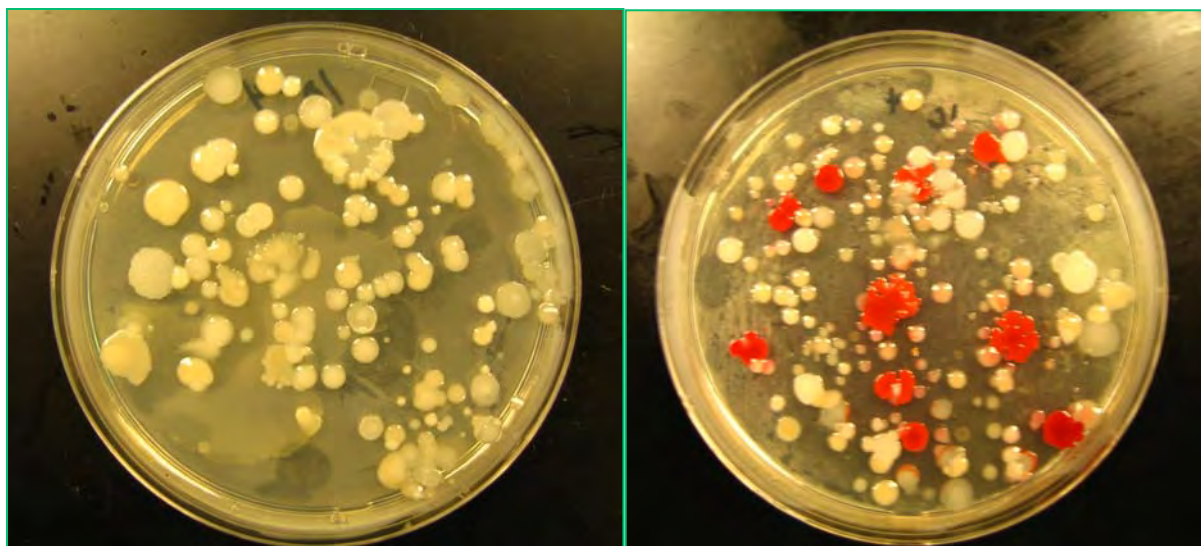


Figure 71. Morphological Differences in Bacterial Populations after Exposure to Xanthan Biopolymers without (left) and with (right) Sorbed Metals.

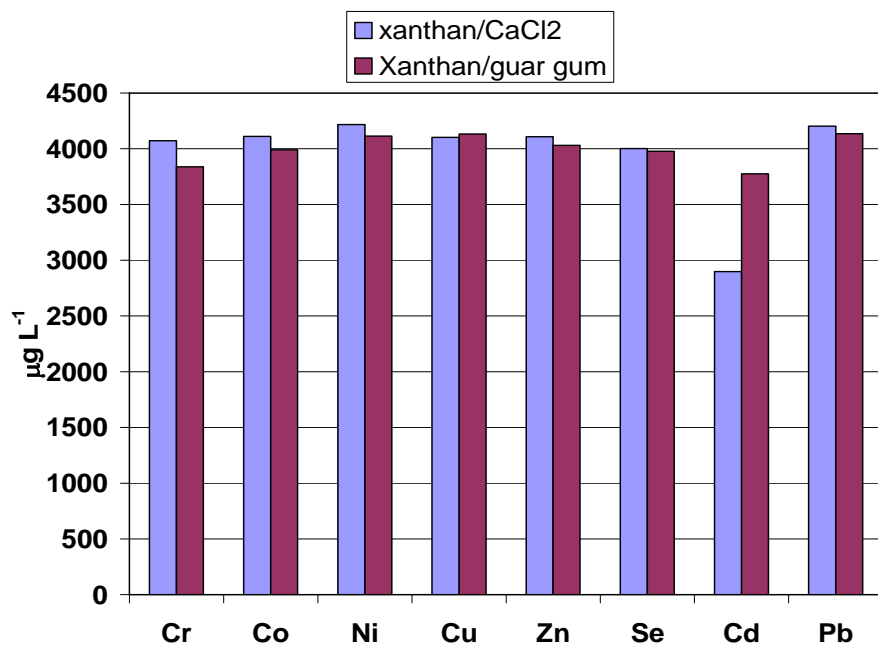


Figure 72. Metals Remaining in Biopolymers after 3 Months of Biodegradation (initial concentration of the spike solution was 5000 µg L⁻¹).

TASK 3. EVALUATION OF THE RESISTANCE OF CAPS TO PHYSICAL DISTURBANCE

Evaluation of Biopolymer Resistance to Physical Disturbance

Various biopolymers were cross-linked with and without coating on sand or amendments (Tables 1 and 2). The cross-linked biopolymer products had increased viscosity and shear strength (results not shown here). They also had an evident cohesiveness, some of them looking and acting literally like “glues” when wet (Picture 15). These physical characteristics indicate that some biopolymers have potential use in active caps as an adhesive, binding cap materials together, and for removal of contaminants.

Shaker Tests

The shaker suspension-simulation device was used to test the suspension resistance of sand, biopolymer coated sands, and organoclay. Five suspension thresholds were established: fine top particles disturbed, motion of top particles, cloudiness, full re-suspension of top layer, and full re-suspension of the bottom layer. The oscillations of the grid used to produce these motions were converted into shear stresses. These stresses were compared with those calculated with Shield’s curve equations, which are indicators of the stability of non-cohesive particles in a bed. Full re-suspension of the bottom layer of sand was not achieved (Figure 73). The deepest penetration into the 7cm high sand layer was 1.5 cm. The maximum speed that the motor was able to achieve was approximately 650 rpm. In the paper by Tsai and Lick (1986) maximum speed derived from the given oscillation periods was 750 rpm. Full re-suspension of the bottom layer may have been achieved if the motor would have reached higher speeds.

Dried biopolymer coated sands CGB3 and XCc treated with addition of HCl in the preparation process performed similarly to plain sand. The biopolymer coatings in these products did not become viscous after rewetting and did not aid in preventing suspension of the sediment columns (Figure 73). However, the dry coated sand CGB3 prepared without HCl (Table 2) produced a viscous gel immediately upon rewetting and was resistant to suspension (Figure 74). The gel properties of the rewetted biopolymer significantly increased the shear stresses required for resuspension of sediments (Figure 73). Even at maximum rotational speed very little disturbance of CGB3 was observed and the top layer was never resuspended (Figure 74).

Additional suspension experiments were conducted to test the stability of multiple biopolymer materials when placed in viscous slurry rather than first drying and then rewetting. The results of these tests are displayed in Figure 75. The slurry products performed very well in the suspension experiments. Initial oscillations of the grid caused the uppermost portions of the slurries to pulse vertically but no sloughing of the samples occurred. Increased shear stresses resulted in minor sloughing of small particles but no resuspension occurred. Sand with biopolymers, e.g., xanthan cross linked with guar gum (XG), was suspension resistance even at a speed of 11 m/s (Figure 76). Mixtures of biopolymer XG, sand, and other amendments such as organoclay and/or apatite were also suspension resistant at a speed 11 m/s (Figure 77). The

significant resistance of the slurry products to suspension shows promise for future applications as a stand-alone active cap or as armament for other amendments.

Organoclay (PM-199) without biopolymers was not suspension resistant. If placed in a flowing aquatic environment, a cap of organoclay would erode like a plain sand cap (Figure 78).

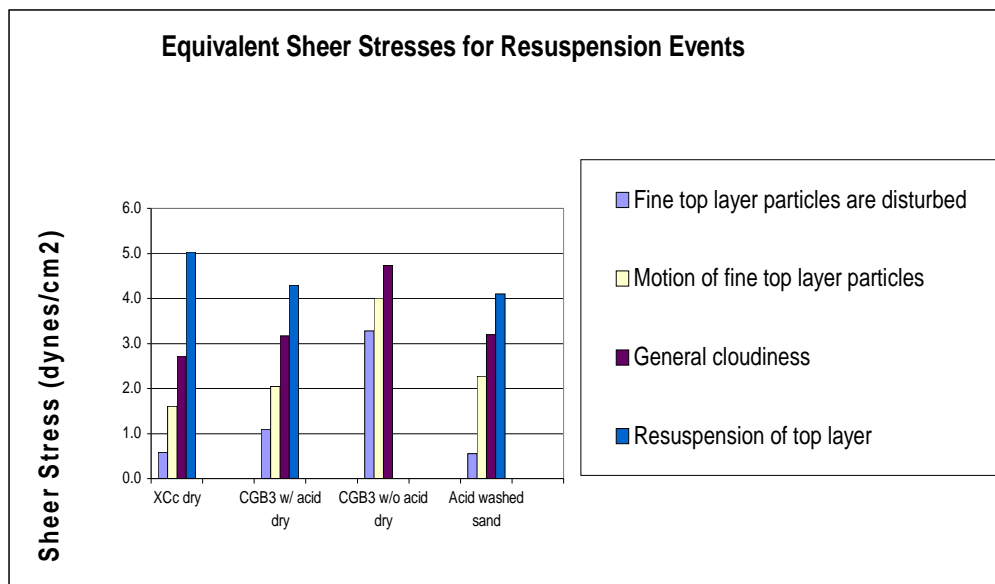


Figure 73. Effects of Equivalent Shear Stresses on Resuspension of Sand and Three Types of Dry and Rewetted Biopolymer Coated Sand.

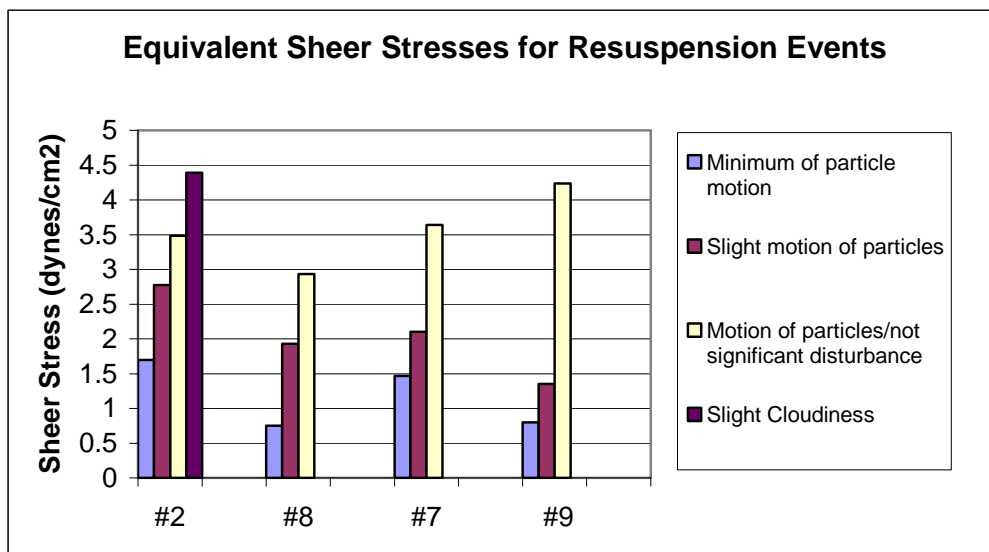


Figure 74. Effects of Equivalent Shear Stresses on Sand and Slurries of Biopolymer Coated Sand: 2 – sand with chitosan/guar gum/borax, 7 – sand with xanthan/guar gum and apatite, 8 – sand with xanthan/guar gum and organoclay (PM-199), 9 – sand with xanthan/guar gum and apatite, and organoclay.



A



B

Figure 75. Plain Sand Resuspension at 3.7 m/s (A) and Erosion at (11 m/s) (B).



A



B

Figure 76. Coated Sand with Xanthan and Guar Gum did not Erode at 3.7 m/s (A) or 11m/s (B).



A



B

Figure 77. Sand and Organoclay (PM-199) Mixed with Biopolymers Xanthan and Guar Gum did not Erode at 3.7m/s (A) or 11m/s (B).



Figure 78. Resuspension of Organoclay (PM-199) leading to Cloudiness (A) and Surface Suspension (B).

Adjustable Shear Stress Erosion and Transport (ASSET) Flume

The materials evaluated in the shaker and ASSET flume tests are listed in Table 2 where they have been assigned product numbers. The products included:

- #4 XCc - sand and xanthan/chitosan cross-linked with calcium chloride and glutaraldehyde,
- #5 XG - sand and 2.5% guar gum cross-linked with xanthan (Kelzan brand)
- #6 XG Coyote - sand and 5% guar gum cross-linked with xanthan (Coyote brand)
- #6 XG Kelzan - sand and 5% guar gum cross-linked with xanthan (Kelzan brand)
- #7 AXG - sand, 12.5% apatite and 5% guar gum cross-linked with xanthan (Kelzan brand)
- #8 OXG - sand, 12.5% organoclay, and 5% guar gum cross-linked with xanthan (Kelzan brand)
- #9 XG/AO - sand, 12.5% organoclay, 12.5% apatite, and 5% guar gum cross-linked with xanthan (Kelzan brand)

Erosion rates as a function of shear stress and depth were obtained for six of the seven materials after 2, 10, and 175 days of consolidation at shear stresses of 0.25, 0.5, 0.75, 1.0, 1.5, 2.0, 3.0 and 4.0 N/m². After preliminary tests of the #7 AXG material at 2 and 5 days, the sample did not show promise as an erosion resistant cap material and was dropped from further testing. The ASSET flume erosion tests enabled stability evaluation of nearly the entire thickness of the cap (~10 cm) under simulated flow conditions that ranged from quiescent to the shear environment in extreme storm events. The erosion rate ratio analysis is used to compare average erosion behavior at distinct intervals within a core. An example of how the two methods correlate is shown for the #9 XG/AO and #8 OXG samples after 10 days of consolidation (Figure 79). Graphics A and B in Figure 79 show that erosion decreases with increasing depth in the #9 XG/OA cap material while graphics C and D show increased erosion in the center of the core with the most erosion resistant layer at the bottom.

The individual erosion behavior of the six dominant cap materials is shown in Figure 80. The six graphics compare the erosion behavior at 2, 10 and 175 days of consolidation at each erosion interval as well as the core average. This enables the evaluation of the erosion behavior of each cap material as a function of consolidation time and depth within the core sample. For example,

the #4 XCC and #9 XG/OA samples display a general hardening or resistance to erosion with increasing core age. Both samples also show that each core became more stable at depth at all ages except for the second depth interval in the 2 day #9 XG/OA sample. It is important to note that the scale on the #9 XG/OA plot is expanded by two orders of magnitude and shows that the oldest, 175 days of consolidation, sample is the most stable or erosion resistant core of all. The #6 XG Kelzan sample shows the opposite trend in that it becomes softer or less erosionally stable as the sample ages. This same sample shows that the surface layer at all ages is always the easiest to erode with general, but not consistent trends, of hardening at depth. The remaining cores, #5 XG, #6 XG Coyote, and #8 OXG, show inconsistent erosion behavior with sample age and depth within the core.

The core average erosion rates for the six primary materials are compared at 2, 10, and 175 days of consolidation along with the time average erosion rate for each material (Figure 81). Sand mixed with XG (xanthan gum) Coyote and XG Kelzan generally became more difficult to erode with depth for all shear stresses. Erosion was in the form of small aggregates (~0.5-2 mm) that often formed small runnel-like features in the surface of the core parallel to the flow path and left a fairly uniform and smooth surface layer. The material was very cohesive and exhibited behaviors consistent with naturally cohesive sediments (Roberts et al, 1998).

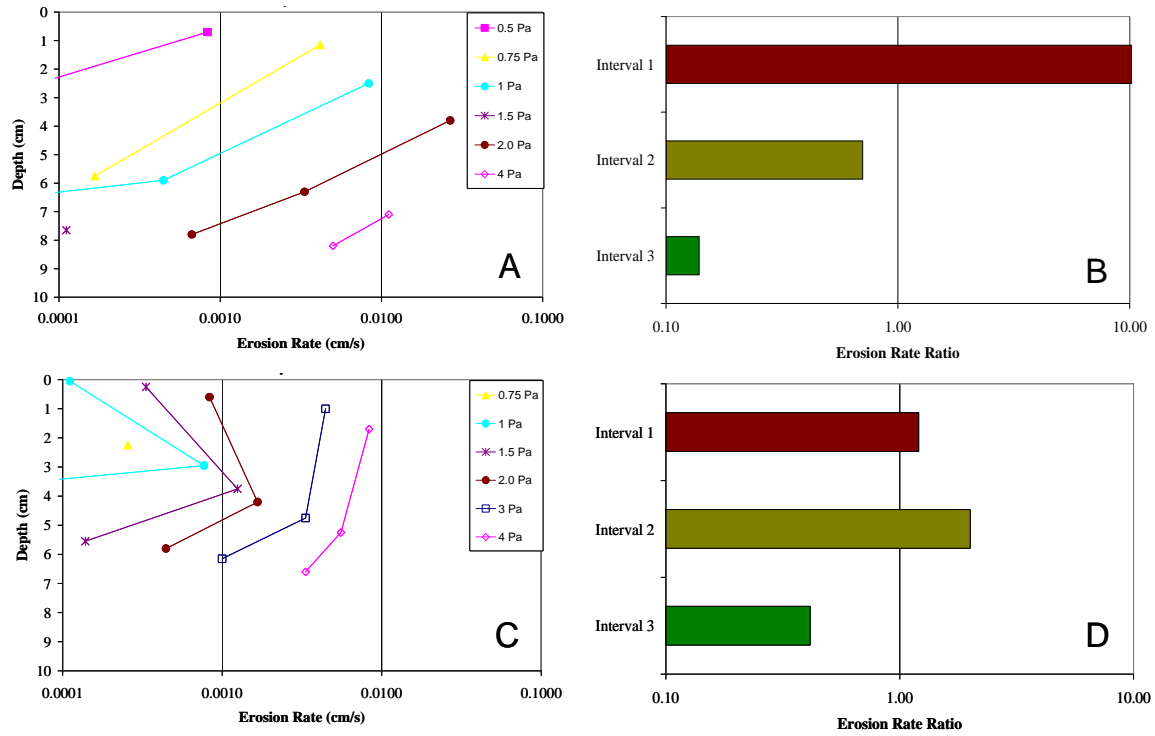


Figure 79. (A) #9 XG/AO 10 Day Consolidation Erosion Rate as a Function of Depth at Shear Stresses of 0.5, 0.75, 1.0, 1.5, 2.0, and 4.0 Pa. (B) #9 XG/AO 10 Day Consolidation Erosion Rate Ratio for the 3 Erosion Intervals. (C) #8 OXG 10 Day Consolidation Erosion Rate as a Function of Depth at Shear Stresses of 0.75, 1.0, 1.5, 2.0, 3.0, and 4.0 Pa. (D) #8 OXG 10 Day Consolidation Erosion Rate Ratio for the 3 Erosion Intervals.

The erosive behavior of AXG differed from that of the other materials (Table 37). The erosion resistance of some materials increased with time as indicated by core average critical shear stress shown in Figure 88. Comparisons between the two and 10 day consolidation periods showed that XCC, XG (2.5% biopolymer), XG Kelzan, OXG Kelzan, and XG/AO Kelzan became harder to erode as they became more consolidated (Table 37 and Figures 81 and 82). Only xanthan/guar gum, mixed with apatite and organoclay showed long term (175 day) physical stability (Figures 81 and 82). The critical shear stress for this material exceeded 2Pa in the 175 day consolidation test indicating its promise as a cap material (Figure 82).

Table 37. Summary of Erosion Properties for 2, 10 and 175 Days of Consolidation.

Sample ID	Critical Shear Stress Range (Pa)	Erosion Rate Range at 1.0 Pa (cm/s)	Erosion Rate Generally Decreases with Depth
2 Day Consolidation			
#4 XCC	0.17 - 0.51	0.0083 - 0.013	Yes
#5 XG	0.73 - 0.99	0.00011 - 0.00067	Yes
#6 XG Coyote	0.86 - 1.90	$<10^{-4}$ - 0.00022	Yes
#6 XG Kelzan	0.73 - 1.73	$<10^{-4}$ - 0.00033	Yes
#7 AXG	0.28 - 0.75	0.00067 - 0.0083*	No, center layer easiest to erode
#8 OXG	0.30 - 0.73	0.00017 - 0.0033	No, easier with depth except for second depth interval
#9 XG/AO	0.30 - 1.2	$<10^{-4}$ - 0.0033	No, center layer easiest to erode although bottom layer was most erosion resistant
10 Day Consolidation			
#4 XCC	0.28 - 0.71	0.00095 - 0.00278	Yes
#5 XG	0.73 - 1.45	$<10^{-4}$ - 0.00022	Yes
#6 XG Coyote	0.28 - 0.73	0.00017 - 0.002	No, surface and bottom layers easier to erode
#6 XG Kelzan	0.73 - 1.65	$<10^{-4}$ - 0.00067	Yes
#7 AXG (5-day)**	0.25 - 0.75	0.00067 - 0.0035	No, center layer easiest to erode
#8 OXG	0.60 - 1.36	$<10^{-4}$ - 0.00077	No, center layer easiest to erode
#9 XG/AO	0.28 - 1.45	$<10^{-4}$ - 0.00083	Yes
175 Day Consolidation			
#4 XCC	0.98 - 1.06	$<10^{-4}$ - 0.00011	Yes
#5 XG	0.65 - 1.61	$<10^{-4}$ - 0.0005	Yes
#6 XG Coyote	0.61 - 0.98	0.00011 - .000056	Yes
#6 XG Kelzan	0.73 - 0.98	0.00011 - .000044	Yes, but second depth interval was most erosion resistant
#8 OXG	0.24 - 0.86	0.00022 - .00303	Yes
#9 XG/AO	0.73 - 3.3	$<10^{-4}$ - 0.00033	Yes

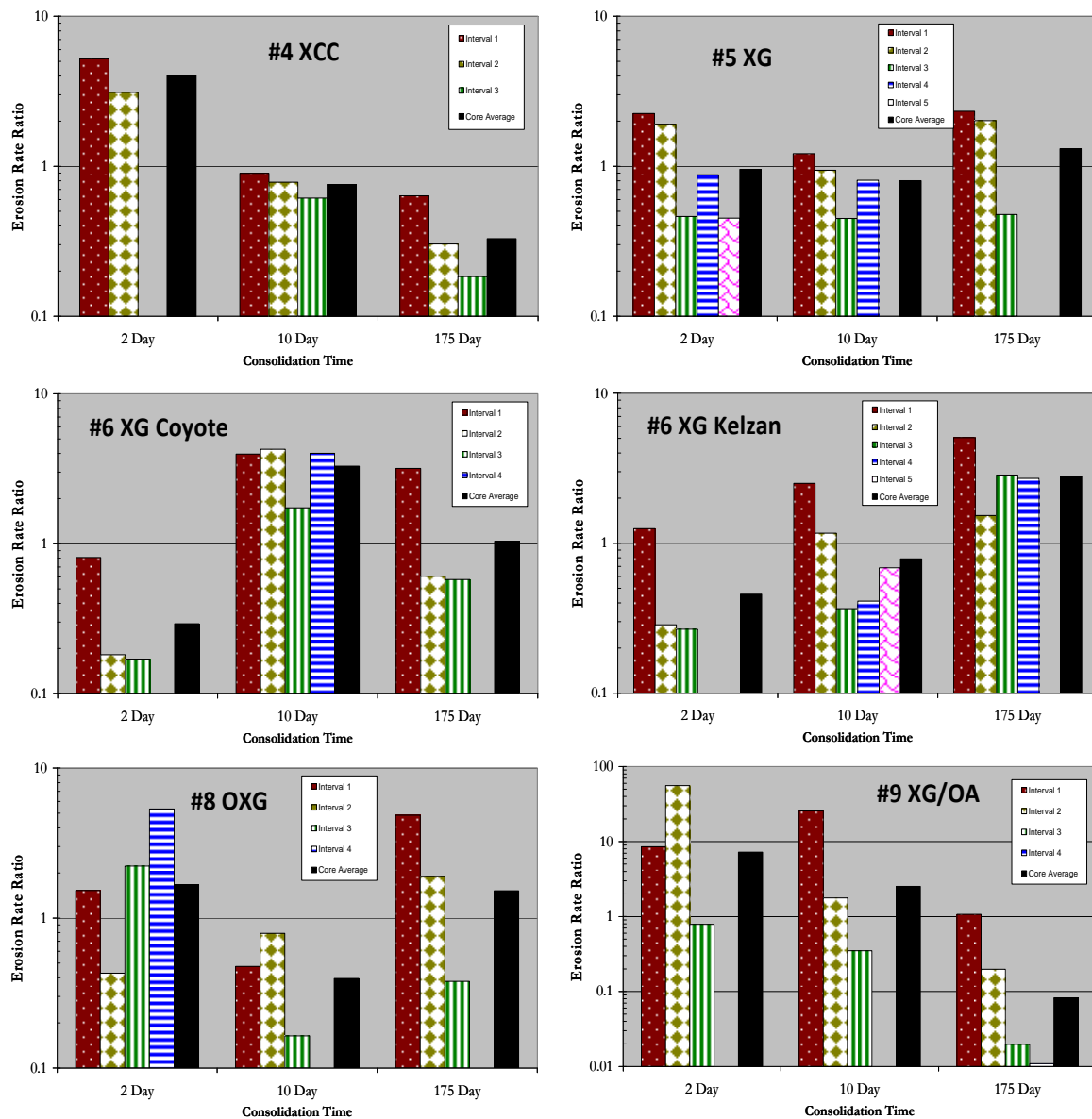


Figure 80. Erosion Rate Ratio for Six Primary Cap Materials comparing All Erosion Intervals and Core Average Erosion at Consolidation Times of 2, 10, and 175 Days.

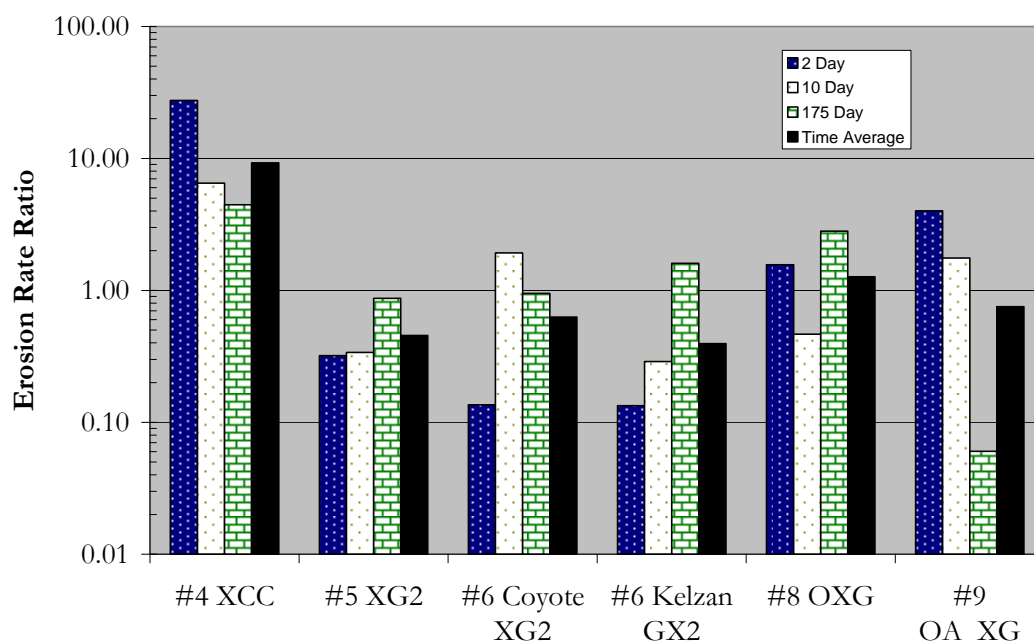


Figure 81. Comparison of Core Average Erosion Rates at 2, 10, and 175 Day Consolidation Including the Time Average of All Three.

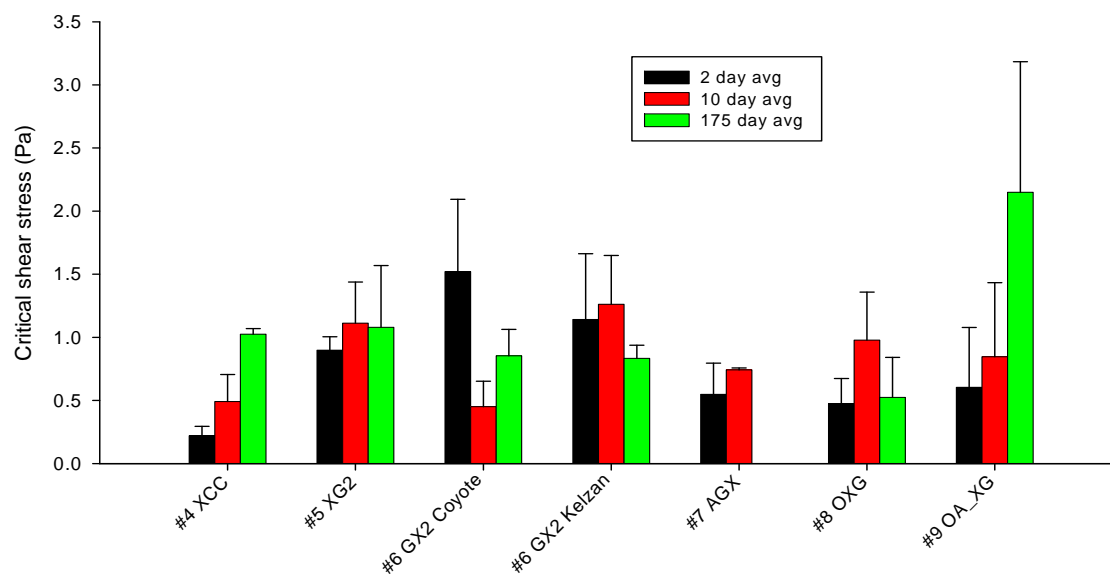


Figure 82. Critical Shear Stress Comparison among Biopolymer Materials at 2, 10, and 175 Days. Each value is an average of measurements taken at two to five different depths in a core sample. Error bars represent standard deviations.

TASK 4. GENERATION OF CONCEPTUAL AND MATHEMATICAL MODELS FOR CONTAMINANT ATTENUATION

Mathematical modeling is an essential tool for evaluating sediment caps due to the lengthy transport times associated with contaminant transport in sediment caps and the inherent spatial variability in natural environments.

The goal of this task was to develop appropriate modeling approaches for design and evaluation of sediment caps that incorporate all the complexities of sediment cap systems. An essential part of the design of sediment caps is dictated by reduction of surficial pore water concentrations, sediment particle concentrations, and contaminant fluxes; therefore any modeling approach should provide a method for evaluating the cap's effect on these parameters.

To summarize, sorption onto cap materials, desorption resistance from sediments, sorption onto dissolved organic matter, pore water advection, sediment deposition/erosion, molecular diffusion, pore water dispersion, bioturbation/bioirrigation, and contaminant decay are the processes that control fate and transport of contaminants in sediment caps. Desorption resistance, deposition, and decay represent natural attenuation mechanisms that reduce environmental risk. Sorption onto dissolved organic matter, pore water advection, molecular diffusion, and pore water dispersion transport contaminants from the underlying sediment to the surface of the cap. The designer has essentially no control over these processes, leaving sorption onto cap materials as the primary design parameter. However, it is critical that the impact of each of the processes listed above be determined at a particular site for assessment of optimal sediment remediation design. Effective contaminated sediment management requires an understanding of the role of these processes which frequently requires the use of mathematical models. Table 38 provides a summary of the processes affecting contaminant transport in sediments.

The following sections provide examples of the expected behavior of contaminants in various sediment capping scenarios.

Table 38. Effects of Transport Processes on Sediment Capping Effectiveness.

Contaminant Transport Process	Designer Control Ability	Impact on Capping Effectiveness
Sediment desorption resistance	None	Positive; desorption resistance increases transport times through caps
Sorption onto cap materials	High	Positive; increasing sorption increases transport times through caps
Sorption dissolved matter onto organic	None	Negative; increased dissolved organic matter levels increase the total pore water mass thereby decreasing breakthrough time
Pore Advection Water	Little	Generally negative; pore water upwelling is the major source of contaminant breakthrough in sediment caps, although in rare pore water down flow cases it has a positive effect
Deposition	None	Positive; high rates bury contaminants, decreasing surficial concentrations
Molecular Diffusion	None	Negative; molecular diffusion decreases the concentration gradients across the cap, although the rate is generally slow in sediment caps
Pore Dispersion Water	Little	Negative; pore water dispersion increases transport through the cap, which decreases the contaminant breakthrough time

Transport of Metals through Active Caps – 1-D Metal Transport Modeling

The results of the modeling are shown in Figures 83 through 90. Each figure shows the sediment pore water concentration and subsequent depletion due to advection and diffusion into the overlying materials. For this analysis, a steady state advective flux of 1 cm/hr (Darcy velocity) was used with a cap thickness of 5 cm. All results presented are relative to these fixed parameters. Figures 83 and 84 show the results for Case 1 where there is no cap and, contaminants are allowed to leach out of the sediment into the overlying water column and subsequently out of the system. For each contaminant, the transport process is dominated by advection and each contaminant is completely removed from the model in under 5 days. Because

the transport process is dominated by advection and there is no sorption processes involved with this simulation, the breakthrough curve for each metal is identical.

Figures 85 and 86 show the results for Case 2 where there is a sand cap overlying the contaminated sediments. Since there is no sorption in the sand cap, this case is similar to Case 1 (no cap). As with Case 1, each contaminant is completely removed from the system in under 5 days.

Figures 87 and 88 show the results for Case 3 where there is an apatite cap overlying the contaminated sediments. Compared to Case 2 (sand cap), these figures clearly show the apatite cap delayed contaminant breakthrough. Except for cobalt, nickel and selenium, breakthrough is delayed for at least 1 year. Furthermore, except for nickel and selenium, it takes several years to clear the metals from the model. Therefore, due primarily to sorption processes, the apatite cap appears to be a barrier against transport of the contaminants compared to the sand cap and no cap cases.

Figures 89 and 90 show the results for Case 4 where there is an organoclay cap overlying the contaminated sediments. These figures show the organoclay cap also delayed contaminant breakthrough. Except for lead, nickel, and zinc, breakthrough is delayed for at least 1 year and it takes several years to clear the metals from the model. As with the apatite cap, due primarily to sorption processes, the organoclay cap appears to be a barrier against transport of the contaminants compared to the sand cap and no cap cases.

As stated earlier, the results presented are normalized to the applied advective flux of 1 cm/hr and a cap thickness of 5 cm. The actual field performance of each cap material will depend on such factors as cap thickness and hydrogeologic conditions. However, the relative performance each material should be similar to that demonstrated in this modeling exercise.

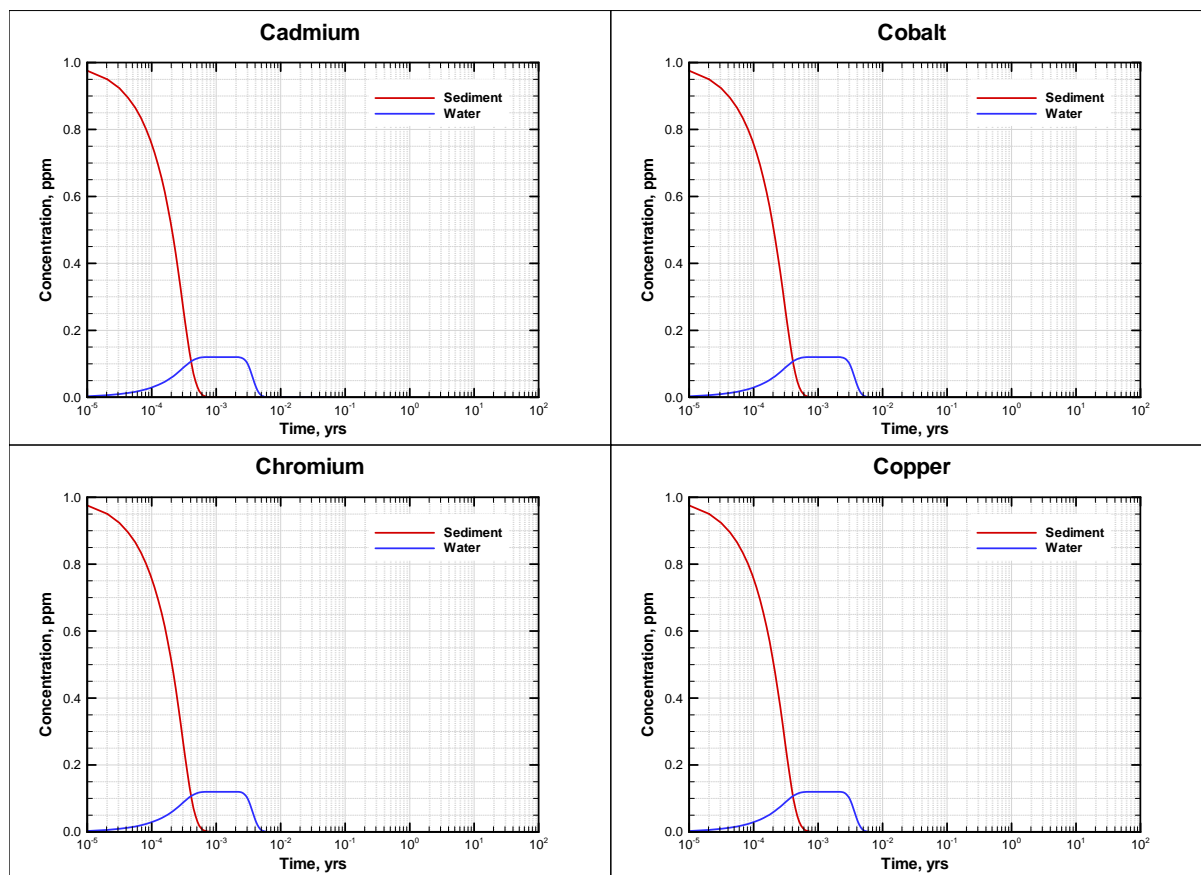


Figure 83. Breakthrough Curves for Cd, Co, Cr, and Cu for the No cap Case. The sediment concentration curves are plotted against the left y-axis and all others against the right y-axis.

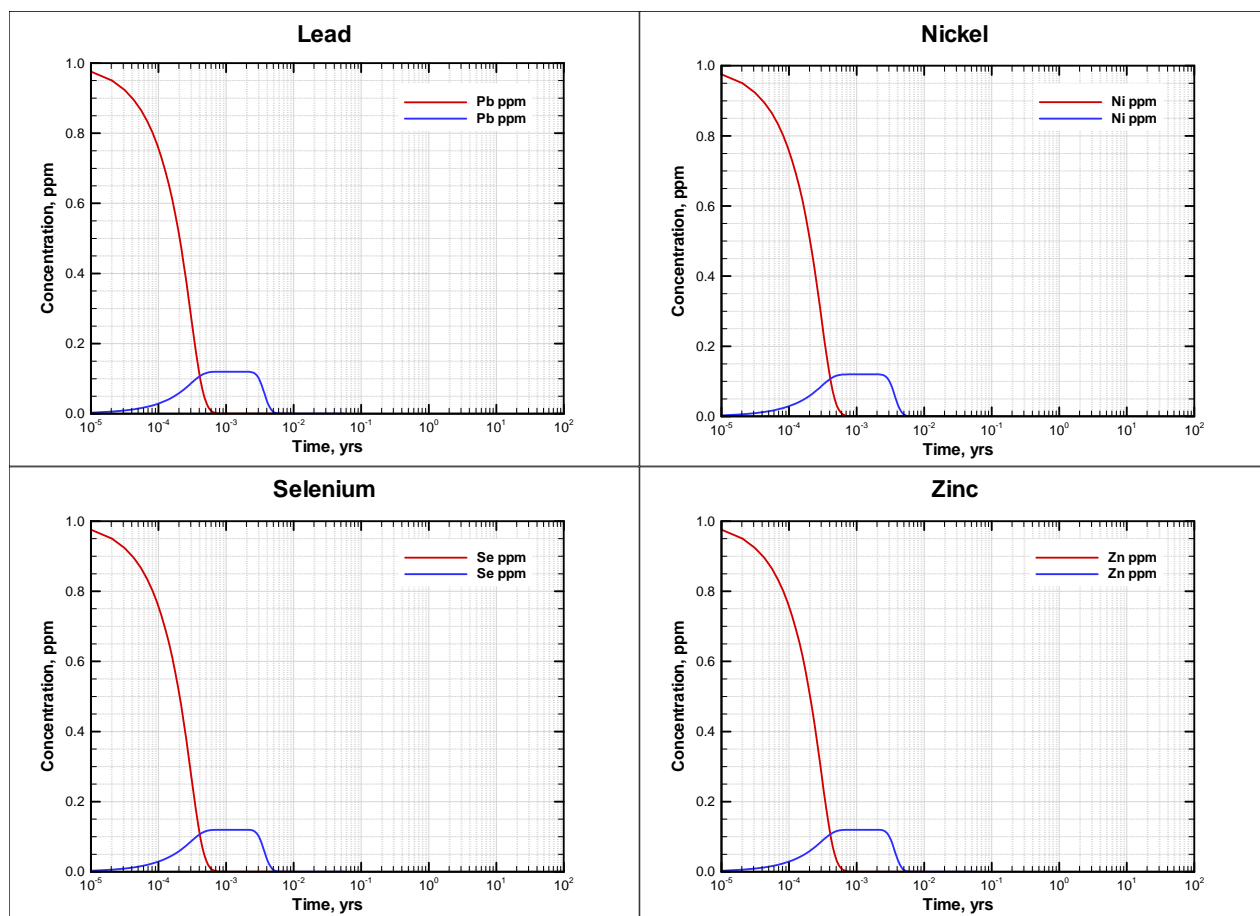


Figure 84. Breakthrough Curves for Pb, Ni, Se, and Zn for No Cap Case. The sediment concentration curves are plotted against the left y-axis and all others against the right y-axis.

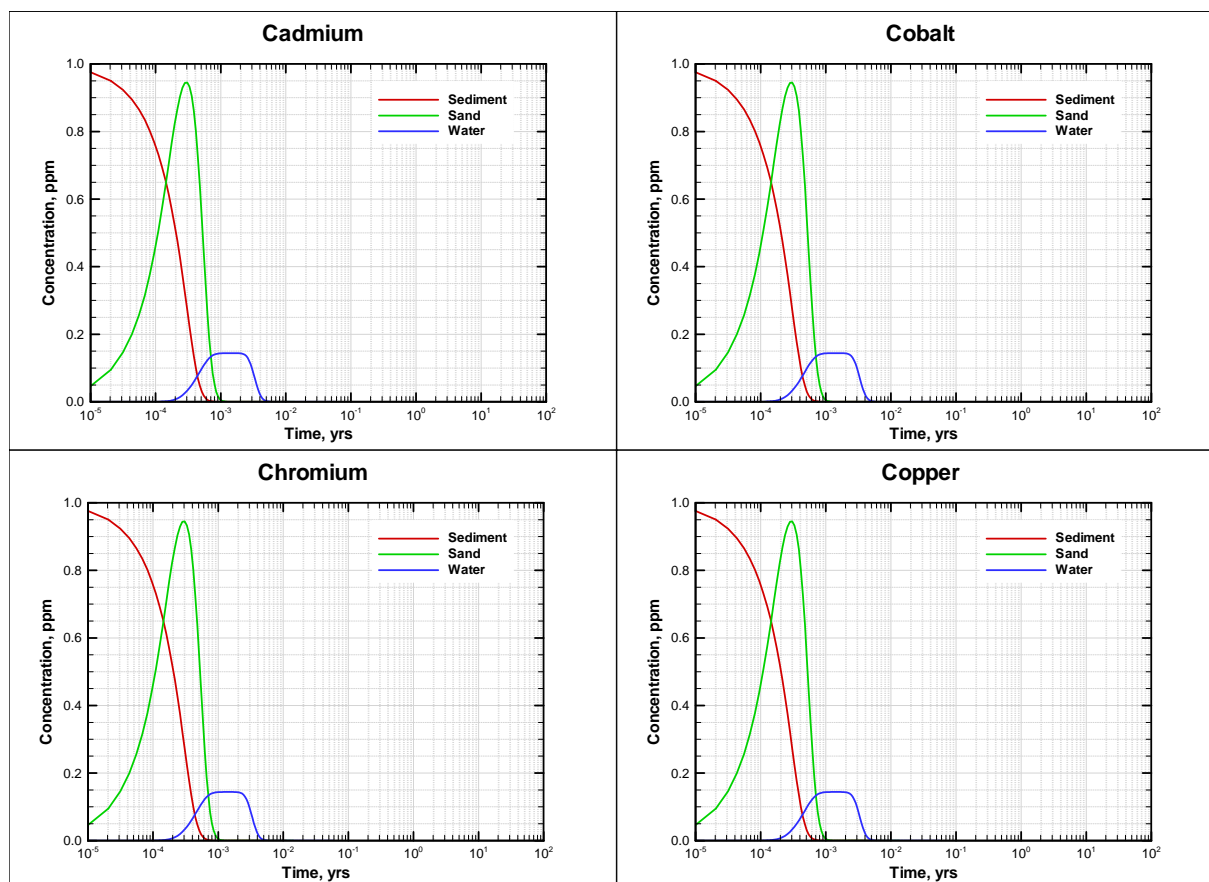


Figure 85. Breakthrough Curves for Cd, Co, Cr, and Cu for Sand Cap Case. The sediment concentration curves are plotted against the left y-axis and all others against the right y-axis.

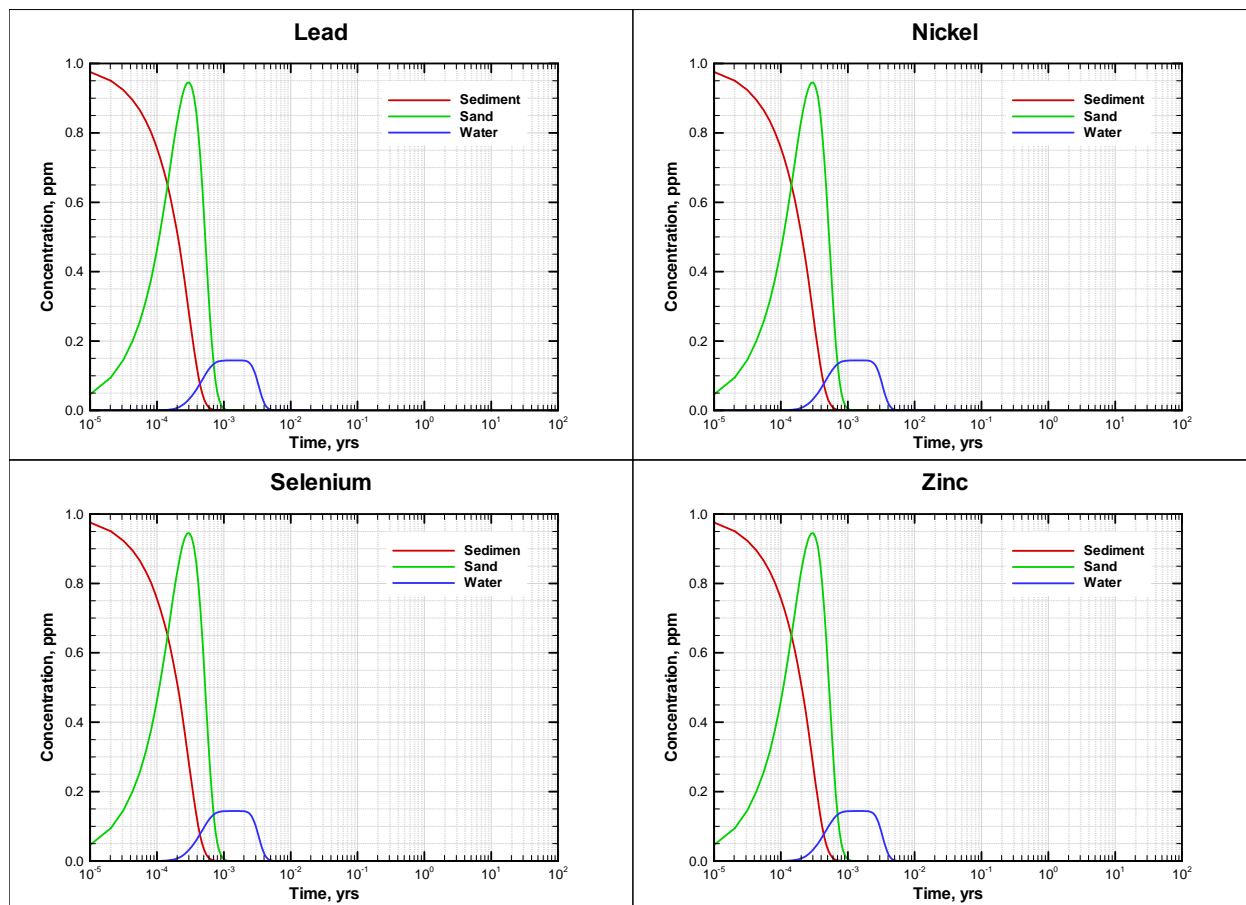


Figure 86. Breakthrough Curves for Pb, Ni, Se, and Zn for Sand Cap Case. The sediment concentration curves are plotted against the left y-axis and all others against the right y-axis.

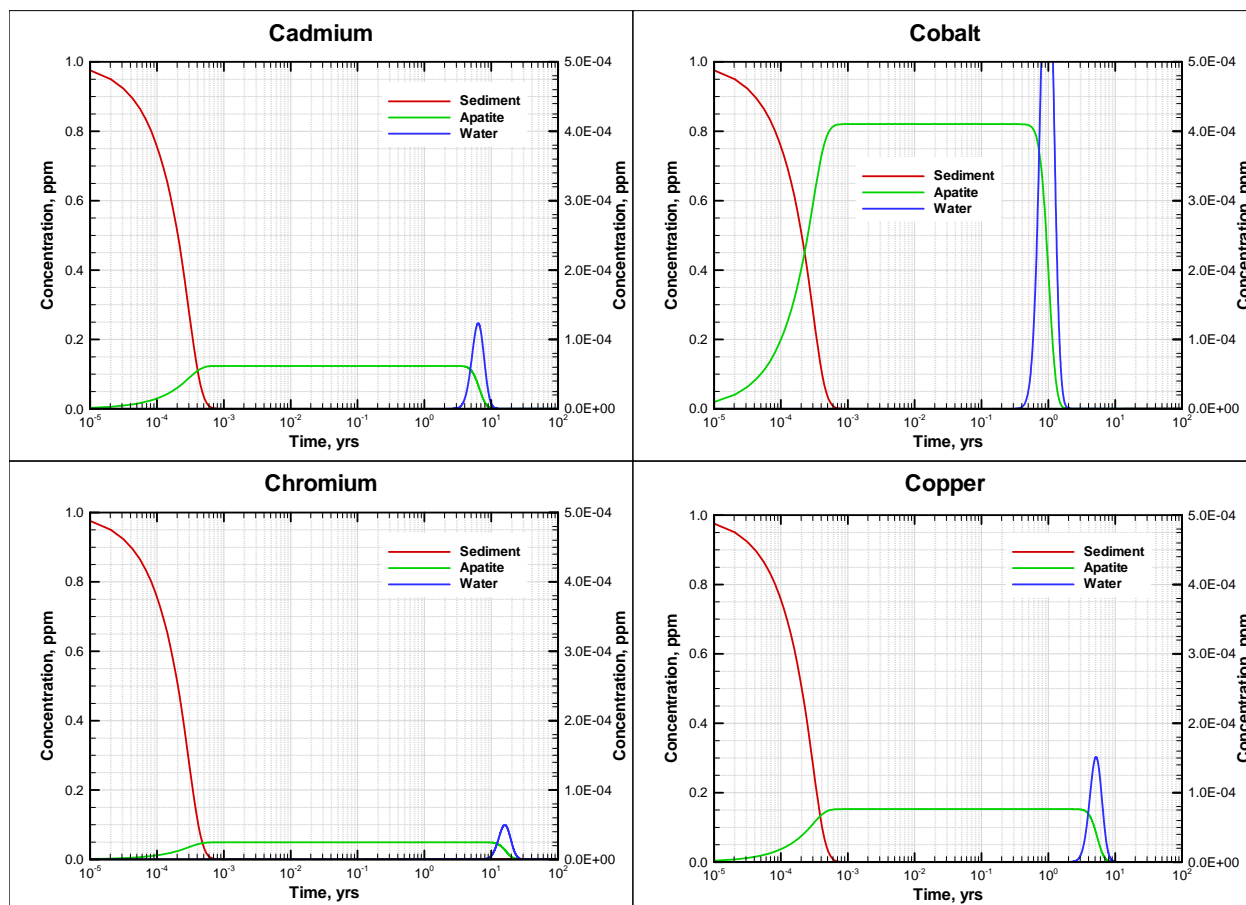


Figure 87. Breakthrough Curves for Cd, Co, Cr, and Cu for Apatite Cap Case. The sediment concentration curves are plotted against the left y-axis and all others against the right y-axis.

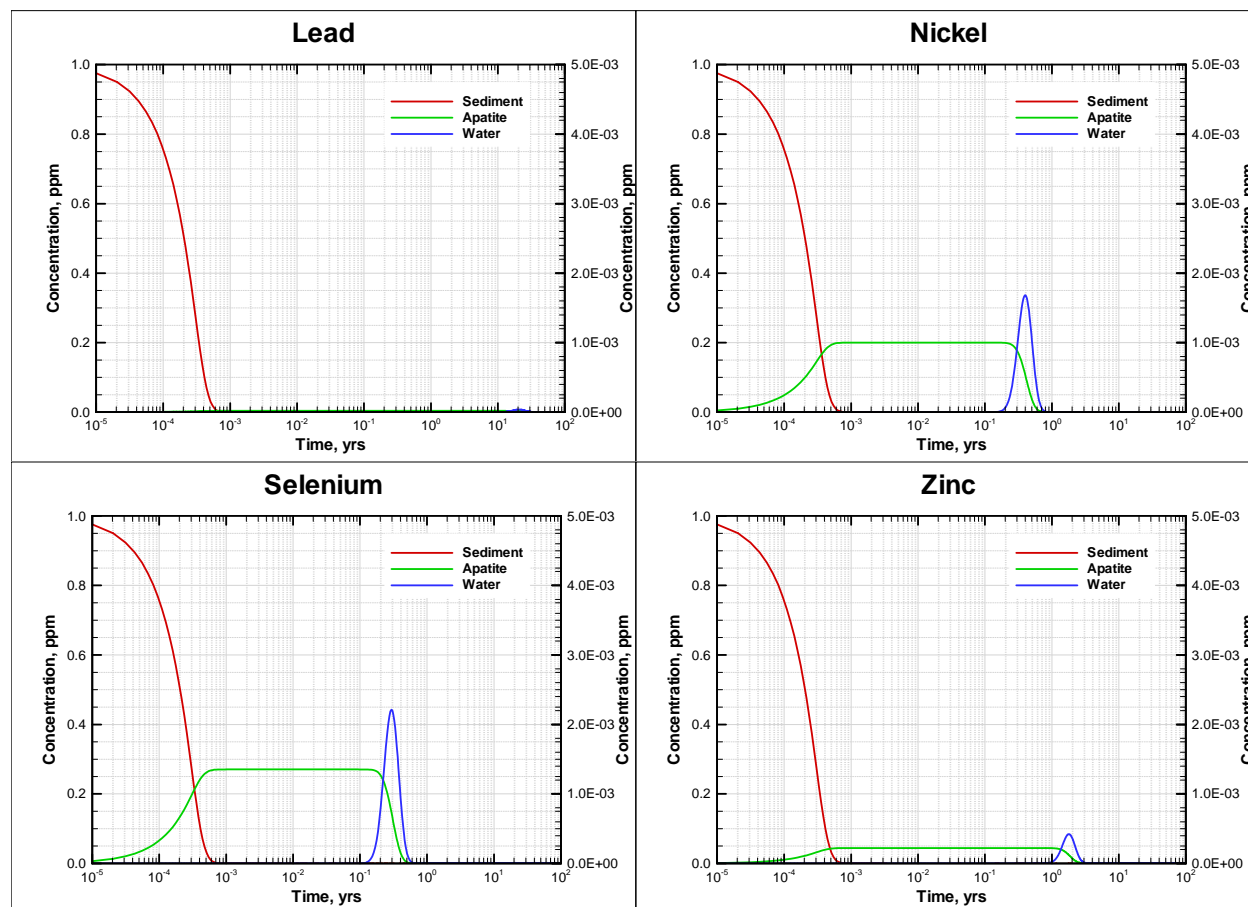


Figure 88. Breakthrough Curves for Pb, Ni, Se, and Zn for Apatite Cap Case. The sediment concentration curves are plotted against the left y-axis and all others against the right y-axis.

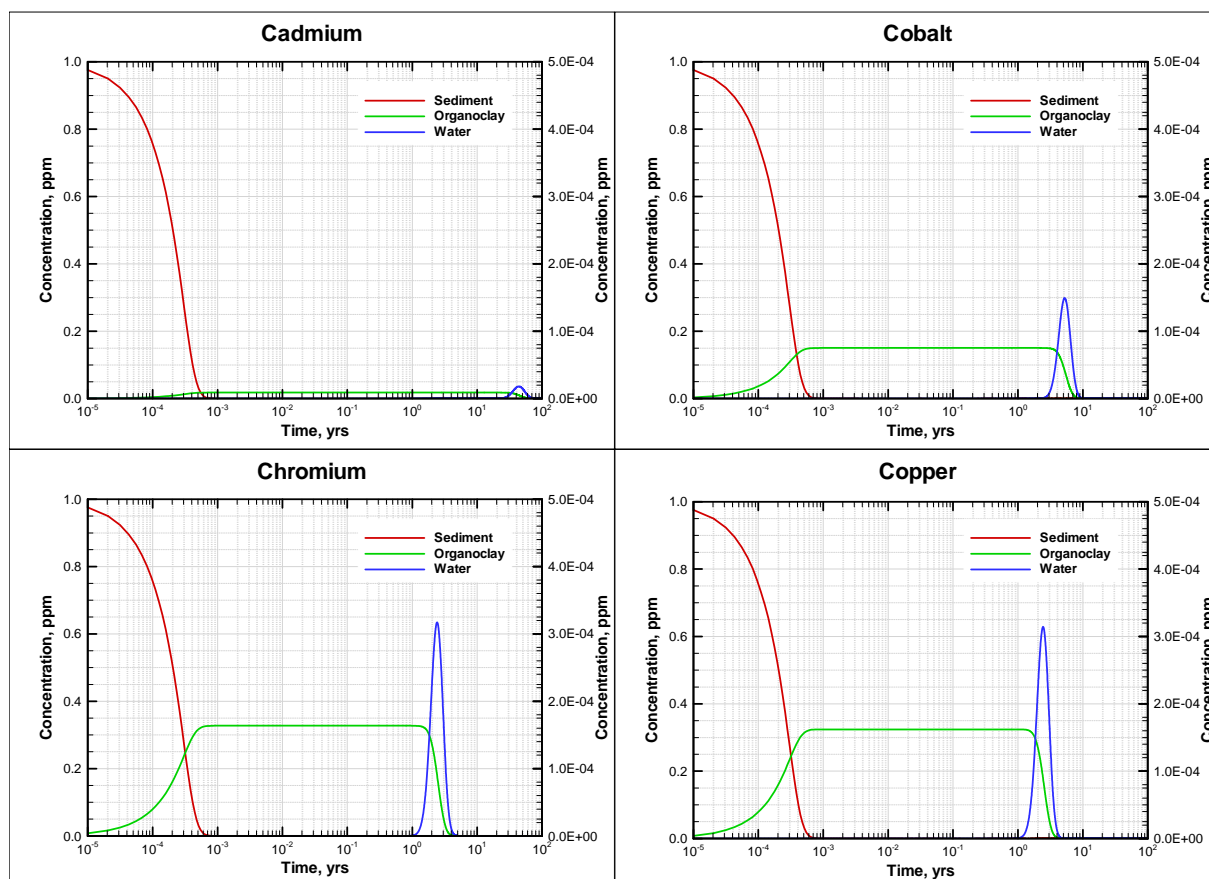


Figure 89. Breakthrough Curves for Cd, Co, Cr, and Cu for Organoclay Cap Case. The sediment concentrations curves are plotted against the left y-axis and all others against the right y-axis.

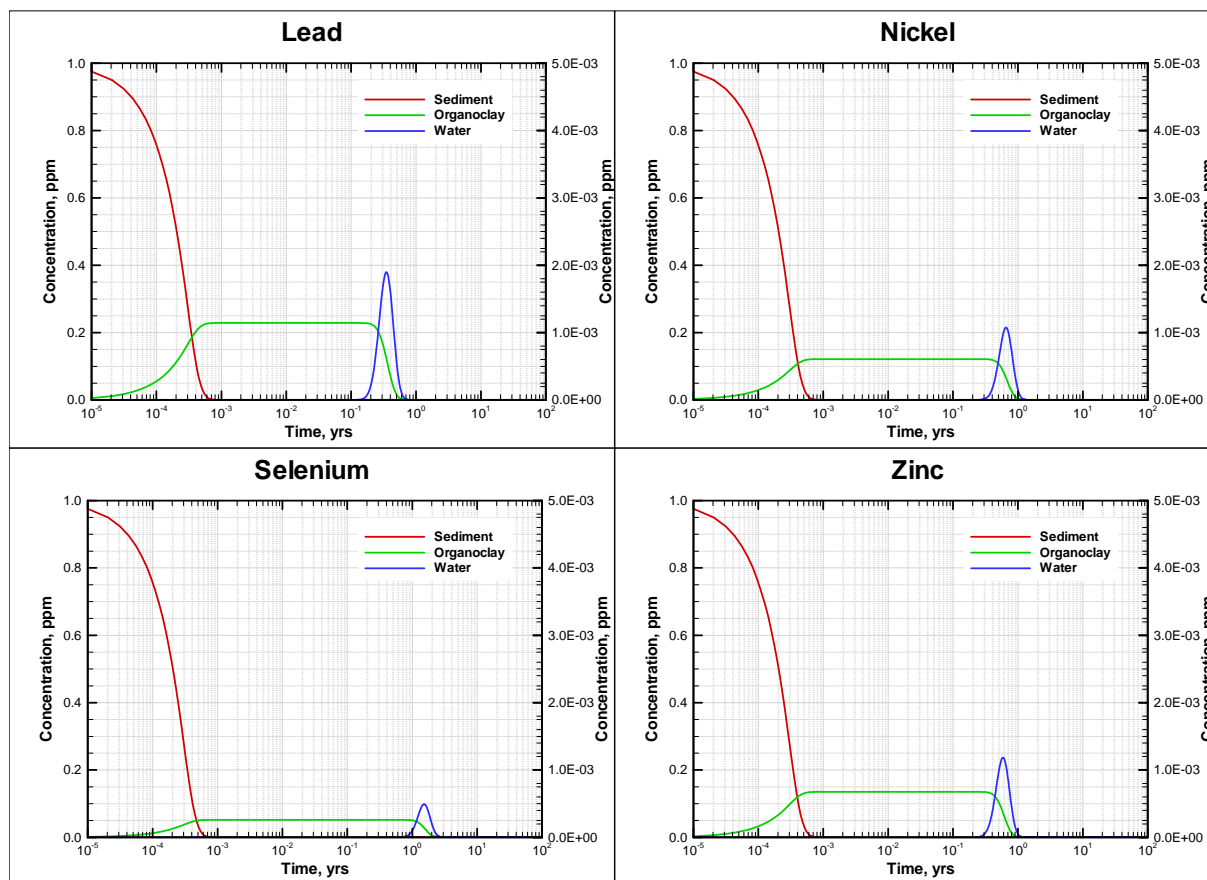


Figure 90. Breakthrough Curves for Pb, Ni, Se, and Zn for Organoclay Cap Case. The sediment concentration curves are plotted against the left y-axis and all others against the right y-axis.

The results of the diffusive and advective transport are a function of the thickness of the column and the flow rate of the spike solution. These results may be scaled in a linear fashion for different flow rates and contaminant concentrations to predict the cap thickness necessary to delay metals breakthrough for a specified period of time. Figure 91 presents an example of how the results from the apatite simulation may be scaled for different flow rates to estimate the cap thickness necessary to delay contaminant breakthrough for a specified time period.

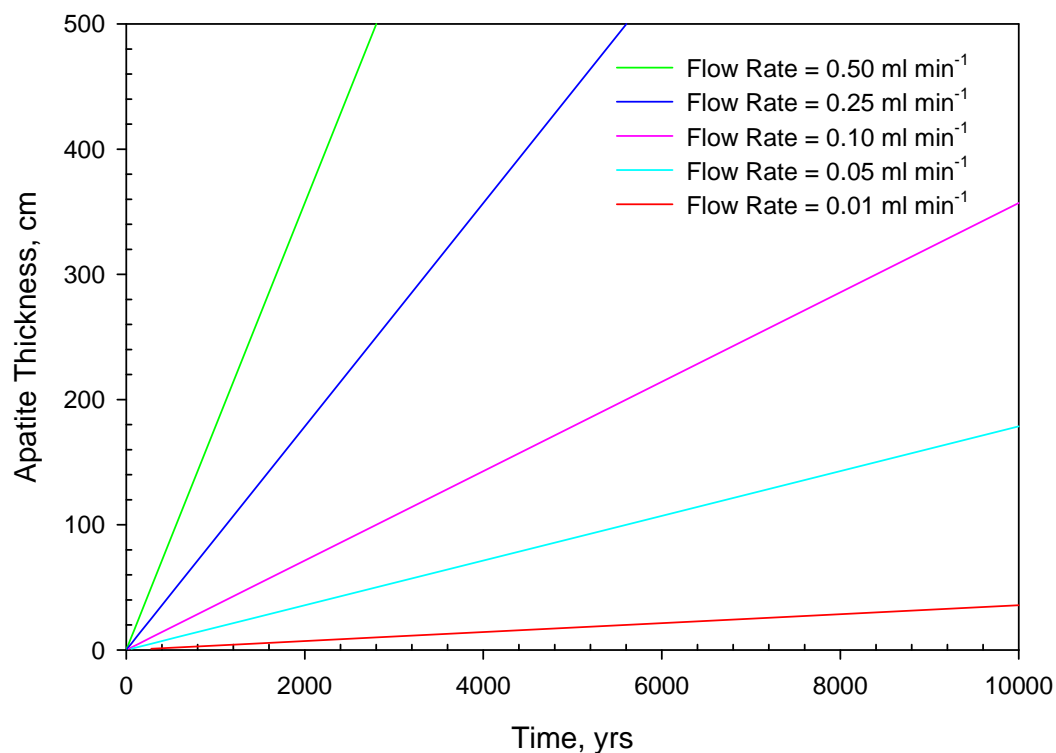


Figure 91. Apatite Thickness as a Function of Breakthrough Time for Cr Concentration of $2 \mu\text{g L}^{-1}$.

Results from this study show that reactive amendments, such as apatite, can significantly delay the breakthrough of certain contaminants compared to sand. This illustrates the promise of amendments such as apatite for use in active cap systems. In addition to the breakthrough experiments conducted as part of this study, a simple numerical model was used to estimate the required cap thickness to delay contaminant breakthrough for a specified time period for various flow rates. The numerical model serves as a cost effective tool for use in the design of active cap systems.

TASK 5. FIELD DEPLOYMENT

SUBTASK 5.1. SELECTION AND CHARACTERIZATION OF A STUDY SITE FOR A PLOT STUDY

Site Selection

In Task 5 active caps developed in the laboratory were evaluated in the field to demonstrate their effects on contaminant mobility and toxicity, their durability and resistance to erosion, and their acceptability to benthic organisms. Several potential sites were investigated in an effort to find a location that was accessible and that exhibited the necessary physical and chemical characteristics for a successful field demonstration. Potential sites were limited to streams rather than standing waters because of the need to assess the resistance of the caps to the erosive effects of strong currents. Sites with comparatively shallow water were sought to permit cap construction without specialized equipment and to facilitate sampling and observation during the course of the study. Two potential study sites on the Savannah River Site were selected for field investigation following preliminary surveys of maps and sediment contaminant records; the sites were located on Tims Branch and Steel Creek (Figure 5). Of these, the site on Steel Creek was chosen for the field deployment because of its greater width and depth, which provide more realistic conditions and permit larger experimental plots.

Steel Creek is a third order stream averaging about 6-8 m wide and 30-40 cm deep during typical low flow conditions. Base flow discharge and mean current measured were 0.45 f/s and 0.95 f/s, respectively. However, flood flows occurring during periods of heavy rainfall are many times higher. The bottom substrate in Steel Creek is composed primarily of sand in high energy areas and silt in depositional environments. Limited amounts of gravel also occur. The banks support shrubs and trees and substantial stands of emergent aquatic plants occur along the stream banks during the growing season. The stream supports a diverse aquatic macroinvertebrate fauna that has the potential to colonize the experimental caps.

Data collected indicate that several metal contaminants occur in the studied area as a result of past discharges from industrial facilities located in the Steel Creek headwaters. Contaminant concentrations for several metals substantially exceed those in Tinker Creek, a nearby uncontaminated stream (Table 39).

Field work was initiated by obtaining all required permits including:

1. Savannah River Site Environmental Evaluation Checklist (EEC) NEPA review/Environmental Permit,
2. Permit for Site Use – SRS,
3. Nationwide Permit (NWP) Number 18, and
4. Hazard Assessment Package (HAP).

Table 39. Metal Concentrations in Sediments from the Proposed Steel Creek Study Area and in Tinker Creek, a Nearby Uncontaminated Stream.

Metal	Steel Creek		Tinker Creek	
	Concentration (mg/kg)	Number Samples	Concentration (mg/kg)	Number samples
Ag	4.5	77	2.0	21
Al	3,780	64	2,435	24
As	9.7	92	1.2	22
Ba	23.8	95	16.7	23
Be	0.16	62	0.29	20
Cd	1.32	84	0.70	21
Cr	16.3	99	4.0	32
Cu	7.2	93	3.5	24
Hg	0.11	93	0.04	22
Mn	950	78	4.7	15
Ni	4.1	95	2.5	23
Pb	58.9	95	4.4	24
Sb	5.2	81	5.0	21
Se	7.1	84	0.94	20
Sn	135	31	5.06	10
V	12.0	52	4.8	24
Zn	38.5	93	5.4	24

Characteristics and Chemistry of Surface Water and Pore Water before Cap Placement

The surface and pore water properties of the samples collected before cap placement are presented in Table 40. The average surface water pH was 7.0, and it was similar in all plots (Table 40). The average dissolved oxygen for all eight plots was 7.0 mg/L, and the average electrical conductivity was 62.2 $\mu\text{S}/\text{cm}$ (Table 40). The average dissolved oxygen value for the pore water samples from the eight plots was 3.3 mg/L; much lower than for surface water (Table 40). Also, ORP values were lower for the pore water samples than for the surface water; average values were 147.5 and 287.9mV, respectively, for pore and surface water (Table 40).

Dissolved organic carbon (DOC) plays a major role in biogeochemistry processes in the aquatic environment. It interacts with metal mobility and bioavailability, acid-base chemistry, and solubility-dissolution of metal ions. Mobility, bioavailability, and toxicity of metals is largely controlled by the presence of DOC.

Average dissolved organic carbon (DOC) concentrations were 7.8 ppm and 10.1 ppm for surface and pore water, respectively (Figure 92 and 93). Slightly higher DOC concentrations were observed in the pore water samples (Figure 93). Metal concentrations were lower in pore water

than in surface water, possibly because the higher DOC concentrations in pore water helped bind metals (Table 41, Figure 94 and 95). The average metal concentrations in surface water for As, Pb, Sb, Se, and Zn exceeded 50 ppb (Figure 94). In the pore water only the Se and Zn concentrations were higher than 50 ppb (Figure 95).

Sediment Properties before Cap Placement

The particle size distribution was approximately 90% sand and 10% silt and clay. Total carbon content in the top 5 cm was 0.2 %, slightly increased with sediment depth up to 10 cm (Figure 96), and again decreased in deeper sediment (10 to 20 cm) (Figure 96). In general, the total carbon content in Steel Creek sediment was comparable to that in the sediment from other creeks on the Savannah River Site. The sediment pH was lowest in the top layer (6.4) and increased with sediment depth.

Background metal concentrations in the creek sediments were 9.7, 1.3, 16.3, 7.2, 4.1, 59, 5.2, 7.1, 12, and 40.0 ppm; respectively, for As, Cd, Cr, Cu, Ni, Pb, Se, V, and Zn. Most of these metal concentrations substantially exceed those in Tinker Creek, a nearby uncontaminated stream. Metals are transported in creeks or river by binding to suspended sediment. Eventually, metals settle onto bed sediment, filter down into sediment pores, and equilibrium is established at the sediment-interstitial water interface. In anaerobic sediment, a naturally occurring constituent called acid-volatile sulfide (AVS) is present (Hansen et al., 1996). Initially, the majority of AVS contained in the anaerobic sediment is bound to Fe as solid iron monosulfide (FeS). If divalent metals, such as Cd, Cu, Cr, Pb, Ni, or Zn are present, the iron in FeS becomes displaced and one of these metals rapidly bind to AVS with strong affinity (Di Toro et al., 1992; Hansen et al., 1996). The metals are then bound in sediment and removed from the interstitial water. The concentration of bioavailable metals, or metals that are unbound and available to organisms, can be estimated from the value of metal to AVS concentrations. In this study AVS and simultaneously extracted metals (SEM) was extracted from eight sediment samples with cold one-molar hydrochloric acid following the method of Allen et al. (1991). A SEM to AVS value greater than one means excess metals are present in the sediment relative to AVS. These unbound metals have the potential to be significantly more bioavailable than those bound to sulfides (Berry et al., 1996). The average AVS values for the tested sediment samples from each plot are presented in Figure 97. The highest values of AVS were observed in plot 2, 6, and 4. With more AVS, metals have less potential to be bioavailable to benthic organisms.

Table 40. Properties of Surface and Pore Water Collected from each Plot in Steel Creek before Cap Deployment.

Parameters	Unit	Plots								AVG	STDEV
		1	2	3	4	5	6	7	8		
Surface water											
Electrical Conductivity (EC)	μS/cm	62	62.3	62	63	62	63	61	62	62.2	0.6
Dissolved oxygen (DO)	mg/L	6.99	6.98	6.89	7.15	7.03	7	6.98	7.07	7.0	0.1
pH		7.01	6.89	6.97	7.17	7.01	6.97	7.05	6.9	7.0	0.1
Oxidation/reduction potential (ORP)		281	283	275	316	285	275	303	285	287.9	14.3
Pore Water											
Electrical Conductivity (EC)	μS/cm	81	96	83	92	73	68	67	65	78.1	11.8
Dissolved oxygen (DO)	mg/L	3.17	4.58	4.65	1.5	1.49	5.4	2.09	3.65	3.3	1.5
pH		6.78	6.77	6.89	6.77	6.69	6.75	6.7	6.7	6.8	0.1
Oxidation/reduction potential (ORP)		166.8	176.9	168.6	89.6	36.5	215.2	157.9	168.2	147.5	56.7

Table 41. Average Element Concentrations in Surface Water (n=9) from the Steel Creek Experimental Area.

Element	1-SW ppb	2-SW ppb	3-SW ppb	4-SW ppb	5-SW ppb	6-SW ppb	7-SW ppb	8-SW ppb	9-SW ppb	AVG ppb	STDEV ppb
Ag	7.7	6.1	7.7	7.7	16.8	13.8	17.6	18.4	16.8	12.5	5.1
Al	86.3	48	64.7	67.6	118.6	111.8	121.6	135.3	121.6	97.3	31.2
As	27.2	10.3	32.2	34.2	70	95.8	133.6	115.7	114.7	70.4	46.0
B	13.2	14.3	13.2	13.2	24.4	21.4	22.4	25.5	22.4	18.9	5.3
Ba	26.2	25.1	24.6	25.6	26.9	26.7	26.4	26.2	26.2	26.0	0.8
Be	1.8	1.1	1.1	0.8	1.3	0.9	1.1	0.9	0.7	1.1	0.3
Ca	8,585	8,474	8,563	8,576	9,083	9,039	9,404	9,378	9,355	8,939	391.7
Cd	0	0	0	4.5	17.9	9	0	4.5	6.7	4.7	6.0
Co	5.7	5.7	9.2	5.7	13.8	13.8	13.8	16.7	16.1	11.2	4.6
Cr	16.1	8.8	12.1	15.4	32.6	27.4	32.6	38.6	36	24.4	11.3
Cu	8	8	10.9	13.7	25.1	22.2	25.1	25.1	20.8	17.7	7.5
Fe	395	367.6	374.4	400.5	408.7	427.9	401.9	417	403.2	399.6	19.0
K	509.4	368.9	439.1	439.1	614.8	579.7	597.2	579.7	527	517.2	85.2
Mg	672.2	649.9	662.3	659.8	756.5	721.8	766.4	766.4	771.3	714.1	52.6
Mn	36.8	24.9	24.9	30.6	27.2	29.5	28.3	28.3	29.5	28.9	3.6
Mo	18.5	11	13.5	12.3	18.5	19.7	21.6	19.1	18.5	17.0	3.7
Na	3,931	3,528	4,075	3,857	4,003	4,094	4,209	3,679	3,769	3,905	218.3
Ni	11.5	5.1	11.5	10.7	24.2	23.4	29.8	29.8	28.2	19.4	9.6
P	0	254.9	61.5	8.8	175.8	131.9	101.1	167	228.6	125.5	90.6
Pb	21.5	21.5	48.2	21.5	92.8	86.1	119.5	119.5	92.8	69.3	41.4
Sb	59.5	59.5	59.5	59.5	119	59.5	59.5	119	59.5	72.7	26.2
Se	214.3	189.3	198.7	148.6	273.8	247.2	251.9	245.6	248.7	224.2	39.5
Si	3,117	2,957	3,068	3,111	3,370	3,387	3,547	3,499	3,522	3,286	224.0
Sr	25.5	24.7	24.9	24.7	25.6	25.6	26.2	25.9	25.8	25.4	0.5
Tl	3,259	1,361	1,930	2,215	6,772	8,766	7,500	12,250	9,146	5,911	3,861
V	62.2	11.1	10.4	7.3	13.6	12.3	14.5	14.8	13.6	17.8	16.8
Zn	47.7	45.3	54.1	38.9	49.4	40.1	56.4	48.2	47.1	47.5	5.7

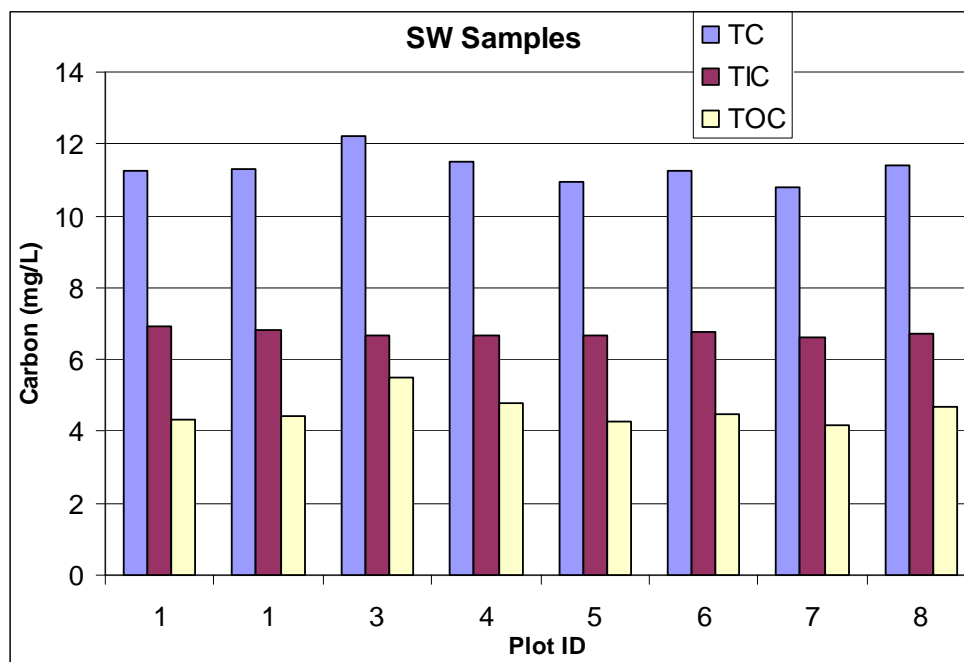


Figure 92. Total Carbon (TC), Total Inorganic Carbon (TIC), and Total Organic Carbon (TOC) in Surface Water Collected at each Plot before Cap Deployment.

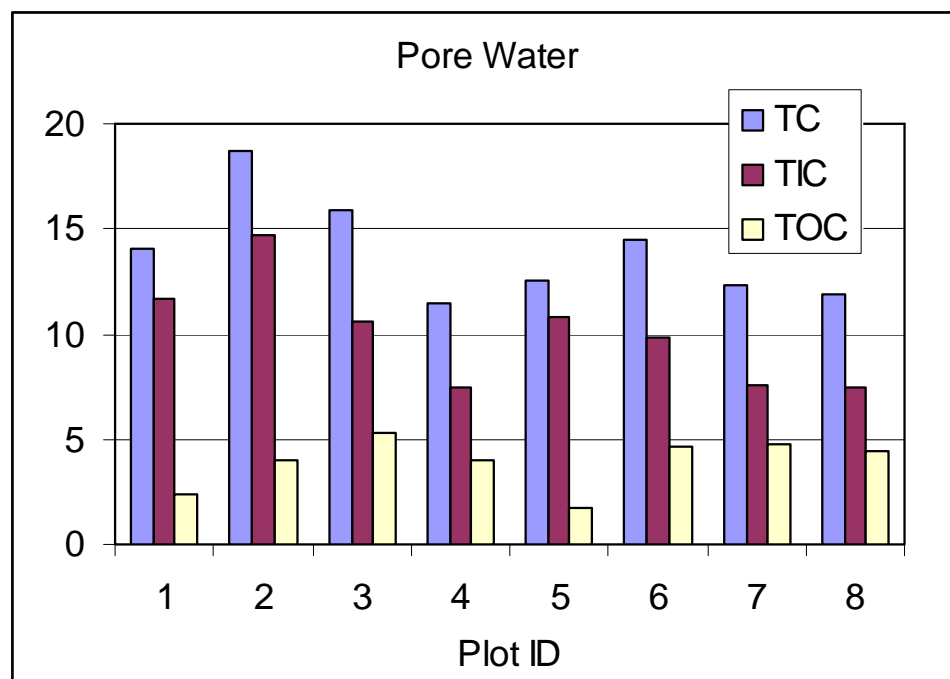


Figure 93. Total Carbon (TC), Total Inorganic Carbon (TIC), and Total Organic Carbon (TOC) in Pore Water Collected at each Plot before Cap Deployment.

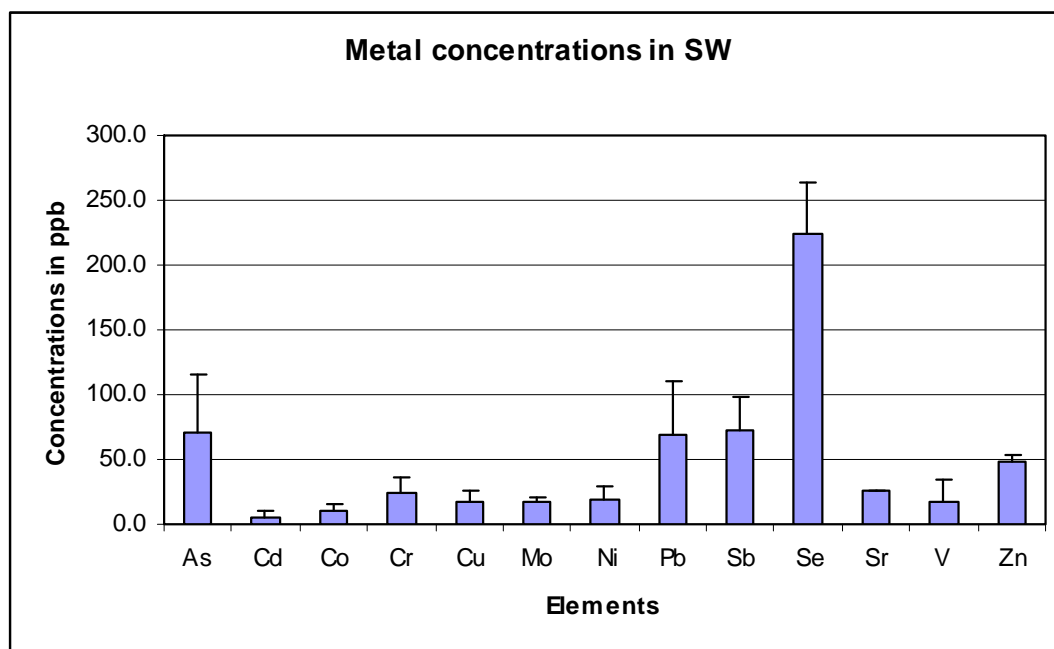


Figure 94. Average Metal Concentrations in Surface Water (n=9) from Steel Creek Experimental Area.

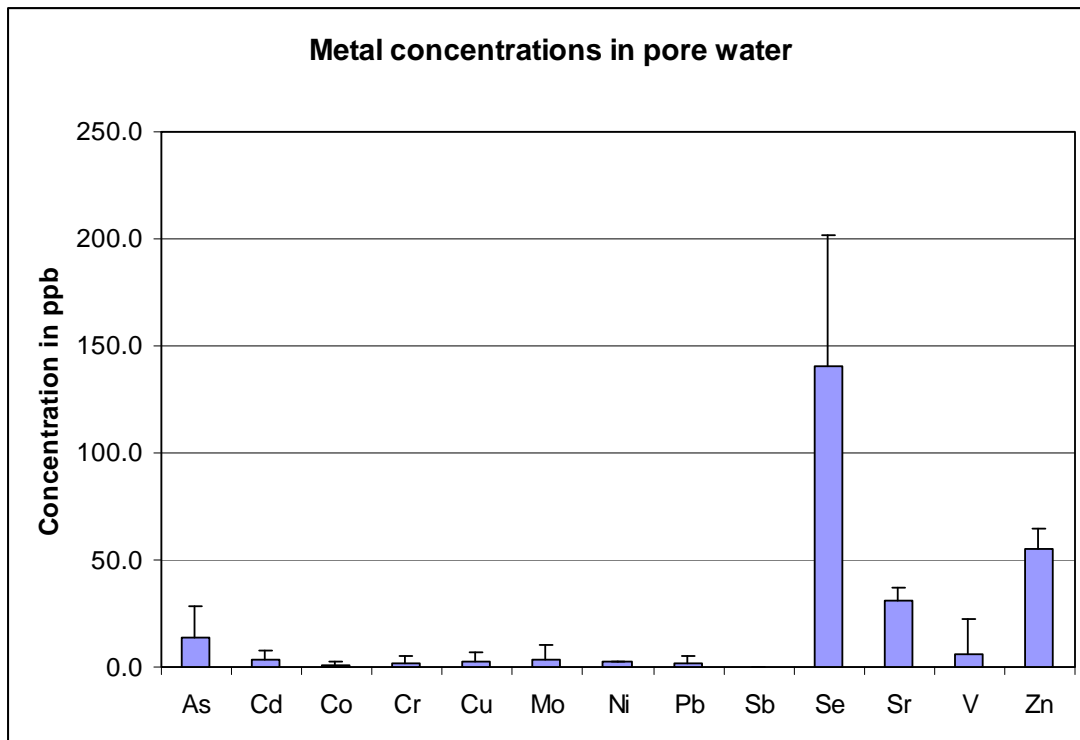


Figure 95. Average Metal Concentrations in Pore Water (n=20) from Steel Creek Experimental Area.

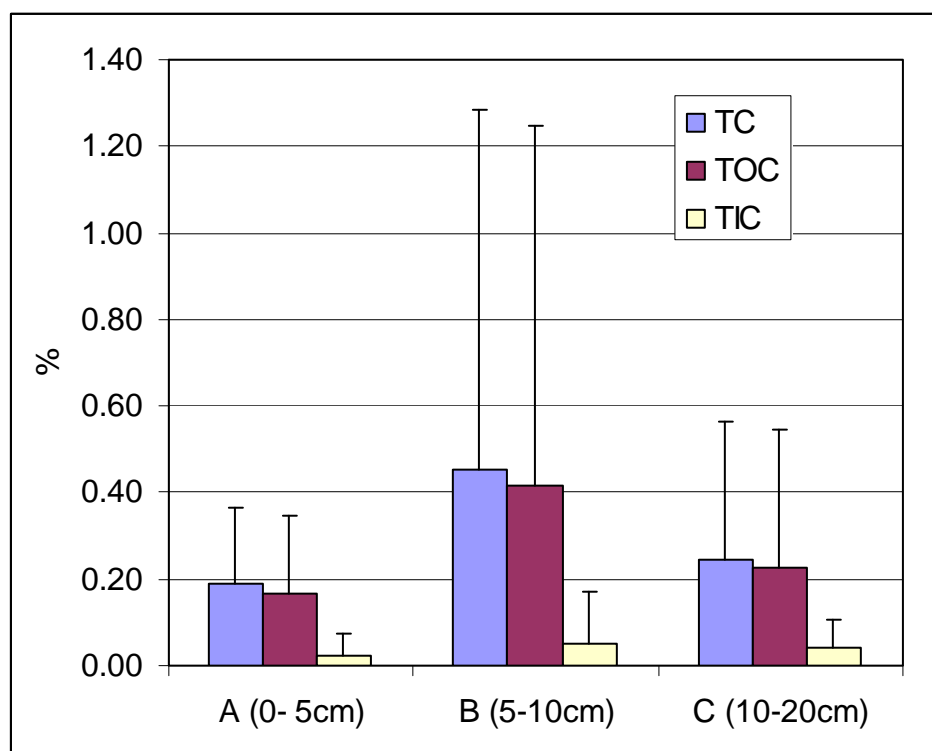


Figure 96. Total Carbon Content (TC), Total Inorganic Carbon (TIC), and Total Organic Carbon (TOC) in Sediment Core Samples (n = 8) Collected at each Plot before Cap Deployment; the core samples were divided in three parts: A 0-5 cm, B 5-10 cm, and C 10-20 cm.

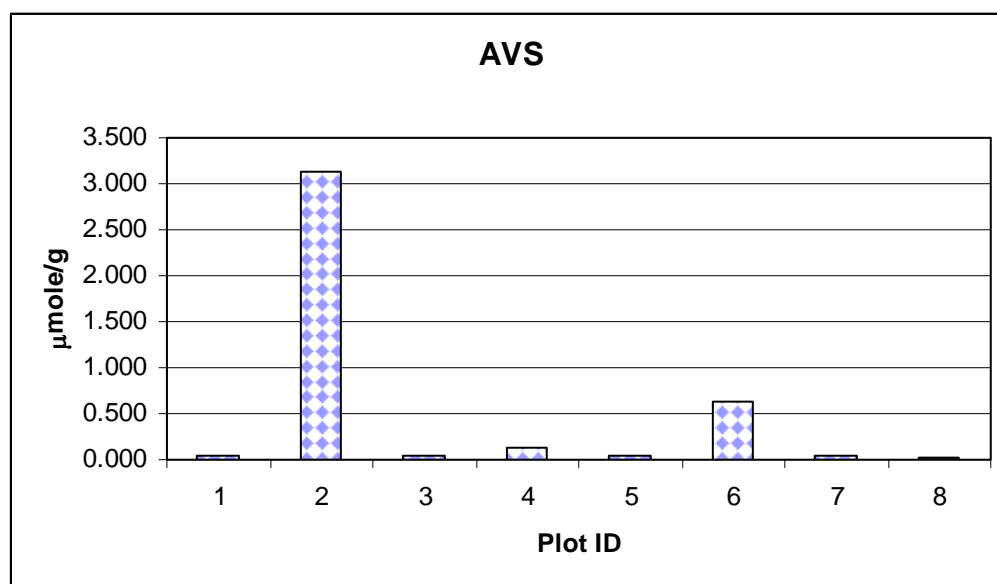


Figure 97. Acid-Volatile Sulfide Concentrations ($\mu\text{mole sulfide} \times \text{gram dry sediment}^{-1}$) in Samples from each Plot.

SUBTASK 5.2. FIELD DEPLOYMENT - CAP CONSTRUCTION

The field deployment in Steel Creek, SRS, included eight plots with four treatments: two control treatments consisting of uncapped sediments (i.e., no amendments added); two caps composed of a single six inch layer of 50% apatite and 50% sand (Figures 6 and 8; Picture 17); two caps composed of two layers including a two inch layer of biopolymer/sand slurry over a four inch layer of 50% apatite and 50% sand (Figures 6 and 8; Picture 18); and two caps composed of three layers including a two inch top layer of biopolymer/sand slurry, a two inch middle layer of 50% apatite and 50% sand, and a two inch bottom layer of 25% organoclay and 75% sand (Figures 6 and 8; Picture 19). The experimental plots were constructed within a 500 foot segment of Steel Creek near the SC Route 125 bridge. The control plots were located in the front and at the end of the experimental area (Figure 6). The two replicates for each of the three cap treatments (each 6 feet wide, 6 feet long, and 6 inches thick) were split between two locations: an eroded area with the an average flow rate of 0.9 f/s (plots 1, 2, 6, and 7) and a more depositional area with a lower average flow rate of 0.4 f/s (plots 3, 4, 8, and 5) Figure 6. The leading edge of each cap was preceded by a sloped transition zone rising from the sediment to the top of the cap to prevent the undercutting likely to occur with a vertical leading edge (Figure 7, Pictures 17, 18, and 19). The transition zone was composed of sand (in apatite/sand plots) or biopolymer/sand slurry in plots with a top layer composed of biopolymer/sand slurry (xanthan crossed lined with guar gum). The cap boundaries (four corners) were permanently marked with 4 foot long PVC pipes to ensure accurate sample collection during the course of the study and to provide a basis for assessing possible changes in cap dimensions as a result of erosion.

An aluminum frame was used during the construction of each plot (Figure 7; Picture 8) to deflect downstream flow, stabilize the working area, reduce turbulence, and avoid loss of amendment materials. The frame was carefully removed wall-by-wall when construction was completed and all cap materials had settled (Picture 9). Cap layers that contained low density materials, such as biopolymers, were applied as slurry to prevent material separation and differential settling. After cap placement sediment cores (5 per plot) were collected to confirm and characterize cap-layer thickness. The average cap thickness was about 6 inches (Picture 20). Thickness of individual layers, in the caps composed of three layers, was about 2 inches.

The test plots were evaluated for 12 months for contaminant immobilization, environmental impact, and erosion resistance.



Picture 17. Plot 3 -- One-layer Cap Composed of Apatite (50%) and Sand (50%) with a Sand Transition Zone. Two sets of pore water sampler tubes were located near the top of the cap (white tubes for samplers beneath the cap and black tubes for samplers in the middle of the cap).



Picture 18. Plot 4 Cap Composed of Two Layers including a Two Inch Layer of Biopolymer/Sand Slurry over a Four Inch Layer of 50% Apatite and 50% Sand.



Picture 19. Plot 8 – Three-layer Cap Composed of Biopolymer/Sand Slurry, a Two Inch Middle Layer of 50% Apatite and 50% Sand, and a Two Inch Bottom Layer of 25% Organoclay and 75% Sand.



Picture 20. The Average Cap Thickness was about 6 Inches.

SUBTASK 5.3. POST-CAP MONITORING

Characteristics and Chemistry of Surface Water and Pore Water after Cap Placement

The surface water properties of samples collected before, one, two, five, nine, and twelve months after cap placement are presented in Table 42. The average surface water pH before cap placement was 7.0. The pH values for surface water during the twelve month monitoring period following cap placement ranged from 7 to 7.8. The pH increased slightly (to 7.3) one month after cap placement, returned to pH 7 after two months, and again increased to 7.8 after nine months (Table 42). The highest EC of the surface water was observed one month after cap placement (80.9 $\mu\text{S}/\text{cm}$). The EC values of the surface water twelve months after cap placement were similar to the EC values before cap placement (Table 42).

The addition of cap materials influenced pore water chemistry, especially pH, EC, and the ORP (Figures 98, 99, and 100). The pH of pore water from the apatite/sand (A/S) and biopolymer/apatite/organoclay/sand (B/A/O/S) caps twelve months after cap placement continued to be higher than in pore water from outside the caps (Figure 98 and Table 43). The pH of pore water samples collected from all test caps and beneath the caps remained elevated during the twelve month sample period compared with the control plots or the measurements before cap placements (Figure 98).

As was expected, the highest EC values in pore water were observed beneath and within the three layer cap with organoclay (Figure 99 and Table 44). The EC in pore water beneath this cap increased from 68 $\mu\text{S}/\text{cm}$ before cap placement to 703 $\mu\text{S}/\text{cm}$ one month after cap placement (Figure 99). However, twelve months after cap placement, the EC of pore water collected from under these caps was only slightly elevated compared with pore water collected from these plots before cap placement or outside the plots (Figure 99).

The caps contributed to changes in the ORP of pore water in sediment under the caps as indicated by samples collected one, two, five, nine, and twelve months after cap placement (Figure 100 and Table 45). Generally, the ORP values beneath the caps were substantially lower than the ORP values before cap placement and from the control plots (Figures 100 and Table 45).

Average DOC concentrations in surface water from the test area changed little during the twelve month evaluation period (Figure 101). The slight changes in the DOC concentration in the surface water samples during this period were likely due to temperature changes or differences in floodplain run-off of organic detritus. However, DOC concentrations in pore water changed as a likely result of the addition of active caps materials. The organoclay in the three layer cap (biopolymer/apatite/organoclay/ sand) had a particularly large influence on the TC content. One month after placement of this cap, TC in the pore water collected beneath the plot increased to 42 mg/L compared with 9.9 mg/L in the control plots (Figure 102). It later declined to about 25 mg/L and continued to decrease for another 10 months to TC values comparable to the measurement from these plots before cap placement or outside the plots (Figure 102).

Concentrations of some metals, e.g., Cr, Ni, Pb, Se, and V in surface water were lower during the twelve months after cap placement than before cap placement (Figure 103). The concentrations of elements such as Ca, P, P, and Mg did not change after cap placement. Only the concentration of Na in surface water increased after cap placement and remained elevated for a period of twelve months, likely due to the addition of organoclay (Figure 103).

Metal concentrations in pore water samples collected from each type of cap and beneath each cap two, five, and 12 months after cap placement are presented in Figures 104 and 105. For the A/S cap the clearest reduction of metal concentrations was observed for As, Cd, Cr, Mo, Pb, and Zn. Reduction of metal concentrations in pore water were less clear for the biopolymer/apatite sand and biopolymer/apatite/organoclay/sand caps, especially twelve months after cap placement (Figure 105 and Table 46). Reduction of metal concentrations in pore water was related to the sequestering agents and to changes in pore water chemistry resulting from the caps. Parameters modified by cap placement included oxidation-reduction (redox) potential and pH (Figures 98 and 100). These parameters may have major effects on metal speciation in pore water.

Generally, metal concentrations in pore water from within and beneath the caps decreased during the twelve months after cap placement; however, concentrations of elements such as Ca, K, Na, and P increased, especially P concentrations within the A/S cap and Na within B/A/O/S cap. Application of apatite in active caps raises questions about the release of P, since it is well known that P can cause eutrophication if present in sufficient concentrations. Cap placement did not significantly increase the P concentration in surface water (Figure 103), but P concentrations increased in pore water collected from within the caps especially in the first five months after cap placement (Figures 106 and 107). However, five months after cap placement, the P concentrations in pore water collected outside the caps were similar to P concentrations in control plots (Figure 107 and Table 47).

Table 42. Properties of Surface Water Collected Before and One, Two, Five, Nine, and Twelve Months after Cap Placement; EC - electrical conductivity, DO – dissolved oxygen, pH, and ORP - oxidation/reduction potential.

Parameters	Unit	Plots								AVG	STDEV
		1	2	3	4	5	6	7	8	n = 8	n = 8
Before Cap Placement											
EC	μS/cm	62	62.3	62	63	62	63	61	62	62.2	0.6
DO	mg/L	7.0	7.0	6.9	7.2	7.0	7.0	7.0	7.1	7.0	0.1
pH		7.0	6.9	7.0	7.2	7.0	7.0	7.1	6.9	7.0	0.1
ORP		281	283	275	316	285	275	303	285	287.9	14.3
After One Month											
EC	μS/cm	81	81	81	81	81	80	81	81	80.9	0.4
DO	mg/L	6.8	6.9	7.2	6.9	7.2	6.8	6.9	7.0	7.0	0.2
pH		7.4	7.4	7.3	7.0	7.2	7.4	7.4	7.4	7.3	0.1
ORP		89.4	96.5	63.4	82.3	45.7	104	95	76	81.5	19.3
After Two Months											
EC	μS/cm	53	52	52	52	53	52	53	52	52.4	0.5
DO	mg/L	12.2	11.8	10.0	10.4	9.5	10.9	11.4	10.4	10.8	0.9
pH		7.3	6.8	7.0	7.0	7.0	6.8	6.8	7.1	7.0	0.2
ORP		63.5	104.2	70.3	82.4	79	109	94.2	75	84.7	16.3
After Five Months											
EC	μS/cm	65	65	66	65	66	65	65	66	65.4	0.5
DO	mg/L	6.7	6.9	7.3	7	6.8	7	6.8	7.6	7.0	0.3
pH		7.2	7.4	7.2	7.4	7.4	7.5	7.3	7.3	7.3	0.1
ORP		115	103.7	102	104	69	122	112	94.7	102.8	16.1
After Nine Months											
EC	μS/cm	64	64	65	64	64	64	64	64	64.1	0.4
DO	mg/L	3.7	3.3	3.6	3.7	3.6	3.6	3.7	3.5	3.6	0.1
pH		7.8	7.9	7.7	7.8	7.7	8.1	7.8	7.7	7.8	0.1
ORP		75	63	64	76	69	68	76	76	70.9	5.6
After Twelve Months											
EC	μS/cm	69	65	65	69	64	69	64	70	66.9	2.6
DO	mg/L	6.7	7.2	10.9	10.0	8.7	9.9	3.7	7.1	8.0	2.3
pH		7.8	7.9	6.9	6.8	7.7	7.1	6.9	7.3	7.3	0.4
ORP		75	63	110	60	69	81	96	128	85.3	24.1

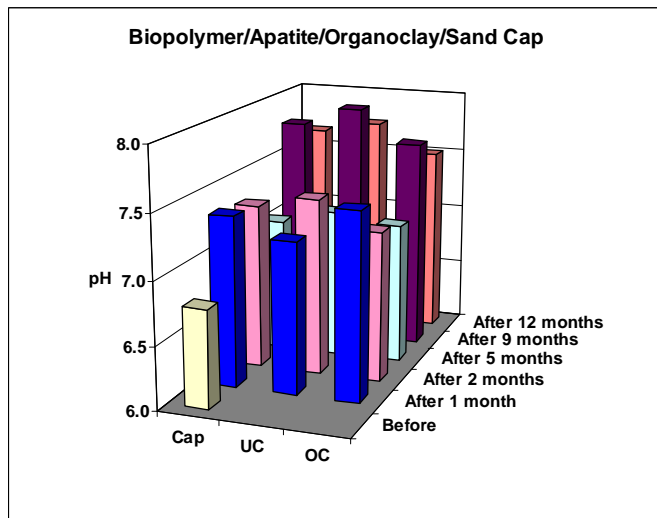
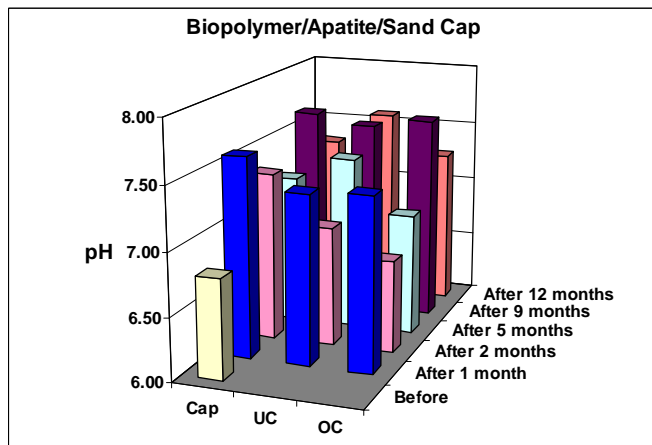
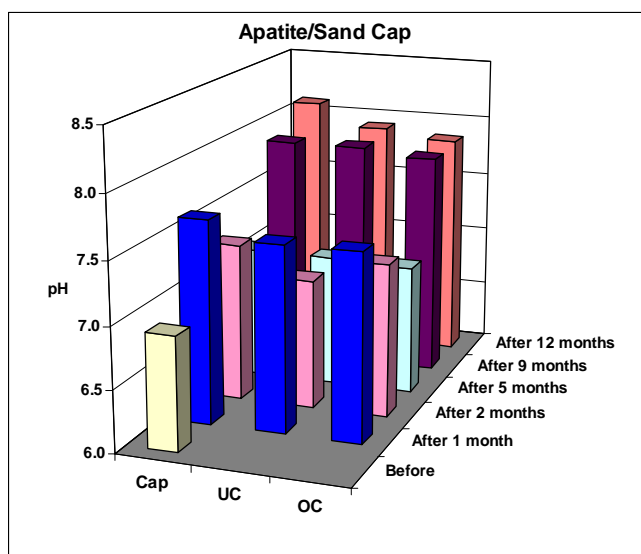


Figure 98. Effect of Cap Amendments on pH of Pore Water – 12 Month Evaluation; Cap – pore water collected within the cap, UC – pore water collected beneath the cap, OC – pore water collected outside the cap.

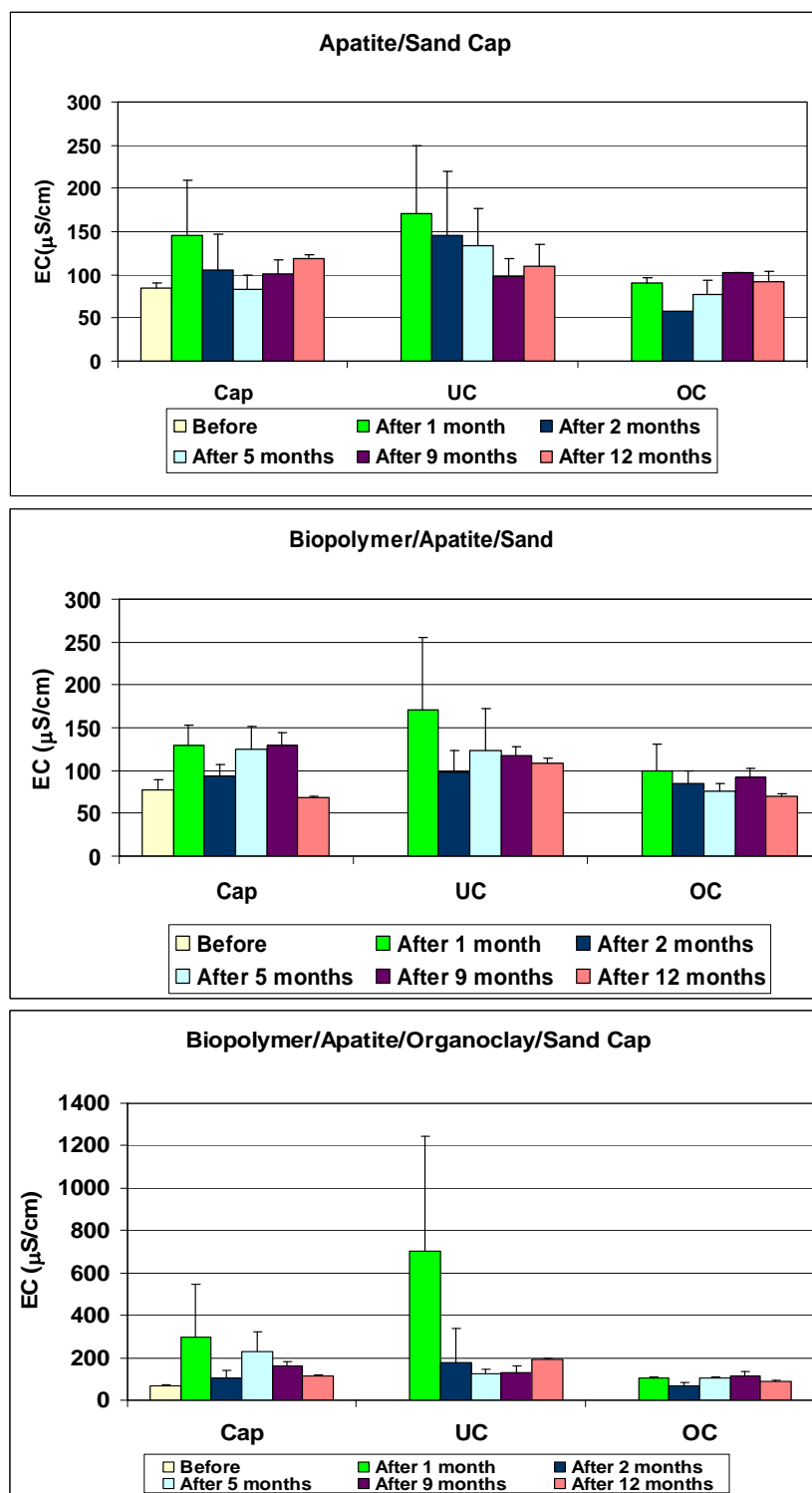


Figure 99. Effect of Cap Amendments on Electrical Conductivity (EC) of Pore Water – 12 Month Evaluation; Cap – pore water collected within the cap, UC – pore water collected beneath the cap, OC – pore water collected outside the plot.

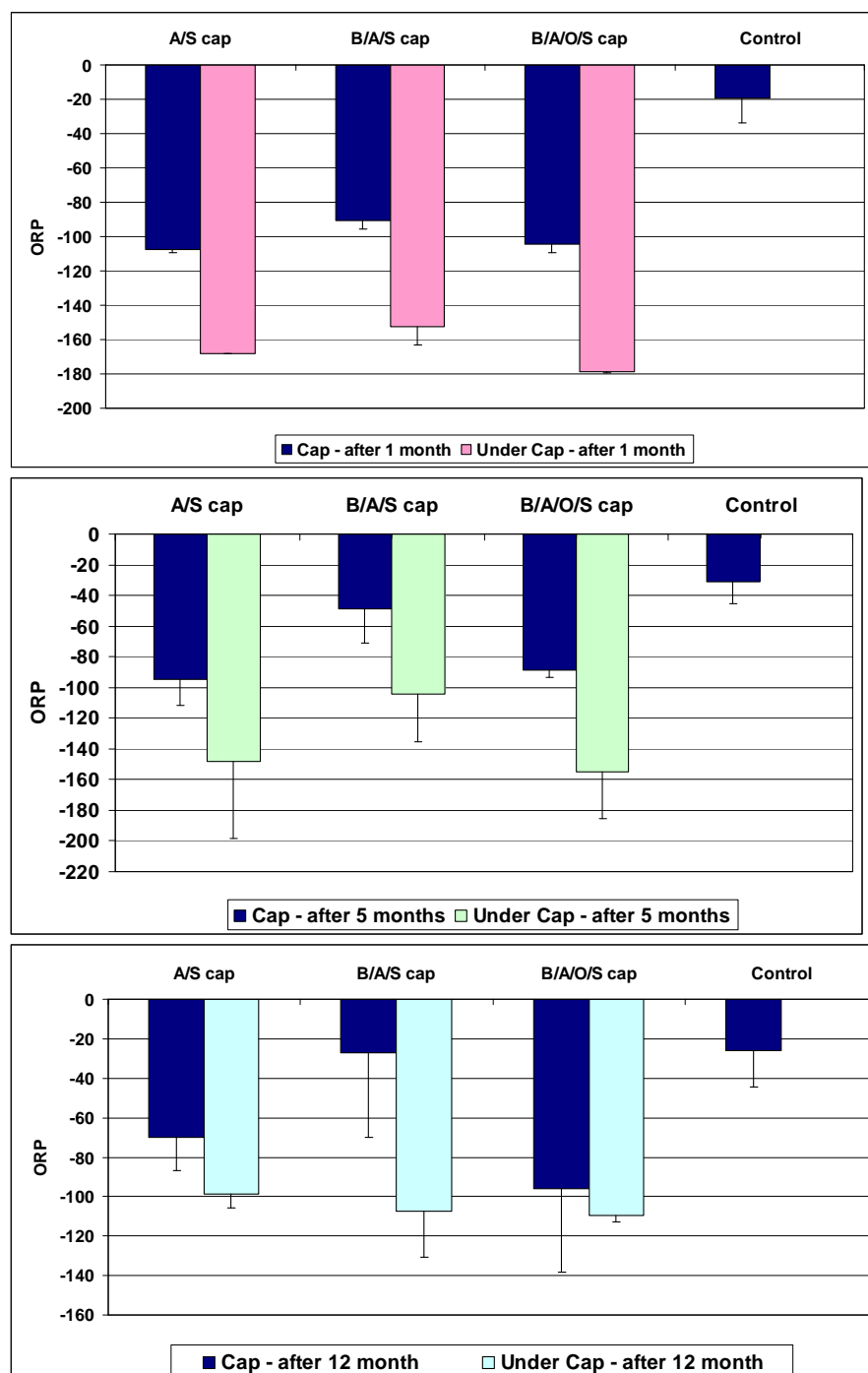


Figure 100. Effect of Cap Amendments on ORP Values of Pore Water –12-Month Evaluation; A/S – apatite/sand, B/A/S – biopolymer/apatite/sand; B/A/O/S - biopolymer/apatite/organoclay/sand.

Table 43. Effect of Cap Amendments on the pH Values of Pore Water -12 Month

Evaluation; A/S – apatite/sand, B/A/S – biopolymer/apatite/sand; B/A/O/S – biopolymer/apatite/organoclay/sand; C- cap, B – beneath cap, O – outside cap, PW – pore water, A1M – after one month, A2M – after 2 months, A5M – after 5 months, A9M – after 9 months, and A12M – after 12 months.

Treatments	A/S Avg	B/A/S Avg	B/A/O/S Avg	Control Avg	A/S Stdev	B/A/S Stdev	B/A/O/S Stdev	Control Stdev
Before	6.92	6.80	6.78	7.01	0.33	0.07	0.09	0.12
CPW-A1M	7.65	7.60	7.36		0.09	0.24	0.17	
BCPW-A1M	7.51	7.36	7.21	7.13	0.24	0.17	0.06	0.05
OCPW-A1M	7.51	7.39	7.48		0.25	0.03	0.24	
CPW-A2M	7.29	7.35	7.32		0.44	0.00	0.28	
BCPW-A2M	7.05	6.96	7.41	6.86	0.23	0.37	0.39	0.08
OCPW-A2M	7.25	6.74	7.20		0.36	0.17	0.22	
CPW-A5M	7.08	7.20	7.08		0.08	0.10	0.11	
BCPW-A5M	7.07	7.40	7.19	6.92	0.02	0.09	0.13	0.04
OCPW-A5M	7.05	6.97	7.13		0.07	0.13	0.04	
CPW-A9M	7.88	7.65	7.80		0.06	0.09	0.09	
BCPW-A9M	7.88	7.58	7.95	7.64	0.06	0.09	0.28	0.09
OCPW-A9M	7.83	7.65	7.69		0.01	0.04	0.20	
CPW-A12M	8.11	7.31	7.65		0.09	0.03	0.07	
BCPW-A12M	7.93	7.58	7.74	6.71	0.12	0.03	0.06	0.07
OCPW-A12M	7.86	7.26	7.51		0.06	0.04	0.07	

Table 44. Effect of Cap Amendments on the EC Values of Pore Water – 12 Month

Evaluation; A/S – apatite/sand, B/A/S – biopolymer/apatite/sand; B/A/O/S – biopolymer/apatite/organoclay/sand; C- cap, B – beneath cap, O – outside cap, PW – pore water, A1M – after one month, A2M – after 2 months, A5M – after 5 months, A9M – after 9 months, and A12M – after 12 months.

Treatments	A/S Avg	B/A/S Avg	B/A/O/S Avg	Control Avg	A/S Stdev	B/A/S Stdev	B/A/O/S Stdev	Control Stdev
Before	85.33	77.50	68.50	75.00	5.86	11.33	3.42	4.69
CPW-A1M	145.00	129.75	297.50		64.31	23.64	249.89	
BCPW-A1M	170.75	171.25	702.67	90.50	78.18	84.22	540.98	9.95
OCPW-A1M	90.33	99.75	103.75		5.69	30.61	4.35	
CPW-A2M	106.00	93.67	103.33		41.50	13.65	35.81	
BCPW-A2M	146.00	98.00	177.50	77.75	74.01	25.06	159.86	26.13
OCPW-A2M	58.00	85.00	69.67		0.00	14.76	15.31	
CPW-A5M	83.00	125.33	226.67		16.46	26.73	96.10	
BCPW-A5M	133.67	124.00	126.00	86.00	43.25	48.07	21.93	9.54
OCPW-A5M	77.50	75.67	106.00		16.26	9.45	5.29	
CPW-A9M	101.50	129.67	160.00		16.26	13.65	21.21	
BCPW-A9M	98.50	118.00	130.50	95.50	20.51	10.15	33.23	13.96
OCPW-A9M	103.00	92.33	116.33		0.00	10.12	21.36	
CPW-A12M	119.50	69.00	112.50		3.54	1.41	4.95	
BCPW-A12M	110.50	109.00	193.50	79.00	24.75	5.66	2.12	10.80
OCPW-A12M	92.50	70.00	90.00		12.02	2.83	5.66	

Table 45. Effect of Cap Amendments on the ORP Values of Pore Water – 12 Month Evaluation; A/S – apatite/sand, B/A/S – biopolymer/apatite/sand; B/A/O/S – biopolymer/apatite/organoclay/sand; C- cap, B – beneath cap, O – outside cap, PW – pore water, A1M – after one month, A2M – after 2 months, A5M – after 5 months, A9M – after 9 months, and A12M – after 12 months.

Treatments	A/S Avg	B/A/S Avg	B/A/O/S Avg	Control Avg	A/S Stdev	B/A/S Stdev	B/A/O/S Stdev	Control Stdev
CPW-A1M	-108	-91	-105	-19	2	5	5	14
BCPW-A1M	-168	-153	-179		0	11	1	
OCPW-A1M	-43	-18	-90		19	23	40	5
CPW-A2M	-84	-25	-57	-16	35	7	47	
BCPW-A2M	-109	-63	-106		1	16	9	
OCPW-A2M	-39	-11	-70			26	14	
CPW-A5M	-95	-49	-89	-31	17	22	5	14
BCPW-A5M	-148	-104	-155		50	31	30	
OCPW-A5M	-32	-45	-64		12	22	26	
CPW-A9M	-82	-113	-128	-36	17	42	42	19
BCPW-A9M	-67	-127	-160		7	23	3	
OCPW-A9M	-45	-59	-108		33	6	5	
CPW-A12M	-70	-27	-96	-26	6	1	18	4
BCPW-A12M	-99	-107	-110		0	21	4	
OCPW-A12M	-58	-27	-28		14	6	12	

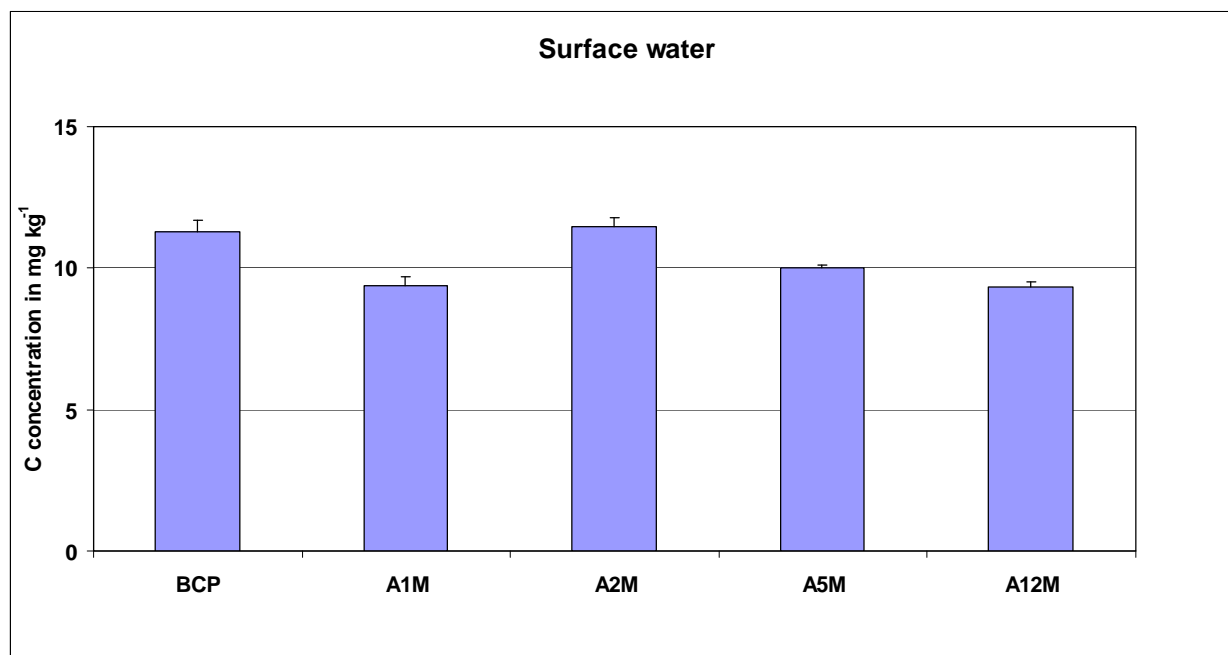


Figure 101. Total Carbon in Surface Water Collected before Cap Placement and One, Two, and Five, and 12 Months after Cap Placement.

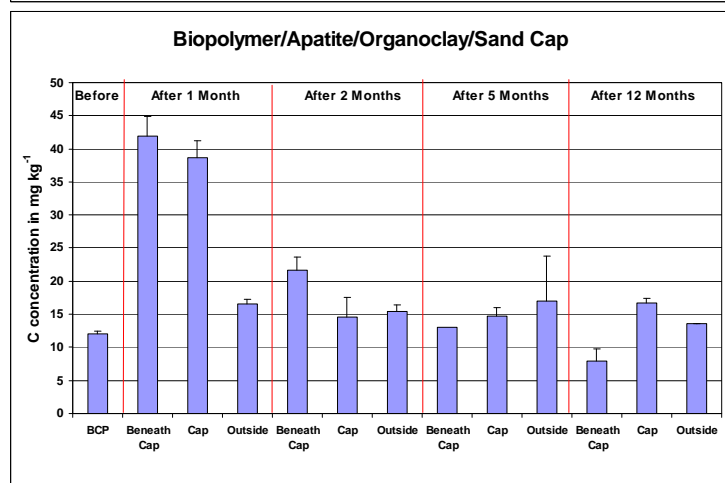
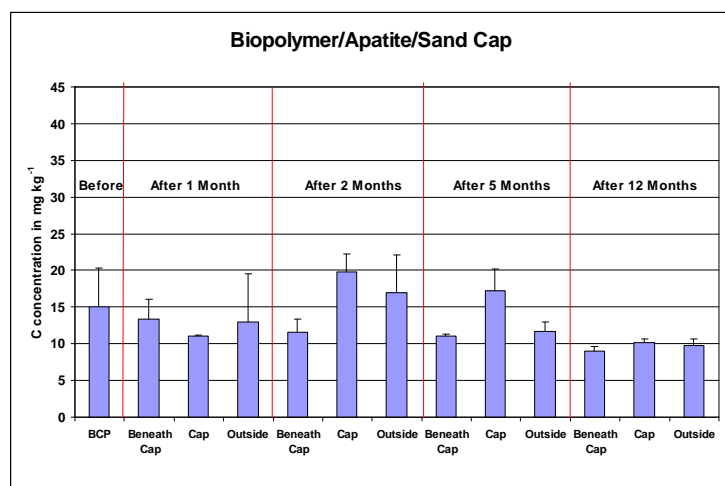
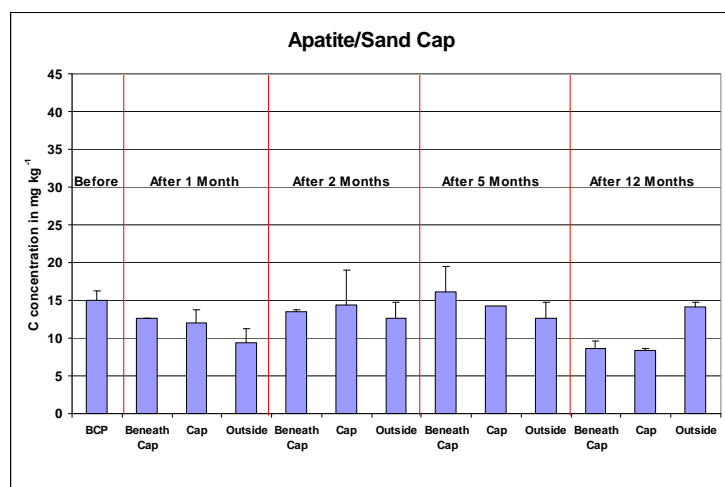


Figure 102. Total Carbon Concentrations in Pore Water Samples Collected from each Type of Cap before Cap Placement (BCP), and One, Two, Five, and 12 Months after Cap Placement. Pore water was collected within each cap (cap), beneath each cap (beneath cap), and outside of each cap (outside).

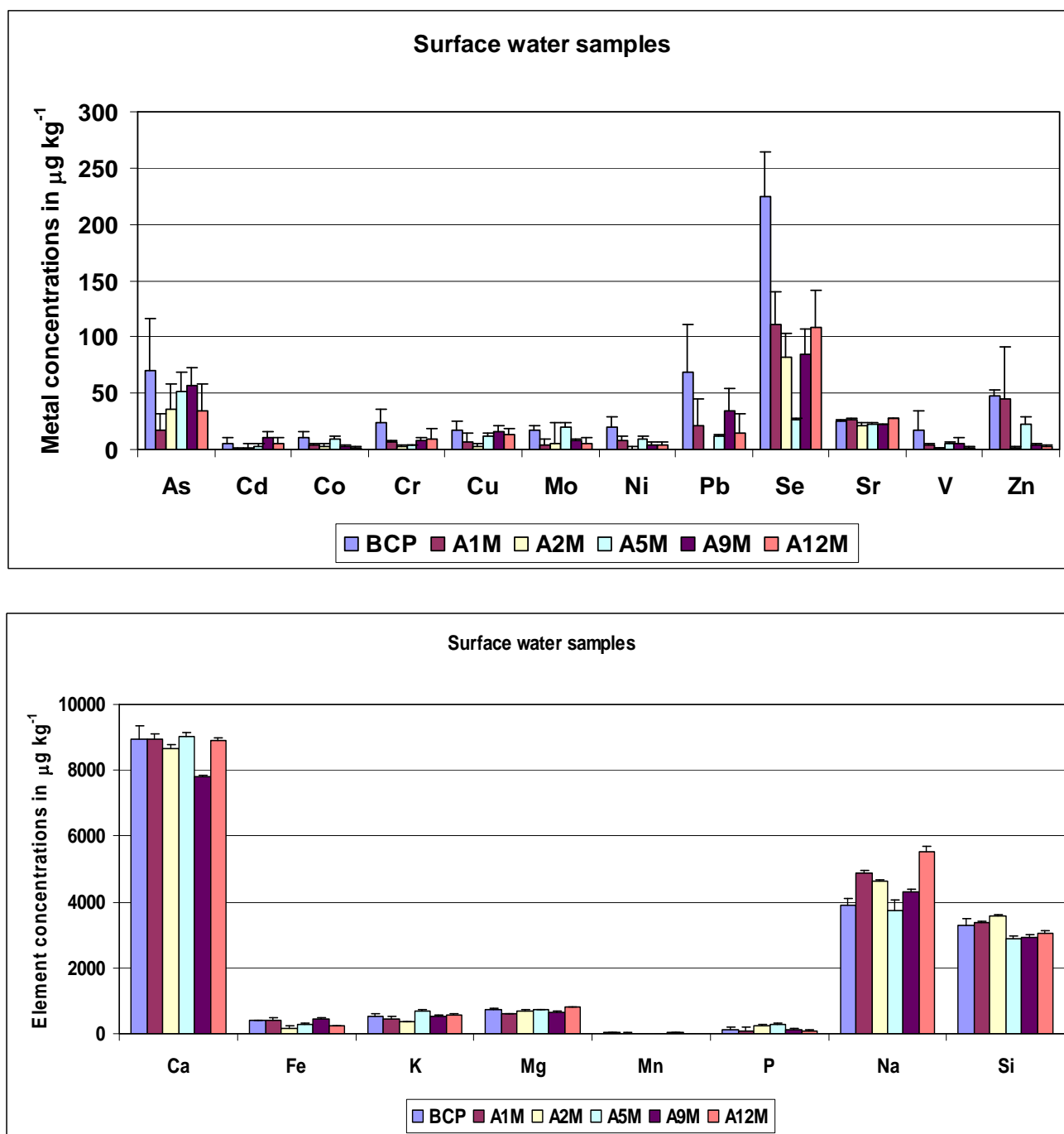


Figure 103. Element Concentrations in Surface Water; BCP- before cap placement, A1M – One Month after Cap Placement, A2M - two months, A5M – five months, A9M – nine months, A12M – twelve months.

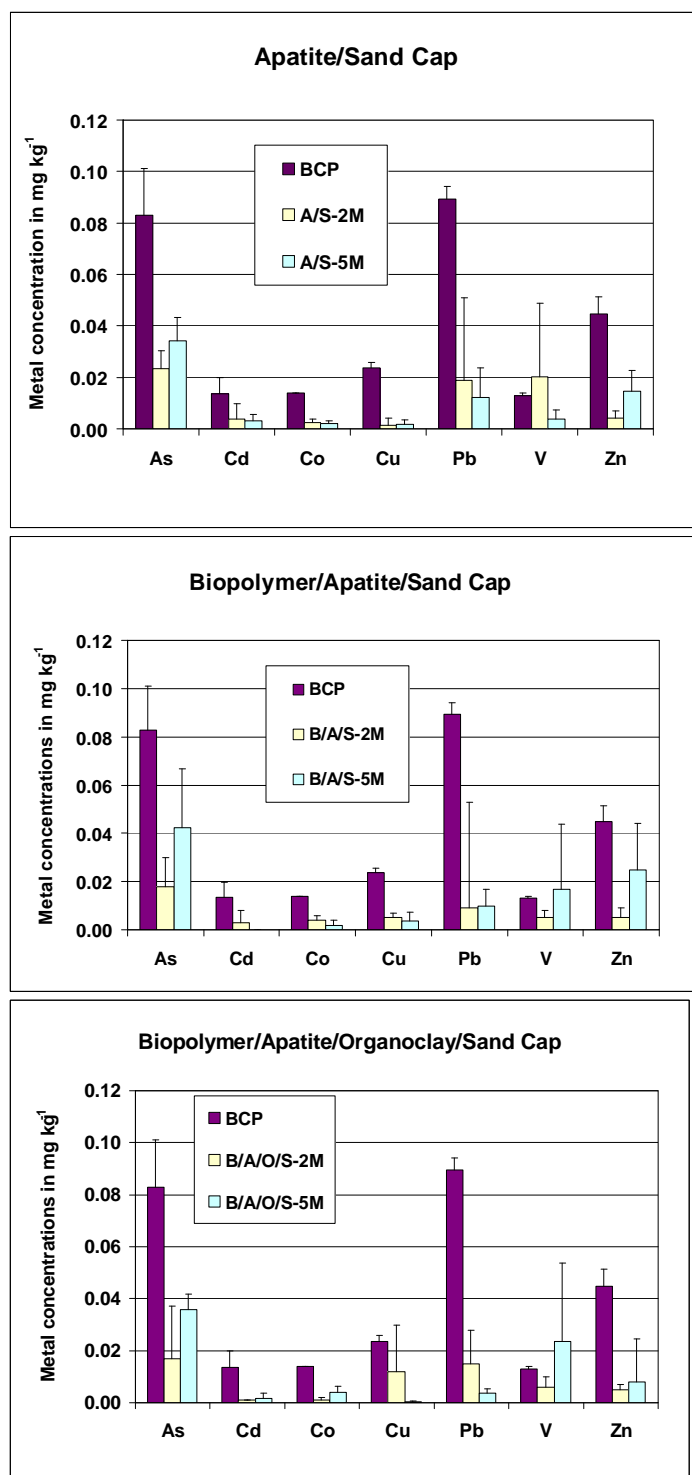


Figure 104. Effect of Cap Materials on Metal Concentrations in Pore Water Two and Five Months after Cap Placement; BCP- before cap placement (n = 8), 2M – pore water collected two months after cap placement(n = 8 for each type of cap), 5M- pore water collected five months after cap placement (n = 8 for each type of cap); A/S – apatite/sand, B/A/S – biopolymer/apatite/sand; B/A/O/S – biopolymer/apatite/organoclay/sand.

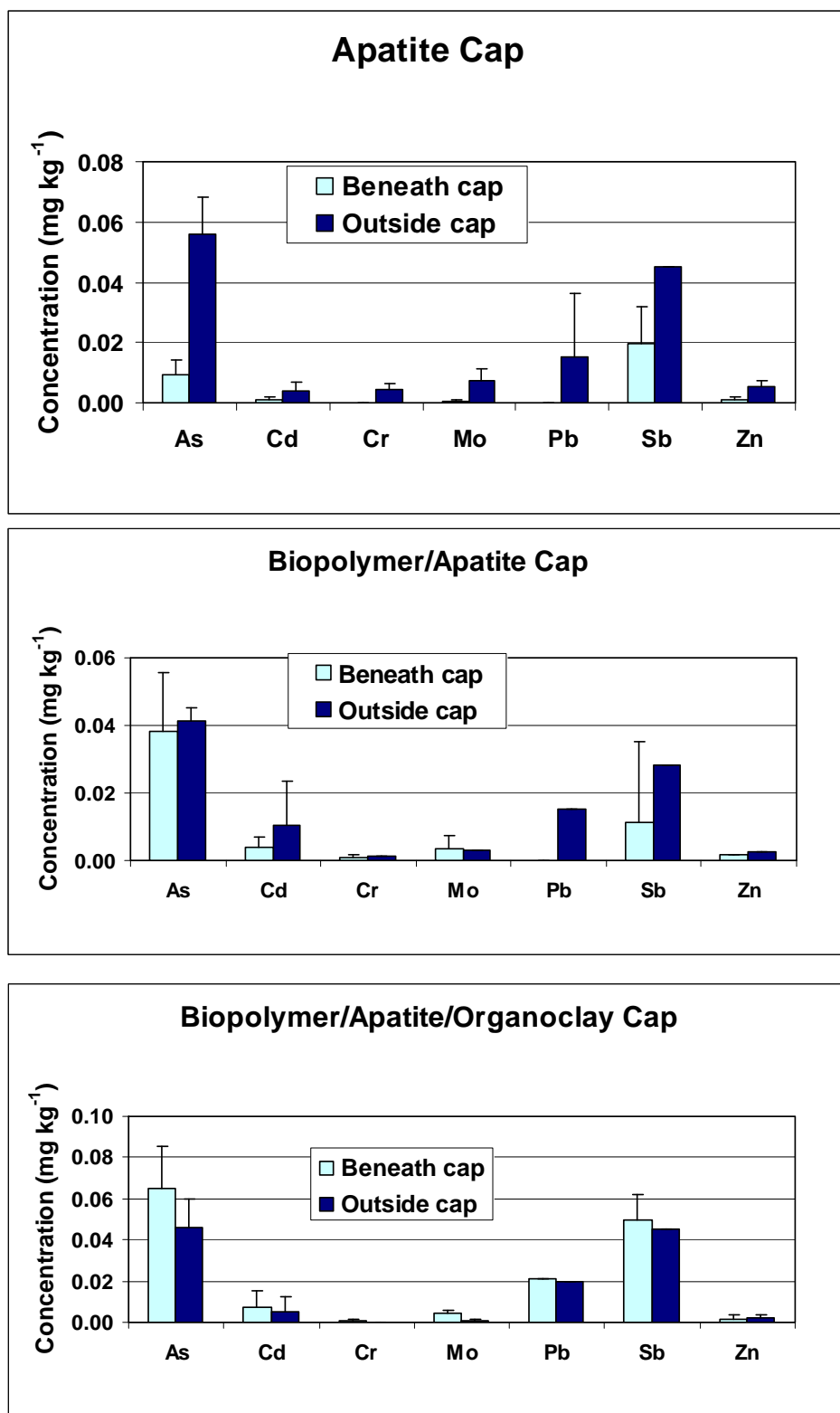


Figure 105. Effect of Cap Materials on Metal Concentrations in Pore Water 12 Months after Cap Placement.

Table 46. Effect of Cap Amendments on Element Concentration (mg kg⁻¹) in Pore Water – 12 Month Evaluation; A – apatite/sand, BA – biopolymer/apatite/sand; BAO – biopolymer/apatite/organoclay/sand; C- cap, B – beneath cap, O – outside cap; Before – element concentration in pore water before cap placement; AVG – averages; STDEV – standard deviations.

Element	BEFORE AVG	A-C AVG	A-BC AVG	A-O AVG	BA-C AVG	BA-BC AVG	BA-O AVG	BAO-C AVG	BAO-BC AVG	BAO-O AVG
Ag	0.0153	0.0000	0.0000	0.0006	0.0000	0.0000	0.0000	0.0000	0.0002	0.0000
Al	0.1152	0.0951	0.0501	0.1718	0.0708	0.0025	0.0256	0.0893	0.0281	0.1470
As	0.0829	0.0307	0.0095	0.0561	0.0312	0.0383	0.0415	0.0378	0.0647	0.0459
B	0.0229	0.0095	0.0090	0.0181	0.0083	0.0139	0.0066	0.0072	0.0109	0.0072
Ba	0.0268	0.0119	0.0097	0.0316	0.0229	0.0318	0.0191	0.0276	0.0390	0.0240
Be	0.0011	0.0004	0.0003	0.0011	0.0006	0.0009	0.0003	0.0003	0.0004	0.0003
Ca	9.0610	22.1900	18.5900	13.1080	8.7725	12.2715	8.7325	20.7100	30.1200	13.9250
Cd	0.0135	0.0008	0.0008	0.0038	0.0064	0.0038	0.0105	0.0038	0.0071	0.0053
Co	0.0138	0.0000	0.0000	0.0000	0.0000	0.0000	0.0000	0.0000	0.0000	0.0000
Cr	0.0300	0.0000	0.0000	0.0042	0.0000	0.0008	0.0014	0.0000	0.0005	0.0010
Cu	0.0237	0.0065	0.0065	0.0026	0.0036	0.0124	0.0000	0.0055	0.0162	0.0033
Fe	0.4183	0.3461	0.2159	1.8266	0.9148	2.3594	0.4048	1.2652	0.9404	1.2670
K	0.5973	0.4783	1.1339	0.5835	0.6639	0.5155	0.4907	0.4351	0.7258	0.4846
Mg	0.7392	1.1315	0.9080	0.6808	0.6794	0.7787	0.7096	0.8823	1.5115	0.6592
Mn	0.0284	0.0147	0.0186	0.0593	0.0428	0.6883	0.0287	0.2375	0.4103	0.0814
Mo	0.0191	0.0012	0.0005	0.0075	0.0000	0.0035	0.0030	0.0032	0.0045	0.0005
Na	4.0485	5.4305	5.7455	5.3890	5.6045	5.2700	5.5580	5.4250	5.5760	5.5180
Ni	0.0238	0.0000	0.0003	0.0000	0.0000	0.0000	0.0000	0.0000	0.0000	0.0000
P	0.1539	0.4563	0.2344	0.2131	0.3672	0.1148	0.0680	0.3459	0.0631	0.0853
Pb	0.0895	0.0000	0.0000	0.0151	0.0000	0.0000	0.0151	0.0000	0.0201	0.0200
Sb	0.0893	0.0113	0.0198	0.0451	0.0113	0.0282	0.0000	0.0282	0.0536	0.0451
Se	0.2605	0.1929	0.1549	0.1357	0.0789	0.1244	0.0770	0.1617	0.2652	0.1090
Si	3.3785	2.9900	3.5500	3.1275	2.9770	3.4085	3.0070	2.9575	3.9615	3.2020
Zn	0.0448	0.0043	0.0011	0.0056	0.0024	0.0017	0.0024	0.0010	0.0017	0.0024
Element	BEFORE STDEV	A-C STDEV	A-BC STDEV	A-O STDEV	BA-C STDEV	BA-BC STDEV	BA-O STDEV	BAO-C STDEV	BAO-BC STDEV	BAO-O STDEV
Ag	0.0021	0.000	0.000	0.001	0.000	0.000	0.000	0.000	0.000	0.000
Al	0.0048	0.029	0.023	0.151	0.054	0.004	0.036	0.041	0.007	0.057
As	0.0182	0.025	0.005	0.012	0.022	0.018	0.004	0.011	0.021	0.014
B	0.0021	0.002	0.004	0.002	0.000	0.003	0.001	0.002	0.003	0.002
Ba	0.0001	0.001	0.001	0.001	0.007	0.019	0.001	0.004	0.010	0.001
Be	0.0003	0.000	0.000	0.000	0.000	0.000	0.000	0.000	0.000	0.000
Ca	0.0311	1.768	6.180	4.641	0.091	3.548	0.469	0.212	6.223	1.520
Cd	0.0063	0.001	0.001	0.003	0.009	0.003	0.013	0.003	0.008	0.007
Co	0.0000	0.000	0.000	0.000	0.000	0.000	0.000	0.000	0.000	0.000
Cr	0.0037	0.000	0.000	0.002	0.000	0.001	0.000	0.000	0.001	0.000
Cu	0.0021	0.006	0.006	0.000	0.001	0.003	0.000	0.001	0.006	0.005
Fe	0.0136	0.073	0.109	1.201	0.654	3.029	0.306	0.631	0.005	0.177
K	0.0248	0.052	0.770	0.061	0.035	0.070	0.105	0.096	0.157	0.026
Mg	0.0245	0.086	0.140	0.161	0.081	0.006	0.027	0.088	0.517	0.012
Mn	0.0016	0.007	0.016	0.026	0.038	0.926	0.012	0.109	0.058	0.019
Mo	0.0008	0.000	0.001	0.004	0.000	0.004	0.000	0.002	0.001	0.001
Na	0.0643	0.276	0.284	0.341	0.046	0.174	0.130	0.423	0.600	0.115
Ni	0.0006	0.000	0.000	0.000	0.000	0.000	0.000	0.000	0.000	0.000
P	0.0310	0.093	0.027	0.153	0.020	0.118	0.059	0.021	0.010	0.070
Pb	0.0047	0.000	0.000	0.021	0.000	0.021	0.000	0.000	0.028	0.000
Sb	0.0421	0.000	0.012	0.000	0.000	0.024	0.000	0.024	0.012	0.000
Se	0.0188	0.002	0.059	0.032	0.014	0.029	0.060	0.025	0.051	0.026
Si	0.0120	0.048	0.759	0.148	0.105	0.571	0.006	0.339	0.118	0.072
Zn	0.0066	0.000	0.001	0.002	0.001	0.000	0.000	0.003	0.002	0.001

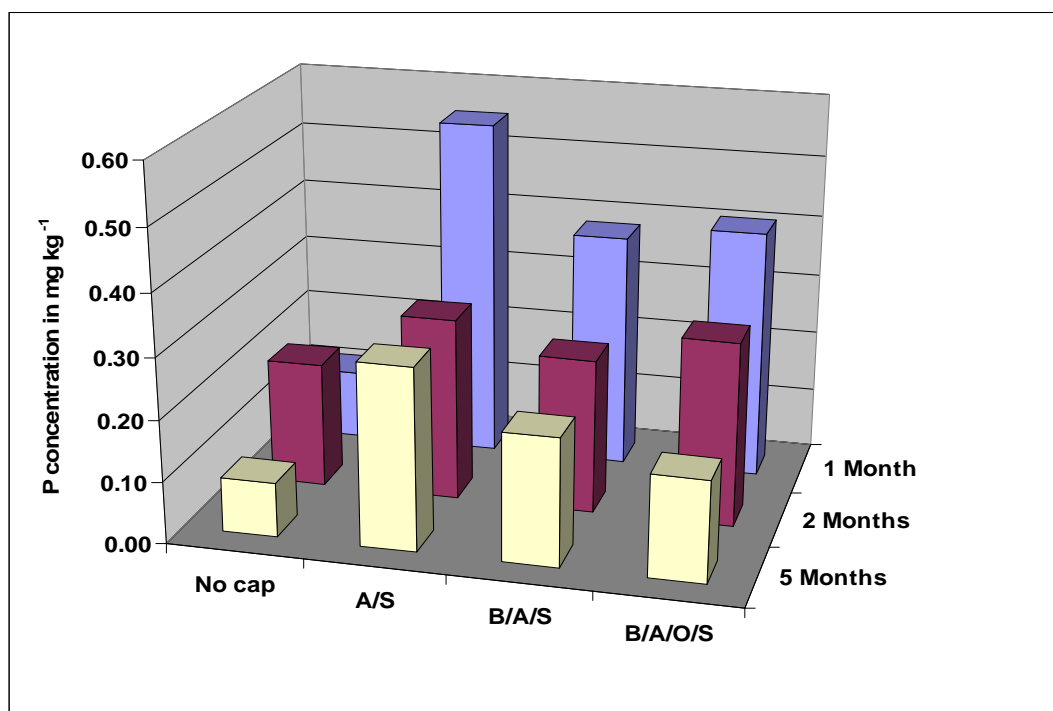


Figure 106. Average P Concentrations (ppm) in Pore Water Collected within and beneath each Cap. The P concentrations are presented for three sampling events: one, two and five months after cap placement; A/S – apatite/sand, B/A/S – biopolymer/apatite/sand; B/A/O/S – biopolymer/apatite/organoclay/sand.

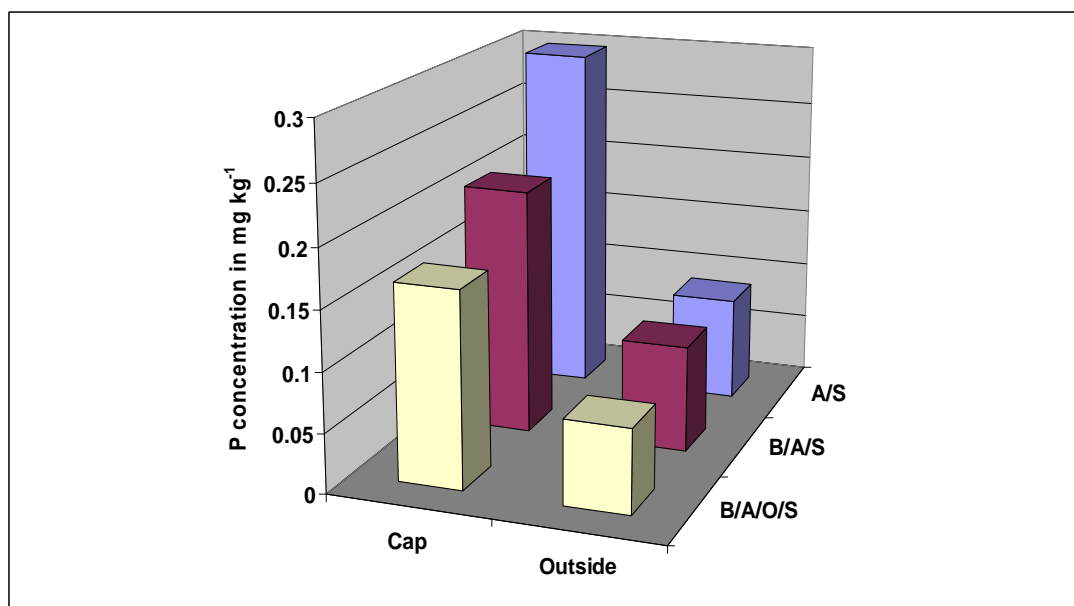


Figure 107. Average P Concentrations (ppm) in Pore Water Collected within and outside each Cap. The P concentrations are presented only for one sampling event - five months after cap placement; A/S – apatite/sand, B/A/S – biopolymer/apatite/sand; B/A/O/S – biopolymer/apatite/organoclay/sand.

Table 47. Average P Concentration (ppm) in Pore Water Collected within, beneath, and outside of each Cap. The P concentrations are presented for four sampling events: one, two, five, and 12 months after cap placement; A – apatite/sand, BA – biopolymer/apatite/sand; BAO – biopolymer/apatite/organoclay/sand; C- cap, B – beneath cap, O – outside cap; Before – element concentration in pore water before cap placement; Avg – averages; Stdev – standard deviations.

	Control	A-C	A-BC	A-O	BA-C	BA-BC	BA-O	BAO-C	BAO-BC	BAO-O
After 1 Month										
Avg	0.11	0.55	0.39	0.27	0.38	0.25	0.21	0.41	0.21	0.17
Stdev	0.05	0.74	0.14	0.11	0.16	0.16	0.07	0.04	0.11	0.06
After 2 Months										
Avg	0.2	0.3	0.23	0.15	0.25	0.21	0.04	0.3	0.2	0.09
Stdev	0.18	0.12	0.11	0.07	0.24	0.10	0.04	0.15	0.12	0.12
After 5 Months										
Avg	0.09	0.25	0.13	0.09	0.21	0.88	0.09	0.17	0.10	0.07
Stdev	0.05	0.16	0.11	0.01	0.10	0.05	0.16	0.12	0.08	0.01
After 12 Months										
Avg	0.16	0.46	0.23	0.21	0.37	0.11	0.07	0.35	0.06	0.09
Stdev	0.03	0.09	0.03	0.15	0.02	0.12	0.06	0.02	0.01	0.07

Sediment Characterization Twelve Months after Cap Placement

Twelve months after cap placement the average pH values for sediment from control plots were slightly higher than the average pH values for sediment from control plots six month earlier. The pH values for two tested layers, 0 – 2.5 and 2.5 – 5 cm, were 5.8 and 5.9, respectively (Figure 108). The addition of apatite in a one layer cap (A/S cap) or in a two layer cap (B/A/S cap) increased the pH values to about 6.2 -6.4 (Figure 108). The six month evaluation showed that the pH of sediment beneath a three layer cap composed of biopolymer/apatite/organoclay/sand (B/A/O/S) remained almost the same as in the control plot (i.e., 4.5 and 4.6 for the 0-2.5 and 2.5 – 5 cm layers, respectively). However, the twelve month evaluation showed an increase in the average pH values of sediment from the B/A/O/S plot to about 6.4 (Figure 108).

Total carbon content six and 12 months after cap placement remained at about the same level in the sediment beneath the A/S cap, but increased substantially in the sediment beneath the B/A/S and B/A/O/S caps (Figure 109). Higher concentrations of carbon in sediment beneath the caps with biopolymer suggest that biopolymers were biodegrading with time and releasing carbon to the sediment. Similar results were obtained in the laboratory studies (Knox et al., 2008). The relationship between carbon, especially dissolved organic carbon, and metal ions or organic contaminants is extremely important because it affects the retention and mobility of these contaminants in sediments and waters (Adriano 2001).

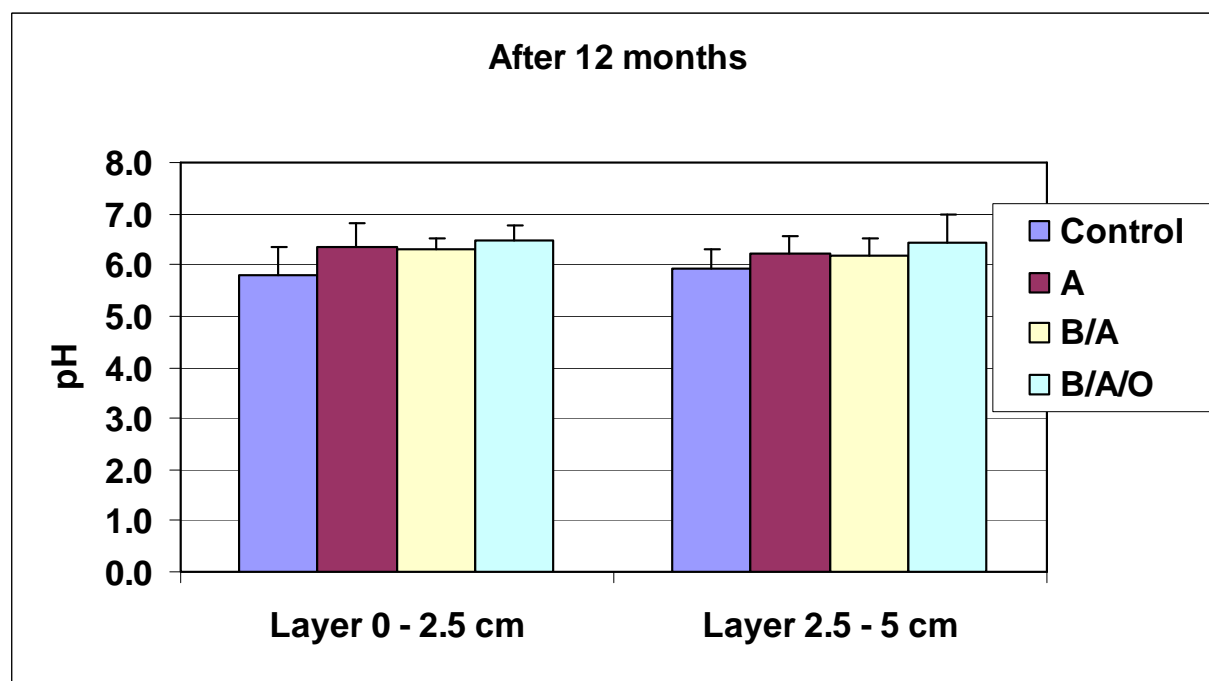
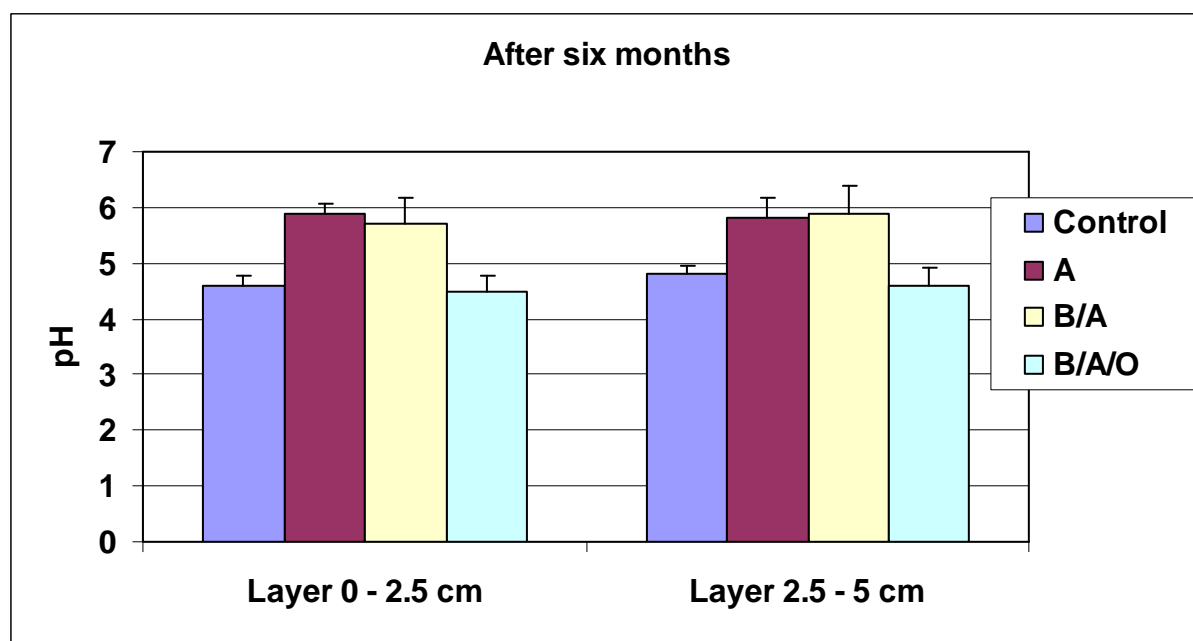


Figure 108. Effect of Cap Amendments on Sediment pH Values; Sediment Samples Collected Six and 12 Months after Cap Placement: Control, untreated sediment, A – apatite cap, B/A – biopolymer/apatite cap, B/A/O – biopolymer/apatite/organoclay cap.

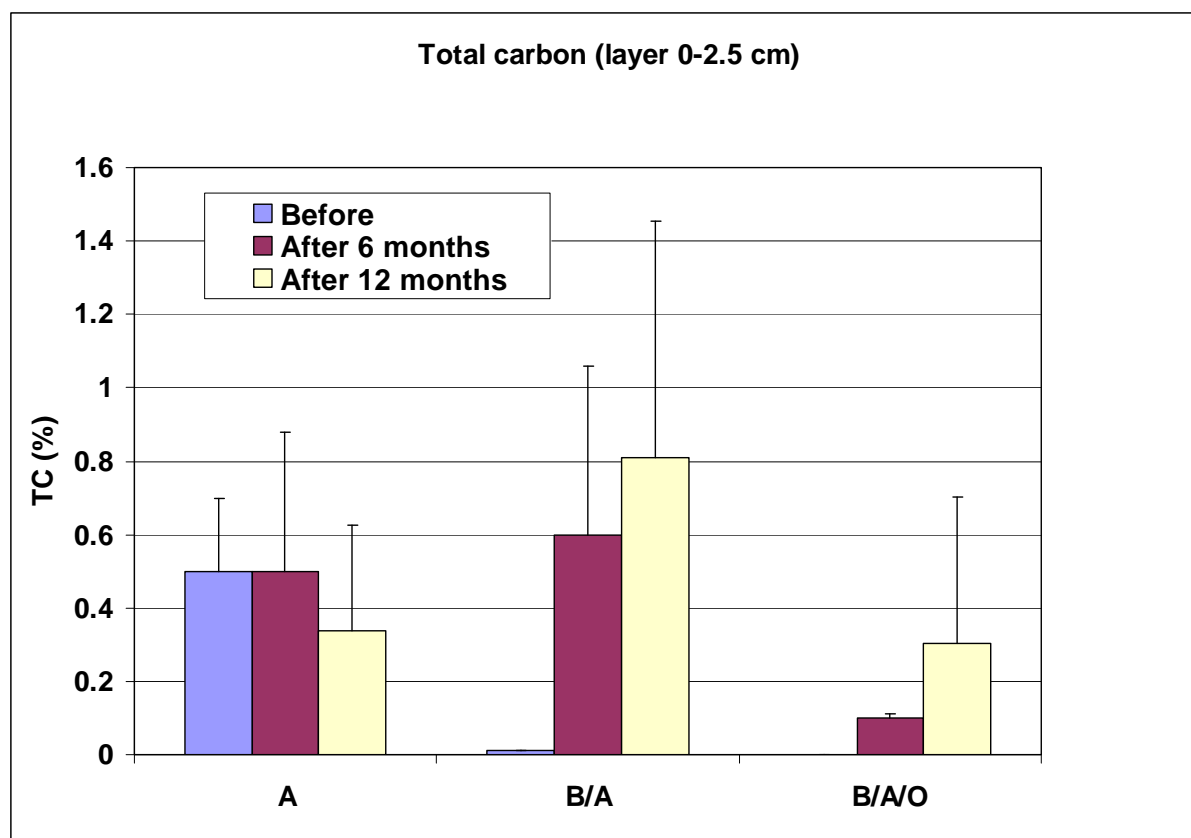


Figure 109. Effect of Cap Amendments on Total Carbon (TC) Content in Sediment beneath Caps; Sediment Samples Collected before, six, and 12 Months after Cap Placement; A – apatite cap, B/A – biopolymer/apatite cap, B/A/O – biopolymer/apatite/organoclay cap.

Simultaneously Extracted Metals/Acid Volatile Sulfide (SEM/AVS) Evaluation of Sediment

There is ongoing debate in the scientific literature on how to evaluate the potential mobile pool of metals for sediment contaminated with metals to cause injury to aquatic organisms. One school of thought is that bioavailability (i.e., uptake by organisms and subsequent toxicity) is controlled primarily by the dissolved metal concentration in the sediment pore water. Proponents of this theory contend that using SEM/AVS molar ratios to estimate sediment pore water for cadmium, copper, mercury, nickel, lead, and zinc (generally present as divalent species) provides a better indicator of sediment toxicity than total mass concentrations on a dry weight basis (Allen et al., 1991; Di Toro et al., 1992; DeWitt et al., 1996; Hansen et al., 1996). AVS is usually the dominant-binding phase for divalent metals in sediment. Metal sulfide precipitates are typically very insoluble, and this limits the amount of dissolved metal availability in sediment pore water. For an individual metal, when the amount of AVS exceeds the amount of the SEM metal (i.e., the SEM/AVS molar ratio is below 1), the metal concentration in the sediment pore water will be low because of the limited solubility of the metal sulfide. For a suite of divalent metals, the sum of the SEM metals must be considered, with the assumption that the metal with the lowest K_{sp} value (least soluble) will form the most stable complex with the AVS (i.e., the lowest K_{sp} metal will “out-compete” the other metals and bind with the AVS).

The other school of thought uses an empirical approach that matches metal sediment chemistry to biological effect data to determine toxic effect levels (Persaud et al., 1992; Ingersoll et al., 1996; MacDonald et al., 1996). Dietary factors (i.e., sediment ingestion) are one important pathway to biotic uptake for the empirical approach (Lee et al., 2000). Recent articles have reported that though metal concentrations in sediment pore water may be controlled by geochemical equilibration with metal sulfide, metal exposure and subsequent toxicity is most likely influenced by sediment ingestion (Long et al., 1998; Lee et al., 2000).

In this study, AVS, SEM, SEM/AVS, and other measures of sediment chemistry were evaluated to assess their potential applicability for evaluating sediment remediation by active caps.

For this report, the concentrations of metals and sulfide in sediment are given in units of μmol analyte/g sediment. The molar-based units are required to allow for easy comparison between the pool of available sulfide (AVS) and the pool of divalent metals (SEM).

The ratio of simultaneously extracted metal to acid –volatile sulfide (SEM/AVS) can provide important information regarding metal availability in anaerobic sediments. The AVS, SEM, and SEM/AVS results for the sediment samples collected before, six and twelve months after cap placement are presented in Figures 110 and 111. The AVS pool from the control plot and the plot treated with an apatite cap increased over the 12 month study period (Figure 110). The AVS pool in the plot treated with a three layer biopolymer/apatite/organoclay (B/A/O) cap increased during the first six months of the study and then declined slightly (Figure 110). SEM concentrations decreased over a period of 12 months in the apatite plot and B/A/O plots. The SEM/AVS ratio decreased over time to low levels in all plots but the decrease was greater in the plot with the apatite cap than in the control plot (Figure 112). SEM/AVS concentrations measured over time can be used to compute rates of SEM/AVS change for each treatment (Figure 112). The rate of decrease in SEM/AVS in sediment beneath the apatite cap was significantly faster than in sediment in the control plot as indicated by a comparison of the regression slopes between the two trend lines ($t=3.00$, $df=12$, $P\leq 0.05$) (Figure 112 and Table 48).

The differences in the SEM/AVS ratio before and twelve months after cap placement were statistically significant ($P\leq 0.05$) for both the apatite and B/A/O plot plots ($t=287.6$ [$df=4$] and $t=6.78$ [$df=4$], respectively, for apatite and B/A/O plots) (Figure 111). The changes in SEM/AVS that occurred over time are the result of changes in AVS and SEM during the time that elapsed from before cap placement to the end of the 12 month study period. To some extent these changes could be related to seasonal factors (Grabowski et al., 2001). It is very well documented that seasonal changes and redox conditions control Fe-S-P concentrations in the sediments, pore waters, and overlying water and, therefore, the AVS concentrations in sediments (Grabowski et al., 2001). However, the significantly more rapid decrease in SEM/AVS that occurred beneath the caps than in the control plot indicates a treatment effect associated with capping that resulted in decreased metal bioavailability. These results show that the pilot-scale active caps in Steel Creek were effective in lowering SEM/AVS values during the one year test period.

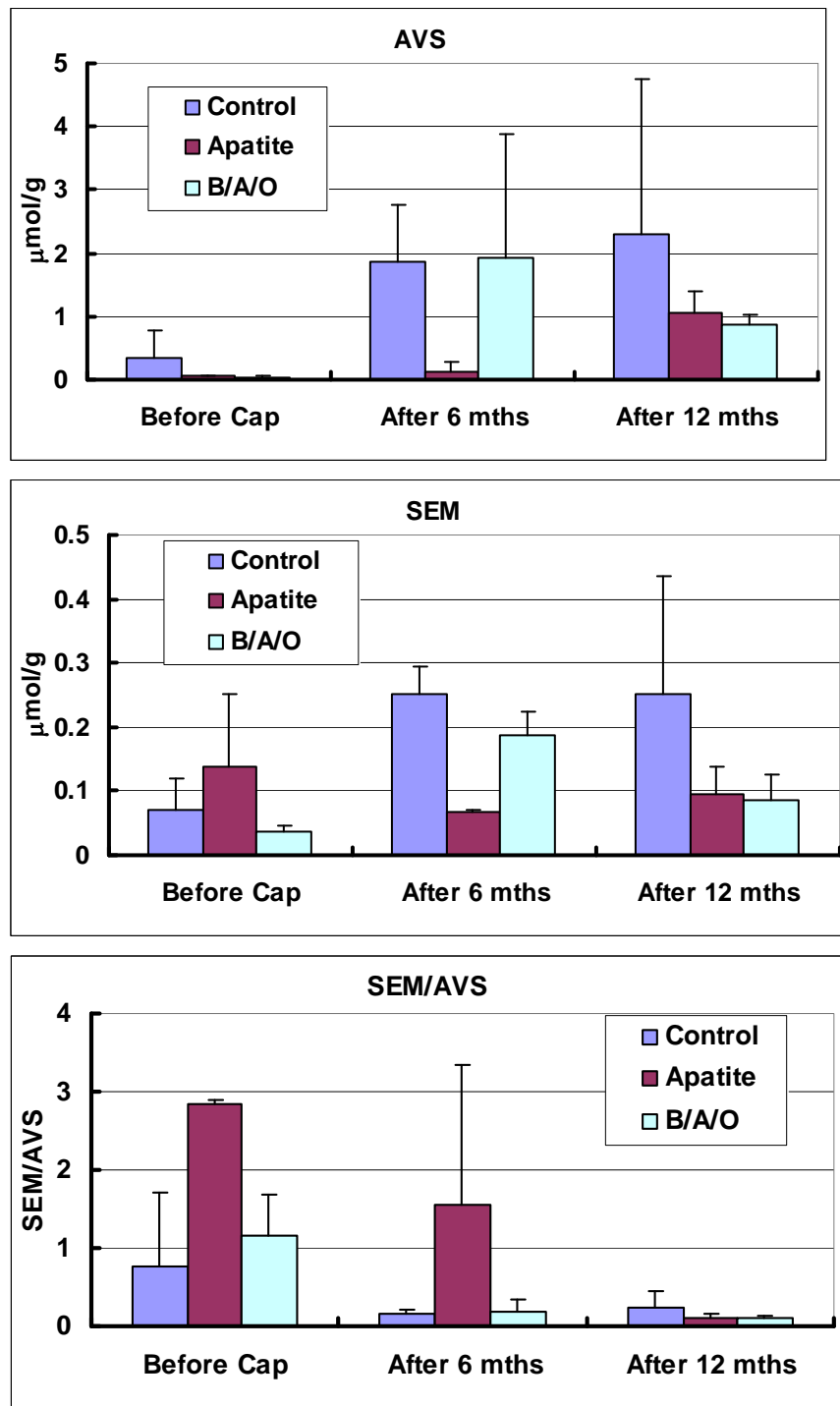


Figure 110. AVS, SEM, and SEM/AVS in Steel Creek Sediment before and after Cap Placement; treatments: control (untreated sediment), biopolymer/apatite/organoclay (B/A/O) cap, and apatite cap.

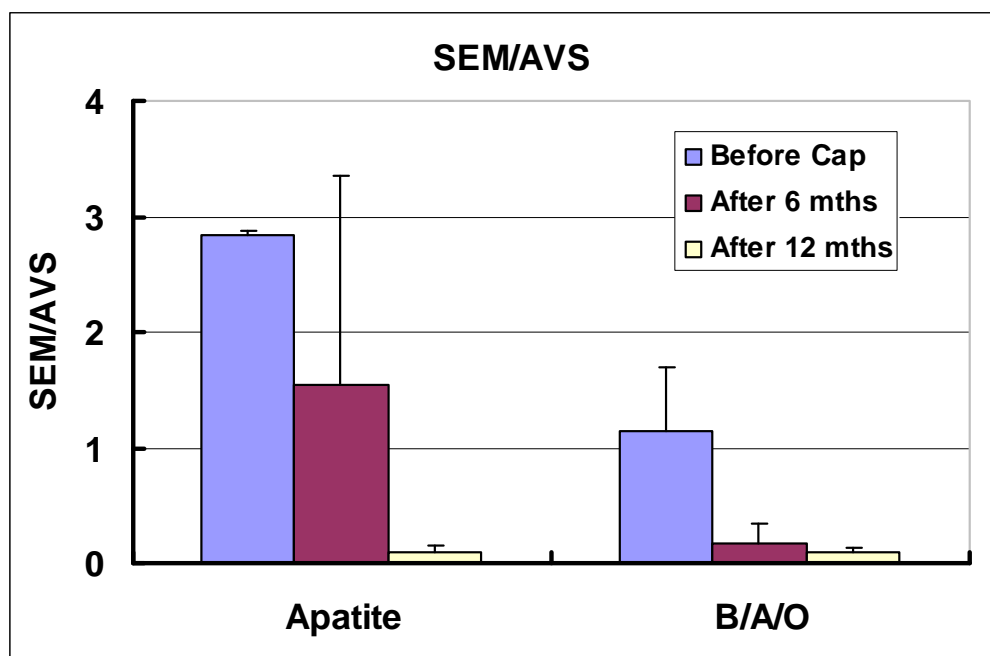


Figure 111. Effect of Cap Amendments on the SEM/AVS Ratio in the Sediment beneath the Caps in Steel Creek – 12 Month Evaluation.

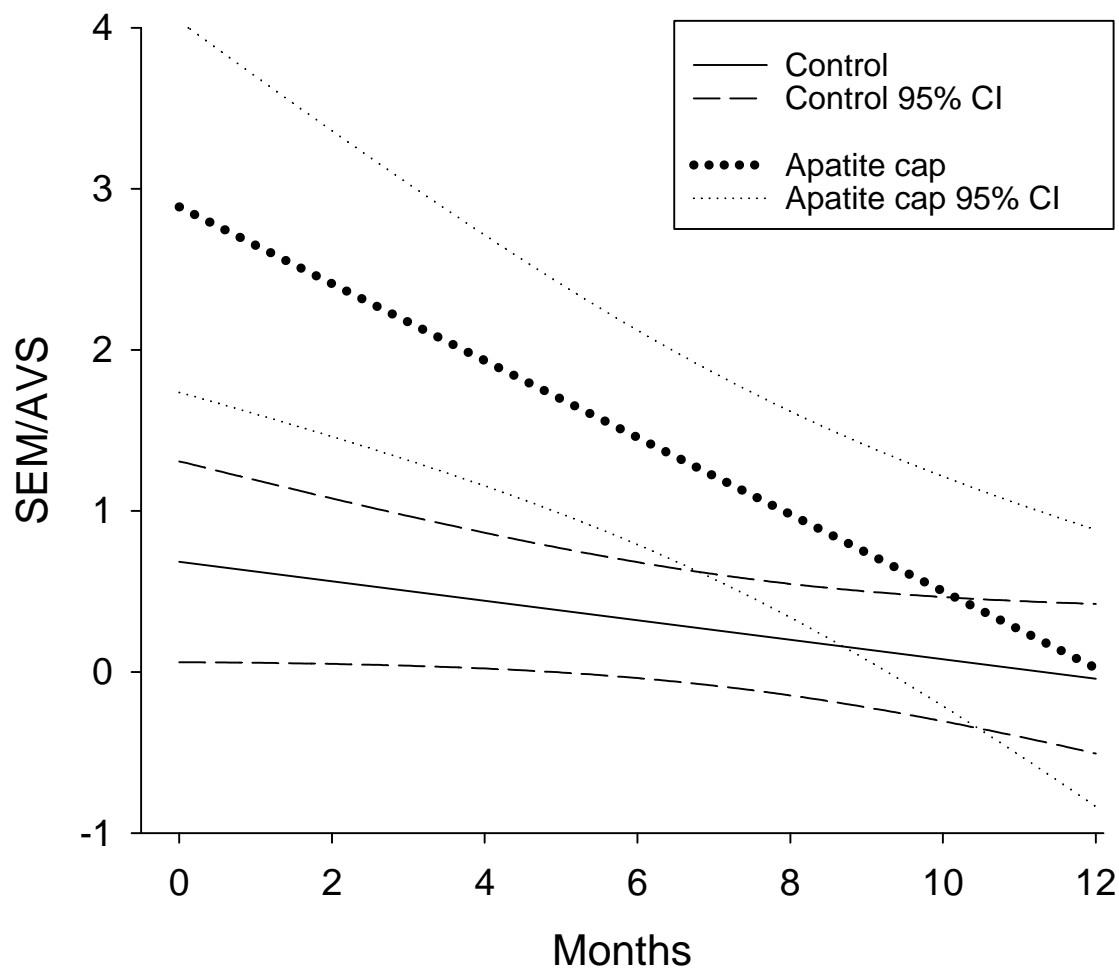


Figure 112. Regression Lines and 95% Confidence Intervals (CIs) Describing Temporal Changes in the SEM/AVS Ratio in Sediment Located in the Control Plot and beneath the Apatite Cap during the One Year Test Period.

Table 48. Statistical Comparison of Regression Slopes Describing Temporal Changes in the SEM/AVS Ratio in Sediment Located in the Control Plot and beneath the Apatite Cap during the One Year Test Period.

Apatite cap						Control cap					
N = 8 R = 0.658 Rsqr = 0.433 Adj Rsqr = 0.338 Standard Error of Estimate = 0.398						N = 8 R = 0.881 Rsqr = 0.776 Adj Rsqr = 0.739 Standard Error of Estimate = 0.736					
	Coefficient	Std. Error	t	P			Coefficient	Std. Error	t	P	
Constant	0.684	0.255	2.687	0.036		Constant	2.888	0.471	6.133	<0.001	
time	-0.061	0.028	-2.139	0.076		time	-0.239	0.0523	-4.562	0.004	
Analysis of Variance:						Analysis of Variance:					
	DF	SS	MS	F	P		DF	SS	MS	F	P
Regression	1	0.726	0.726	4.576	0.076	Regression	1	11.285	11.285	20.815	0.004
Residual	6	0.951	0.159			Residual	6	3.253	0.542		
Total	7	1.677	0.240			Total	7	14.537	2.077		

Test of differences between slopes

	Apatite	Control
slope	-0.239	-0.061
SE	0.052	0.028
SE dif	0.059	
t	-3.002	
df	12	
critical t for df1,12 , p=0.05=2.179		

Evaluation of Zone of Influence (ZOI) – Laboratory Study

The laboratory study investigating the ZOI was conducted for six months with four types of simulated caps: sand, apatite, organoclay, and a three layered cap composed of biopolymer, apatite and organoclay. Lead concentrations in water extracted from sediment 0 to 10 cm below the apatite cap were significantly lower than in water extracted from sediment below the sand cap (Figure 113). Other metals such as Cd, Co, Cr, Sb, and Zn were reduced in the first 2.5 cm of sediment below the caps with amendments (Figure 114). Metal concentrations in water extracts from the sediment below the sand cap remained the same as in the sediment without a cap.

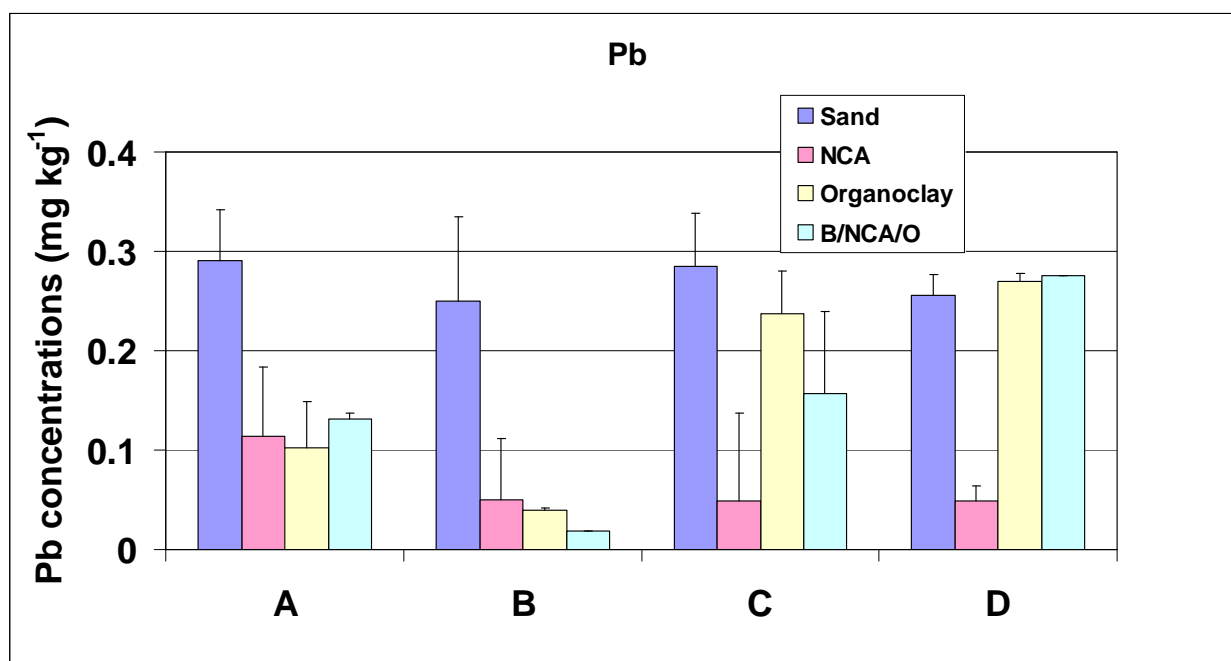


Figure 113. Lead Concentration in Water Extracts from Sediment Collected from below Each Cap; four types of caps were evaluated: sand, NCA – apatite, organoclay, and B/NCA/O – biopolymer, apatite and organoclay; A – layer 0-1.5 cm, B – layer 1.5-2.5 cm, C – layer 2.5-5 cm, and D – layer 5-10cm.

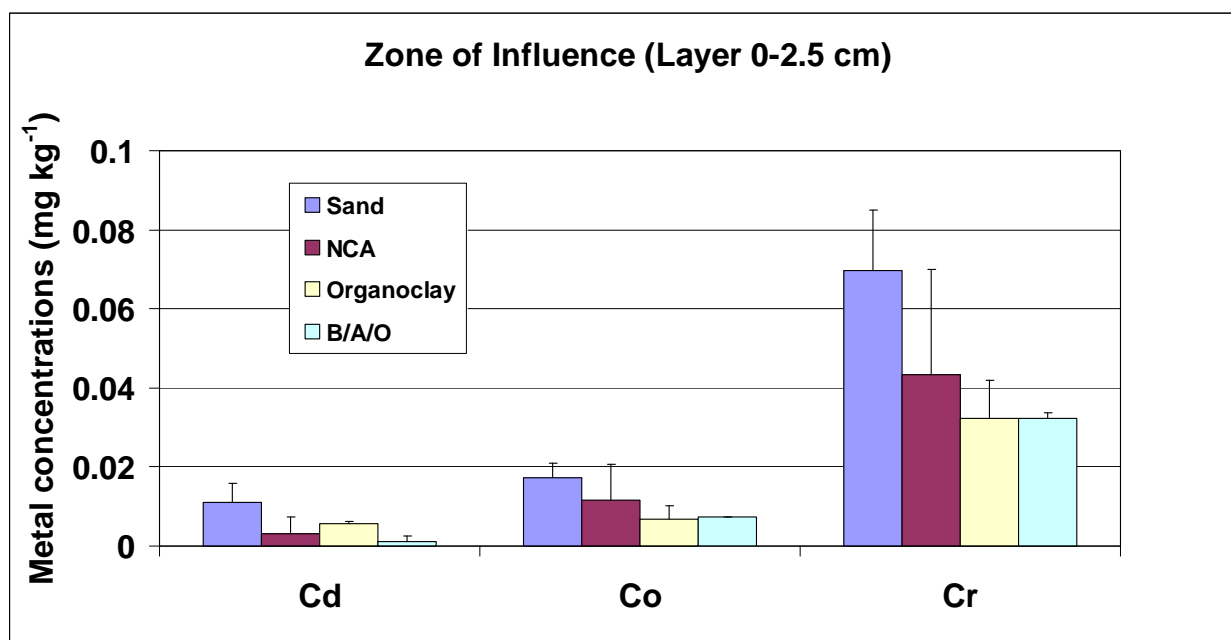
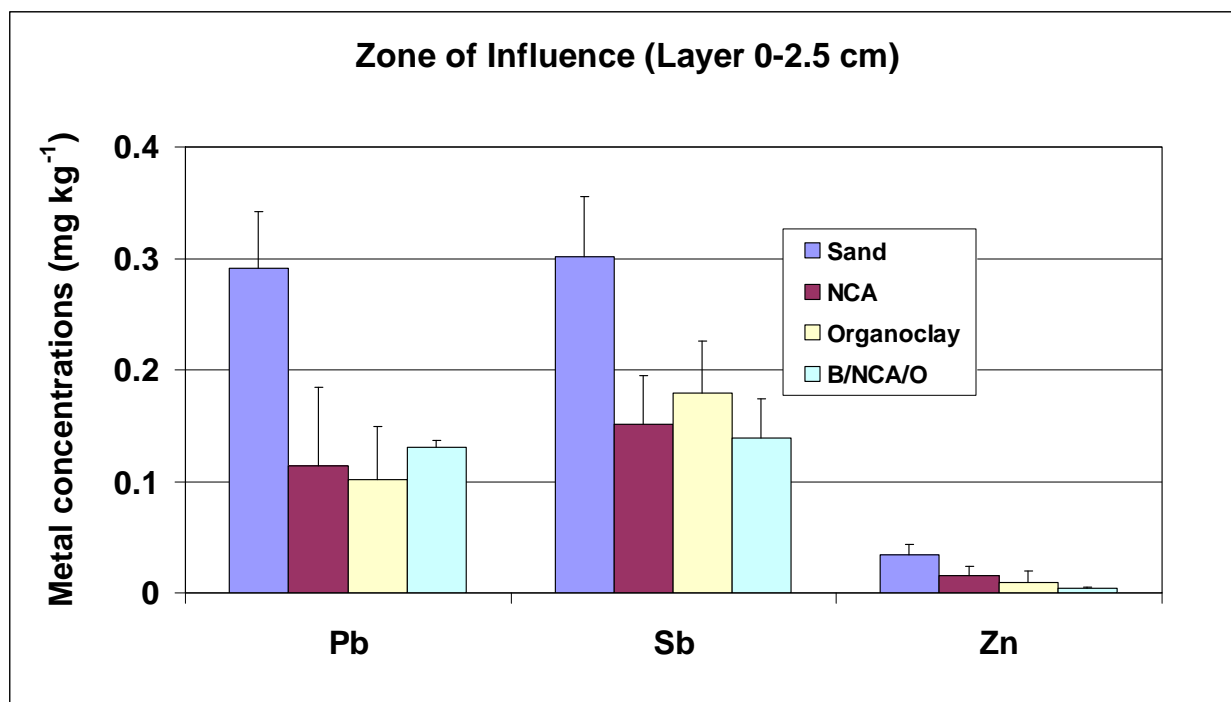


Figure 114. Metal Concentrations in Water Extracts from Sediment Collected from below each Cap; four types of caps were evaluated: sand, NCA – apatite, organoclay, and B/NCA/O – biopolymer, apatite and organoclay cap.

Evaluation of Zone of Influence (ZOI) –Field Study

The ZOI concept was also evaluated in the field by collecting sediment cores from the test plots six and twelve months after cap placement. The sediment samples from two layers beneath the caps were extracted with a double acid method. This method was used in this study to assess the available pool of metals in the sediment below the caps and to evaluate the ZOI of sequestering agents that were used in the caps. The data from the double acid extraction method are presented in Figures 115, 116, and 117. The concentration of metals (Cd, Co, Cu, Zn, and As) in the double acid extracts of the sediment samples collected from beneath the apatite and apatite biopolymer caps six and twelve months after cap placement declined with sediment depth (Figures 115, 116, and 117). In the sediment beneath the biopolymer/apatite/organoclay cap, where organoclay was placed at the bottom, most extracted metal concentrations were reduced only in the first sediment layer (0 – 2.5 cm). Most extracted metal concentrations lower in the sediment (2.5 – 5.0 cm or below 5 cm) were similar to those in the control plot (Figures 116 and 117). These data show that the downward migration of the amendments used in active caps can neutralize contaminants located deeper in the sediment profile (i.e. in the zone of influence).

Also, these data and SEM data revealed that a cap composed of thin layers of amendments (2 inches per layer) does not work for removal of both inorganic and organic contaminants. If organoclay is used as the bottom layer, and apatite as the middle layer, metal immobilization is much less effective than in caps composed only of apatite, or with apatite as the bottom layer (Figures 116 and 117). Therefore, mixing amendments in one layer could be the best design for active caps that remediate both inorganic and organic contaminants.

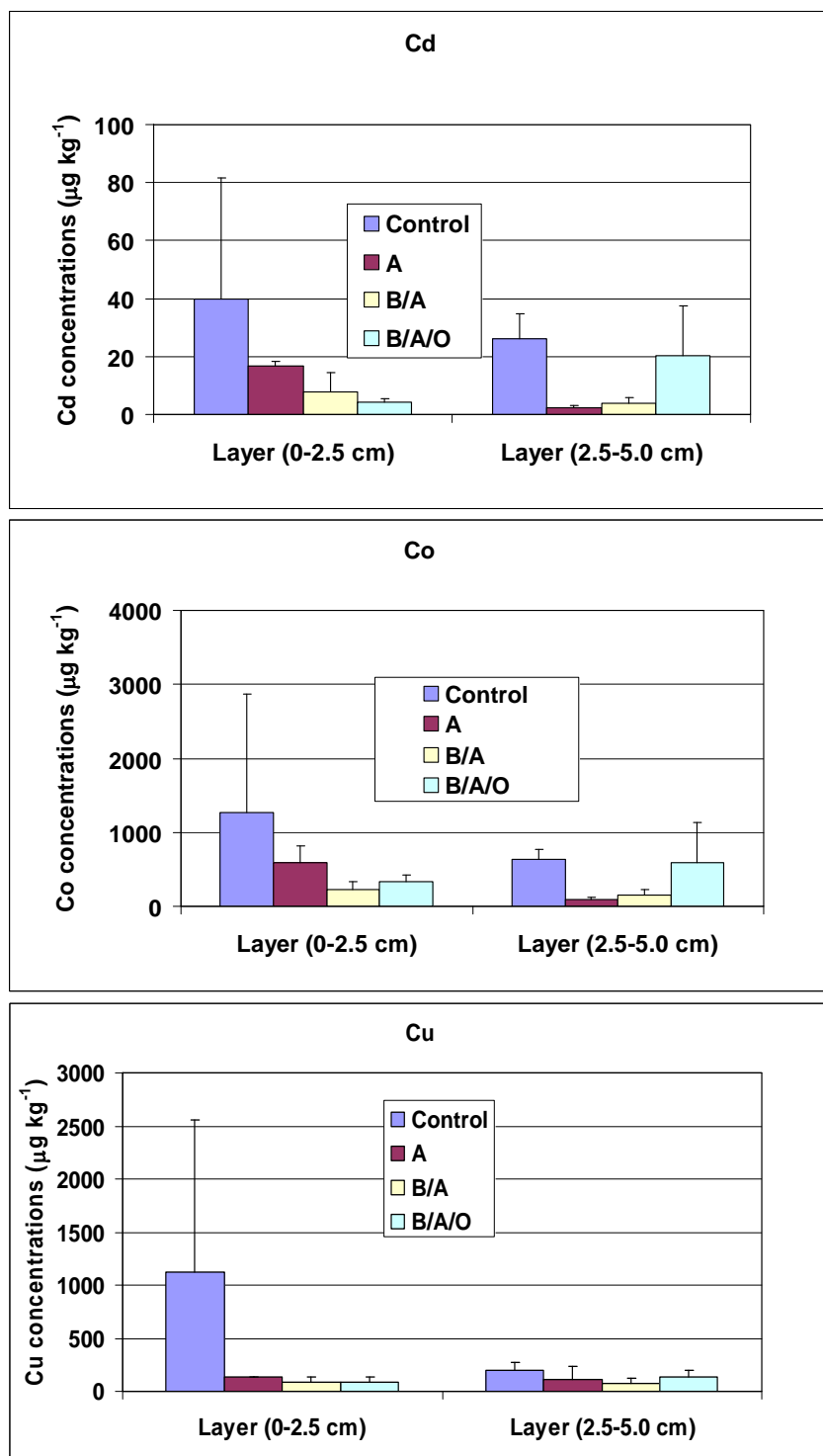


Figure 115. Double Acid Extractions of Metals from Sediment Layers beneath the Caps – Six Month Evaluation; A- apatite cap, B/A – biopolymer/apatite cap, and B/A/O – biopolymer/apatite/organoclay cap.

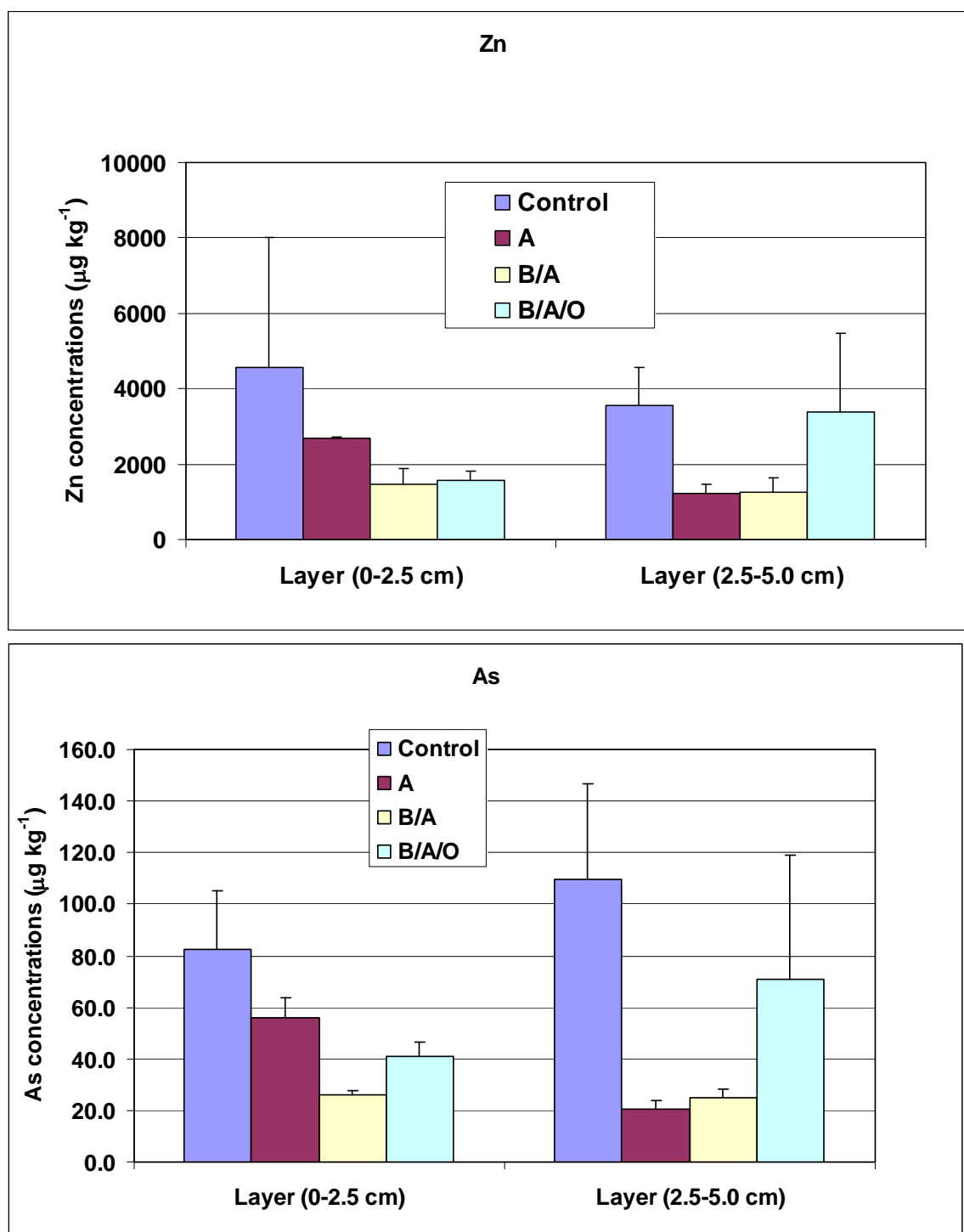


Figure 116. Double Acid Extractions of Metals from Sediment Layers beneath the Caps – Six Month Evaluation; A- apatite cap, B/A – biopolymer/apatite cap, and B/A/O – biopolymer/apatite/organoclay cap.

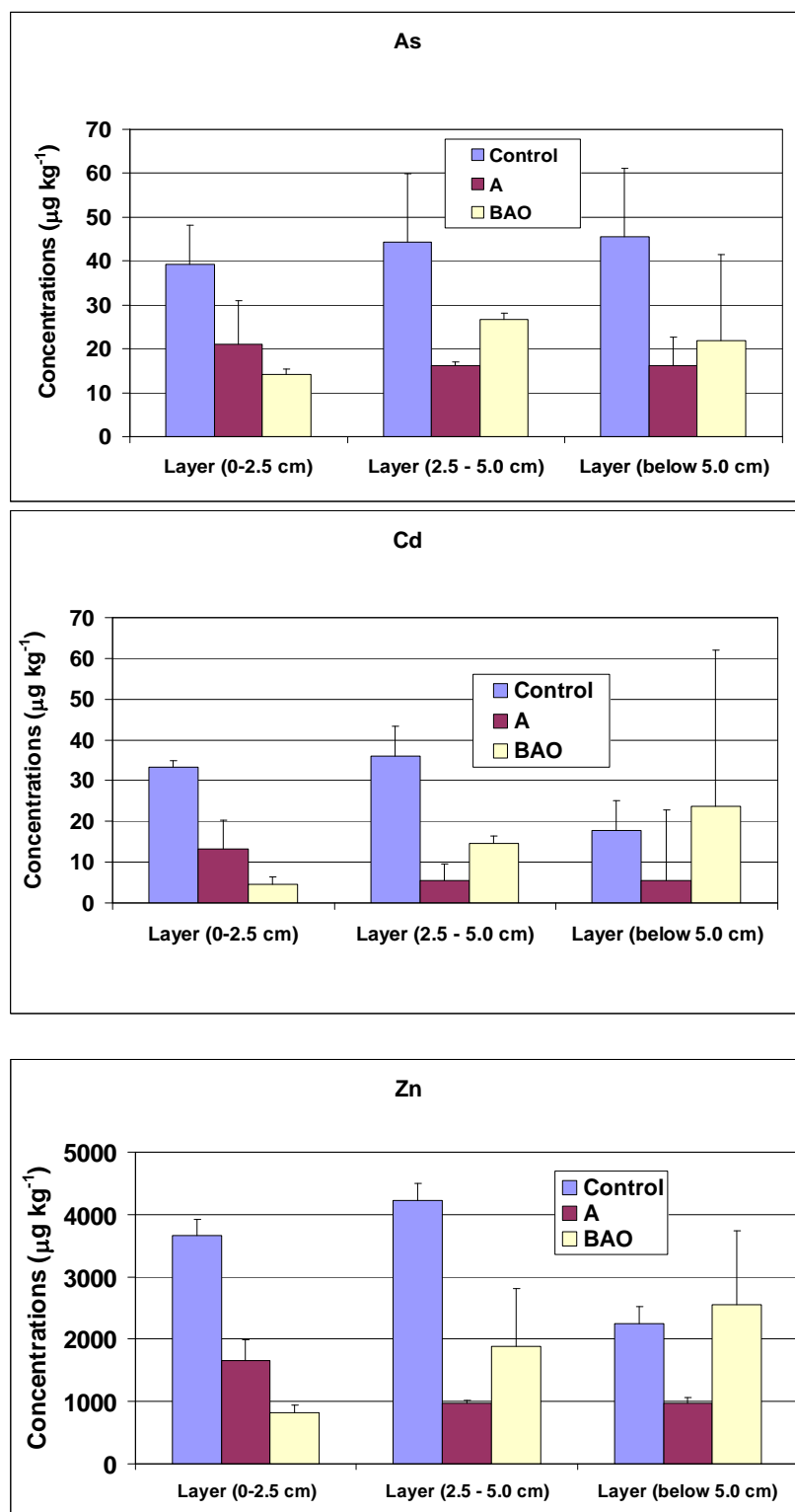


Figure 117. Double Acid Extractions of Metals from Sediment Layers beneath Caps – 12 Month Evaluation; A- apatite cap, B/A – biopolymer/apatite cap, and B/A/O – biopolymer/apatite/organoclay cap.

Effect of Active Caps on Metal Bioavailability – Comparison of DGT Probes and Pore Water Results

Sediment and water DGT probes were evaluated in the field for determination of the bioavailable pool of metals (Picture 21). DGT results collected directly in the field agreed with DGT results collected from sediment cores held under controlled conditions in the lab (Figure 118). For most elements, metal concentrations in pore water collected in the field were slightly higher than metal concentrations measured by DGT. Exceptions included Pb and Zn (Figure 118).

Generally, metal concentrations in pore water samples and measured in-situ by DGT were lower beneath the apatite cap than in untreated sediment (Figure 119). The ANOVA of the DGT data indicated that DGT measurements generated in the field did not differ significantly from DGT measurements generated in the laboratory, thus confirming the comparability of in-situ and ex-situ DGT data (Table 49 and Figure 118). More research is needed, but these preliminary results indicate that DGT methods can be used successfully on ex-situ sediment cores including deep cores collected from below sediment caps. Not surprisingly, the main effect of “metal” was significant ($P < 0.001$) indicating that concentrations differed among metals. Of greater interest was a significant ($P < 0.001$) interaction between metal and treatment, indicating that the apatite caps lowered sediment pore water concentrations for some metals but not others. Specifically, concentrations of cobalt, copper, zinc, and lead were lower in the sediments beneath the apatite caps than in the sediments from the control plots; whereas concentrations of other metals did not differ between treatments (Figure 119).

The ANOVA of the DGT results and results from analysis of pore water samples collected with sippers indicated that the main effects of treatment (apatite cap vs. control plot), sample type (DGT vs. pore water samples) and metal were all significant ($P = 0.012$ or less) (Table 50). There were also significant two-way interactions between treatment and sample type ($P = 0.023$) and between sample type and metal ($P < 0.001$). These results show that the DGT measurements differed from the pore water measurements, and that these differences were inconsistent among metals and between treatments. Specifically, metal concentrations in pore water samples were somewhat higher than metal concentrations measured by DGT with the exceptions of Pb and Zn (Figures 118 and 119). Additionally, pore water measurements tended to indicate greater differences between treatments than did DGT measurements.

Table 49. Analysis of Variance of Metal Concentrations Measured by DGT in Sediment from Apatite Caps and Control Plots. Data were collected from the field (i.e., with DGT probes deployed in-situ) and from sediment samples maintained in the laboratory.

Source	Type III SS	df	Mean Squares	F-ratio	p-value
Treatment (apatite vs. control)	0.158	1	0.158	3.541	0.065
Location (laboratory vs. field)	0.008	1	0.008	0.181	0.672
Metal	58.644	6	9.774	218.842	0.000
Treatment * Location	0.023	1	0.023	0.512	0.477
Treatment * Metal	2.788	6	0.465	10.406	0.000
Location * Metal	0.126	6	0.021	0.468	0.829
Treatment * Location * Metal	0.225	6	0.038	0.840	0.544
Error	2.501	56	0.045		

Table 50. Analysis of Variance of Metal Concentrations Measured by DGT and by Collection of Pore Water Samples Using Sippers. Data were collected from sediments located beneath apatite caps and from control plots with untreated sediment.

Source	Type III SS	df	Mean Squares	F-ratio	p-value
Treatment (apatite vs. control)	0.365	1	0.365	12.886	0.001
Sample type (DGT vs. pore water)	0.186	1	0.186	6.557	0.012
Metal	13.889	6	2.315	81.665	0.000
Treatment * Sample type	0.151	1	0.151	5.329	0.023
Treatment * Metal	0.309	6	0.052	1.819	0.103
Sample type * Metal	1.965	6	0.327	11.552	0.000
Treatment * Sample type * Metal	0.231	6	0.039	1.359	0.239
Error	2.778	98	0.028		



Picture 21. Sediment DGT Probe.

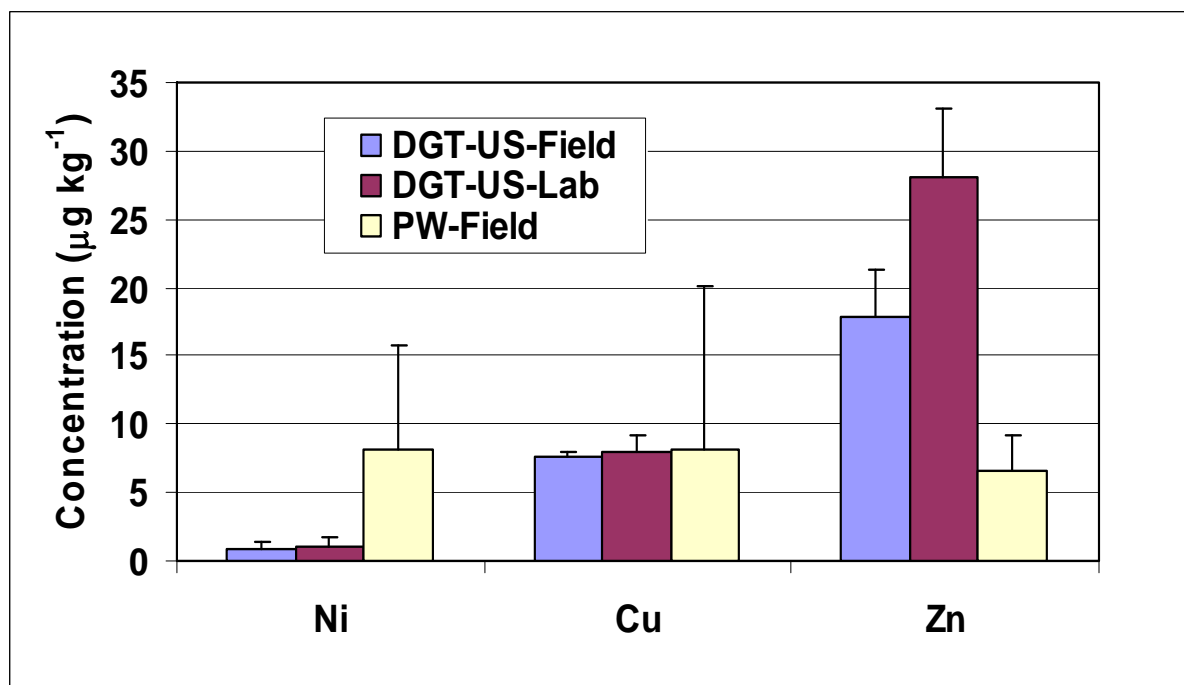
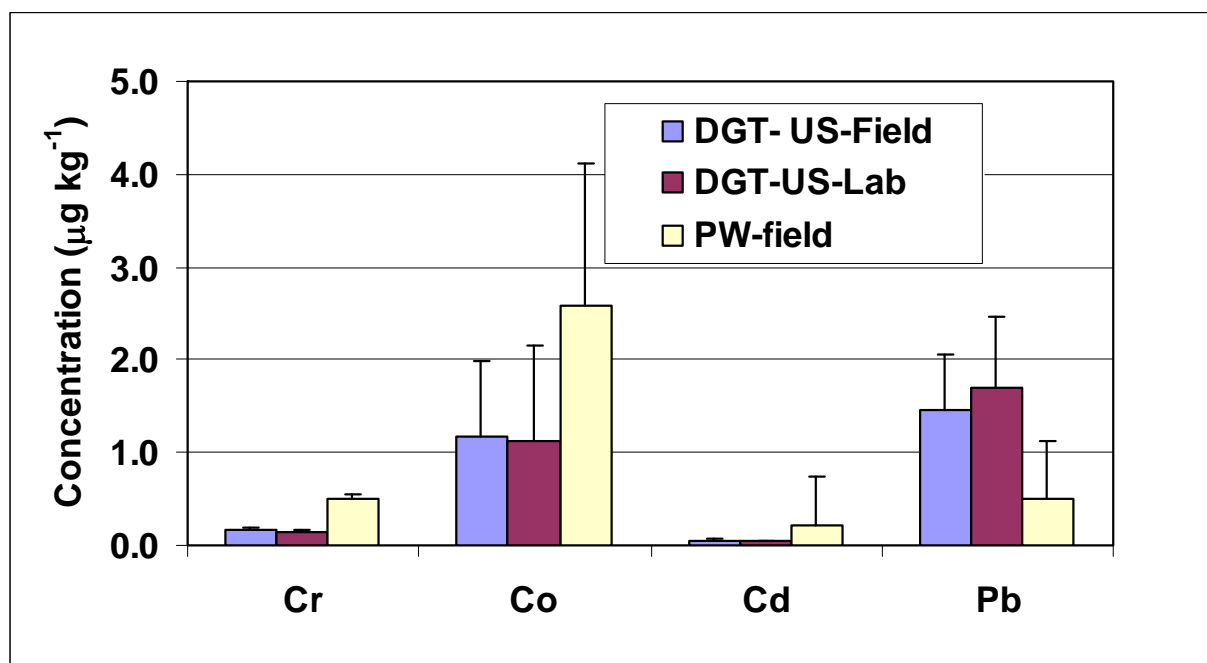


Figure 118. Metal Concentrations Measured by Field and Laboratory DGT and in Pore Water Collected with Sippers in Field; US – untreated sediment, PW – pore water.

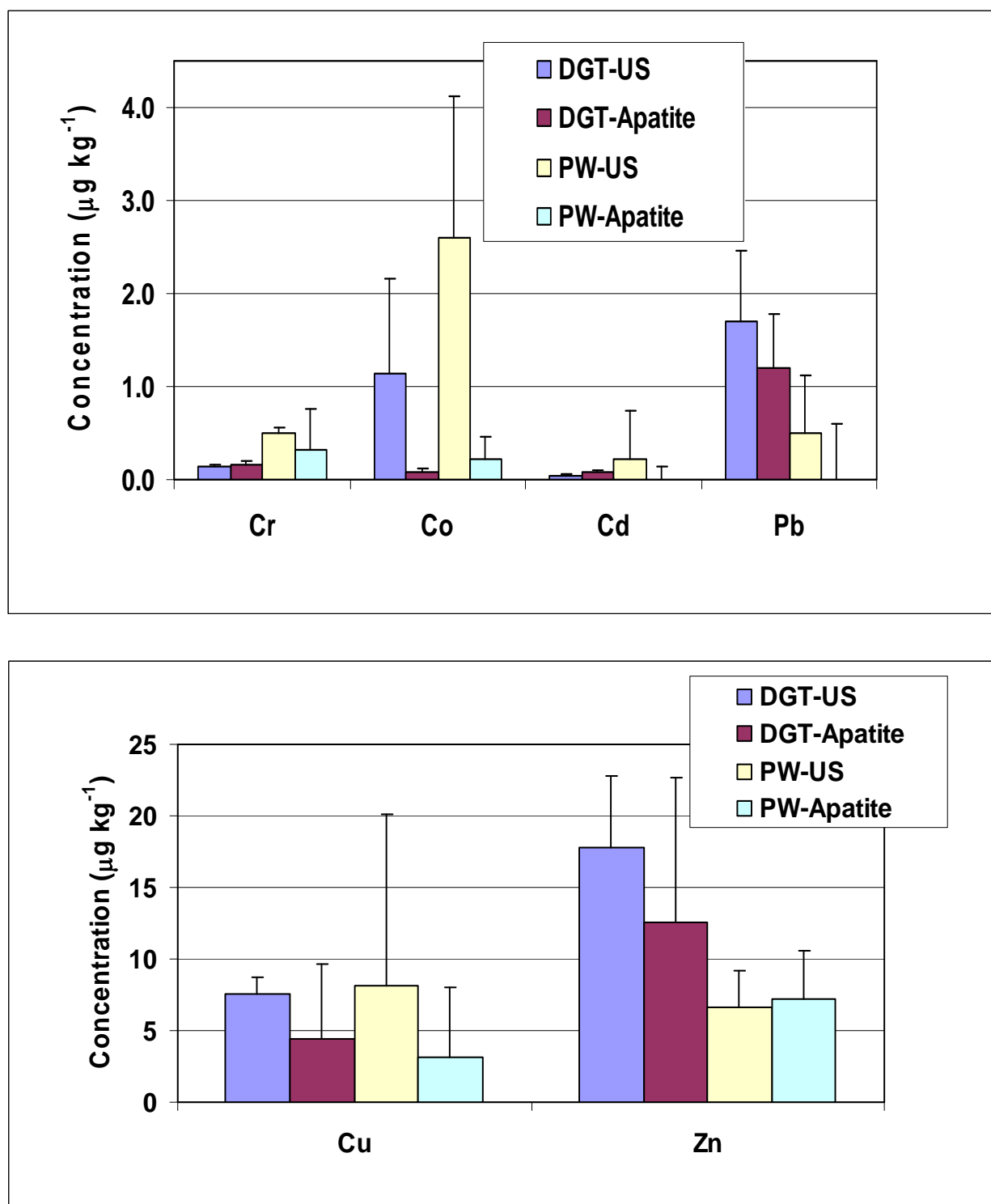


Figure 119. Effect of Apatite Active Cap on Metals in Sediments – DGT in Comparison with Pore Water Results; US – untreated sediment, PW – pore water.

Cap Erosion

Cap erosion was determined by measuring the following variables: visual examination of the stream bottom, assessment of the composition of core samples from the experimental caps, cap dimensions, and concentrations of carbon and phosphorus in sediments outside the plots.

Visual examination of the stream bottom sediment in and around the test plots was conducted every week, for four weeks and then every month. Generally, the caps placed in areas of high flow (0.9-1.2 fps) showed substantial erosion within the first month. The apatite/sand cap eroded the fastest, and material from this cap was transported up to 20 feet downstream within one month (Table 51, Picture 22). However, the caps with sand mixed with biopolymer as the top layer, showed no movement of the lower layers composed of apatite or organocay/sand. The caps located in depositional areas with flow rates under 0.4 fps showed little evidence of erosion during the first six months (Table, Pictures 23 and 24).

Assessment of cores taken from the capped plots helped determine if materials were being removed from the cap surface by erosion or if stream sediments were being deposited on the surface of the cap. In high flow areas, the deposition of native sediments on the top of caps varied from 1 inch in some locations to 5 inches in others. Deposition was unrelated to cap type, but rather was associated with flow rate and the location of the cap in the stream channel. In the first quarter of the year there were at least 3 storm events during which stream flow exceeded 3 fps. The plots in depositional areas with flows generally under 0.4 fps showed small or marginal deposition of native sediment on top of the caps even after heavy storms.

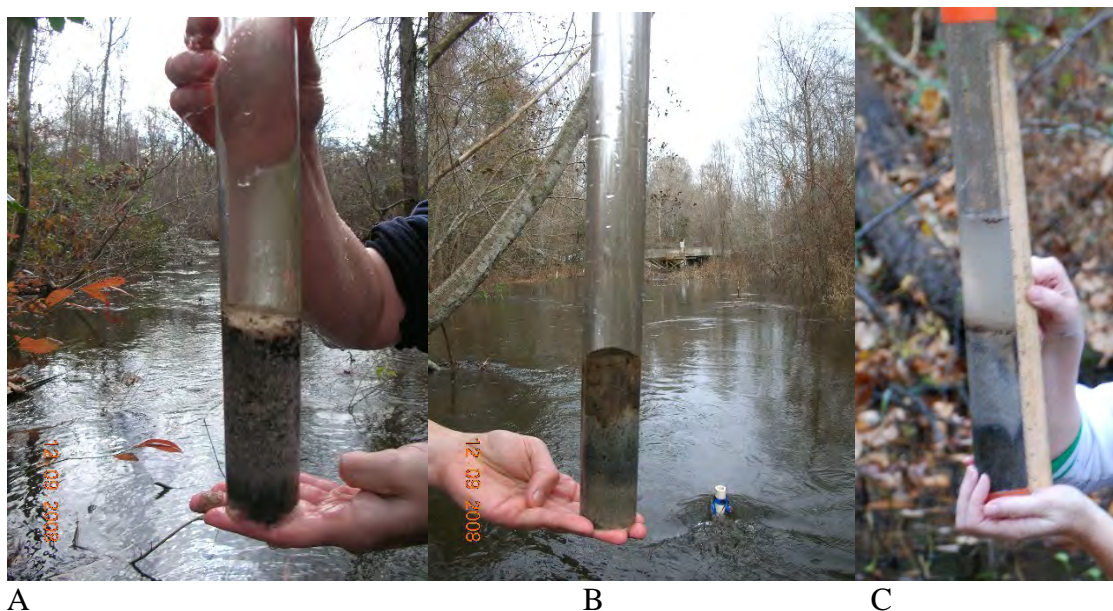
After two months, caps with a top layer of biopolymer/sand started to show evidence of degradation in both high flow and low flow (depositional) areas. These field data are consistent with the laboratory evaluation of biopolymer xanthan/guar gum by the ASSET flume, which showed that this biopolymer began to degrade after two months. Although the top layer of the biopolymer caps showed erosion after two months, examination of cores samples showed that the biopolymer prevented movement of the material beneath the biopolymer layer. This was also suggested by P concentrations in pore water collected outside of the biopolymer/apatite/sand cap, which were lower than the P concentrations in the pore water outside of the apatite/sand cap. This difference suggested faster erosion of apatite when it was not protected by a biopolymer layer.

Table 51. Twelve month Evaluation of Cap Thickness; A/S- apatite/sand cap, B/A – biopolymer/apatite sand cap, and B/A/O – biopolymer/apatite/organoclay sand cap.

		Weeks					Months								
Plot #	Replicates	0 cm	1 cm	2 cm	3 cm	4 cm	1 cm	2 cm	3 cm	4 cm	5 cm	6 cm	9 cm	12 cm	
High Flow Areas															
2 (B/A)	2-1	15.0	15.2	14.0	14.5	13.7	14.4	13.0	14.0	10.0	8.0	6.0	5.0	4.0	
	2-2	15.0	14.5	14.0	13.8	13.5	14.0	12.5	11.5	9.0	7.5	5.0	6.0	2.0	
	2-3	15.7	15.9	15.3	15.0	14.0	15.1	13.0	12.0	8.5	8.0	6.0	6.0	4.0	
	2-4	14.7	14.3	14.6	14.5	13.5	14.2	13.0	10.0	4.0	5.0	0.0	0.0	1.0	
		15.1	15.0	14.5	14.5	13.7	14.4	12.9	11.9	7.9	7.1	4.3	4.3	2.8	
7 (B/A/O)		0.4	0.7	0.6	0.5	0.2	0.5	0.3	1.7	2.7	1.4	2.9	2.9	1.5	
	7-1	15.0	14.5	14.0	14.2	13.7	14.1	12.5	10.0	9.5	7.0	6.0	4.0	2.0	
	7-2	14.8	15.0	14.0	13.8	13.5	14.1	13.2	12.0	11.0	6.0	6.0	5.0	2.0	
	7-3	15.0	14.7	14.2	13.0	13.0	13.7	13.0	10.5	3.0	1.0	0.0	0.0	0.0	
	7-4	14.6	14.3	13.8	13.5	13.0	13.7	12.0	9.5	8.0	4.0	4.0	3.0	3.0	
1 (A/S)		14.9	14.6	14.0	13.6	13.3	13.9	12.7	10.5	7.9	4.5	4.0	3.0	1.8	
		0.2	0.3	0.2	0.5	0.4	0.2	0.5	1.1	3.5	2.6	2.8	2.2	1.3	
	1-1	15.0	12.5	10.0	8.3	8.0	9.7	7.5	6.0	4.9	5.0	4.5	3.0	3.0	
	1-2	15.0	11.0	9.5	8.0	6.8	8.8	6.0	5.5	5.0	4.0	3.0	2.0	2.5	
	1-3	15.4	10.0	8.5	7.5	6.2	8.1	5.5	4.5	4.0	3.0	4.0	2.0	2.0	
	1-4	14.8	9.5	9.0	7.5	6.5	8.1	5.0	5.0	5.0	6.0	5.5	1.5	1.5	
		15.1	10.8	9.3	7.8	6.9	8.7	6.0	5.3	4.7	4.5	4.3	2.1	2.3	
		0.3	1.3	0.6	0.4	0.8	0.8	1.1	0.6	0.5	1.3	1.0	0.6	0.6	
	Depositional Areas														
	4 (B/A)	4-1	15.0	15.0	14.5	14.0	13.7	14.3	14.0	13.7	14.0	12.5	12.0	14.0	15.0
4-2		15.0	14.5	14.0	13.8	13.5	14.0	13.5	13.0	12.0	12.0	12.5	13.0	7.0	
4-3		15.7	15.2	15.3	15.0	14.0	14.9	15.0	13.6	12.5	13.0	12.0	11.0	10.0	
4-4		14.7	14.3	14.6	15.0	16.0	15.0	16.0	12.5	12.5	12.0	13.0	10.0	11.0	
		15.1	14.8	14.6	14.5	14.3	14.5	14.6	13.2	12.8	12.4	12.4	12.0	10.8	
8 (B/A/O)		0.4	0.4	0.5	0.6	1.2	0.5	1.1	0.6	0.9	0.5	0.5	1.8	3.3	
	8-1	15.0	14.5	14.0	14.2	14.0	14.2	15.0	13.0	12.0	13.0	12.5	12.0	12.0	
	8-2	14.8	15.0	14.0	15.0	13.5	15.0	16.0	12.8	11.5	12.0	12.0	13.0	12.0	
	8-3	15.0	14.7	15.0	14.0	15.0	14.7	14.5	12.3	13.0	12.0	12.0	12.0	9.0	
	8-4	14.6	14.3	13.8	15.0	13.5	14.2	13.0	12.5	12.0	11.0	10.5	3.0	15.0	
3 (A/S)		14.9	14.6	14.2	14.6	14.0	14.5	14.6	12.7	12.1	12.0	11.8	10.0	12.0	
		0.2	0.3	0.5	0.5	0.7	0.4	1.3	0.3	0.6	0.8	0.9	4.7	2.4	
	3-1	15.0	14.5	14.0	14.2	13.7	14.1	14.0	12.5	13.0	12.5	13.0	9.0	11.0	
	3-2	15.0	15.0	14.0	13.8	13.5	14.1	14.0	12.8	12.0	11.8	12.0	13.0	12.0	
	3-3	15.4	14.7	16.0	14.0	13.5	14.6	15.0	13.0	12.5	12.0	11.0	13.0	10.0	
	3-4	14.8	14.3	13.8	16.0	15.0	16.0	14.5	13.0	13.0	13.0	11.0	12.0	11.0	
		15.1	14.6	14.5	14.5	13.9	14.7	14.4	12.8	12.6	12.3	11.8	11.8	11.0	
		0.3	0.3	1.0	1.0	0.7	0.9	0.5	0.2	0.5	0.5	1.0	1.9	0.8	



Picture 22. One Layer Cap Composed of Apatite (50%) and Sand (50%) in Creek Channel with High Flow One Month after Deployment. Erosion of the plot was visible within the first week (Picture A). After one month the cap material was transported up to 20 feet (Picture B) and about one or two inches of native sediment was deposited on the top of cap.



Picture 23. Sediment Cores from Caps in Depositional Areas (Flow Rate Lower than 0.4fps) after Two Months: A) plot #3 – Apatite/Sand cap; B) plot #4 – Biopolymer/Apatite/Sand cap; C) plot #8 – Biopolymer/Apatite/Organoclay/Sand. Two months after cap placement, the cap thickness in all plots in depositional areas was about 6 inches.



Picture 24. Sediment Cores Collected from Depositional Areas after Six Months - biopolymer/apatite/organoclay/sand cap (A), apatite/sand cap (B), and biopolymer/apatite/sand cap (C).

Cap Erosion – Field Evaluation by Adjustable Shear Stress Erosion Transport (ASSET) Flume

Erosion rate data have been collected for eight core samples, two from control plots (native sediment; samples 1 and 2), three from the biopolymer/apatite/organoclay/sand plot (samples 3, 4, and 5), and three from the apatite/sand plot (samples 6, 7, and 8). The data are presented as erosion rates and critical shear stresses for the initiation of erosion as a function of depth from the sediment surface. The non-linear relationship between erosion rate and bed shear stress can make it difficult to quantify variability in the erosion behavior within a single core and between many cores. As such, the data are also presented in the form of an erosion rate ratio that produces a single numerical value for a particular erosion rate data series that accounts for this non-linear relationship. The erosion rate ratio is used to make direct comparisons between erodibility within a single core (i.e., to identify changes with depth), between similar cores, and between all tested cores to aid in the identification of the most erosion resistant cap material.

In this analysis, each core was sub-sampled into separate depth intervals. Following the methods of Roberts et al. (1998), Roberts and Jepsen (2001), and Jepsen et al. (1996 and 1997), the erosion rate for each depth interval can be approximated by a power law function of sediment density and applied shear stress. Non-cohesive sediments do not show variation of erosion rate with density, therefore the density term is dropped. For each depth interval, the measured erosion rates and applied shear stress were calculated using equation 17.

From this analysis an average erosion rate for the entire core was also determined, and the erosion rate at each depth interval was directly compared to this average. The results are an erosion rate ratio which provides an estimation of the erosion susceptibility of each depth interval relative to the core average. In addition, an average erosion rate of similar cores and for all cores was determined. Also, the erosion rate for each depth interval within a core as well as each cores average erosion rate was compared to the specified average.

Figure 120 compares the erosion rate of each depth interval for each core as well as the core average erosion rate with the average erosion rate for all sediment cores tested. For clarity, Figure 121 re-plots only the core average erosion rate compared with the average erosion rate for all cores. Figure 128 further refines Figures 121 and 122 by comparing the average erosion rate of the three different material types to the overall average across all material types.

Generally, there was little difference between the average erosion rates of the cores and material types. For example, all cores and material types have an average erosion rate that differed from the overall mean by a factor of two or less. The results indicated that the cap most resistant to erosion was the cap with apatite and sand, which became increasingly harder to erode with depth.

The results from the erosion tests in the field are consistent with the laboratory evaluation of biopolymers. In the laboratory and field, long-term (six months or more) tests of the biopolymers

showed that guar gum cross-linked with xanthan (Kelzan) became less erosion resistant after two months. Therefore, the application of xanthan/guar gum in the field as the top layer of an active cap is beneficial for a short time for erosion resistance. Another benefit of biopolymer is during the construction of caps. In this study, biopolymers reduced sediment suspension and facilitated the settling of other amendments that were placed below the biopolymer layer. A remaining benefit of biopolymer addition was an increased pool of carbon in the sediment beneath the caps and lower release of metals and other elements, especially P, in comparison with apatite only. However, more research is needed on the type of biopolymer to apply to caps and the best way to deliver biopolymers to caps. A three layered cap composed of biopolymer on the top, apatite in middle, and organoclay on the bottom, is not ideal for biopolymer interaction with other amendments, which could serve as cross-link reagents. A very important aspect of biopolymer application in remedial work concerns the biodegradability of biopolymers, especially under extreme aquatic conditions (e.g., high summer temperature; changeable ratio of Fe-S-P in sediment, pore and surface water chemistry; and other factors).

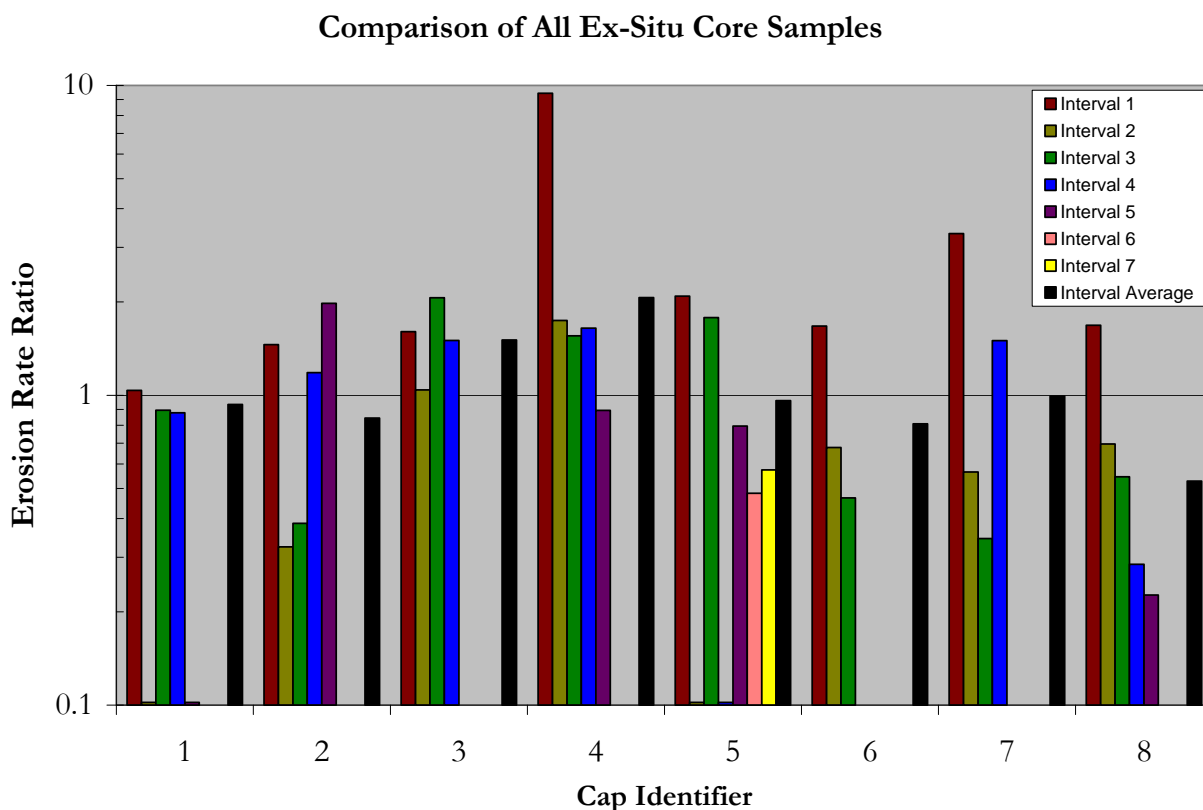


Figure 120. Erosion Rate Ratio - Comparison of All Samples: control plot – samples 1 and 2; biopolymer/apatite/organoclay plot – samples 3, 4, and 5; apatite/sand plot – 6, 7, and 8.

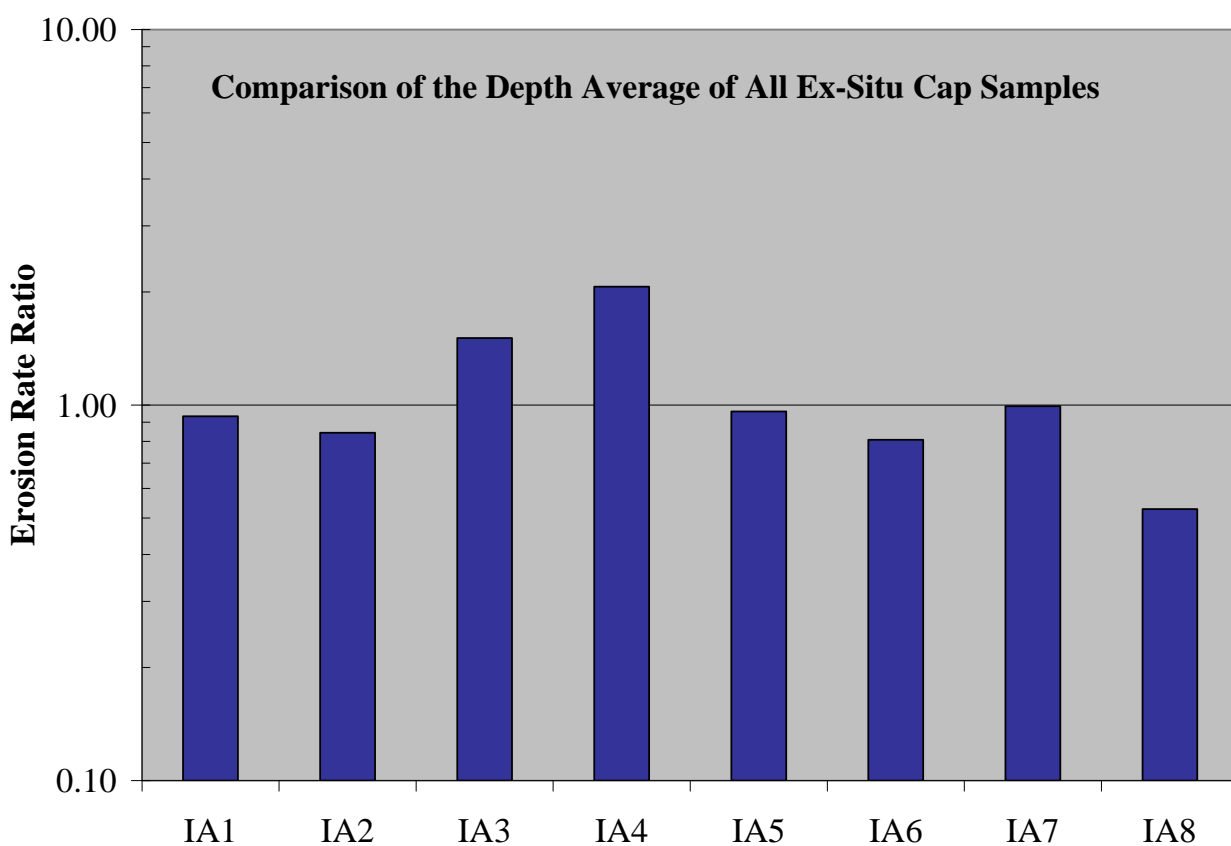


Figure 121. Erosion Rate Ratio - Comparison of the Depth Average for all Samples: control plot – samples 1 and 2; biopolymer/apatite/organoclay plot – samples 3, 4, and 5; apatite/sand plot – 6, 7, and 8; A – average.

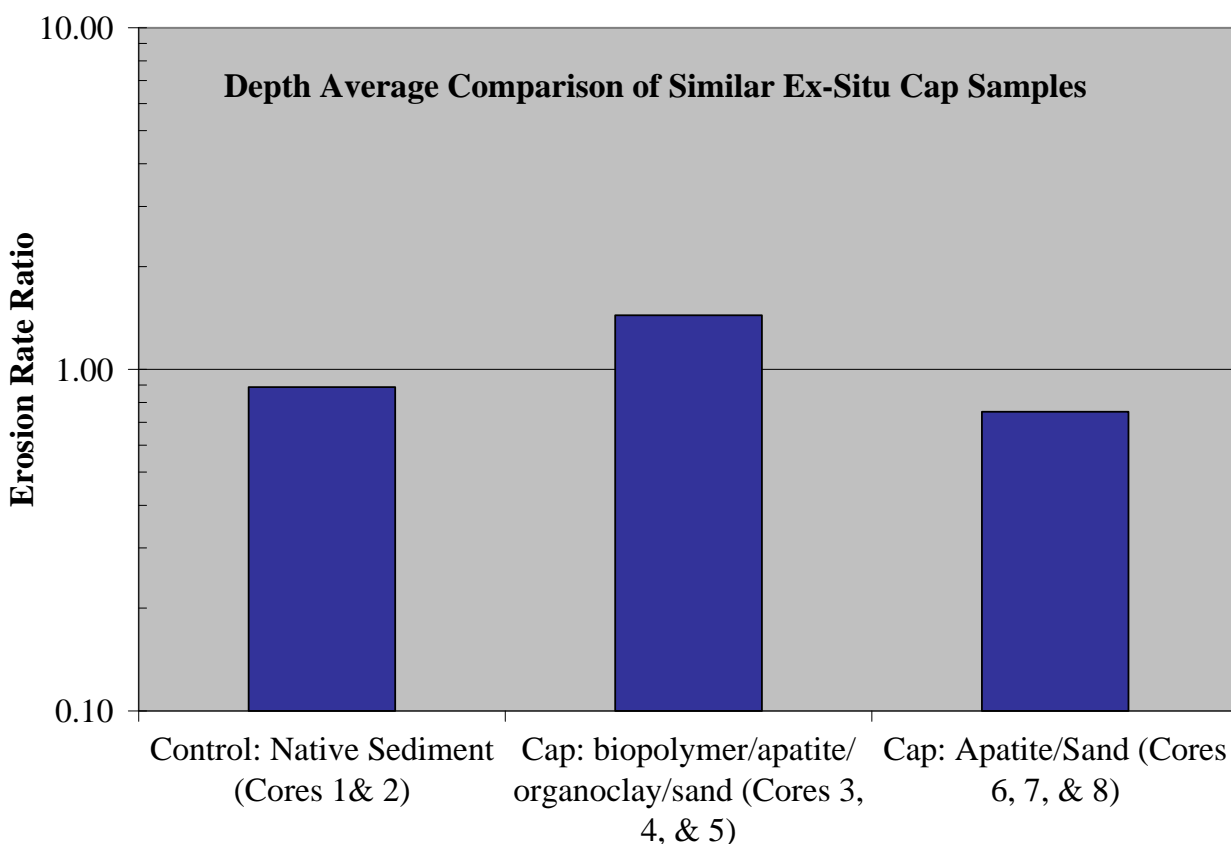


Figure 122. Erosion Rate Ratio - Comparison of Material Types: native material (control plot – samples 1 and 2), biopolymer/apatite/organoclay material (samples 3, 4, and 5) and apatite/sand material (samples – 6, 7, and 8).

Active Biomonitoring

The scope of this study was limited to determining whether likely active cap amendments were directly harmful to benthic organisms. However, there are other issues regarding the effects of active cap amendments on aquatic life. Amendments might provide less than optimal substrate for colonization by benthic organisms because of particle size, texture, or other physical characteristics. This would not be surprising because even slight variations among natural substrates can have large impacts on the structure of benthic assemblages. Avoidance of capped areas by benthic organisms could be beneficial. However, if full restoration of the benthic community is desirable, it may be necessary to provide a superposed “habitat layer” of natural substrate over the amendments that comprise the active cap.

The survival of benthic organisms was assessed in amendments used in pilot-scale caps constructed in Steel Creek, located on the Savannah River Site. Three types of benthic organisms including *Hyaella azteca*, *Lumbriculus variegatus*, and the Asiatic clam *Corbicula fluminea* were held in small screened cages that were partially buried within caps composed of 50% apatite and 50% sand (Plot 3); 2.5% biopolymer (guar gum and xanthan), 50% apatite, and

47.5% sand (Plot 4); biopolymer, apatite, organoclay, and sand in three layers (Plot 8); and in a control plot composed of Steel Creek sediment (Plot 5). Four cages were placed in each cap except for the biopolymer, apatite, organoclay, and sand cap (Plot 8). Eight cages were placed in the latter: four cages within the 2.5% biopolymer, 50% apatite, and 47.5% sand layer and four cages within the 25% organoclay and 75% sand layer.

Active biomonitoring was initiated on November 13th, 2008 by placing *Lumbriculus variegatus* (about 2.0 g) in 15 cm long, 2.5 cm diameter screened cages along with amendments or native substrates similar to those in the caps (or control plot) in which the cages were placed. Percent recovery of California blackworms *Lumbriculus variegates* after 28 days in the field averaged 84% in cages from Plot 5 (native sediment), 90% in cages from Plot 3 (apatite and sand), 68% in cages from Plot 8 (organoclay and sand layer), 36% in cages from Plot 8 (biopolymer, apatite, and sand), and 26% in cages from Plot 4 (biopolymer, apatite, and sand) (Figures 123 and Picture 25). Analysis of variance indicated that these differences were significant ($P < 0.05$). The lowest recovery and greatest inter-replicate variability occurred among cages that contained substrates with biopolymers (Figure 123). Examination of blackworms recovered from cages with such substrates suggested that only individuals that remained on or near the substrate surface were able to survive. Additional examination of blackworms in the laboratory indicated they were unable to efficiently burrow through biopolymers because of the high viscosity of these materials.

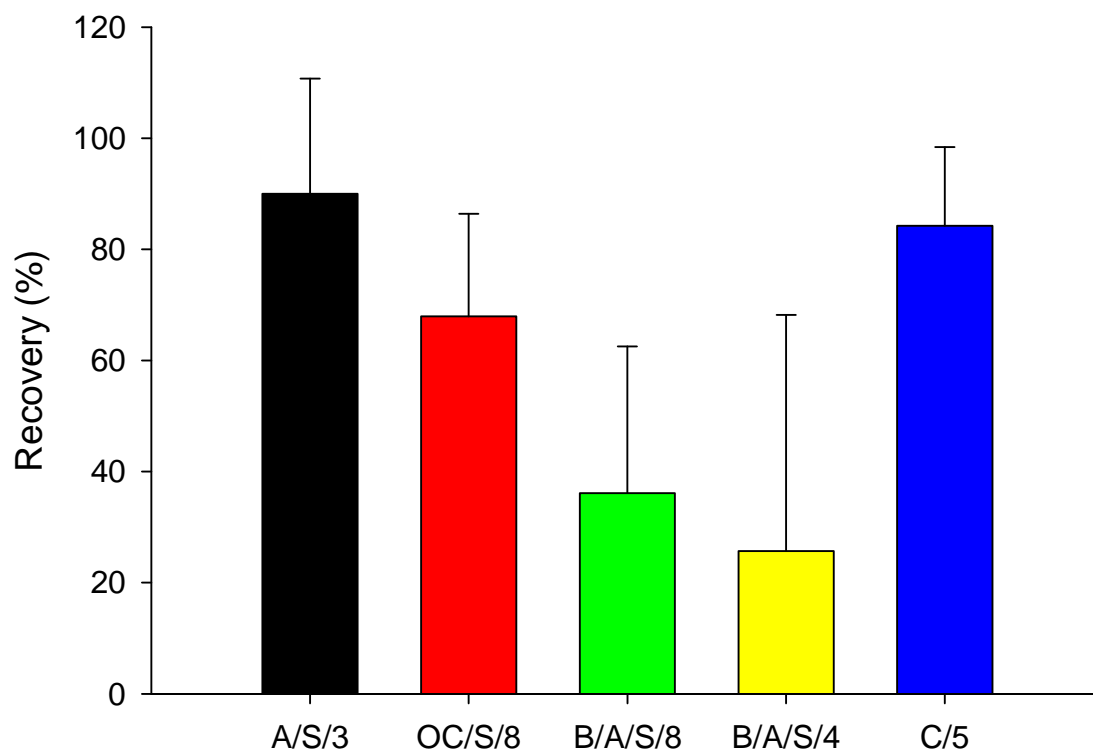
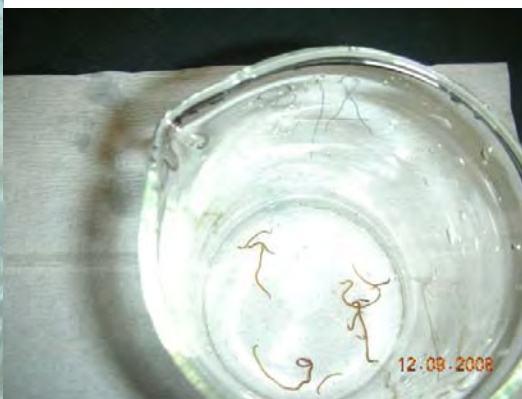


Figure 123. Percent Recovery (average and standard deviation, n=4) Based on Aggregate Weight of California Blackworms Held for 28 Days in Screened Cages Buried within Experimental Active Caps composed of Different Materials (A/S/3 = apatite and sand, Plot 3; OC/S/8 = organoclay and sand, Plot 8; B/A/S/8 = biopolymer, apatite, and sand, Plot 8; B/A/S/4 = biopolymer, apatite, and sand, Plot 4; C/5 = natural substrate, Control Plot 5).



Control



B/A/S cap



B/A/S cap



A/S cap



O/S cap

Picture 25. **California Blackworms after One Month of Exposure to Amendments in Field;**
 B/A/S – biopolymer/apatite/sand; A/S – apatite/sand; O/S – organoclay/sand.

The field study results indicated that blackworm survival was depressed in substrates that contained biopolymers, probably because of physical effects rather than chemical toxicity. These physical effects may have been related to suffocation following entrapment of the worms in the biopolymer matrix. These results contrast with the results of previously conducted sediment bioassays with the amphipod *Hyaella azteca*, which showed no mortality in the presence of biopolymer coated sand (Paller and Knox, 2010). This difference may be related to the behavior of these organisms. California blackworms live by burrowing within sediments. In contrast, *Hyaella* is epibenthic and can live on the sediment surface rather than within the sediments (Wang et al., 2004), thereby avoiding entrapment within the biopolymer matrix. Additional laboratory studies focusing on the relative behaviors of these organisms on biopolymer substrates will be required to test this hypothesis.

Another difference between California blackworms and *Hyaella* is that the latter was more sensitive to organoclay, showing significant mortality in sediments mixed with as little as 5% organoclay. In contrast, blackworms were not significantly affected by up to 20% organoclay. These results were similar to those obtained with another annelid worm, *Ilyodrilus*, which did not exhibit significant mortality in sediments mixed with as much as 50% organoclay (Knox et al., 2007). This difference is likely a consequence of the greater sensitivity of *Hyaella*, which is known to be affected by a variety of chemicals (Wang et al., 2004).

Survival of the bivalve *Corbicula fluminea* held for four weeks in cages within the experimental plots in Steel Creek averaged 97.5% in native sediment in control plot 5; 97.5% in apatite and sand in plot 3; 35% in biopolymer, apatite, and sand in plot 4; 97.5% in the organoclay and sand layer in plot 8; and 25% in the biopolymer, apatite, and sand layer in plot 8 (Figure 124). These differences in survival were statistically significant ($P < 0.05$), with the lowest survival in substrates that contained biopolymers. Differences in average weight among surviving clams from different caps or cap layers were not significant indicating no discernable differences in growth. However, the potential for growth during the study period was minimal because of low ambient temperatures.

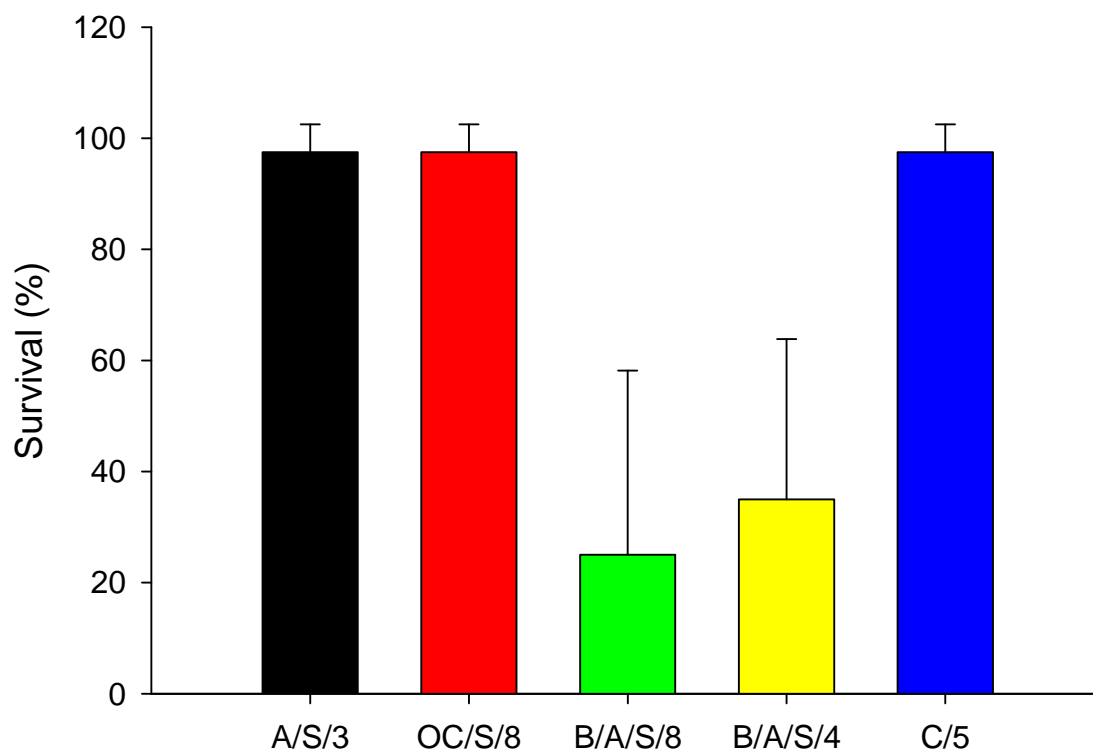


Figure 124. Survival of *Corbicula fluminea* Held in Cages within Experimental Active Caps in Steel Creek (A = apatite, OC = organoclay, S = sand, B = biopolymer, C = control [native sediment], numbers refer to plot designations).

Survival of *Hyalella azteca* held for nine days in cages within the plots in Steel Creek averaged 85.0% in native sediment in control plot 5; 67.5% in apatite and sand in plot 3; 45% in biopolymer, apatite, and sand in plot 4; 85% in the organoclay and sand layer in plot 8; and 52.5% in the biopolymer, apatite, and sand layer in plot 8 (Figure 125). The lowest survival occurred in substrates that contained biopolymers; however, differences in survival among plots were not statistically significant ($P < 0.05$).

The results observed with all organisms indicated that only caps containing biopolymer were associated with significant mortality as a likely result of physical entrapment and/or suffocation in the viscous biopolymer matrix. Organisms held in caps containing apatite or organoclay mixed with sand did not suffer significant mortality suggesting that apatite and organoclay are unlikely to have deleterious effects when applied in the proportions used in this study. The results of these field studies differed from the results of previous laboratory bioassays conducted under this project, which showed that organoclay was toxic to the amphipod *Hyalella azteca*. This difference may be attributable to the greater sensitivity of *Hyalella* or to differences between laboratory and field conditions, in particular differences associated with continuous flow in the stream and static conditions in the laboratory.

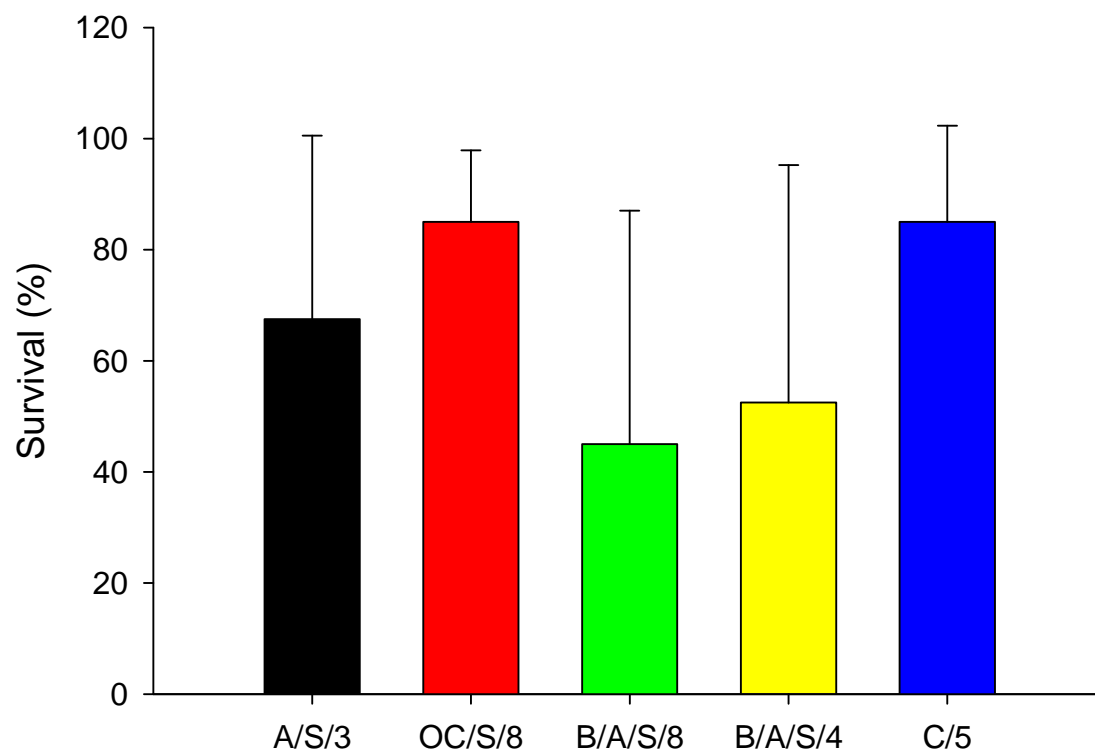


Figure 125. Survival of *Hyalella azteca* Held in Cages within Experimental Active Caps in Steel Creek (A = apatite, OC = organoclay, S = sand, B = biopolymer, C = control [native sediment], numbers refer to plot designations).

SUMMARY AND CONCLUSIONS

The laboratory studies of this project determined the best active cap materials, active cap composition, and the effects of active cap components on metal bioavailability, retention, and toxicity. Modeling procedures were used or developed to assess diffusive and advective transport through active caps composed of promising amendments. Procedures were developed for making biopolymer materials, and the basic physical properties of several biopolymer materials were assessed and compared. Specific conclusions from the laboratory studies include the following:

- Apatite, organoclays, and the biopolymer, chitosan, are effective amendments for removing metals from both fresh and salt water. They also exhibit high retention (80% or more) of most metals indicating reduced potential for remobilization of contaminants to the water column
- Organoclays are the best amendment for containing organic contaminants. Kinetic studies showed long-term retardation of contaminant migration through a layer of organoclay
- After comparing more than 20 biopolymer products, chitosan/guar gum cross-linked with borax and xanthan/chitosan cross-linked with calcium chloride were identified as having potential for inclusion in active caps to produce a barrier that resists erosion
- Active caps composed of apatite or organoclay can delay contaminant breakthrough due to diffusion by hundreds or thousands of years when compared with passive caps composed of sand
- Biopolymer coated sand and NC apatite do not harm aquatic organisms, indicating the suitability of these material for aquatic applications. The EPA TCLP procedure showed that the amendments do not leach hazardous metals
- Results from bench-scale diffusion experiments showed that contaminants were released into the water from uncapped sediments after six months but not from capped sediments. These results confirmed modeling data, which showed that even sand can prevent metal release by diffusive transport over short time periods
- Bench-scale experiments on advective transport of metals through simulated caps composed of apatite and sand showed that all metals were sorbed by the apatite and breakthrough was delayed relative to sand
- A shaker and an Adjustable Shear Stress Erosion and Transport (ASSET) flume were used to evaluate the ability of biopolymers to improve the erosion resistance of active sediment caps. The shaker results showed that plain sand was easily resuspended with slight agitation, but slurries of biopolymer and sand or biopolymer, sand, apatite, and/or organoclay were resistant to erosion even with strong agitation. The ASSET flume test showed that XG Coyote (guar gum cross-linked with xanthan Coyote brand) and XG Kelzan (guar gum cross-linked with xanthan Kelzan brand) were very cohesive. After ten days of consolidation, XG

Coyote became easier to erode, but XCC (xanthan cross-linked with chitosan and calcium chloride), XG Kelzan, OXG (O-organoclay) Kelzan, and XG/AO Kelzan became harder to erode. XG Kelzan was selected for the field deployment based on erosion test results. The significant resistance of the slurry products to erosion shows promise for the application of these materials as a stand-alone active cap or as armament for other amendments

- Modeling approaches that incorporate the complexities of sediment cap systems were developed for the design and evaluation of sediment caps. Numerical models that estimate the required cap thickness to delay contaminant breakthrough for a specified time period for various flow rates constitute a cost effective tool for use in the design of active cap systems

Steel Creek at the Savannah River Site (SRS), Aiken, SC was chosen for a field deployment of the capping technologies developed in the laboratory. Steel Creek is a third order stream about 6-8 m wide and 30-40 cm deep during low flow conditions. Contaminant concentrations for several metals substantially exceed those in uncontaminated streams. The field deployment in Steel Creek, SRS, included eight plots with four treatments: two control treatments consisting of uncapped sediments (i.e., no amendments added); two caps composed of a single six inch layer of 50% apatite and 50% sand; two caps composed of two layers including a two inch layer of biopolymer/sand slurry over a four inch layer of 50% apatite and 50% sand; and two caps composed of three layers including a two inch top layer of biopolymer/sand slurry, a two inch middle layer of 50% apatite and 50% sand, and a two inch bottom layer of 25% organoclay and 75% sand. An aluminum frame was used to deflect downstream flow, reduce turbulence, and avoid loss of amendment materials during the construction of each cap. The leading edge of each cap was preceded by a sloped transition zone rising from the sediment to the top of the cap to prevent undercutting likely to occur with a vertical leading edge. Upper cap layers that contained low density materials, such as biopolymers, were applied as a slurry to prevent material separation and differential settling. After cap placement, sediment cores (5 per plot) were collected to confirm and characterize cap thickness. The average cap thickness was about 6 inches. The thickness of individual layers in the caps composed of three layers was about 2 inches. The test plots were evaluated for contaminant immobilization, environmental impact, and erosion for twelve months. Baseline sediment, surface water, and pore water samples from the test area were collected and characterized for metals and other parameters such as pH, total organic carbon, total inorganic carbon, and redox potential before cap deployment.

Specific conclusions from the field studies include the following:

- Metal concentrations in pore water within and beneath each cap even one year after cap placement were lower than metal concentrations in pore water collected before cap placement or outside the caps
- Active caps lowered SEM/AVS in the sediment beneath the caps resulting in substantially lower metal bioavailability during the one year test period

- Double acid extract data show that downward migration of the amendments used in active caps can neutralize contaminants located deeper in the sediment profile (i.e. in the zone of influence)
- The mobile pool of metals in remediated contaminated sediments can be successfully evaluated using SEM/AVS ratios, DGT sediment probes, and by measuring metal concentrations in pore water
- Short-term erosion tests (two months) revealed that biopolymers increased cap resistance to erosion. However, field studies showed that biopolymers were not physically stable after six months
- Addition of biopolymers reduced sediment suspension during cap construction and facilitated the rapid settling of other amendments that were placed below the biopolymer layer. Biopolymers also increased the pool of carbon in the sediment beneath the cap and lowered the release of some elements, especially P, in comparison with apatite only
- Active biomonitoring showed that all test organisms survived well in all experimental caps except those containing biopolymer (guar gum cross-linked with xanthan)

REFERENCES

- ACRI (Analytical & Computational Research, Inc.). 2004. *PORFLOW Version 5.0 User's Manual*, Revision 5, Analytical & Computational Research, Inc., Los Angeles, California.
- Adriano, D.C. 2001. Trace Elements in Terrestrial Environments. Biogeochemistry, Bioavailability, and Risk of Metals. Second Edition, Springer-Verlag, New York.
- Allen, H.E., Gongmin, F., Boothman, W., DiToro, D., and Mahony, J.D. 1991. Analytical Method for Determination of Acid Volatile Sulfide in sediment. Submitted to U.S Environmental Protection Agency, Office of Water, Washington, DC.
- Alther, G. 2002. Organoclays remove organics and metals from water, p. 223-231. *In* P.T. Kostecki, E.J. Calabrese, and J.Dragun (eds) Contaminated Soils, Vol.7, Amherst Scientific Publishers, Amherst, MA.
- Amacher, M.C. 1996. Nickel, cadmium and lead. P.739-768. *In* D.L. Sparks (ed.) Methods of soil analysis. Part 3. SSSA Book Ser. 5. SSSA, Madison, WI.
- American Society for Testing and Materials. 1993. Standard test method for 24-h batch-type measurement of contamination sorption by soils and sediments. Designation D 4646-87. ASTM, Philadelphia, PA.
- Barnett, M.O., Jardine, P.M., and Brooks, S.C. 2002. U(VI) adsorption to heterogeneous subsurface media: Application of a surface complexation model. *Environ. Sci. Technol.*, 36(5), 937-942.
- Benjamin, M.M. and Leckie, J.O. 1981. Multiple-site adsorption of Cd, Cu, Zn, and Pb on amorphous iron oxyhydroxide. *J. Colloid Interface Sci.*, 78, 209-221.
- Berkeley, R.C.W. 1979. Chitin, Chitosan and Their Degradative Enzymes. *In* Microbial Polysaccharides, eds. R.C.W. Berkeley, C.W. Goody and D.C. Elwood. Academic Press. New York.
- Berry, W.J., Hansen, D.J., Mahony, J.D., and Robson, D.L. 1996. Predicting the toxicity of metal-spiked laboratory sediments using acid-volatile sulfide and interstitial water normalizations. *Environ. Tox. Chem.*, 15(12), 2067-2079.
- Bertsch, P.M., Hunter, D.B., Sutton, S.R., Bajt, S., and Rivers, M.L. 1994. In situ chemical speciation of uranium in soils and sediments by micro X-ray absorption spectroscopy. *Environ. Sci. Technol.*, 28, 980-984.
- Bervoets, L., Meregalli, G., DeCooman, W., Goddeeris, B., and Blust, R. 2004. Caged midge larvae (*Chironomus riparius*) for the assessment of metal bioaccumulation from sediments in situ. *Environ. Tox. Chem.*, 23, 443-454.

Bilinski, H., Kozar, S., Plavsic, M., Kwokal, Z., and Branica, M. 1991. Trace metal adsorption on inorganic solid phases under estuarine conditions. *Mar. Chem.*, 32, 225-233.

Bodek, I., Lyman, W.J., Reehl, W.F., and Roseblatt, D.H. (editors). 1988. *Environmental inorganic chemistry, properties, processes, and estimation methods*. Pergamon Press, New York, NY.

Bostick, W.D., Stevenson, R.J., Jarabek, R.J., and Conca, J.L. 2003. Use of apatite and bone char for the removal of soluble radionuclides in authentic and simulated DOE groundwater. *Adv. in Environ. Res.*, 3(4), 488-498.

CCME. 2005. *Canadian Water Quality Guidelines*. Canadian Council of Ministers of the Environment, Winnipeg, Manitoba. (<http://www.ec.gc.ca/ceqg-rcqe/water.htm>)

Chen, X.B., Wright, J.V., Conca, J.L., and Peurrung L.M. 1997. Effect of pH on heavy metals sorption on mineral apatite. *Environ. Sci. Technol.*, 31, 624-631.

Chlopecka, A. and Adriano, D.C. 1996. Mimicked in situ stabilization of metals in a cropped soil: Bioavailability and chemical forms of Zn. *Environ. Sci. Technol.*, 30, 3294-3303.

Choy, B. and Reible, D.D. 2000. *Diffusion models of environmental transport*. CRC Press LLC, Boca Raton, FL.

Contaminants of Concern for Effects on Aquatic Biota. Oak Ridge National Laboratory, Oak Ridge, TN. ES/ER/TM-96/R2. (<http://www.hsrd.ornl.gov/ecorisk/reports/html>).

Deans, J.R. and Dixon, B.G. 1992. Uptake of Pb^{2+} and Cu^{2+} by novel biopolymers. *Water Res.* 26 (4), 469-472.

DeWitt, T.H., Swartz, R.C., Hansen, D.J., McGovern, D., and Berry, W.J. 1996. Bioavailability and chronic toxicity of cadmium in sediment to the estuarine amphipod *leptocheirus plumulosus*. *Environ. Tox. Chem.*, 15, 2095-2101.

Di Toro, D.M., Mahony, J.D., Hansen, D.J., and Scott, K.J. 1992. Acid volatile sulfide predicts the acute toxicity of cadmium and nickel in sediments. *Environ. Sci. Technol.*, 26, 96-101.

Dudley, L.M., McLean, J.E., Furst, T.H., and Jurinak, J.J. 1988. Sorption of copper and cadmium from the water soluble fraction of an acid mine waste by two calcareous soils. *Soil Sci.*, 145, 207-214.

Dudley, L.M., McLean, J.E., Sims, R.C., and Jurinak, J.J. 1991. Sorption of Cd and Cu from acid mine waste extract by two calcareous soils: Column studies. *Soil Sci.*, 151, 121-135.

Eiden, C.A., Jewell, C.A., and Wightman, J.P. 1980. Interaction of Lead and Chromium with Chitin and Chitosan. *J. App. Pol. Sci.*, 25, 1587-1599.

ERD (Environmental restoration Division). 1999. Ecological screening values (ESVs). Manual: ERD-AG-003, P.7.1, Revision 0. Savannah River Site, Aiken, SC.

Evans, A.G., Bauer, L.R., Haslow, J.S., Hayes, D.W., Martin, H.L., McDowell, W.L., and Pickett, J.B. 1992. Westinghouse Savannah River Company, report no. WSRC-RP-92-315.

Forstner, U. and Wittmann, G.T.W. 1979. Metal pollution in the aquatic environment. Springer-Verlag, Berlin.

Grabowski, L.A., Houpis, J.L.J., Woods, W.I., and Johnson, K.A. 2001. Seasonal bioavailability of sediment-associated heavy metals along the Mississippi river floodplain. *Chemosphere*, 45, 643-651.

Hansen, D.J., Berry, W.J., Mahony, J.D., Boothman, W.S., Di Toro, D.M., Robson, D.L., Ankley, G.T., Ma, D., Yan, Q., and Pesch, C.E. 1996. Predicting the toxicity of metal-contaminated field sediments using interstitial concentrations of metals and acid-volatile sulfide normalizations. *Environ. Tox. Chem.*, 15, 2080-2094.

Hickey, M.G. and Kittrick, J.A. 1984. Chemical partitioning of cadmium, copper, nickel, and zinc in soils and sediments containing high levels of heavy metals. *J. Environ. Qual.*, 13, 372-376.

Griscom, S.B., Fisher, N.S., and Luoma, S.N. 2000. Geochemical influences on assimilation of sediment-bound metals in clams and mussels. *Environ. Sci. Technol.*, 34, 91-99.

Ingersoll, G.C., Haverland, P.S., and Brunson, E.L. 1996. Calculations and evaluation of sediment effect concentrations for amphipod *Hyaella azteca* and the midge *Chironomus riparius*. *J. Great Lake Res.*, 22, 602-623.

Jensen, M.P., Nash, K.L., Morss, L.R., Appelman, E.H., and Schmidt, M.A. 1996. Immobilization of actinides in geomeia by phosphate precipitation. Humic and fulvic acids: Isolation, structure and environmental role. *ACS Symp. Ser.* 651:272-285.

Jepsen, R., Roberts, J., and Lick, W. 1996. Effects of Bulk Density on Sediment Erosion Rates. *Water, Air, and Soil Pollution*, 99, 21-31.

Jepsen, R., Roberts, J., and Lick, W. 1997. Long Beach Harbor Sediment Study, Report Submitted to the U.S. Army Corps of Engineers, DACW09-97-M-0068.

Kabat-Pendias, A. 2001. Trace Elements in soils and plants. 3rd Edition, CRC Press, Boca Raton, FL, USA.

Khor, E. 2001. Chitin: Fulfilling a Biomaterials Promise. Elsevier Science Ltd., Amsterdam.

Knox, A.S., Seaman, J., Mench, M.J., and Vangronsveld J. 2000a. Remediation of metal- and radionuclide- contaminated soils by in situ stabilization techniques. *In* I.K. Iskandar, Environmental Restoration of Metals-Contaminated Soils, CRC Press, Boca Raton, FL.

Knox, A.S., Seaman, J., and Pierzynski, G. 2000b. Chemo-phytostabilization of metals in contaminated soils. *In* D.L. Wise, et al., Remediation of Hazardous Waste Contaminated Soils, 2nd Edition, Marcel Dekker, Inc.

Knox, A. S., Kaplan, D. I., Adriano, D.C., and Hinton, T.G. 2003. Evaluation of Rock Phosphate and Phillipsite as Sequestering Agents for Metals and Radionuclides. *J. Environ. Qual.*, 32, 515-525.

Knox, A. S., Kaplan, D.I., and Hang, T. 2004. Phosphate Mineral Sources Evaluation and Zone-of-Influence Estimates for Soil Contaminant Amendments at the T-Area Outfall Delta (U). Technol. Rep. WSRC-TR-2003-00579, Rev. 0. Westinghouse Savannah River Company, Aiken, SC.

Knox, A.S., Paller, M., Nelson, E., Specht, W., and Gladden, J. 2006a. Contaminant assessment and their distribution and stability in constructed wetland sediments, *J. Environ. Qual.*, 35, 1948-1959.

Knox, A.S., Kaplan, D.I., and Paller, M.H.. 2006b. Natural phosphate sources and their suitability for remediation of contaminated media. *Sci. Total Environ.*, 357, 271-279.

Knox, A.S., Paller, M.H., Nelson, E.A., Specht, W.L., Halverson, N.V., and Gladden, J.B. 2006. Metal distribution and stability in constructed wetland sediments. *J. Environ. Qual.*, 35, 1948-1959.

Knox, A.S., Paller, M.H., Reible, D. D., and Petrisor, I.G. 2007a. Innovative in-situ remediation of contaminated sediments for simultaneous control of contamination and erosion. Annual Report 2007, WSRC-RP-2007-00666.

Knox, A. S., Paller, M. H., Reible, D. D., and Petrisor, I. 2007b. Sequestering Agents for Metal Immobilization - Application to the Development of Active Caps in Fresh and Salt Water Sediments, Conference Proceedings, the 4th International Conference on Remediation of Contaminated Sediments, January 22-25, 2007, Savannah, GA.

Knox, A.S., Dixon, K.L., Paller, M.H., Reible, D.D., Roberts, J.J., and Petrisor, I.G.. 2008a. Innovative in-situ remediation of contaminated sediments for simultaneous control of contamination and erosion. Annual Report 2008, SRNL-RP-2008-01216.

Knox, A.S., Paller, M.H., Reible, D. D., Ma, X., and Petrisor, I.G. 2008b. Sequestering Agents for Active Caps – Remediation of Metals and Organics. *Soil and Sediment Contamination: An International Journal*, 17(5), 516-532.

Knox, A.S., Paller, M.H., Dixon, K.L., Reible, D.D., and Roberts, J. 2009. Innovative in-situ remediation of contaminated sediments for simultaneous control of contamination and erosion. Annual Report 2009, SRNL-RP-2009-01497.

Krupka, K.M. and Serne, R.J. 2002. Geochemical factors affecting the behavior of antimony, cobalt, europium, technetium, and uranium in vadose sediments. Technical Report, PNNL-14126, Pacific Northwest National laboratory, Richland, WA.

Lagaly, G. 1984. Clay-Organic complexes and interactions. *Phil. Trans. R. Soc. London*, A-311, pp. 315-332.

Lee, B.G., Griscom, S.B., Lee, J.S., Choi, H.J., Koh, C.H., Luoma, S.N., and Fisher, N.S. 2000. Influences of dietary uptake and reactive sulfide on metal bioavailability from aquatic sediments. *Science*, 287, 282-284.

Leppert, D. 1990. Heavy metal sorption with clinoptilolite zeolite: alternatives for treating contaminated soil and water. *Mining Eng.*, 42(6), 604-608.

Li, Y.H. and Gregory, S. 1974. Diffusion of ions in sea water and in deep sea sediments. *Geochimica et Cosmochimica Acta*, 38, 703 -714.

Li, Y., Yang, I.C.Y., Lee, K.I., and Yen, T.F. 1993. Subsurface Application of *Alcaligenes eutrophus* for Plugging of Porous Media. *Microbial Enhanced Oil Recovery – Recent Advances* (E.T. Premuzic and A. Woodhead, Eds.), Elsevier Amsterdam, 65-77.

Long, E.R., MacDonal, D.D., Cabbage, J.C., and Ingersoll, C.G. 1998. Predicting the toxicity of sediment-associated trace metals with simultaneously extracted trace metal: acid-volatile sulfide concentrations and dry weight-normalized concentrations: a critical comparison. *Environ. Tox. Chem.*, 17, 972-974.

Lu, X.X., Reible, D.D., and Fleeger, J.W. 2006. Bioavailability of polyaromatic hydrocarbons in field contaminated Anacostia River (Washington DC) sediment. *Environ. Toxicol. & Chem.*, 25(11), 2869-2874.

Luoma, S.N., and Bryan, G. 1982. A statistical study of environmental factors controlling concentrations of heavy metals in the bivalve *Scrobicularia plana* and the polychaete *Nereis diversicolor*. *Est Coast Shlf Sci.* 15, 95-108.

Luoma, S.N. and Rainbow, P.S. 2005. Why is metal bioaccumulation so variable? Biodynamic as a unifying concept. *Environ. Sci. Technol.* 39, 921-1931.

Ma, Q.Y., Logan, T.J., Traina, S.J., and Ryan, J.A. 1994a. Effects of NO_3^- , Cl^- , F^- , SO_4^{2-} , and CO_3^{2-} on Pb^{2+} immobilization by hydroxyapatite. *Environ. Sci. Technol.*, 28, 408-418.

Ma, Q.Y., Traina, S.J., Logan, T.J., and Ryan, J.A. 1994b. Effects of aqueous Al, Cd, Cu, Fe(II), Ni, and Zn on Pb immobilization by hydroxyapatite. *Environ. Sci. Technol.*, 28, 1219-1228.

Ma, Q.Y., Logan, T.J., and Traina, S.J. 1995. Lead immobilization from aqueous solutions and contaminated soils using phosphate rocks. *Environ. Sci. Technol.*, 29, 1118-1126.

Ma, L.Q. and Rao, G.N. 1997. The effect of phosphate rock on Pb distribution in contaminated soils. *J. Environ. Qual.*, 26, 259-264.

Martin, G.R., Yen, T.F., and Karimi, S. 1996. Application of Biopolymer Technology in Silty Soil Matrices to Form Impervious Barriers. In: *Proceedings of 7th Australia New Zealand Conference on Geomechanics* (M.B. Jaksa, W.S. Kaggwa, and D.A. Cameron, Eds.), International Association of Engineering Geology and International Society for Rock Mechanics, Adelaide, Australia, 1996, 814-819.

McDonald, D.D., Carr, R.S., Calder, F.D., Long, E.R., and Ingersoll, C.G. 1996. Development and evaluation of sediment quality guidelines for Florida coastal waters. *Ecotoxicol.* 5, 253-278.

McKay, G., Blair, H.S., and Findon, A. 1989. Equilibrium studies for the sorption of metal ions onto chitosan. *Ind. J. of Chem.*, 28A, 356-360.

McLean, J.E. and Bledsoe, B.E. 1992. Ground water issue: Behavior of metals in soil. EPA/540/S-92/018 (archived at URL: www.epa.gov/swertio1/tsp/download/issue14.pdf).

McNeil, J., Taylor, C., and Lick, W. 1996. Measurements of the Erosion of Undisturbed Bottom Sediments with Depth. *J. Hyd. Eng.*, 122(6), 316-324.

Moody, T.E. and Wright, J. 1995. Adsorption isotherms: North Carolina apatite induced precipitation of lead, zinc, manganese, and cadmium from Bunker Hill 4000 Soil. Technical Report BHI-00197, Bechtel Hanford, Richland, WA.

Nash, K.L., Jensen, M.P., Hines, J.J., Freidrich, S.A., and Redko, M. 1997. Phosphate mineralization of actinides by measured addition of precipitating anions. TTP# CH2-6-C3-22. Chem. Div., Argonne National Laboratory, Argonne, IL.

Nash, K.L., Jensen, M.P., and Schmidt, M.A. 1998a. Actinide immobilization in the subsurface environment by in-situ treatment with a hydrolytically unstable organophosphorus complexant: Uranyl uptake by calcium phytate. *J. Alloys and Compounds*, 271-273, 257-261.

Nash, K.L., Jensen, M.P., and Schmidt, M.A. 1998b. In-situ mineralization of actinides of groundwater cleanup: Laboratory demonstration with soil from the Fernald Environmental

Management Project. 507-518. In W.W. Schultz and N.J. Lombardo (ed.) Science and technology for disposal of radioactive tank waste. Plenum Press, New York.

Paller, M.H. and Knox, A.S. 2010. Amendments for the remediation of contaminated sediments: Evaluation of potential environmental impacts. *Sci. Tot. Environ.*, 408, 4894-4900.

Persaud, D., Jaagumagi, R., and Hayton, A. 1992. Guidelines for the protection and management of aquatic sediment quality in Ontario. Water Resources Branch, Ontario Ministry of the Environment, Toronto, Ontario, Canada.

Ponizovsky, A. and Tsadilas, C.D. 2003. Lead(II) retention by Alfisol and clinoptilolite: cation balance and pH effect. *Geoderma*, 115, 303– 312.

Quevauviller, P., Rauret, G., Lopez-Sanchez, J.F., Rubio, R., Ure A., and Muntau, H. 1997. Certification of trace metal extractable contents in a sediment reference material (CRM 601) following a three-step sequential extraction procedure. *Sci. Tot. Environ.*, 205, 223-234.

Reible, D.D., Lampert, D., Constant, W.D., Mutch, R.D., and Zhu, Y. 2006. Active Capping Demonstration in the Anacostia River, Washington, DC, Remediation: The Journal of Environmental Cleanup Costs, Technologies and Techniques, 17 (1), 39-53.

Roberts, J. and Jepsen, R. 2001. Development for the Optional Use of Circular Core Tubes with the High Shear Stress Flume. SNL report to the US Army Corps of Engineers, Waterways Experiment Station.

Roberts, J., Jepsen, R., Gotthard, D., and Lick, W. 1998. Effects of Particle Size and Bulk Density on Erosion of Quartz Particles. *J. Hyd. Eng.*, 124(12), 1261-1267.

Rogers, V.A. 1990. Soil Survey of Savannah River Plant Area, Parts of Aiken, Barnwell, and Allendale Counties, South Carolina. U.S. Department of Agriculture, Soil Conservation Service. In cooperation with U.S. Department of Energy; U.S. Department of Agriculture Forest Service: South Carolina Agricultural Experiment Station; and South Carolina Land Resources Conservation Commission.

Ruby, M.V., Davis, A., Schoof, R. Eberle, S., and Sellstone, C.M. 1996. Estimation of lead and arsenic bioavailability using a physiologically base extraction test. *Environ. Sci. Technol.*, 30, 422-430.

Schlichting, H. 1979. *Boundary-Layer Theory*. Seventh Edition, McGraw-Hill.

Schmuhl, R., Krieg, H.M., Keizer, K. 2001. Adsorption of Cu(II) and Cr(VI) ions by chitosan: Kinetics and equilibrium studies. *Water SA*, 27(1), 1-7.

Singh, S.P., Ma, L.Q., and Harris, W.G. 2001. Heavy metal interactions with phosphatic clays: Sorption and desorption behavior. *J. Environ. Qual.* 30, 1961-1968.

Smith, L.A., Means, J.L., Chen, A., Alleman, B., Chapman, C.C., Tixler, J.S., Brauning, S.E., Gavaskar, A.R., and Royer, M.D. 1995. Remediation option for metals-contaminated sites. Lewis Publisher, Boca Raton, FL, USA.

Soundarajan, R., Barth, E.F., and Gibbons, J.J. 1990. Using an organophilic clay to chemically stabilize waste containing organic compounds. Hazard. Mater. Control, 3(1), 42-45.

Sowder, A.G., Khijniak, T., Morris, P.J., and Bertsch, P.M. 1999. Evaluation of effect of apatite amendments on Uranium and nickel toxicity in aged contaminated sediments. Paper #PB7-05, presented at "Migration'99", Lake Tahoe, NV (UCRL-ID-13526).

Stewart, T.L. and Fogler, H.S. 2001. Biomass Plug Development and Propagation in Porous Media. Biotechnology and Bioengineering, February 5, 353-363.

Suter, G.W. and Tsao, C.L. 1996. Toxicological Benchmarks for Screening Potential
Suzuki, T., T. Hatsushika, and M. Miyake. 1982. Synthetic Hydroxyapatite as inorganic cations exchangers. J. Chem. Soc., Faraday Trans. I., 78, 3605-3611.

Suzuki, T., Hatsushika, T., and Hayakawa, Y. 1981. Synthetic Hydroxyapatite employed as inorganic cation-exchangers. J. Chem. Soc., Faraday Trans. I. 77, 1059-1062.

Tessier, A., Campbell, P.G.C., and Bisson, M. 1979. Sequential extraction procedure for the speciation of particulate trace metals. Anal. Chem., 51, 844-850.

Tessier, A., Couillard, Y., Campbell, P.G.C., and Auclair, J.C. 1993. Modeling Cd partitioning in oxic lake sediments and Cd concentrations in the freshwater bivalve *Anodonta grandis*. Limnol. Oceanogr. 38, 1-17.

Tsai, C-H. and Lick, W. 1986. A portable device for measuring sediment resuspension. J. Great Lakes Res., 12(4), 314-321.

Udaybhaskar, P., Iyengar, L., and Prabhakara Rao, A.V.S. 1990. Hexavalent chromium interaction with chitosan. J. Appl. Polym. Sci., 39, 739-747.

U.S. EPA. 1992. Toxicity Characteristic Leaching Procedure, SW-846, Method 1311.

U.S. EPA. 1998. Appendix B. Palermo, M.R., Maynard, S., Miller, J., and Reible, D.D. Guidance for In-Situ Subaqueous Capping of Contaminated Sediments", Assessment and Remediation of Contaminated Sediments (ARCS) Program, Great Lakes National Program Office, US EPA 905-B96-004.

U.S. EPA-ORD. 1999. Monitored Natural Attenuation of Petroleum Hydrocarbons. EPA/600/F-98/021. Washington D.C.: Office of Research and Development, National Risk Management Research Laboratory.

U.S. EPA. 2000. Methods for measuring the toxicity and bioaccumulation of sediment-associated contaminants with freshwater invertebrates. Second Edition. Washington, D.C: U.S. Environmental Protection Agency, EPA 600/R-99/064.

U.S. EPA. 2009. National Recommended Water Quality Criteria. Office of Water, Washington, DC. 2009. (<http://www.epa.gov/ost/criteria/wqctable/>).

Vankar, P.S. and Tiwari, V. 2001. Toxic metal removal by using Cyclodextrins, *Analytical-Science.com*, BioAnalytical and BioAssays, 2001_BA006.

Viana, P.Z., Yin, K., and Rockne, K.J. 2008. Modeling active capping efficacy. 1. Metal and organometal contaminated sediment remediation. *Environ. Sci. Technol.*, 42, 8922-8929.

Wan Ngah, W.S. and Liang, K.H. 1999. Adsorption of Gold (III) Ions onto Chitosan and N-Carboxymethyl Chitosan: Equilibrium Studies. *Ind. Eng. Chem. Res.*, 38, 1411-1414.

Wang, F., Goulet, R.G., and Chapman, P.M. 2004. Testing sediment biological effects with the freshwater amphipod *Hyaella azteca*: the gap between laboratory and nature. *Chemosphere*, 57, 1713–1724.

Wise, A. 1986. Influence of calcium on trace metal interactions with phytate. p.151-160. In E. Graf (ed.) *Phytic acid: Chemistry and applications*. Pilatus Press, Minneapolis, MN.

Wright, J.V., Peurrung, L.M., Moody, T.E., Conca, J.L., Chen, X., Didzerekis, P.P., Wyse, E. 1995. In Situ Immobilization of Heavy Metals: Apatite Mineral Formations. Technical Report to the Strategic Environmental Research and Development Program, Department of Defense, Pacific Northwest National Laboratory, Richland; 154pp.

Xu, S., Sheng, G., and Boyd, S.A. 1997. Use of organoclays in pollutant abatement. *Adv. Agron.*, 59, 25-62.

Yang, T.C. and Zall, R.R. 1984. Absorption of metals by natural polymers generated from seafood processing wastes. *Ind. Eng. Chem. Prod. Res. Dev.*, 23, 168-172.

Yen, T.F. 2001. In-situ Stabilization of Subsurface Contaminants Using Microbial Polymers. In: *Proceedings, Industry Partnerships for Environmental Science and Technology DOE-NETL*, Morgantown, WV, 2001.

Yen, T.F., Yang, I.C.Y, Karimi, S., and Martin, G.R. 1996. Biopolymers for Geotechnical Applications. Reprinted from the North American Water and Environment Congress, American Society of Civil Engineers, 6 p.

Zachara, J.M., Girvin, D.C., and Schmidt, R.L., 1987. Chromate adsorption on amorphous iron oxyhydroxide in the presence of major groundwater ions. *Environ. Sci. Technol.*, 21, 589-594.

Zhang, F., Ryan, J.A., and Yang, J. 1998. In vitro soil solubility in the presence of hydroxyapatite. *Environ. Sci. Technol.*, 32, 2763-2768.

Zhang, H. and Davison, W. 1995. Performance characteristic of the technique of diffusion gradients in thin-films (DGT) for the measurement of trace metals in aqueous solution. *Anal. Chem.*, 67, 3391-3400.

Zhang, H. and Davison, W. 2001. In situ speciation measurements. Using DGT to determine inorganically and organically complexed metals. *Pure Appl. Chem.*, 73, 9-15.

Zhang, Z.Z., Sparks, D.L., and Scrivner, N.C. 1993. Sorption and desorption of quaternary amine cations on clays. *Environ. Sci. Technol.*, 27, 1625-1631.

APPENDIX 1- ADDITIONAL DATA

Table 1. Commercially Available Amendments Collected for Contaminant Removal/Immobilization Experiments

Product Name	Company	Product Description	Short Name*
Biopolymers			
Coyote Brand Algin SA	Gum Technology Corp., P.O. Box 35206, Tucson, AZ	Natural bend of sodium alginates. Sodium alginate is the sodium salt of alginic acid. It is an extract of seaweed and is used as a thickener in the food industry and as a gelling agent and emulsifier.	CBA-SA
Coyote Brand Guar HV, High Viscosity Guar	Gum Technology Corp., P.O. Box 35206, Tucson, AZ	Guar gum is a thickening agent extracted from the guar bean (<i>Cyamopsis tetragonoloba</i>). Solutions with different gum concentrations can be used as emulsifiers and stabilizers because they prevent oil droplets from coalescing. Guar gum is also used as suspension stabilizer.	CBG-HV
Coyote CMC-300, Carboxy Methyl Cellulose	Gum Technology Corp., P.O. Box 35206, Tucson, AZ	CMC, is a cellulose derivative. Its functional properties depend on the degree of substitution of the cellulose structure and on the chain length of the cellulose backbone. CMC has high viscosity and is used in food science as a viscosity modifier or thickener, and to stabilize emulsions. It is also a constituent of many non-food products such as toothpaste, laxatives, water-based paints, detergents, and various paper products.	CMC-300

Coyoye Brand Xanthan Gum 80 mesh	Gum Technology Corp., P.O. Box 35206, Tucson, AZ	Xanthan gum is a natural gum polysaccharide used as a food additive and rheology modifier. It is produced by the fermentation of glucose or sucrose by the <i>Xanthomonas campestris</i> bacterium. Xanthan gum can produce a large increase in the viscosity of a liquid by adding a very small quantity of gum (1%). It is used in foods to stabilize colloidal oil and solid materials. In the oil industry xanthan gum is used in large quantities to thicken drilling fluids. These fluids carry the solids cut by the drilling bit back to the surface. It is more stable than other gums under a wide range of temperatures and pHs.	XG
Chitosan 90%	AIDP, Inc., 17920 E. Ajax Circle, City of Industry, CA 91748	Chitosan is derived from chitin extracted from recycled crab and shrimp shells. It is used as a nutraceutical and a plant growth enhancer. Chitosan is also used for filtration in water processing. Chitosan causes fine sediment particles to bind together and be removed during sand filtration. Chitosan also removes phosphorous, heavy minerals, and oils from water.	BPC
Chitosan High Density	AIDP, Inc., 17920 E. Ajax Circle, City of Industry, CA 91748	Chitosan is derived from chitin extracted from recycled crab and shrimp shells. It is used as a nutraceutical and a plant growth enhancer. Chitosan is also used for filtration in water processing. Chitosan causes fine sediment particles to bind together and be removed during sand filtration. Chitosan also removes phosphorous, heavy minerals, and oils from water.	BPC-HD

Kelzan S (xanthan gum)	CP Kelco U.S., Inc., 123 N. Wacker Dr., Suite 2000, Chicago, IL, 60606	Xanthan gum is a natural gum polysaccharide used as a food additive and rheology modifier. It is produced by the fermentation of glucose or sucrose by the <i>Xanthomonas campestris</i> bacterium. Xanthan gum can produce a large increase in the viscosity of a liquid by adding a very small quantity of gum (1%). It is used in foods to stabilize colloidal oil and solid materials. In the oil industry xanthan gum is used in large quantities to thicken drilling fluids. These fluids carry the solids cut by the drilling bit back to the surface. It is more stable than other gums under a wide range of temperatures and pHs.	BPKS
Kelzan (xanthan gum)	CP Kelco U.S., Inc., 123 N. Wacker Dr., Suite 2000, Chicago, IL, 60606	Xanthan gum is a natural gum polysaccharide used as a food additive and rheology modifier. It is produced by the fermentation of glucose or sucrose by the <i>Xanthomonas campestris</i> bacterium. Xanthan gum can produce a large increase in the viscosity of a liquid by adding a very small quantity of gum (1%). It is used in foods to stabilize colloidal oil and solid materials. In the oil industry xanthan gum is used in large quantities to thicken drilling fluids that carry solids cut by the drilling bit back to the surface. It is more stable than other gums under a wide range of temperatures and pHs.	BPK

Phosphates

North Carolina Apatite	Aurora, NC	Mined rock phosphate, dominant mineral phase: hydroxyapatite. Apatite minerals have the ability to capture and hold radioactive and metal contaminants.	NCA
Washed Phosphate Ore	Calcium Silicate Corporation Clumbia, TN	Mined rock phosphate. Phosphate minerals have the ability to capture and hold radioactive and metal contaminants.	RPT

Biological Apatite	PIMS-NW, Richland, WA www.pimsnw.com	Biological apatite is ground fish bone. It has fewer impurities than other forms of apatite and contains about 27% total phosphate, most of which is available. Biological apatite is more soluble than rock phosphates.	BA
Calcium Phytate	Dong Li Phytate Ltd., China	Calcium Inositol Hexaphosphate or Phytic acid calcium salt. Molecular formula:Ca ₆ C ₆ H ₆ O ₂₄ P ₆	CaP
Organoclays			
Clayfloc™ 200	Biomin Inc., P.O.Box 20028, Ferndale, MI 48220	Modified montmorillonite, granular solid, removes heavy metals in acidic conditions	OCB-200
Clayfloc™ 202	Biomin Inc., P.O.Box 20028, Ferndale, MI 48220	Modified montmorillonite, granular solid, removes heavy metals in acidic conditions	OCB-202
Clayfloc™ 750	Biomin Inc., P.O.Box 20028, Ferndale, MI 48220	An organoclay-based flocculent (modified bentonite). Removes organic contaminants and anions	OCB-750
PM-199	CETCO Remediation Technologies	Organoclay (starting material bentonite clay), organoclay surfactant: dimethyl ammonium chloride. Removes mostly organic contaminants	OC-PM-199
AquaBlok#8	AquaBlok, Toledo, Ohio 43614	Clay mineral/aggregate composite particle material. Grayish/white pebble, various sizes	AB8
AquaBlok#ZVI	AquaBlok, Toledo, Ohio 43614	Clay mineral/Zero Valent Iron/aggregate composite particle material. Yellow/bronish pebble, various sizes	ABZVI

Zeolites		
Phillipsite	Steelhead Specialty Minerals Spokane, WA	<p>Potassium-sodium-aluminosilicate. $K, Na_5 [(AlO_2)_5 (SiO_2)_{11}] 10 H_2O$. Phillipsite is a natural zeolite.</p> <p>Zeolite is a mineral with a naturally-occurring negative charge that can hold positive ions. In addition, Zeolite has an open framework molecular structure (very porous) with a very high surface area that is capable of adsorbing and absorbing many different types of gases, hydrocarbons, heavy metals, and low-level radioactive elements.</p>
Clinoptilolite	Steelhead Specialty Minerals Spokane, WA	<p>Clinoptilolite has a cage-like structure consisting of SiO_4 and AlO_4 tetrahedra joined by shared oxygen atoms. The negative charges of the AlO_4 units are balanced by the presence of exchangeable cations - notably calcium, magnesium, potassium and sodium. These ions can be readily displaced by other substances such as heavy metals and ammonium ions. This phenomenon is known as cation exchange, and it is the very high cation exchange capacity of clinoptilolite that provides many of its very useful properties.</p>

APPENDIX 2- PUBLICATIONS

Reports:

1. Knox, A.S., M.H. Paller, D.D. Reible, and I.G. Petrisor. 2006. Innovative in-situ remediation of contaminated sediments for simultaneous control of contamination and erosion. Annual Report 2006, WSRC-RP-2006-01149.
2. Knox, A.S., M.H. Paller, D.D. Reible, and I.G. Petrisor. 2007. Innovative in-situ remediation of contaminated sediments for simultaneous control of contamination and erosion. Annual Report 2007, WSRC-RP-2007-00666.
3. Knox, A.S., K.L. Dixon, M.H. Paller, D.D. Reible, J. Roberts, and I.G. Petrisor. 2008. Innovative in-situ remediation of contaminated sediments for simultaneous control of contamination and erosion. Annual Report 2008, SRNL-RP-2008-01216.
4. Knox, A.S., M.H. Paller, K.L. Dixon, D.D. Reible, and J. Roberts. 2009. Innovative in-situ remediation of contaminated sediments for simultaneous control of contamination and erosion. Annual Report 2009, SRNL-RP-2009-01497.

Papers:

1. Knox, A. S., M.H. Paller, D.D. Reible, and I.G. Petrisor. 2007. Sequestering agents for metal immobilization – application to the development of active caps in fresh and salt water sediments. Conference Proceedings of the Fourth International Conference on Remediation of Contaminated Sediments, Savannah, Georgia, January 22-25, 2007, Battelle Press: ISBN 978-1-57477-159-6.
2. Knox, A.S., M.H. Paller, D.D. Reible, X. Ma, and I.G. Petrisor. 2008. Sequestering agents for active caps – remediation of metals and organics, *Soil and Sediment Contamination: An International Journal*, 17(5): 516-532.
3. Knox, A.S., R. Brigmon, D. Kaplan, and M. Paller. 2008. Interactions among phosphate amendments, microbes and uranium mobility in contaminated sediments. *Science of the Total Environment*, 395: 63-71.
4. Paller, M.H. and A.S. Knox. 2010. Amendments for the remediation of contaminated sediments: Evaluation of potential environmental impacts, *Science of the Total Environment*, 408, 4894-4900.
5. Knox, A.S., J. Roberts, M.H. Paller and D.D. Reible. 2010. In-situ remediation of contaminated sediments – active capping technology. Conference proceedings of the 15th International Conference on Heavy Metals in the Environment (15th ICHMET2010), Gdansk, Poland, 19-23 September, 2010

Book Chapters:

1. Knox, A. S., I.G. Petrisor, C. Turick, J. Roberts, M.H. Paller, D. D. Reible, and C.R. Forrest. 2010. Life span of biopolymer sequestering agents for contaminant removal and erosion resistance. In “Biopolymers”, ISBN 978-953-7619-X-X, Sciyo, 2010.

MS Theses:

1. Galjour Dufreche, J. 2008. Evaluation of organoclay as an active capping amendment for the control of dissolved PAH contamination, MS Thesis, The University of Texas at Austin, May 2008.
2. Forrest, C.R., 2008. Evaluation of biopolymer coated sands as capping materials, MS Thesis, The University of Texas at Austin, May 2008.

Abstracts:

1. Knox, A.S., M.H. Paller, I.G. Petrisor, and D.D. Reible. 2006. Sequestering agents for contaminants in sediments - Application to the Development of Active Caps, the SERDP/ and ESTCP Partners in Environmental Technology Technical Symposium & Workshop, Washington, D.C., November 28-30, 2006.
2. Knox, A.S., M.H. Paller, I.G. Petrisor, and D.D. Reible. 2006. Sequestering agents for inorganic contaminants in sediments, the 4th International Conference on Remediation of Contaminated Sediments, January 22-25, 2007, Savannah, GA.
3. Knox, A.S., M.H. Paller, I.G. Petrisor, and D.D. Reible. 2006. Sequestering agents for active caps – their effects on contaminant mobility, bioavailability, and microbial activity, the 9th International In-situ and On-situ Bioremediation Symposium, May 7-10, 2007, Baltimore, Maryland.
4. Knox, A.S., M.H. Paller, and D.D. Reible. 2007. Effect of apatite and organoclay on metal bioavailability in contaminated sediments, the 3rd International Conference on Environmental Science and Technology, Houston, TX, August 6-9, 2007.
5. Knox, A.S., M.H. Paller, and D.D. Reible. 2007. Sequestering agents for metals and organic contaminants - application in remediation of contaminated sediments, the American Society of Agronomy, Soil Science Society of America International Annual Meetings, New Orleans, LA, November 4-8, 2007.
6. Knox, A.S., M.H. Paller, D.D. Reible, X. Ma, and I.G. Petrisor. 2007. In-situ remediation of sites contaminated with waste mixtures, the 5th International Conference on Oxidation and Reduction Technologies for In-Situ Treatment of Soil and Groundwater, Niagara Falls, New York, USA, September 24-27, 2007.
7. Knox, A.S., M.H. Paller, D.D. Reible, and I.G. Petrisor 2007. Active caps for remediation of mixtures of contaminants and resistance to erosion – a comprehensive evaluation, SERDP/ and ESTCP Partners in Environmental Technology Technical Symposium & Workshop, Washington, D.C., December 4-6, 2007.
8. Paller, M.H. and A.S. Knox. 2007. Evaluation of the potential side effect of sequestering agents used for the development of active caps for contaminated sediments, SERDP/ and ESTCP Partners in Environmental Technology Technical Symposium & Workshop, Washington, D.C., December 4-6, 2007.
9. Galjour, J., L. Moretti, S. Ma, X.X. Lu, D.D. Reible, A.S. Knox, and M.H. Paller. 2007. Evaluation of the applicability and effectiveness of organoclay as active capping materials. SERDP/ and ESTCP Partners in Environmental Technology Technical Symposium & Workshop, Washington, D.C., December 4-6, 2007.
10. Forrest, C., S. Ma, D.D. Reible, I.G. Petrisor, and A.S. Knox. 2007. Evaluation of biopolymer coated sands as capping materials. SERDP/ and ESTCP Partners in

- Environmental Technology Technical Symposium & Workshop, Washington, D.C., December 4-6, 2007.
11. Galjour, J., L. Moretti, S. Ma, X.X. Lu, D.D. Reible, A.S. Knox, and M.H. Paller. 2008. Evaluation of the applicability and effectiveness of organoclay as active capping materials. Pittcon Conference & Expo, New Orleans, LA, March 2-7, 2008.
 12. Knox, A.S., D.I. Kaplan, M.H. Paller, and D.D. Reible. 2008. Use of apatite for chemical stabilization of contaminants in soils and sediments. Pittcon Conference & Expo, New Orleans, LA, March 2-7, 2008.
 13. Paller, M.H., and A.S. Knox. 2008. Potential side-effects of sequestering agents used in active caps for remediating contaminated sediments. North Atlantic Chapter of the Society for Environmental Toxicology and Chemistry, Bar Harbor, Maine, June 6, 2008.
 14. Knox, A.S. and M. Paller. 2008. Role of apatite in remediation of metal contaminated sediments, North Atlantic Chapter of the Society for Environmental Toxicology and Chemistry, Bar Harbor, Maine, June 6, 2008.
 15. Knox, A.S. 2008. Role of apatite in manipulation of metal bioavailability in soils and sediments. SETAC North America 29th Annual Meeting, November 16-20, 2008, Tampa, FL.
 16. Knox, A.S., D.D. Reible, M.H. Paller, and I.G. Petrisor. 2008. Effect of active caps components on contaminant bioavailability and toxicity in contaminated sediments. SETAC North America 29th Annual Meeting, November 16-20, 2008, Tampa, FL.
 17. Knox, A.S., D.D. Reible, M.H. Paller, and I.G. Petrisor. 2009. Active caps for remediation of mixture of contaminants and resistance to erosion. 5th International Conference on Remediation of Contaminated Sediments, February 2-5, 2009, Jacksonville, FL.
 18. Galjour, J., L. Moretti, X.X. Lu, F. Yan, D.D. Reible, A.S. Knox, M.H. Paller, and J. Olsta. 2009. Organoclay for the control of dissolved and separate phase contaminants: laboratory and field studies. 5th International Conference on Remediation of Contaminated Sediments, February 2-5, 2009, Jacksonville, FL.
 19. Knox, A.S., D.D. Reible, M.H. Paller, I.G. Petrisor, K.L. Dixon, and J. Roberts 2009. Active caps for the remediation of mixtures of contaminants and resistance to erosion. The 10th International Conference on the Biogeochemistry of Trace Elements, Special Symposium on Fate and transport of metals in contaminated sediments – new approaches in remediation, July 13-16, 2009, Chihuahua, Chih. Mexico.
 20. Paller, M.H., A. S., Knox, D. D. Reible, X. Lu, and M.C. Brim. 2009. Potential toxicity of amendments used for treating contaminated sediments. 10th International Conference on the Biogeochemistry of Trace Elements, Special Symposium on Fate and transport of metals in contaminated sediments – new approaches in remediation, July 13-16, 2009, Chihuahua, Chih. Mexico.
 21. Dixon, K.L. and A.S. Knox. 2009. Sequestration of metals in active cap materials: A laboratory and numerical evaluation. 10th International Conference on the Biogeochemistry of Trace Elements, Special Symposium on Fate and transport of metals in contaminated sediments – new approaches in remediation, July 13-16, 2009, Chihuahua, Chih. Mexico.
 22. Knox, A.S., M.H. Paller, and D.D. Reible. 2009. Field deployment of active caps – assessment of metal bioavailability and erosion resistance. SETAC North America 30th Annual Meeting, November 19-23, 2009, New Orleans, LA.

23. Paller, M.H., Knox, A.S., D.D. Reible, X. Lu, and M.C. Brim. 2009. Field deployment of active caps – biomonitoring of amendment toxicity. SETAC North America 30th Annual Meeting, November 19-23, 2009, New Orleans, LA.
24. Knox, A.S. and M.H. Paller. 2009. Monitoring of active caps – application of diffusive gradients in thin-film (DGT) technology for assessment of metal bioavailability in sediments. Conference on DGT and the Environment, 7th to 9th October, 2009, Santa Margherita di Pula, Sardinia, Italy.
25. Knox, A.S., D.D. Reible, M.H. Paller, K.L. Dixon, J. Roberts, and I.G. Petrisor. 2009. Field deployment of active caps – assessment of metal bioavailability, erosion, and toxicity. SERDP and ESTCP Partners in Environmental Technology Technical Symposium & Workshop, Washington, D.C., December 1-3, 2009.
26. Dixon, K.L. and A.S. Knox. 2009. Sequestration of metals in active cap materials: a laboratory and numerical evaluation. SERDP and ESTCP Partners in Environmental Technology Technical Symposium & Workshop, Washington, D.C., December 1-3, 2009.
27. Knox, A.S. 2009. In-situ remediation of contaminated sediments using sequestering agents – effect on metal bioavailability and toxicity, SERDP and ESTCP Partners in Environmental Technology Technical Symposium & Workshop, Washington, D.C., December 1-3, 2009.
28. Knox, A.S., M.H. Paller, D.D. Reible. 2010. In situ remediation of contaminated sediments – active capping technology. The 15th International Conference on Heavy Metals in the Environment (15th ICHMET2010), September 19-23, 2010, Gdansk, Poland.
29. Knox, A.S., M.H. Paller, and K.L. Dixon. 2010. Effect of active caps on contaminant bioavailability – measurement and prediction of the bioavailable pool of contaminants in sediments. the International Annual Meeting of the American Society of Agronomy/Crop Science Society of America/Soil Science Society of America (ASA/CSSA/SSSA), Long Beach, CA, November 1-4, 2010.
30. Knox, A.S. and M.H. Paller. 2010. New approaches for monitoring in situ remediation of contaminated sediments – zone of influence (ZOI). SETAC North America 31th Annual Meeting, November 7-11, 2010, Portland, Oregon.
31. Knox, A.S., M.T. Whiteside, and M.H. Paller. 2010. Application of diffusive gradients in thin film (DGT) technology for assessment of metal bioavailability in remediated sediments. SETAC North America 31th Annual Meeting, November 7-11, 2010, Portland, Oregon.
32. Knox, A.S., M.H. Paller, K.L. Dixon, and D.D. Reible. 2010. Field performance of active caps – assessment of contaminant immobilization, erosion resistance, and toxicity. SERDP and ESTCP Partners in Environmental Technology Technical Symposium & Workshop, Washington, D.C., November 30 - December 2, 2010.
33. Knox, A.S., M.H. Paller, K.L. Dixon, and D.D. Reible. 2011. In situ remediation of contaminated sediments - new approaches for monitoring active caps. Sixth International Conference on Remediation of Contaminated Sediments, New Orleans, Louisiana, February 7-10, 2011.

Presentations:

Oral Presentations at Professional Meetings/Invited presentations and others

1. Knox, A.S., M.H. Paller, D.D. Reible, and I.G. Petrisor. 2007. Sequestering Agents for Inorganic Contaminants in Sediments, the Fourth International Conference on Remediation of Contaminated Sediments, January 22-25, 2007, Savannah, Georgia.
2. Knox, A.S., M.H. Paller, D.D. Reible. 2007. Effect of Apatite and Organoclay on Metal Bioavailability in Contaminated Sediments, the 3rd International Conference on Environmental Science and Technology, Houston, TX, August 6-9, 2007.
3. Knox, A. S., M.H. Paller, D.D. Reible, X. Ma, and I. Petrisor. 2007. In-Situ Remediation of Sites Contaminated with Waste Mixtures, the 5th International Conference on Oxidation and Reduction Technologies for In-Situ Treatment of Soil and Groundwater, Niagara Falls, New York, USA, September 24-27, 2007.
4. Knox, A.S., M.H. Paller, and D.D. Reible. 2007. Sequestering Agents for Metals and Organic Contaminants-Application in Remediation of Contaminated Sediments, the 100th American Society of Agronomy, Soil Science Society of America International Annual Meetings, New Orleans, LA, November 4-8, 2007.
5. Knox, A.S., D. Kaplan, M.H. Paller, D.D. Reible. 2008. Use of apatite for chemical stabilization of contaminants in soils and sediments, Pittsburgh Conference on Analytical Chemistry and Applied Spectroscopy "PITTCON CONFERENCE & EXPO, New Orleans, LA, March 2-6, 2008.
6. Reible, D.D., J. Galjour, L. Moretti, X. Lu, S. Ma, A.S. Knox and M.H. Paller. 2008. Evaluation of the applicability and effectiveness of organoclays as active capping materials, Pittsburgh Conference on Analytical Chemistry and Applied Spectroscopy "PITTCON CONFERENCE & EXPO, New Orleans, LA, March 2-6, 2008.
7. Knox, A.S. 2008. Active caps for the remediation of mixtures of contaminants and resistance to erosion, the Federal Remediation Technologies Roundtable (FRTR), Arlington, VA, June 5, 2008.
8. Paller, M.H. and A.S. Knox. 2008. Potential side-effects of sequestering agents used in active caps for remediating contaminated sediments, North Atlantic Chapter of the Society for Environmental Toxicology and Chemistry, Bar Harbor, Maine, June 6, 2008.
9. Knox, A.S. and M. Paller. Role of Apatite in Remediation of Metal Contaminated Sediments, North Atlantic Chapter of the Society for Environmental Toxicology and Chemistry, Bar Harbor, Maine, June 6, 2008.
10. Knox, A.S. 2008. Role of apatite in manipulation of metal bioavailability in soils and sediments, the SETAC North America 29th Annual Meeting, Tampa, FL, November 16-20, 2008.
11. Knox, A.S., D. Reible, and M.H. Paller. Effect of active caps components on contaminant bioavailability and toxicity in contaminated sediments. The SETAC North America 29th Annual Meeting, Tampa, FL, November 16-20, 2008.
12. Knox, A.S., D. Reible, and M.H. Paller, and I. Petrisor. 2009. Active caps for remediation of mixture of contaminants and resistance to erosion. The 5th International Conference on Remediation of Contaminated Sediments, Jacksonville, FL, February 2-5, 2009.
13. Galjour, J., L. Moretti, S. Ma, X.X. Lu, D.D. Reible, A.S. Knox, and M.H. Paller, and J. Olsta. 2009. Organoclay for the control of dissolved- and separate-phase contaminants:

- laboratory and field studies. The 5th International Conference on Remediation of Contaminated Sediments, Jacksonville, FL, February 2-5, 2009.
14. Knox, A.S. 2009. Use of apatite for chemical stabilization of contaminants in soils and sediments, the CSRAGS meeting, USC Aiken, SC, January 27, 2009.
 15. Knox, A.S. 2009. Innovative in-situ remediation of contaminated sediments for simultaneous control of contamination and erosion, the University of Wuppertal, Germany, October 12, 2009.
 16. Knox, A.S. 2009. In-situ remediation of contaminated sediments using sequestering agents – effect on metal bioavailability and toxicity, SERDP and ESTCP Partners in Environmental Technology Technical Symposium & Workshop, Washington, D.C., December 1-3, 2009.
 17. Knox, A.S., M.H. Paller, D.D. Reible. 2010. In situ remediation of contaminated sediments – active capping technology, 15th International Conference on Heavy Metals in the Environment (15th ICHMET2010), Gdansk, Poland, September 19-23, 2010.
 18. Paller, M.H., A.S. Knox, D.D. Reible, and X. Lu. 2010. Potential toxicity of sequestering agents used in active caps, 15th International Conference on Heavy Metals in the Environment (15th ICHMET2010), Gdansk, Poland, September 19-23, 2010.
 19. Knox, A.S., M.H. Paller, and K.L. Dixon. 2010. Effect of active caps on contaminant bioavailability – measurement and prediction of the bioavailable pool of contaminants in sediments, the International Annual Meeting of the American Society of Agronomy/Crop Science Society of America/Soil Science Society of America (ASA/CSSA/SSSA), Long Beach, CA, November 1-4, 2010.
 20. Knox, A.S. and M.H. Paller. 2010. New Approaches for monitoring in situ remediation of contaminated sediments – Zone of Influence (ZOI). SETAC North America 31th Annual Meeting, Portland, Oregon, November 7-11, 2010.

Poster Presentations at Professional Meetings

1. Knox, A.S., M.H. Paller, D.D. Reible, and I.G. Petrisor. 2006. Sequestering agents for contaminants in sediments - application to the development of active caps, SERDP and ESTCP Partners in Environmental Technology Technical Symposium & Workshop, Washington, D.C., November 28-30, 2006.
2. Knox, A.S., M.H. Paller, D.D. Reible, and I.G. Petrisor 2007. Active caps for remediation of mixtures of contaminants and resistance to erosion - a comprehensive evaluation. SERDP/ and ESTCP Partners in Environmental Technology Technical Symposium & Workshop, Washington, D.C., December 4-6, 2007.
3. Paller, M.H. and A.S. Knox. 2007. Evaluation of the potential side effects of sequestering agents used for the development of active caps for contaminated sediments, SERDP/ and ESTCP Partners in Environmental Technology Technical Symposium & Workshop, Washington, D.C., December 4-6, 2007.
4. Galjour, J., L. Moretti, S. Ma, X.X. Lu, D.D. Reible, A.S. Knox, and M.H. Paller. 2007. Evaluation of the applicability and effectiveness of organoclay as active capping materials. SERDP/ and ESTCP Partners in Environmental Technology Technical Symposium & Workshop, Washington, D.C., December 4-6, 2007.
5. Forrest, C., S. Ma, D.D. Reible, I. Petrisor, and A.S. Knox. 2007. Evaluation of Biopolymer Coated Sands as Capping Materials. SERDP/ and ESTCP Partners in

- Environmental Technology Technical Symposium & Workshop, Washington, D.C., December 4-6, 2007.
6. Knox, A.S., M.H. Paller, K.L. Dixon, D.D. Reible, I.G. Petrisor, and J. Roberts. 2008. Active caps for remediation of sediment contaminants and resistance to erosion – transition from the laboratory to the field, SERDP/ and ESTCP Partners in Environmental Technology Technical Symposium & Workshop, Washington, D.C., December 1-4, 2008.
 7. Knox, A.S., C.E. Turick, and M.H. Paller. 2008. Methods for evaluating the life span of biopolymers used for contaminants sequestration and erosion control. SERDP/ and ESTCP Partners in Environmental Technology Technical Symposium & Workshop, Washington, D.C., December 1-4, 2008.
 8. Knox, A.S., M.H. Paller, and D.D. Reible. 2009. Field deployment of active caps – assessment of metal bioavailability and erosion resistance. SETAC North America 30th Annual Meeting, New Orleans, LA, November 19-23, 2009.
 9. Paller, M. H., Knox, A.S., D.D. Reible, X. Lu, and M.C. Brim. 2009. Field deployment of active caps – biomonitoring of amendment toxicity. SETAC North America 30th Annual Meeting, November 19-23, 2009, New Orleans, LA.
 10. Knox, A.S. and M.H. Paller. 2009. Monitoring of active caps – application of diffusive gradients in thin-film (DGT) technology for assessment of metal bioavailability in sediments. Conference on DGT and the Environment, 7th to 9th October, 2009, Santa Margherita di Pula, Sardinia, Italy.
 11. Knox, A.S., D.D. Reible, M.H. Paller, K.L. Dixon, J. Roberts, and I.G. Petrisor. 2009. Field deployment of active caps – assessment of metal bioavailability, erosion, and toxicity. SERDP and ESTCP Partners in Environmental Technology Technical Symposium & Workshop, Washington, D.C., December 1-3, 2009.
 12. Dixon, K.L. and A.S. Knox. 2009. Sequestration of metals in active cap materials: a laboratory and numerical evaluation. SERDP and ESTCP Partners in Environmental Technology Technical Symposium & Workshop, Washington, D.C., December 1-3, 2009.
 13. Knox, A.S., M.T. Whiteside, and M.H. Paller. 2010. Application of diffusive gradients in thin film (DGT) technology for assessment of metal bioavailability in remediated sediments. SETAC North America 31th Annual Meeting, Portland, Oregon, November 7-11, 2010.
 14. Knox, A.S., M.H. Paller, K. L. Dixon, and D.D. Reible. 2010. Field performance of active caps – assessment of contaminant immobilization, erosion resistance, and toxicity, SERDP and ESTCP Partners in Environmental Technology Technical Symposium & Workshop, Washington, D.C., November 30 - December 2, 2010.

APPENDIX 3 - TRANSITION PLAN

The expected outcome of this research work is a definitive understanding of active capping technology and the ability of active capping to remediate/reduce contaminant bioavailability in sediments. This will result in setting more defensible cleanup goals and establishing more realistic cleanup priorities while still ensuring the protection of human health and the environment. This enhanced understanding will increase the confidence of site managers to incorporate active capping technology into site management decisions. Results from this project are being promoted to DoD, scientists, and the public via DoD websites, presentations in internationally recognized scientific symposia, publication in peer-reviewed scientific journals, and reports. Feedback from international symposium/session attendees provides guidance that will be used to adjust the conceptual framework to improve the effectiveness of active capping technology.

The following sessions/symposiums were organized in 2009 and 2010 or planned for 2011:

1. A special symposium on **“Fate and transport of metals in contaminated sediments – new approaches in remediation”** was organized by Anna Knox (SRNL), Danny Reible (UT, Austin, TX), Michael Paller (SRNL), and Domy Adriano (SREL). The symposium was a part of the 10th International Conference on the Biogeochemistry of Trace Elements. The symposium was held in Chihuahua, Chih., Mexico, July 15, 2009.
2. A session titled **“Risk Assessment and Prediction of Contaminant Bioavailability in Soils and Sediments,”** which covers both metals and organic contaminants, was a part of the ASA-CSSA-SSSA annual meeting (Division S02 Soil Chemistry, Cosponsor S11 Soils and Environmental Quality), Oct. 31-Nov. 4, 2010, Long Beach, California. The organizers of the session were: Anna S. Knox and Ronald T. Checkai. <https://www.acsmeetings.org/poster-oral-papers>.
3. A special session **“Heavy Metals in Sediments and Remediation Technologies”** was organized by Anna Knox (SRNL), Jörg Rinklebe (University of Wuppertal, Germany), and Michael Paller (SRNL). The symposium was a part of the 15th International Conference on Heavy Metals in the Environment (15th ICHMET2010), September 19-23, 2010, Gdansk, Poland (<http://www.pg.gda.pl/chem/ichmet>).
4. A special symposium **“Bioavailability of Contaminants in Sediments – Implications for Remedial Technologies”** will be a part of the International Conference of Biogeochemistry of Trace Elements (ICOBTE) World Conference 2011. The ICOBTE World Conference will be held in Florence, Italy in July 2011. The symposium organizers are Anna Sophia Knox (SRNL), Danny D. Reible (University of Texas, TX), Jörg Rinklebe (Wuppertal University, Germany), Michael H. Paller (SRNL), and Domy C. Adriano (UGA)